

14-Sep-15 08:20 – 10:10	Oral	Sea to Sky Ballroom A
MOAA — Facilities I		
Chair: J. Knobloch (HZB)		

MOAA01 FRIB Project: Moving to Production Phase08:20 *K. Saito, J. Wei (FRIB)*

The Facility for Rare Isotope Beams (FRIB) is based upon a high power heavy ion driver linac under construction at Michigan State University under a cooperative agreement with the US DOE. The construction of conventional facilities already started in the summer, 2013, and the accelerator production began from the summer, 2014. FRIB will accelerate all the stable ion beams from proton to uranium beyond a beam energy of 200 MeV/u and up to a beam power of 400 kW to produce a great number of various rare isotopes using SRF linac. The FRIB SRF driver linac makes use of four kinds of SRF structures. Totally 332 two gap cavities and 48 cryomodules are needed. All SRF hardware components have been validated and are now moving to production. The SRF infrastructure also has been constructed in MSU campus. This talk will present FRIB project and challenges regarding SRF technologies. The status of SRF linac hardware validation and their production, SRF infrastructure status and plan shall be addressed. The information that can be relevant for future large scale proton/ion SRF linacs will also be provided.

MOAA02 Recent Progress with EU-XFEL08:40 *D. Reschke (DESY)*

The superconducting accelerator of the European XFEL consists of the injector part and the main linac. The injector includes one 1.3 GHz accelerator module and one 3.9 GHz third-harmonic module, while the main linac will consist of 100 accelerator modules, operating at an average design gradient of 23.6 MV/m. The fabrication and surface treatment by industry as well as RF acceptance tests of the required 808 superconducting 1.3 GHz cavities are close to an end by the time of SRF15. The accelerator module assembly, testing and installation in the tunnel is in full swing. First steps of commissioning have been made. The status and results of cavity and module RF tests at 1.3 GHz and 3.9 GHz are presented.

MOAA03 Progress on Chinese ADS project09:00 *Y. He (IMP/CAS) W.M. Pan (IHEP)*

An overview of C-ADS project progress since SRF2013 shall be presented. Operational experience with integrated hardware and beam tests and SRF infrastructure shall be reported. An overview of cavity and cryomodule progress can be presented keeping in mind that a detailed ADS cavity report will also be presented in a separate talk.

MOAA04 Overview of Recent SRF Developments for ERLs09:20 *S.A. Belomestnykh (BNL) S.A. Belomestnykh (Stony Brook University)*

This talk reviews SRF technology for Energy Recovery Linacs (ERLs). In particular, recent developments and results reported at the ERL2015 Workshop are highlighted. The talk covers facilities under construction, commissioning or operation, such as cERL at KEK, BERLinPro at HZB and R&D ERL at BNL, as well as facilities in the development phase. Future perspectives will be discussed.

MOAA05 Status of the RISP Superconducting Heavy Ion Accelerator09:45 *D. Jeon (IBS)*

Construction of the RISP heavy ion accelerator facility is in progress in Korea. The driver linac is a superconducting linac that can accelerate uranium to proton beams, delivering 400 kW beam power to various targets. Prototyping and test of the superconducting cavities and cryomodules are proceeding. Prototype superconducting cavities were fabricated through domestic vendors and their vertical tests were performed in collaboration with TRIUMF. Vertical tests showed good performance of the prototype cavities, which verified that there were no significant issues of the cavity design and fabrication. SRF Test Facility is under construction to be completed by early 2016. Progress report of the RAON accelerator systems is presented.

14-Sep-15 10:40 – 12:50	Oral	Sea to Sky Ballroom A
MOBA — Fundamentals I - High-Q		
Chair: C.E. Reece (JLab)		

MOBA01 SRF Linac for LCLS-II: Design Approaches, R&D and First Test Results10:40 *M.C. Ross (SLAC)*

This talk will describe the LCLS-II SRF linac stressing the challenges inherent in the technical specifications, the design approaches and the R&D program. Recent progress will be reported.

MOBA02 Efficient Magnetic Flux Expulsion During Cooldown11:00 *A. Romanenko (Fermilab)*

The talk will report recent experimental results and theoretical understanding of the magnetic flux expulsion during cooldown provided by large thermal gradients. The complete expulsion of the magnetic flux can lead to record-high Qs at accelerating gradients of ~20 MV/m. High Qs were achieved in ambient magnetic fields up to 190 mG. These findings open up a way to ultra-high quality factors at low temperatures and show an alternative to the sophisticated magnetic shielding implemented in modern superconducting accelerators.

MOBA03 Mean-Free-Path Dependence of the Losses From Trapped Magnetic Flux in SRF Cavities11:15 *D. Gonnella (Cornell University (CLASSE), Cornell Laboratory for Accelerator-Based Sciences and Education)*

One important characteristic of nitrogen-doped cavities is their very high sensitivity to increased residual surface resistance from trapped ambient magnetic flux. We have performed a systematic study on the losses by trapped flux, and their dependence on the mean-free-path (MFP) of the niobium RF penetration layer. Cavities with a wide range of MFP values were tested in uniform ambient magnetic fields to measure trapped magnetic flux and resulting increase in RF surface resistance. MFP values were determined from surface impedance measurements. The measured MFP dependence of the increased residual surface resistance from trapped ambient magnetic flux is compared to theoretical predictions.

MOBA04 High-Q Operation of SRF Cavities: The Impact of Thermocurrents on the RF Surface Resistance

11:30 *J.M. Vogt (HZB)*

For CW applications much effort is being expended to minimize the power dissipation (surface resistance) of niobium cavities. Previous studies have shown that residual resistance can be reduced by performing a thermal cycle, a procedure of warming up a cavity after initial cooldown to about 20K and cooling it down again. It was postulated that thermocurrents during cooldown generate additional trapped magnetic flux that impacts the cavity quality factor. Here, we present a more extensive study that includes measurements of two additional passband modes and that confirms the effect. A change in surface resistance of more than a factor seven was observed. In this paper, we also discuss simulations that support the claim. While the layout of the cavity LHe tank system is cylindrically symmetric, we show that the temperature dependence of the material parameters results in a non-symmetric current distribution.

MOBA05 Nature and Mechanisms of Flux Trapping During Quench in Superconducting Cavities

11:50 *M. Checchin (Fermilab)*

Achievable gradients in superconducting radio frequency cavities are primarily limited by the RF field breakdown due to quench. This phenomenon was extensively studied and several well-known mechanisms have been understood, such as thermal breakdown, multipacting, field emission, and the local overcoming of the critical field. On the other hand, the degrading effect of quench on quality factor is still not well understood and remains an open question for the SRF community. Recent tests on a high-Q cavity in a well-controlled magnetic field environment show Q changes with quench that vary directly with the ambient field conditions at the time of quench, showing in this case no evidence for trapped flux from thermo-electric currents induced by the quenches. This experiment nicely illustrates the flux expulsion and Q recovery with quench phenomenon previously reported by others. Additional attention will be also given to some new insight into the quench mechanism of nitrogen-doped cavities.

MOBA06 N Doping: Progress in Development and Understanding

12:05 *A. Grassellino (Fermilab)*

Significant progress was made recently with N2 doped cavities. This talk will summarize all developments with N-doped Nb cavity work at FNAL in the past two years.

MOBA07 Lessons Learned From Nitrogen Doping at JLab - Exploration of Surface Resistance and Quench Field Trade-Offs With Varied Interstitial Atom Diffusion of Niobium Cavity Surfaces

12:20 *A.D. Palczewski, G. Ciovati, P. Dhakal, R.L. Geng, C.E. Reece, H. Tian (JLab)*

Interstitial diffusion of atomic species into the surface of niobium has been found to yield significantly reduced srf surface resistance and lowered quench fields. This talk summarizes systematic efforts to explore the trade-offs of these phenomena with a goal of learning how to maximize Q0 in the 30 MV/m regime. The talk also summarizes N-doped cavity progress at JLab for LCLS-II.

MOBA08 Niobium Impurity-Doping Studies at Cornell and CM Cooldown Dynamic Effect on Q0

12:35 *M. Liepe, B. Clasby, R.G. Eichhorn, B. Elmore, F. Furuta, G.M. Ge, D. Gonnella, T. Gruber, D.L. Hall, G.H. Hoffstaetter, J.J. Kaufman, P.N. Koufalas, J.T. Maniscalco, T.I. O'Connell, P. Quigley, D.M. Sabol, J. Sears, E.N. Smith, V. Veshcherevich (Cornell University (CLASSE), Cornell Laboratory for Accelerator-Based Sciences and Education)*

As part of a multi-laboratory research initiative on high Q0 niobium cavities for LCLS-II and other future CW SRF accelerators, Cornell has conducted an extensive research program during the last two years on impurity-doping of niobium cavities and related material characterization. In this talk we report on the performance of doped cavities in vertical and cryomodule tests, and on detailed material characterization using SIMS and microwave impedance measurements. We show that higher nitrogen doping levels result in a reduced quench field. We report on the results from five cryomodule tests of nitrogen-doped 9-cell cavities, which include studies on the sensitivity to ambient magnetic fields, performance degradation from vertical to horizontal test, and impact of the RF power coupler on cavity performance. We further present measurements on the impact of the cool-down dynamics on thermoelectric currents and flux trapping, and discuss important differences between vertical and horizontal cavity tests.

14-Sep-15 14:20 – 17:30

Poster

Sea to Sky Ballroom BC

MOPB — Poster Session

MOPB001 RF Performance of Ingot Nb Cavities of Medium-Low Purity

G. Ciovati (JLAB) P. Dhakal, P. Kneisel, G.R. Myneni, J.K. Spradlin (JLab)

Superconducting radio-frequency cavities made of ingot niobium with residual resistivity ratio (RRR) greater than 250 have proven to have similar or better performance than fine-grain Nb cavities of the same purity, after standard processing. The high purity requirement contributes to the high-cost of the material. As superconducting accelerators operating in continuous-wave typically require cavities to operate at moderate accelerating gradients, using lower purity material could be advantageous not only to reduce cost but also to achieve higher Q0-values, because of the well-known dependence of the BCS-surface resistance on mean free path. In this contribution we present the results from cryogenic RF tests of 1.3-1.5 GHz single-cell cavities made of ingot Nb of medium (RRR=100-150) and low (RRR=60) purity from different suppliers. Cavities made of medium-purity ingots routinely achieved peak surface magnetic field values greater than 70 mT with Q0-values above $1.5 \cdot 10^{10}$ at 2 K. The performance of cavities made of low-purity ingots were affected by significant pitting of the surface after chemical etching.

MOPB002 Observation of High Field Q-Slope in 3 GHz Nb Cavities

G.V. Ereemeev, E.E. Hannon (JLab)

A degradation of the unloaded quality factor is commonly observed above about 100 mT in elliptical niobium cavities. The cause of this degradation has not been fully understood yet, but the empirically found solution of heating to about 100-120 C for 24-48 hrs., eliminates the degradation in electropolished fine grain or large grain niobium cavities. While numerous experiments related to this phenomenon have been done at 1.3 GHz and 1.5 GHz, little data exists at other frequencies and the frequency dependence of this degradation is not clear. We have measured the unloaded quality factor of 3 GHz fine grain niobium cavities, which were chemically polished as the final treatment before RF tests in a vertical Dewar and observed the characteristic degradation in two of the cavities. The measurement of the quality factor degradation at different bath temperatures points to a field-dependent rather than a temperature-related effect.

- MOPB003 Superconducting Cavity for the Measurements of Frequency, Temperature, RF Field Dependence of the Surface Resistance**
H. Park, S.U. De Silva, J.R. Delayen (ODU) H. Park (JLab)
 In order to better understand the contributions of the various physical processes to the surface resistance of superconductors the ODU Center for Accelerator Science is developing a half-wave resonator capable of operating between 325 MHz and 1.3 GHz. This will allow the measurement of the temperature and rf field dependence of the surface resistance on the same surface over the range of frequency of interest for particle accelerators and identify the various sources of power dissipation.
- MOPB004 Understanding the Field Dependence of the Surface Resistance of SRF Cavities**
P.N. Koufalas, D. Gonnella, M. Liepe, J.T. Maniscalco (Cornell University (CLASSE), Cornell Laboratory for Accelerator-Based Sciences and Education)
 An important limiting factor in the performance of SRF cavities in medium and high fields is the intrinsic quality factor and, thus, the surface resistance of the cavity. The exact dependence of the surface resistance on the magnitude of the RF field is not well understood. Here we present an analysis of experimental data of various single-cell cavities prepared and tested at Cornell, including nitrogen-doped cavities that demonstrate an anti-Q slope in the medium field region. We extract the temperature dependent and independent surface resistances for these cavities, analyze field dependencies, and compare with theoretical predictions. These comparisons and analyses provide new insights into the field dependence of the surface resistance and improve our understanding of the mechanisms behind the effect.
- MOPB005 Developing a Setup to Measure Field Dependence of BCS Surface Resistance**
J.T. Maniscalco, T. Gruber, M. Liepe, J. Sears (Cornell University (CLASSE), Cornell Laboratory for Accelerator-Based Sciences and Education)
 The surface resistance of SRF cavities has been shown experimentally to depend on the strength of the field. Several theories have recently been proposed to describe this phenomenon. In this paper we compare experimental results to the theoretical predictions. We also present work on the development of a cavity setup for measuring the field-dependence with an applied DC magnetic field.
- MOPB006 Hc2 Measurements of Superconductors**
J.T. Maniscalco, D. Gonnella, D.L. Hall, M. Liepe, E.N. Smith (Cornell University (CLASSE), Cornell Laboratory for Accelerator-Based Sciences and Education)
 Recently, Cornell has improved a method for extracting the upper critical field Hc2 of a thin-film superconductor using four-point resistivity measurements. In the field of superconducting radio-frequency accelerators (SRF), novel materials and processes such as nitrogen-doped niobium and Nb3Sn may allow for improved SRF performance and cost efficiency over traditional niobium. In this paper we present updated results on Hc2 measurements for several of these novel SRF materials, as well as results for niobium prepared normally. We also extract important material properties from these measurements, such as the Ginzburg Landau parameter, the mean free path, and coherence length, which are critical for determining SRF performance.
- MOPB007 Temperature Excursions in Nb Sheets With Imbedded Cracks**
P. Xu (MSU) T.R. Bieler (Michigan State University) C. Compton (FRIB), N.T. Wright (MSU)
 Delamination cracks can form in rolled Nb sheets, and between layers with different microstructures. Such cracks cause resistance to heat conduction from the RF surface to the LHe bath. A delamination crack can negate the advances in manufacturing processes that have enhanced the thermal conductivity of Nb. Here, temperature excesses are calculated as functions of crack size and location, and the power dissipated at an imperfection in the RF surface. A cylindrical section of Nb sheet is modeled as having adiabatic sides. A hemispherical defect is located on the RF surface at the center of this section. A crack is modeled as a void within the sheet. The Kapitza resistance between the Nb surface and LHe is varied. The results indicate that an incipient crack leads to a decrease in the magnetic flux required to cause thermal breakdown. The decrease in the field is gradual with increasing crack radius, until the crack radius nearly equals the section radius, after which the field required for breakdown decreases sharply. To a lesser extent, the field strength for thermal breakdown also decreases with increased crack depth.
- MOPB008 Theoretical Field Limit and Cavity Surface Conditions: Nano-Scale Topography and Submillimeter Pit**
T. Kubo (KEK)
 The recent two theoretical papers^{*,**} are briefly introduced. The former addresses the superheating field (Bs) suppression due to nano-defects distributing almost continuously on the cavity surface^{*}. We introduce a model of the nano-defect. An analytical formula for Bs suppression factor is derived. By using the formula, suppression factors of bulk or multilayer superconductors and those after various surface processing technologies can be evaluated. An application to the dirty Nb processed by EP is also presented as an example. The latter address the magnetic field enhancement (MFE) at the sub-millimeter pit on the surface of cavity, which is thought to cause quench^{**}. There exists the famous well-type pit model, but many of pits are not well-type but have gentle slopes. Impacts of the slope angle on MFE have not been well understood. We introduce a model that can describe a pit with an arbitrary slope angle. A formula to evaluate the MFE factor is derived. A pit with a gentle slope angle yields a much smaller MFE factor than the well-type pit. The formula can be applied to the calculation of MFE factors of real pits with arbitrary slope angles.
- MOPB009 Model of Flux Trapping in Cooling Process**
T. Kubo (KEK)
 Recent findings that cooling conditions affect an amount of trapped magnetic flux attract much attention as a way to achieve a high-Q0 by SRF cavity^{*,**,***}. Q0~2*10¹¹ has already been achieved by the full flux expulsion^{****}. While much experimental studies have been conducted, not much theoretical progress followed on it. In this paper, I introduce a simple model that can explain how trapped fluxoids are expelled in cooling process.
- MOPB010 Field-Dependent Surface Resistance for Superconducting Niobium Accelerating Cavities: The Case of N-Doping**
W. Weingarten (Private Address), R.G. Eichhorn (Cornell University (CLASSE), Cornell Laboratory for Accelerator-Based Sciences and Education)
 The dependence of the Q-value on the RF field (Q-slope) for superconducting RF cavities is actively studied in various accelerator laboratories. Although remedies against this dependence have been found, the physical cause still remains obscure. A rather straightforward two-fluid model description of the Q-slope in the low and high field domains is extended to the case of the recently experimentally identified increase of the Q-value with the RF field obtained by so-called "N-doping".
- MOPB011 How Uniform Are Cool-Downs?**
J.A. Robbins, R.G. Eichhorn (Cornell University (CLASSE), Cornell Laboratory for Accelerator-Based Sciences and Education)
 Since the last SRF conference it has become clear that achieving extremely high quality factors of SRF cavities depend on the cool-down scenario. While some findings favor a fast cool-down, others suggest a slow cycle to be advantageous, and many variations to that have been investigated: the role of thermocurrents, amount of ambient magnetic field and flux trapping. This paper will investigate, how uniformly different cool-down procedures are and if they can explain the more efficient magnetic flux expulsion.

- MOPB012 Calculation of the Thermo-Current Driven Magnetic Field at the RF Layer of a Superconducting Cavity**
J. May-Mann, R.G. Eichhorn (Cornell University (CLASSE), Cornell Laboratory for Accelerator-Based Sciences and Education)
The role of thermo-current and how they may or may not impact the performance of a superconducting cavity has been a mystery for a while. In this paper, we will report on results we gained by simulating field configurations, as they exist during different cool-down scenarios. We will show that the symmetry that exist during an ideal cool-down can be broken. As a result of the symmetry breaking we will demonstrate that a significant amount of magnetic field will exist at the RF layer of the cavity which may reduce the quality factor if partially trapped. Based on our findings, mitigation strategies and beneficial cool-down conditions will be derived.
- MOPB013 Simulation of Geometry Dependent Flux Trapping**
R.G. Eichhorn, J. May-Mann (Cornell University (CLASSE), Cornell Laboratory for Accelerator-Based Sciences and Education)
Trapping or expulsion of ambient magnetic field has become an important factor in the performance of superconducting cavities with very high Q. As experimental data is limited, we set up a numerical field calculation model to study this effect in more details. We will report, how the cavity orientation, the movement of the transition to superconductivity front, and the orientation of the magnetic field contributes to the amount of magnetic field being vulnerable for trapping.
- MOPB014 Cool-Down Studies in Horizontally Cooled Cavity**
M. Martinello, M. Checchin, A. Grassellino, O.S. Melnychuk, A. Romanenko, D.A. Sergatskov (Fermilab) M. Checchin (Illinois Institute of Technology)
The cool-down details of superconducting accelerating cavities are found to be crucial parameters that have to be optimize in order to obtain very high quality factors. The temperature all around the cavity is monitored during its cool down across the critical temperature, in order to visualize the different dynamics of fast and slow cool-down, which determine considerable difference in terms of magnetic field expulsion and cavity performance. The study is performed placing a single cell 1.3GHz elliptical cavity perpendicularly to the helium cooling flow, which is representative of how SRF cavities are cooled in an accelerator. Hence, the study involves geometrical considerations regarding the cavity horizontal configuration, underling the different impact of the various magnetic field components on the surface resistance. Experimental data also proves that under established condition, flux lines are concentrated at the cavity top, in the equatorial region, leading to temperature rise.
- MOPB015 Trapped Flux Surface Resistance Analysis for Different Surface Treatment**
M. Martinello, M. Checchin, A. Grassellino, O.S. Melnychuk, S. Posen, A. Romanenko, D.A. Sergatskov (Fermilab) M. Checchin (Illinois Institute of Technology)
The trapped flux surface resistance is one of the main contribution on cavity losses when they are cooled in presence of external magnetic field. The study is focalized on the understanding of the different contributions of the trapped flux surface resistance, and their role as a function of different surface treatment. The study is performed on 1.3 GHz niobium cavities with different surface treatment: electro polishing, 120C baking, and N-doping with various concentration of nitrogen. The different contributions at the trapped flux surface resistance are then analyzed as a function of the mean free path in order to find the best mean free path which minimized this surface resistance contribution.
- MOPB016 New Insights Into Frequency Dependence of Nitrogen Doping and Trapped Flux Losses**
M. Martinello, M. Checchin, A. Grassellino, O.S. Melnychuk, A. Romanenko, D.A. Sergatskov (Fermilab) M. Checchin (Illinois Institute of Technology)
Nitrogen doped niobium cavities appears to be particularly suitable in the case of 1.3 GHz superconducting cavity technology, giving ultra-high quality factors thanks to the very low surface resistances. Of actual importance is to understand whether the implementation of nitrogen doping treatment leads to high performance in the whole frequency range suitable for SRF applications. The work is focused on the surface resistance analysis of 650 MHz, 1.3 GHz and 3.9 GHz cavities, with the primary purpose of verifying the benefits of nitrogen treatment within this range of frequencies. In addition, since 1.3 GHz nitrogen doped niobium cavities have shown high sensitivity to external magnetic field, a deeply study of the trapped flux residual resistance as a function of the resonance frequency will be presented.
- MOPB017 On the Impact of Thermocurrents on the RF Surface Resistance (Undoped Bulk Nb)**
J.M. Vogt, J. Knobloch, O. Kugeler (HZB)
For CW applications much effort is being expended to minimize the power dissipation (surface resistance) of niobium cavities. Previous studies have shown that residual resistance can be reduced by performing a thermal cycle, a procedure of warming up a cavity after initial cooldown to about 20K and cooling it down again. It was postulated that thermocurrents during cooldown generate additional trapped magnetic flux that impacts the cavity quality factor. Here, we present a more extensive study that includes measurements of two additional passband modes and that confirms the effect. A change in surface resistance of more than a factor seven was observed. In this paper, we also discuss simulations that support the claim. While the layout of the cavity LHe tank system is cylindrically symmetric, we show that the temperature dependence of the material parameters results in a non-symmetric current distribution.
- MOPB018 Introduction of Precisely Controlled Microstructural Defects into SRF Cavity Niobium Sheet and Their Impact on Local Superconducting Properties**
M. Wang, T.R. Bieler, D. Kang (Michigan State University) C. Compton (NSCL) C. Compton, C. Compton (FRIB) P.J. Lee (NHFML) A. Polyanskii, Z-H. Sung (ASC)
When SRF cavity shapes are formed from Nb sheets, the metallurgical processing introduces microstructural defects such as dislocations and low-angle grain boundaries that can serve as pinning centers for magnetic flux that may degrade cavity performance. Therefore, the relationship between magnetic flux behavior and microstructural defects in carefully strained SRF Nb sheet was investigated. Laue X-ray and EBSD-OIM crystallographic analyses of large grain ingot slices were used to characterize microstructural defects and then predict which grains and sample orientations will produce desired model defects due to tensile deformation. Grain orientations were chosen to favor specific slip systems, which generate dislocations with special angles with respect to the sample surface. Nb bicrystals were also prepared to investigate the effects of grain boundaries on flux pinning. The generated defect structures were confirmed by OIM and TEM. Cryogenic magneto-optical imaging was used to directly observe the penetration of magnetic flux into the deformed Nb. These model samples have deformation that is similar to that expected in typical cavity forming processes.
- MOPB019 Horizontal Testing and Thermal Cycling of an N-Doped Tesla Type Cavity**
O. Kugeler, J. Knobloch, J.M. Vogt (HZB) A. Grassellino, O.S. Melnychuk, A. Romanenko, D.A. Sergatskov (Fermilab)
An N-doped TESLA type cavity treated at FERMILAB has been tested in the HoBiCaT horizontal test stand. Temperatures and magnetic fields occurring during the superconducting transition were recorded at various positions and directions on the outer cavity surface. Several thermal cycling runs were performed yielding different Q0 factors just like in undoped cavities. The resulting residual and BCS resistance values were correlated to the thermal and magnetic conditions during cooldown and compared to values obtained in a vertical test at Fermilab.

- MOPB020 Derivation of the Trapped Flux Residual Resistance as Function of the Mean Free Path**
M. Checchin, A. Grassellino, M. Martinello, A. Romanenko (Fermilab) M. Martinello (Illinois Institute of Technology)
 In this study a calculation of the fluxoids-related residual surface resistance is presented. The calculation is based on the assumption of the local description of fluxoids in the superconductor, where the magnetic field lines are screened by superconducting currents and confined in a normal conducting core with a finite radius. Independently on the temperature dependent surface resistance, two main mechanisms of dissipation of fluxoids are considered: the oscillation of the magnetic flux lines about a pinning center driven by the Lorenz force acting on them, and the normal conducting resistance associated to the presence of a normal conducting core. The whole calculation is carried out taking in to account the dependence on the mean free path, in order to correlate the fluxoids residual surface resistance to the amount of impurities at the RF surface of SRF cavities.
- MOPB021 Mechanism of Flux Trapping During Superconductive Quench in Niobium Cavities**
M. Checchin, A. Grassellino, M. Martinello, O.S. Melnychuk, A. Romanenko, D.A. Sergatskov (Fermilab) M. Martinello (Illinois Institute of Technology)
 Since the born of SRF technology, it has been observed that the superconducting quench may lead to the lowering of the cavity intrinsic quality factor, and this effect was attributed to magnetic flux trapped at the quench spot during the quench event. Anyway, the complete description of the mechanism at the basis of magnetic flux trapping at the quench spot has been till now not clear and source of discussion in the SRF community. In this study we will describe the real origin and mechanism of magnetic flux trapping at the quench spot, proving that the quench-related quality factor degradation is consequence of the presence of ambient magnetic field during the quench. We proved that the intrinsic quality factor can be totally recovered by quenching in zero magnetic field, up to a certain point. If the degradation is too important then the quality factor cannot be completely recovered and still some magnetic flux will be remained trapped at the quench spot.
- MOPB022 Origin of Premature Quench in Superconducting Nitrogen Doped Cavities**
M. Checchin, A. Grassellino, M. Martinello, O.S. Melnychuk, S. Posen, A. Romanenko, D.A. Sergatskov, Y. Trenikhina (Fermilab) M. Martinello (Illinois Institute of Technology)
 Nitrogen doped superconducting cavities are the most reliable RF accelerating technology able to achieve quality factors of $5 \cdot 10^{10}$ at 2 K for nine cells cavities 1.3 GHz cavities. The main drawback of such technology though, is the early quench that limits the accelerating gradients to about 20 MV/m, against the average of 35 MV/m obtained with the usual EP plus 120 °C bake treatment. In this study we present the early quench phenomenon description by means of temperature mapping during the RF vertical test of single cell cavities and by a detailed investigation on the material properties of the quench spot cut-out. The study is then addressed to the description of the early quench mechanism on nitrogen doped cavities, with particular attention in the explanation of why different doping recipes have different quench fields, in order to define the best dopant content able to maximize the cavity intrinsic quality factor without lowering the quench field.
- MOPB023 Detectors Sensing Second Events Induced by Thermal Quenches of SRF Cavities in He II**
M. Fouaidy, F. Dubois, D. Longuevergne, O. Pochon, J.-F. Yaniche (IPN)
 SRF bulk Nb cavities are often limited by quench due to anomalous losses (heating due normal defects or Field Emission). We continued R&D on Quench Detectors (QD) activity for locating quench in SRF cavities via 2nd sound in superfluid helium. We investigated 2 kinds of QD: Capacitive OST (COST) and Low Response time resistive Thermometers (LRT). A test stand operating in LHe (Temperature: T0) was used for the characterization of the QD by means of precise experimental simulation of SRF cavity quench (pulsed heat flux qP). For improving spatial resolution of QD, smaller COSTs were developed and tested. We investigated the dynamic response of QD as function of different parameters (heater size/geometry, T0, qP) and data are reported. Further, a 2nd Sound Resonator (SSR), with a pair of COSTs at its 2 extremities as 2nd Sound Generator (SSG) and Detector (SSD) respectively and housing also a low heat capacity heater (SSG) and a LRT (SSD) assembly was developed. The first experimental data obtained, with SSR operated in resonating mode or in a shock wave mode are presented. The results concerning locating of quenches in QWR and spoke cavities are discussed.
- MOPB024 SRF Cavity Breakdown Calculation Procedure Using FEA-Software**
R.A. Kostin, A. Kanareykin (Euclid TechLabs, LLC) I.V. Gonin (Fermilab) E.N. Zaplatin (FZJ)
 SRF cavity thermal breakdown can be analyzed analytically using thermodynamics equation. This technique is suitable for simple geometries when surface magnetic field variation can be omitted. Thermal radiation effect which is crucial for SRF gun calculations is also hard to implement properly because of complicated geometry. All of these can be overcome by using multiphysics FEA-software. This paper shows the procedure of cavity thermal breakdown calculation in coupled multiphysics analysis with dependable parameters.
- MOPB025 Quality Factor Field Dependence Down to Very Low Fields**
A. Romanenko, M. Checchin, T.N. Khabiboulline, M. Martinello (Fermilab) M. Checchin, M. Martinello (Illinois Institute of Technology)
 Potential application of SRF cavities for quantum computing requires their operation in the limit of very low fields (down to single photon) and temperatures (<100 mK). If niobium cavities are advantageous for this field depends on the Q value, which can be achieved, and therefore requires detailed studies in the low field Q slope regime. Here we report the first attempt toward such a characterization by extending the low field Q slope measurements in 1.3 GHz single cell cavities down to the lowest possible fields.
- MOPB026 Effect of Hydrogen Injection During Cooling on the Q(e) Curve of Vacuum Furnace Treated Cavities**
A. Romanenko, M. Checchin, A. Grassellino, M. Martinello (Fermilab) M. Checchin, M. Martinello (Illinois Institute of Technology)
 We report on the experiment of controlled hydrogen absorption during the cool down of cavities after vacuum furnace treatment for an extended period of time.
- MOPB027 Studies of Superconducting Properties of N-Doped Samples**
A. Vostrikov, A. Grassellino, A. Romanenko (Fermilab) T. Murat (University of Wisconsin-Madison) A. Vostrikov (University of Chicago)
 We have performed detailed studies using DC and AC magnetometry and electrical resistivity measurements of niobium samples prepared using different nitrogen doping recipes. We compare the results to the samples prepared by standard preparation techniques such as EP with and without additional 120C baking to get insight into driving factors of the lowered quench field in N-doped SRF cavities.

- MOPB028 Preservation of Very High Quality Factors of 1.3 GHz Nine Cells From Bare Vertical Test to Dressed Horizontal Test**
A. Grassellino, M. Checchin, A.C. Crawford, C.J. Grimm, A. Hocker, M. Martinello, O.S. Melnychuk, J.P. Ozelis, A.M. Rowe, D.A. Sergatskov, G. Wu (Fermilab) D. Gonnella (Cornell University (CLASSE), Cornell Laboratory for Accelerator-Based Sciences and Education) M. Liepe (Cornell University) J.M. Vogt (HZB)
In this contribution we will report quality factor evolution of several different nine cell N doped cavities with very high Q. The evolution of the quality factor will be reported from bare to dressed in vertical test to dressed in horizontal test with unity coupling to dressed in horizontal test and CM-like environment/configuration (with RF ancillaries). Cooling studies and optimal cooling regimes will be discussed for both vertical and horizontal tests and comparisons will be drawn also for different styles titanium vessels. Studies of sensitivities to magnetic field in final horizontal configuration have been performed by applying a field around the dressed cavity and varying the cooling; parameters required for a very good flux expulsion will be presented.
- MOPB029 N Doping Recipe Development for Optimal Q and Quench Fields in 1.3 GHz and 650 MHz Single Cell and Nine Cell Nb Cavities**
A. Grassellino, M. Checchin, A.C. Crawford, M. Martinello, O.S. Melnychuk, M. Merio, S. Posen, A. Romanenko, A.M. Rowe, D.A. Sergatskov (Fermilab)
This contribution will report progress in developing an optimal nitrogen doping regime for 650 MHz and 1.3 GHz niobium cavities. Statistics over > 30 cavities will be reported showing clear trends in two-three times larger medium field Q values systematically achieved and the dependence of the quench field on the doping level. Optimal recipes will be highlighted for the "light N doping" regime producing high Q and gradients > 30 MV/m for single cells and > 25 MV/m for nine cells. RF performance of cavities subject to high T bake in presence of partial pressure of different gases will be reported.
- MOPB030 Measurements of Thermal Impedance on Superconducting Radiofrequency Cavities**
P. Dhakal, G.R. Myneni (JLab) G. Ciovati (JLAB)
The thermal impedance of niobium plays an important role in the stability of the superconducting radio frequency cavities used in particle accelerators. During the operation of SRF cavities, the RF power dissipated on the inner surface of the cavities and the heat transport to the helium bath depend on the thermal conductivity of niobium and the Kapitza conductance of the interface between the niobium and superfluid helium. Here, we present the results of measurements done on samples as well as on SRF cavities made of both ingot and fine-grain Nb to explore the effect of the surface preparation and crystal structure on the thermal impedance.
- MOPB032 Trial of Nitrogen Doping for SRF Cavities at KEK**
K. Umemori, H. Inoue, E. Kako, T. Konomi, T. Kubo, H. Sakai, M. Sato, H. Shimizu, K. Shinoe, M. Yamanaka (KEK) H. Hara, K. Sennyu, T. Yanagisawa (MHI)
Recently Nitrogen doping (N-doping) technique was proposed and drastic improvements of Q-values were reported. Since high-Q operation of SRF cavities are very attractive for CW machine, we started investigation on performance of Nitrogen doped SRF cavities. Nitrogen doping systems were prepared on two vacuum furnaces, which have been used for annealing of SRF cavities. Two fine grain single cell cavities have been used for the study. After 800 degree, 3 hours annealing, N-doping were carried out under several Pa of Nitrogen pressure and followed by post annealing. Three kind of different conditions, pressure and duration time, were attempted. After applying EP-2, cavity performances were evaluated by vertical tests. Against our expectations, we observed lower Q-values, at every measurements, than those measured without N-doping. In this presentation, we describe details about N-doping system and parameters and results obtained by vertical tests. Some discussions are also given against our results.
- MOPB033 LCLS-II SRF Cavity Processing Protocol Development and Baseline Cavity Performance Demonstration**
M. Liepe, P. Bishop, H. Conklin, R.G. Eichhorn, F. Furuta, G.M. Ge, D. Gonnella, T. Gruber, D.L. Hall, G.H. Hoffstaetter, J.J. Kaufman, G. Kulina, J.T. Maniscalco, T.I. O'Connell, P. Quigley, D.M. Sabol, J. Sears, V. Veshcherevich (Cornell University (CLASSE), Cornell Laboratory for Accelerator-Based Sciences and Education) M. Checchin, A.C. Crawford, A. Grassellino, C.J. Grimm, A. Hocker, M. Martinello, O.S. Melnychuk, J.P. Ozelis, A. Romanenko, A.M. Rowe, D.A. Sergatskov, W.M. Soyars, R.P. Stanek, G. Wu (Fermilab) A.D. Palczewski, C.E. Reece (JLab)
The "Linac Coherent Light Source-II" Project will construct a 4 GeV CW superconducting RF linac in the first kilometer of the existing SLAC linac tunnel. The baseline design calls for 280 1.3 GHz nine-cell cavities with an average intrinsic quality factor Q_0 of $2.7 \cdot 10^{10}$ at 2K and 16 MV/m accelerating gradient. The LCLS-II high Q_0 cavity treatment protocol utilizes the reduction in BCS surface resistance by nitrogen doping of the RF surface layer, which was discovered originally at FNAL. Cornell University, FNAL, and TJNAF conducted a joint high Q_0 R&D program with the goal of (a) exploring the robustness of the N-doping technique and establishing the LCLS-II cavity high Q_0 processing protocol suitable for production use, and (b) demonstrating that this process can reliably achieve LCLS-II cavity specification in a production acceptance testing setting. In this paper we describe the LCLS-II cavity protocol and analyze combined cavity performance data from both vertical and horizontal testing at the three partner labs, which clearly shows that LCLS-II specifications were met, and thus demonstrates readiness for LCLS-II cavity production.
- MOPB034 Nitrogen Doping of Niobium Cavity in IHEP**
P. Sha (Institute of High Energy Physics (IHEP), Chinese Academy of Sciences)
Nitrogen doping technology has been proved to improve the performance of superconducting cavities obviously. Related research has been carried out in IHEP and PKU, which focused on 1.3-GHz single-cell cavity firstly.
- MOPB035 Nature and Implication of Found Actual Particulates on the Inner Surface of Cavities in a Full-Scale Cryomodule Previously Operated With Beams**
R.L. Geng, J.F. Fischer, O. Trofimova (JLab)
Field emission in an SRF cavity is often the result of small foreign particulates lodging on the cavity inner surface. To avoid these particulate field emitters, careful cleaning and handling of individual cavities and clean room assembly of cavity strings are common practice. Despite these elaborate processes, some particulates persist to stay on the final surface of a beam-ready cavity. Moreover, as will be shown in this contribution, new particulates accumulate after a cryomodule is placed in the accelerator tunnel. The nature of these accumulated particulates on the inner surface of a beam-accelerating cavity is largely unknown for two reasons: (1) lack of access to such surfaces; (2) lack of a workable procedure for investigation without destroying the cavity. In this contribution, we report the first study on found actual particulates on the inner surface of 5-cell CEBAF cavities in a full-scale cryomodule previously operated with beam. The nature of the studied particulates is presented. The implication of the findings will be discussed in view of reliable and efficient operation of CEBAF and future large-scale SRF accelerators.

MOPB036 Nitrogen Doping Study on Niobium Samples*Z.Q. Yang, X.Y. Lu, W.W. Tan, D.Y. Yang, J. Zhao (PKU)*

Nitrogen doping can systematically improve the quality factor of niobium superconducting radio-frequency cavities. And it has been decided to be applied to the LCLS-II program. But the mechanisms of the nitrogen doping effect remain unclear. We studied the nitrogen doping effect through a series of experiments on niobium samples at both room temperature and liquid Helium temperature to seek the physical explanation. The experimental environment is close to that of the Fermilab. The experimental methods involves time of flight secondary ion mass spectrometry, point-contact tunneling, measurement of the RRR, measurement of magnetic hysteresis loop, atomic force microscope analysis and nuclear magnetic resonance analysis. The BCS resistance of the samples is calculated from the srmp code, using the material parameters measured. The critical state model is applied to evaluate the residual resistance due to the trapped magnetic flux based on the measured magnetic hysteresis loop. Our study shows that the nitrogen doping effect results from the interaction between nitrogen and hydrogen, which can avoid the formation of poorly superconducting hydride and nitride.

MOPB037 Performance of Nitrogen Doped and Standard Treatment Cavities at 4.2K*O.S. Melnychuk, A. Grassellino (Fermilab)*

In many industrial SRF cavity applications 4.2K is a preferred operation temperature. Quality factor of Nitrogen doped cavities and cavities with baseline ILC processing was measured at 4.2K-4.5K at Fermilab vertical test facility for SRF cavities. We present results for 1.3GHz and 650MHz cavities. We also include comparison of 325MHz cavity performance at 4.2K for electro-polished and 120C baked cavities.

MOPB038 Comparison of Quality Factor, Quench Fields, and Field Emission Onset for 1.3GHz Cavities of Different Surface Treatments*O.S. Melnychuk, A. Grassellino (Fermilab)*

We present a summary of performance of 1.3GHz TESLA shape nine-cell SRF cavities characterized in vertical test facilities at DESY and at Fermilab. Quality factor at 5MV/m and at 16MV/m as well as quench field are studied. Comparison of performance between different surface treatments is made. Studies of field emission onset are performed.

MOPB039 Analysis of BCS RF Loss Dependence on N-Doping Protocols*A.D. Palczewski, P. Dhakal, C.E. Reece (JLab)*

During the last one and a half years, as guidance for the nitrogen doping protocols for the LCLS-II prototype cryomodule, JLab has systematically doped 21 total single and multi-cell cavities in order to understand the feasibility and sensitivity of nitrogen doping for the project. For all test RF measurements, each cavity was tested at multiple temperatures in order to understand the field and temperature dependence of the RF losses. Initial analysis of the temperature dependant and independent portion of the RF losses on multiple cavities was presented at IPAC 2015[*]. These results suggest there is a correlation between the doping/electropolish parameters and the temperature dependent RF losses, but the mechanism which would explain this correlation is yet unclear. In this paper we will present a new study on two cavities which seeks to examine the correlation seen in the initial results over a larger doping/EP range and consider interpretation based on characterization of co-treated coupon samples[**]

MOPB040 Performance of Dressed Cavities for the Jefferson Laboratory LCLS-II Prototype Cryomodule*A.D. Palczewski, G.K. Davis (JLab) F. Furuta, G.M. Ge, D. Gonnella, M. Liepe (Cornell University (CLASSE), Cornell Laboratory for Accelerator-Based Sciences and Education)*

Initial vertical RF test results and quench studies for six of the eight undressed 9 cell cavities slated for use in the Jefferson laboratory LCLS-II prototype cryomodule were presented at IPAC2015.* For the final string 2 more cavities AES029 and AES030 (work done at Cornell) are being processed and tested for qualification before helium vessel welding. In addition, AES034 (initial R&D treatment) is being reworked with the current production protocol after a surface reset to improve the overall performance. After final qualification all 8 cavities will be welded into helium vessels and equipped with HOM couplers. In this paper we will present the final three vertical RF tests of the bare cavities along with the results after helium vessel welding before installation in the cryomodule string.

MOPB041 Cryomodule Testing of Nitrogen-Doped Cavities*D. Gonnella, B. Clasby, R.G. Eichhorn, B. Elmore, F. Furuta, G.M. Ge, D.L. Hall, Y. He, G.H. Hoffstaetter, J.J. Kaufman, P.N. Koufalas, M. Liepe, J.T. Maniscalco, T.I. O'Connell, P. Quigley, D.M. Sabol, E.N. Smith, V. Veshcherevich (Cornell University (CLASSE), Cornell Laboratory for Accelerator-Based Sciences and Education) A. Grassellino, C.J. Grimm, O.S. Melnychuk, A. Romanenko, D.A. Sergatskov (Fermilab)*

The Linac Coherent Light Source-II (LCLS-II) is a new FEL x-ray source that is planned to be constructed in the existing SLAC tunnel. In order to meet the required high Q0 specification of 2.7×10^{10} at 2 K and 16 MV/m, nitrogen-doping has been proposed as a preparation method for the SRF cavities in the linac. In order to test the feasibility of these goals, four nitrogen-doped cavities have been tested at Cornell in the Horizontal Test Cryomodule (HTC) in five separate tests. The first three tests consisted of cavities assembled in the HTC with high Q input coupler. The fourth test used the same cavity as the third but with the prototype high power LCLS-II coupler installed. Finally, the fifth test used a high power LCLS-II coupler, cavity tuner, and HOM antennas. Here we report on the results from these tests along with a systematic analysis of change in performance due to the various steps in preparing and assembling LCLS-II cavities for cryomodule operation. These results represent one of the final steps to demonstrate readiness for full prototype cryomodule assembly for LCLS-II.

MOPB042 Fundamental Studies on Doped SRF Cavities*D. Gonnella, T. Gruber, P.N. Koufalas, M. Liepe, J.T. Maniscalco (Cornell University (CLASSE), Cornell Laboratory for Accelerator-Based Sciences and Education)*

Recently, doping with nitrogen has been demonstrated to help SRF cavities reach significantly higher intrinsic quality factors than with standard procedures. However, the quench fields of these cavities have also been shown to be reduced. Here we report on fundamental studies of doped cavities, investigating the source of reduced quench field and exploring alternative dopants. We have focused on studying the quench of nitrogen-doped cavities with temperature mapping, critical field measurements using PPMS, and measurements of the flux penetration field using pulsed power to investigate maximum fields in nitrogen doped cavities. We also report on studies of cavities doped with other gases such as Argon and Helium. For these alternative dopants, we also show studies on samples to analyze concentrations of the doping atoms within the niobium. These studies have enabled us to shed light on the mechanisms behind the higher Q and lower quench fields that have been observed in cavities doped with impurities.

MOPB043 Frequency Dependence Studies of Nitrogen Doped SRF Cavities Using Multimode Measurements of an End Group Cavity*Y. Xie, A. Grassellino, A. Romanenko (Fermilab)*

In order to study frequency dependence of rf surface resistance of nitrogen doped cavities, we have developed a single cell srf cavity made of two 9cell end groups with input coupler and high order mode couplers. By exciting several 2GHz and 3GHz higher frequency modes from different coupler ports, we are able to measure frequency dependence of nitrogen doped cavities in a single rf test. The method of multimode excitation and rf test results will be presented.

MOPB044 Feasibility Study of Linear Colliders Using 2.6GHz Nitrogen Doped Cavity

Y. Xie, A. Grassellino, A. Romanenko (Fermilab)

For SRF cavities with higher rf frequency than 1.3GHz, the global thermal runaway effects prohibit using cavities of 2GHz above for linear colliders. With nitrogen doping, we show that 2.6GHz cavity can reach 35MV/m average accelerating gradients thus they can be used for linear colliders. The nitrogen doped 2.6GHz SRF cavities will significantly reduce the cost of future linear colliders or other SRF projects. For prof of principle studies, we present several 2.6GHz nitrogen doped single cell cavities rf testing results.

MOPB045 Study of Slip and Deformation in High Purity Single Crystal Nb for Accelerator Cavities

D. Kang, D.C. Baars, T.R. Bieler (Michigan State University) C. Compton (FRIB) A. Mapar, F. Pourboghrat (MSU)

High purity Nb has been used to build accelerator cavities over the past couple decades, and there is a growing interest in using ingot Nb as an alternative to the fine grain sheets. Plastic deformation governed by slip is complicated in body-centered cubic metals like Nb. Besides the crystal orientation with respect to the applied stress (Schmid effect), slip is also affected by other factors including temperature, strain rate, strain history, and non-Schmid effects such as twinning/anti-twinning asymmetry and non-glide shear stresses. A clear understanding of slip is an essential step towards modeling the deep drawing of large grain ingot slices, hence predicting the final microstructure/performance of cavities. Two groups of single crystals, with and without a prior heat treatment, were deformed to 40% engineering strain in uniaxial tension. Differences in flow stresses and active slip systems between the two groups were observed, likely due to the removal of preexisting dislocations. Crystal plasticity modeling of the stress-strain behavior suggests that the non-Schmid effect is small in Nb, and that the deep drawing process might be approximated with a Schmid model.

MOPB046 Evidence of Surface Carbon and Ordered NbC on Processed Niobium

J. Zasadzinski, A. Korczakowski, M. Warren (IIT) D.C. Ford, Th. Proslie (ANL)

High purity Nb processed according to standard recipes for SRF cavities displays regions with high concentrations of graphitic carbon as measured by Raman spectroscopy and SEM. High resolution TEM studies of such excess C regions reveal nanoscale inclusions of NbC that are coherent with the Nb host. NbC is also observed in Raman spectroscopy and displays a strongly enhanced two-phonon signal compared to bulk NbC. Raman data are compared to phonon mode calculations using density functional theory. It is found that the excess C regions can develop from strain alone and thus may be relevant for the initial deep drawing step of SRF cavity processing.

MOPB047 Secondary Electron Yield of Electron Beam Welded Areas of SRF Cavities

M. Basovic, S. Popović, M. Tomovic, L. Vušković (ODU) F. Čučkov, A. Samolov (University of Massachusetts Boston)

Secondary Electron Emission (SEE) is a phenomenon that contributes to the total electron activity inside the Superconducting Radiofrequency (SRF) cavities during the accelerator operation. SEE is highly dependent on the state of the surface. During electron beam welding process, significant amount of heat is introduced into the material causing the microstructure change of Niobium (Nb). Currently, all simulation codes for field emission and multipacting are treating the inside of the cavity as a uniform, homogeneous surface. Due to its complex shape and fabricating procedure, and the sensitivity of the SEE on the surface state, it would be interesting to see if the Secondary Electron Yield (SEY) parameters vary in the surface area on and near the equator weld. For that purpose, we have developed experimental setup that can measure accurately the energy distribution of the SEY of coupon-like like samples. To test the influence of the weld area on the SEY of Nb, dedicated samples are made from a welded plate using electron beam welding parameters common for cavity fabrication. SEY data matrix of those samples will be presented.

MOPB048 First Observation of Premature Magnetic Flux Penetration on Low Angle Grain Boundaries (LAGBs) of Mechanically Deformed High Purity Single Grain SRF Niobium

Z-H. Sung, S. Chetri, A. Polyanskii (ASC) T.R. Bieler, M. Wang (Michigan State University) C. Compton (NSCL) D.C. Larbalestier, P.J. Lee (NHMFL)

We have studied the mechanism of dislocation-magnetic field interactions in SRF Nb so as to determine the effect of dislocation decorated cell structures on RF cavity performance. To introduce small amounts of mechanical deformations, we tensile-tested a single SRF-grade Nb coupon, and then the tested coupon was sliced into small pieces by EDM in order to properly align the dislocation slip system parallel to the direction of the external magnetic fields. Using vibrometric polishing with BCP process, we removed surface damages to make the surface more representative of the chemistry of a SRF Nb cavity. Magneto-optical imaging showed that low angle grain boundaries (LAGBs) produced by 5 % deformation can preferentially admit magnetic flux. Comparisons of surface topological features before and after cryogenic cooling below $T_c \sim 9.2$ K of Nb with optical and electron microscopy showed that NbHx segregated along the LAGBs, suggesting of degraded superconductivity due to hydride phases. EBSD-OIM study indicated that misorientation across LAGBs is about 0.5 degree, and HR-TEM analysis suggests that the LAGBs might be formed by consecutive connection of geometrically necessary boundaries.

MOPB049 High Flux Three Dimensional Heat Transport in Superfluid Helium and Its Application to a Trilateration Algorithm for Quench Localisation With OSTs

T. Junginger (TRIUMF, Canada's National Laboratory for Particle and Nuclear Physics) P. Horn (TU Dresden) T. Koettig, K.C. Liao, A. Macpherson (CERN) B.J. Peters (KIT)

Oscillating superleak transducers of second sound can be used to localize quench spots on superconducting cavities by trilateration. However propagation speeds faster than the velocity of second sound are usually observed impeding the localization. Dedicated experiments show that the fast propagation cannot be correlated to the dependence of the velocity on the heat flux density, but rather to boiling effects in the vicinity of the hot spot. 17 OSTs were used to detect quenches on a 704MHz one-cell elliptical cavity. Two different algorithms for quench localization have been tested and implemented in a computer program enabling direct crosschecks. The new algorithm gives more consistent results for different OST signals analyzed for the same quench spot.

MOPB050 Characterization of SRF Materials at the TRIUMF muSR Facility

R.E. Laxdal, T.J. Buck, T. Junginger, P. Kolb, Y.Y. Ma, L. Yang, Z.Y. Yao (TRIUMF, Canada's National Laboratory for Particle and Nuclear Physics) S.H. Abidi (University of Toronto) R. Kiefl (UBC & TRIUMF)

MuSR is a powerful tool to probe local magnetism and hence can be used to diagnose flux penetration in Type-II superconductors. Samples produced at TRIUMF and with collaborators in both coin shaped and ellipsoidal geometries have been characterized by applying either transverse or parallel fields between 0 and 300mT and measuring flux entry as a function of applied field. Samples include Nb treated in standard ways including forming, chemistry, and heat treatments. Further, Nb samples have been doped with Nitrogen and coated with a 2 micron layer of Nb3Sn by collaborators from FNAL and Cornell respectively and measured in three field/geometry configurations. Analysis of the method in particular the effects of geometry and the role of pinning will be presented. Results of the measurements will be presented.

- MOPB051 First MuSR Measurements of SRF Samples in Strong Parallel Fields**
S. Gheidi (UBC) T.J. Buck, T. Junginger, R.E. Laxdal, G. Morris (TRIUMF, Canada's National Laboratory for Particle and Nuclear Physics) M. Dehn (TUM/Physik) R. Kiefl (UBC & TRIUMF)
 MuSR is a powerful tool to probe local magnetism and hence can be used to diagnose the entry of magnetic flux in superconductors. First measurements on SRF samples were done with an external DC field applied perpendicular to the sample (transverse geometry) with the muons applied to the sample face. Here the results are strongly impacted by demagnetization, pinning strength and edge effects. A new spectrometer has been developed to allow sample testing with a field varying from 0 to 300mT applied along the sample face (parallel geometry) analogous to rf fields in SRF resonators. The geometry is characterized by a small demagnetization factor reducing the impact of pinning and edge effects on field of first flux entry. The beamline installation and first results comparing transverse and parallel results will be presented.
- MOPB052 Determination of Surface and Bulk Superconducting Properties of Nitrogen Doped SRF Nb**
S. Chetri, D.C. Larbalestier, Z-H. Sung (ASC) P. Dhakal (JLab) P.J. Lee (NHMFL)
 Nitrogen-doped cavities show significant performance improvement in the medium accelerating field regime due to a lowered RF surface resistivity. However, the mechanism of enhancement has not been clearly explained. Our experiments explore how N₂-doping influences Nb bulk and surface superconducting properties, and compare the N₂-doped properties with those obtained previously with conventionally treated samples. High purity Nb-rod was mechanically deformed and post treated based on a typical SRF cavity treatment recipe. The onset of flux penetration at H_{c1}, and the upper and the surface critical fields, H_{c2} and H_{c3}, were characterized by magnetic hysteresis and AC susceptibility techniques. The surface depth profile responsible for superconductivity was examined by changing AC amplitude in AC susceptibility, and the microstructure was directly observed with EBSD-OIM. We are also investigating surface chemistry for detailed composition using XPS. We have found that N₂-doping at 800 °C significantly reduces the H_{c3}/H_{c2} ratio towards the ideal value of ~1.7, and conclude that AC susceptibility is capable of following changes to the surface properties induced by N₂-doping.
- MOPB053 Tunneling Spectroscopy of N-Doped Nb Samples and Hot and Cold Spots in the High Field Q Slope Region**
Th. Proslir, N. Groll (ANL) C. Cao, J. Zasadzinski (IIT) M. Checchin, A. Grassellino, M. Martinello, A. Romanenko (Fermilab)
 We present a tunneling spectroscopy study of N-doped bulk Nb samples made at FNAL under the same conditions as Nb cavities that shows the anti Q-slope effect. The conductance curves reveal a near-ideal BCS density of states with a sharp gap distribution centered around 1.5 meV and low inelastic scattering value of ~ 8% of the gap value. Very similar results were obtained on cut out from cold spots measured in the high field Q slope region. In hot spots cut out however, the spread of gap values is more pronounced, and higher inelastic scattering rates are measured.
- MOPB054 An Investigation of Correlations Between Mechanical and Microstructural Properties of High Purity**
Z. Zhao, T.R. Bieler, D. Kang (Michigan State University) C. Compton (FRIB)
 An understanding of the relationship between mechanical and functional properties, and processing history is essential in order to manufacture polycrystalline niobium cavities with consistent performance. The crystallographic texture (preferred crystal orientation) and microstructure in polycrystalline sheet varies considerably, so identifying its influence on properties is needed to achieve a better understanding of how to control properties of high purity niobium. Samples extracted from many lots produced by Tokyo Denki and Ningxia sheet were examined. Through-thickness texture of the undeformed niobium samples was measured using electron backscattered pattern mapping. Texture is identified with pole figures, orientation distribution function, and grain misorientation relationships. Stress-strain tests were done to identify ultimate tensile stress, elongation, 0.2% yield strength, and hardening rate. From tests on many lots, there is no clear trend between the mechanical and material properties in high purity niobium and correlations between various microstructural and mechanical properties show significant scatter and few apparent correlations.
- MOPB055 Characterization of N-Doping Recipes for the Nb SRF Cavities**
Y. Trenikhina, A. Grassellino, O.S. Melnychuk, A. Romanenko (Fermilab)
 For the future development of the nitrogen doping technology, it's vital to understand the mechanisms behind the performance benefits of N-doped cavities as well as the performance limitations, such as quench field. Following various doping recipes, cavity cutouts and flat niobium samples have been evaluated with XRD, XPS, SEM, SIMS and TEM in order to relate structural and compositional changes in the niobium near-surface to SRF performance. Annealing of Nb cavities with nitrogen for various durations and at various temperatures lead to a layer containing inclusions of non-superconducting Nb nitride phases, followed by unreacted Nb with an elevated N-interstitials concentration. We found that EP of the N-treated cavities removes the unwanted niobium nitride phases, confirming that performance benefits are originating from the elevated concentration of N interstitials. The role of low temperature Nb hydride precipitants in the performance limitation of N-doped cavities was evaluated by TEM temperature dependent studies. Finally, extended characterization of the original cavity cutouts from the N-doped RF tested cavity sheds some light on quenching mechanisms.
- MOPB056 A Differential-Exponential Hardening Model for Crystal Plasticity Modeling of Single Crystals**
A. Mapar, F. Pourboghrat (MSU) T.R. Bieler (Michigan State University) C. Compton (FRIB)
 Stress-strain curves of single crystals usually involves three stages, starting with activation of a single slip system. At this stage there is not much dislocation interaction and therefore the hardening rate is low. The next stage is when other slip systems active and rapidly increase the hardening rate. In the third stage cross slip and dynamic recovery happen and hardening rate decreases. Classical hardening models can only capture the first part of the stress-strain curve. In this study a new hardening model is proposed that can capture the first and second stages of the deformation. This model has been evaluated for Niobium single crystals and has successfully predicted the deformation of tensile samples having different crystal orientations.
- MOPB057 Crystal Plasticity Modeling of Single Crystal Nb**
A. Mapar, F. Pourboghrat (MSU) T.R. Bieler, D. Kang (Michigan State University) C. Compton (FRIB)
 Deformation behavior of niobium (Nb) is not thoroughly studied, although it is widely used in manufacturing superconducting cavities. This deficiency of knowledge limits the predictability in raw material properties for fine grain sheets, which are less anisotropic and easier to deform uniformly than large grain sheets. Studies on modeling and simulation of deformation of Nb are also limited. Therefore design of a new manufacturing procedure becomes a costly process, because models predicting the deformation of Nb are not accurate. A polycrystal is an aggregate of single crystals. Tensile tests were performed on single crystal with different orientations, to study the deformation behavior of Nb. A number of crystal plasticity models were developed, calibrated and finally used to predict the deformation of single crystal tensile samples. This study compares the predictions of these models. This provides a foundation for physically realistic polycrystal deformation models.

MOPB058 **Field Emission from Thermally Oxidized Nb Samples**

S. Lagotzky, G. Müller (Bergische Universität Wuppertal)

Enhanced field emission (EFE) from particulates and surface defects is one of the main field limitations of superconducting Nb cavities required for XFEL and ILC. The activation field E_{act} of such emitters and the emitter number density N at a given E_{act} is strongly influenced by the thickness of the Nb oxide layer*. Combination of this effect with surface cleaning techniques, e.g. dry ice cleaning (DIC), potentially shifts the onset of EFE to even higher E_{act} . Therefore, we have started to investigate a single crystal Nb sample after thermal oxidation (TO) by a heat treatment (HT) in air ($T = 360^{\circ}\text{C}$, $t = 40$ min). Field emission maps showed a first emitter at 100 MV/m, and $N = 30/\text{cm}^2$ at 225 MV/m. SEM analysis of the 10 strongest emitters revealed mainly surface defects and one particulate. Subsequent removal of the oxide by a HT ($T = 400^{\circ}\text{C}$, $t = 1$ h) under UHV resulted in an EFE onset at 75 MV/m and increased N to $60/\text{cm}^2$ at 225 MV/m. In a second step the TO as well as the measurement was repeated after DIC of the surface. The resulting field maps and the SEM analysis of selected emitters will be reported.

MOPB059 **Field Emission Investigation of Centrifugal-Barrel-Polished Nb Samples**

S. Lagotzky, G. Müller (Bergische Universität Wuppertal) A. Navitski (DESY) A.L. Prudnikava, Y. Tamashevich (Uni HH)

Actual and future SRF-accelerators require high accelerating gradient E_{acc} and quality factor Q_0 , which are often limited by enhanced field emission (EFE)* caused by surface roughness or particulates**. Various expensive surface preparation techniques (e.g. BCP, EP, HPR etc.) have been developed to obtain the required surface quality and remove the emitters. Recently, centrifugal barrel polishing (CBP) has been reconsidered to obtain a comparable surface roughness as EP with less effort***. We have started to investigate Nb samples, which were prepared as coupons in a single cell 1.3 GHz cavity by an optimized five step CBP process with a final dry ice cleaning. EFE maps showed the first emitter (1 nA) at 60 MV/m, and 32 emitters at 110 MV/m. SEM/EDX analysis of the emitting sites revealed many Al_2O_3 inclusions with sharp edges. Therefore, subsequent BCP (~20 μm removal) was applied to the sample. Surface analysis as well as EFE characterization of CBP treated Nb coupons with/without BCP step will be presented.

MOPB060 **A GPU Based 3D Particle Tracking Code for Multipacting Simulation**

T. Xin (Stony Brook University) S.A. Belomestnykh, I. Ben-Zvi, J.C. Brutus, V. Litvinenko, I. Pinayev, J. Skaritka, Q. Wu, B. P. Xiao (BNL)

A new GPU based 3D electron tracking code is developed at BNL and benchmarked with both popular existing parallel tracking code and experimental results. The code takes advantage of massive concurrency of GPU cards to track electrons under RF field in 3D Tetrahedron meshed structures. Approximately ten times of FLOPS can be achieved by utilizing GPUs compare to CPUs with same level of power consumption. Different boundary materials can be specified and the 3D EM field can be imported from the result of Omega3P calculation. CUDA_{OpenGL} interop was implemented so that the emerging of multipactors can be monitored in real time while the simulation is undergoing. Code also has GPU farm version that can run on multiple GPUs to further increase the turnover of multipacting simulation.

MOPB061 **Suppression of Upstream Field Emission in RF Accelerators**

F. Marhauser, S.V. Benson, D. Douglas (JLab)

So-called electron loading is the primary cause for cavity performance limitations in modern RF accelerating cavities. In superconducting RF cavities in particular, the onset of parasitic electron effects may start at field levels as low as a few MV/m. Electron loading can be attributed to mainly three phenomena: field emission, multiple impact electron amplification, and RF electrical breakdown. Field emission has been a persistent issue despite advances in SRF technology, whereas RF electrical breakdown and multipacting can be controlled by appropriate cavity design choices. Field emission becomes a major concern when the electrons emitted are captured by the accelerating RF field and directed along the beam axis through a series of cavities or even entire cryomodules. Consequently, electrons can accumulate energy comparable to that of the main beam over similar distances. This can represent a considerable dark current, which can travel downstream or upstream depending on the field-emitting site of origin. In this paper, a method is presented that can significantly suppress the upstream field emission by design.

MOPB062 **Overview of a 12 GeV Electron Accelerator for the MaRIE XFEL at LANL**

T. Tajima (LANL)

The MaRIE (Matter Radiation In the Extremes) project at LANL includes a 12 GeV electron accelerator for its XFEL facility. This accelerator is based on SRF technology with a design cavity gradient of 31.5 MV/m. An overview of the project especially focusing on the R&D for the SRF technology will be presented.

MOPB063 **Design of the Superconducting LINAC for SARAF**

C. Madec (CEA) N. Bazin, L. Boudjaoui, R. Cubizolles, G. Ferrand, P. Hardy, C. Pes, N. Sellami (CEA/IRFU) B. Gastineau, N. Pichoff (CEA/DSM/IRFU)

CEA is committed to delivering a Medium Energy Beam Transfer line and a superconducting linac (SCL) for SARAF accelerator in order to accelerate 5mA beam of either protons from 1.3 MeV to 35 MeV or deuterons from 2.6 MeV to 40.1 MeV. The SCL consists 4 cryomodules equipped with warm diagnostics. The first two identical cryomodules host 6 half-wave resonator (HWR) low beta cavities ($\beta = 0.091$), 176 MHz. As the last two identical welcome 7 HWR high-beta cavities ($\beta = 0.181$), 176 MHz. The beam is focused through the superconducting solenoids located between cavities housing steering coils. A Beam Position Monitor is placed upstream each solenoid. A diagnostic box containing a beam profiler, a bunch length monitor and a vacuum pump will be inserted between 2 consecutive cryomodules. The HWR cavities, the solenoid package and the cryomodules are being designed. These studies will be presented in this poster.

MOPB064 **Plan for High Intensity Proton Driver at KEKB for the Next Generation Neutrino Experiment**

G.-T. Park (KEK)

At J-Parc, a preliminary study is underway to construct a new proton driver that can deliver an intense proton beam with multi-megawatt power. With target energy of 9 GeV, we are focusing on the low-energy section up to 1.2 GeV. In this report, we describe our initial layout for the low energy section, including the low-beta superconducting cavities, and some preliminary decisions of the accelerator parameters for the feasibility of the plan.

MOPB065 **Recent Measurements on the sc 325 MHz CH-Cavity**

M. Busch, M. Amberg, M. Basten, F.D. Dziuba, H. Podlech, U. Ratzinger (IAP) M. Amberg (HIM)

At the Institute for Applied Physics (IAP), Frankfurt University, a sc 325 MHz CH-Cavity has been designed and fabricated. Successful tests at 4 K and 2 K with gradients up to 14.1 MV/m have been performed. The cavity is destined for a 11.4 AMeV 10 mA ion beam at the GSI UNILAC, Darmstadt. Consisting of 7 gaps and a geometrical beta of 0.16 this resonator is designed to provide a gradient of 5 MV/m. Novel features of this structure comprise a compact design, low electric peak fields, improved surface processing possibilities and power coupling. In addition a tuner system based on mechanically deformable bellow tuners attached inside the cavity and driven either by a stepping motor or a piezo actuator will keep the cavity on resonance. This contribution reports about the latest measurements on the cavity with the recently attached helium vessel and a renewed surface processing.

MOPB066 R&D Status of the New Superconducting CW Heavy Ion LINAC@GSI

M. Basten, M. Busch, F.D. Dziuba, D. Mäder, H. Podlech, M. Schwarz (IAP) M. Amberg, K. Aulenbacher, M. Miski-Oglu (HIM) W.A. Barth, V. Gettmann, S. Mickat (GSI)

To keep the ambitious Super Heavy Element (SHE) physics program at GSI competitive a superconducting (sc) continuous wave (cw) high intensity heavy ion LINAC is currently under progress as a multi-stage R&D program of GSI, HIM and IAP*. The baseline linac design consists of a high performance ion source, a new low energy beam transport line, an (cw) upgraded High Charge State Injector (HLI), and a matching line (1.4 MeV/u) which is followed by the new sc-DTL LINAC for post acceleration up to 7.3 MeV/u. In the present design the new cw-heavy ion LINAC comprises constant-beta sc Crossbar-H-mode (CH) cavities operated at 217 MHz. The advantages of the proposed beam dynamics concept applying a constant beta profile are easy manufacturing with minimized costs as well as a straightforward energy variation**. An important milestone will be the full performance test of the first CH cavity (Demonstrator), in a horizontal cryo module with beam. An advanced demonstrator setup comprising a string of cavities and focussing elements is proposed to build from 9 short CH-cavities with 8 gaps. The corresponding simulations and technical layout of the new cw heavy ion LINAC will be presented.

MOPB067 Steps Towards Superconducting CW-LINAC for Heavy Ions at GSI

M. Miski-Oglu, M. Amberg, K. Aulenbacher, W.A. Barth, V. Gettmann (HIM) K. Aulenbacher (IKP) W.A. Barth, M. Heilmann, S. Mickat, S. Yaramyshev (GSI) M. Basten, F.D. Dziuba, H. Podlech, U. Ratzinger (IAP)

Providing heavy ion beams for the ambitious experiment program at GSI, the Universal Linear Accelerator (UNILAC) serves as a powerful high duty factor (25%) accelerator. Beam time availability for SHE-research will be decreased due to the limitation of the UNILAC providing a proper beam for FAIR simultaneously. To keep the GSI-SHE program competitive on a high level, a standalone sc cw-LINAC in combination with the upgraded GSI High Charge State injector is planned to build. In preparation for this the first linac section (financed by HIM and partly by HGF-ARD-initiative) will be tested in 2015 as a demonstrator. After successful testing the construction of an extended cryomodule comprising two further, but shorter CH cavities is foreseen to test until end of 2017. In this contribution the simulation of beam dynamics and the preliminary mechanical layout of the entire string comprising three rf cavities and three solenoids in a cryo environment will be presented. As a final R&D step towards an entire linac an advanced cryo module comprising up to five CH cavities is envisaged for 2019 serving for first user experiments at the coulomb barrier.

MOPB068 Pulsed SC Ion Linac as an Injector to Booster of Electron Ion Collider

P.N. Ostroumov, Z.A. Conway, B. Mustapha (ANL) B. Erdelyi (Northern Illinois University)

The electron-ion collider (EIC) being developed at JLAB requires a new ion accelerator complex (IAC). The IAC includes a new linac and a booster accelerator facility. The new facility is required for the acceleration of ions from protons to lead for colliding beam experiments with electrons in the EIC storage ring. Originally, we proposed a pulsed linac which is based upon a NC front end, < 5 MeV/u, with a SC section for energies > 5 MeV/u and capable of providing 285 MeV protons and ~100 MeV/u lead ions for injection into the IAC booster. A recent cost optimization study of the IAC suggested that lower injection energy into the booster may reduce the overall project cost with ~120 MeV protons and ~40 MeV/u lead ions. Stronger space charge effects in the booster caused by lower injection energy will be mitigated by the booster design. In this paper we discuss both linac options.

MOPB069 Superconducting Linac Upgrade Plan for the Second Target Station Project at SNS

S.-H. Kim, M. Doleans, J. Galambos, M.P. Howell (ORNL) J.D. Mammosser (ORNL RAD)

The beam power of the Linac for the Second Target Station (STS) at the Spallation Neutron Source (SNS) will be doubled to 2.8 MW. For the energy upgrade seven additional cryomodules will be installed in the reserved space at the end of the linac tunnel to produce the linac output energy of 1.3 GeV. The cryomodules for STS will have some changes that do not require changes of overall layout based on the lessons learned from operational experience over the last 10 years and the high beta spare cryomodule developed in house. The average macro-pulse beam current for the STS will be 38 mA that is about 40 % increase from that for the present 1.4 MW operation. Plans for the existing cryomodules to support higher beam current for the STS is also presented in this paper.

MOPB070 Preliminary Conceptual Design of the CEPC SRF System

J.Y. Zhai, J. Gao, T.M. Huang, Z.C. Liu, Z.H. Mi, P. Sha, Y. Sun, H.J. Zheng (IHEP)

CEPC is a circular electron positron collider operating at 240 GeV center-of-mass energy as a Higgs factory, recently proposed by the Chinese high energy physics community. The CEPC study group, together with the FCC and ILC community, will contribute to the development of future high energy colliders and experiments which will ensure that the elementary particle physics remain a vibrant and exciting field of fundamental investigation for decades to come. Superconducting RF (SRF) system is one of the most important technical systems of CEPC and is a key to achieving its design energy and luminosity. It will dominate, with the associated RF power source and cryogenic system, the overall machine cost, efficiency and performance. The CEPC SRF system will be one of the largest and most powerful SRF accelerator installations in the world. The preliminary conceptual design of the CEPC SRF system is summarized in this paper, including the machine layout, key parameter choices and some critical issues such as HOM damping, emphasizing the new technology requirement and R&D focuses.

MOPB071 Technology Readiness Levels Applied to Current SRF Accelerator Technology for ADS

R. Edinger (PAVAC) R.E. Laxdal (TRIUMF, Canada's National Laboratory for Particle and Nuclear Physics)

Accelerator Driven Systems (ADS) are comprised of high power accelerators supplying a proton beam to a reactor vessel. The reactor vessel could contain fuels such as used uranium nuclear fuels or Thorium. The proton beam will be used to produce Neutrons by spallation in the reactor vessel. Technology readiness levels (TRLs) can be used to chart technology status with respect to end goal and as such can be used to outline a road map to complete an ADS system. TRL1 defines basic principles observed and reported, whereas TRL9 is defined as system ready for full scale deployment. SRF technology when applied to ADS reflects a mix of TRL levels since worldwide many SRF Accelerators are in operation. The paper will identify the building blocks of an ADS accelerator and analyze each for technical readiness for industrial scale deployment. The integrated ADS structure is far more complex than the individual systems, but the use of proven subsystems allows to build SRF accelerators that could deliver the beam required. An analysis of the technical readiness of SRF technology for ADS will be presented.

MOPB072 Characterisation of Surface Defects on EXFEL Series and ILC-Higrade Cavities

A. Navitski, E. Elsen, V. Myronenko, J. Schaffran, O. Turkot (DESY) Y. Tamashevich (Uni HH)

Inspection of the inner cavity surface by an optical system is an inexpensive and useful means for surface control and identification of critical or suspicious features. Optical inspection of around 100 EXFEL series and ILC-HiGrade cavities has been performed recently using the high-resolution OBACHT system. It is a semi-automated tool based on the Kyoto camera. To gain information about the 3D topography of surface features or defects, a replica technique has been applied additionally. This is a non-destructive surface-study method reaching resolution down to 1 μm by imprinting the details of the surface onto a hardened rubber. The footprint is subsequently investigated with a microscope or profilometer. Based on these studies, several defects on the surface have been found and classified. Most of the cavity failures leading e.g. to field limitations below 20 MV/m have been identified and corresponding feedback given to the production cycle. Typical surface features and defects as well as their influence on the cavity performance will be presented and discussed.

MOPB073 Surface Analyses and Optimization of Centrifugal Barrel Polishing of Nb Cavities

A. Navitski, E. Elsen, B. Foster, V. Myronenko (DESY) B. Foster, A.L. Prudnikava, Y. Tamashevich (Uni HH)

Centrifugal barrel polishing (CBP) is an acid-free surface-polishing technique based on abrasive media. It considerably reduces the usage of chemicals in the preparation of Nb cavities, typically leaving only a final light electropolishing (EP) and achieves considerably smaller roughness than in chemical treatments alone. CBP addresses in particular the removal of pits, welding spatters, deep scratches, and foreign material inclusions that occasionally occur in the production process. A mirror-smooth surface without chemical contamination is also an important enabling step for thin films. Recent results indicate, however, the need of further optimizations, mainly to reduce the surface damaged layer as well as the pollution by the polishing media. A dedicated study of the CBP process using a "coupon" cavity facilitates better polishing characterisation and optimisation by direct measurements of the roughness, removal rate, and removal profile as well as the amount of contamination left behind and determination of a best combination of the CBP and chemical polishing. Results of the coupon-studies and perspectives of the optimizations will be presented and discussed.

MOPB074 CERN's Bulk Niobium High Gradient SRF Programme: Developments and Recent Cold Test Results

A. Macpherson, K.G. Hernández-Chahín, P. Maesen, F. Pillon, K.M. Schirm, N. Valverde Alonso (CERN) K.G. Hernández-Chahín (DCI-UG)

As part of the development of a bulk niobium high gradient SRF program at CERN, cold testing of prototype SPL cavities is being carried out at CERN's SRF test facility. The Superconducting Proton Linac (SPL) cavity design is a 704 MHz bulk niobium 5-cell elliptical cavity with $\beta=1$, and four prototypes have been procured in industry. Successive cold tests of bare cavities at temperatures between 1.8 and 4.2 K have been used to define and validate the cavity preparation process, with optimisation in CERN's electropolishing and high pressure rinsing achieved. Consequently, there has been a progressive increase in achieved cavity performance toward SPL specifications, along with improved understanding of the RF conditioning and field emission behaviour of the cavity prototypes. Additionally, deployment of novel diagnostic and environmental monitoring have allowed for a detailed study and control of the cryostat test environment and its influence on cavity performance; factors considered include ambient magnetic field, trapped magnetic flux, and thermal electric currents. The current results of this test program are presented and the implications to our testing procedure discussed.

MOPB075 Experiences on Retreatment of XFEL Series Cavities at DESY

A. Matheisen, N. Krupka, S. Saegebarth, P. Schilling, N. Steinhau-Kühl, B. van der Horst (DESY)

For the European XFEL, two industrial companies are responsible for the manufacture and surface preparation of the eight hundred superconducting cavities. The companies had to strictly follow the XFEL specification and document all production and preparation steps. No performance guaranties were required. Each cavity delivered by Industry to DESY is tested in a vertical test at 2K. Resonators not reaching the performances defined for application at the XFEL linear accelerator modules or showing leakage during cold RF tests have undergone a subsequent retreatment at DESY. Nearly 20% of the cavity production required retreatment, most of them by an additional High Pressure Rinsing. Some cavities received additional BCP flash chemical treatment after the initial HPR did not cure the problem. The analysis of retreatments and quality control data available from the retreatment sequences and the workflow of retreatment will be presented.

MOPB076 Horizontal RF Test of a Fully Equipped 3.9 GHz Cavity for the European XFEL in the DESY AMTF

C.G. Maiano, C. Albrecht, R. Bospflug, J. Branlard, L. Butkowski, T. Delfs, J. Eschke, A. Gössel, F. Hoffmann, M. Hüning, K. Jensch, R. Jonas, R. Klos, D. Kostin, W. Maschmann, A. Matheisen, U. Mavrič, W.-D. Möller, K. Mueller, P. Pierini, J. Rothenburg, O. Sawlanski, M. Schmökel, E. Vogel (DESY) A. Bosotti, M. Moretti, R. Paparella, P. Pierini, D. Sertore (INFN/LASA) E.R. Harms (Fermilab) C.R. Montiel (ANL) S. Pivovarov (BINP SB RAS)

In order to validate the cavity package concept before the module preparation for the European XFEL Injector, one 3.9 GHz cavity, complete with magnetic shielding, power coupler and frequency tuner was tested in a specially designed single cavity cryomodule in one of the caves of the DESY Accelerator Module Test Facility (AMTF). The cavity was tested in high power pulsed operation up to the quench limit of 24 MV/m, above the vertical test qualifications and all subsystems under test (coupler, tuner, waveguide tuners, LLRF system) were qualified to design performances.

MOPB077 Vertical Tests of XFEL 3rd Harmonic Cavities

D. Sertore, M. Bertucci, A. Bosotti, J.F. Chen, C.G. Maiano, P. Michelato, L. Monaco, M. Moretti, R. Paparella, P. Pierini (INFN/LASA) A. Matheisen, M. Schmökel (DESY) C. Pagani (Università degli Studi di Milano & INFN)

The 10 cavities of the EXFEL 3rd Harmonic Cryomodule have been tested and qualified, before integration in the He-tank, in our upgraded Vertical Test stand. In this paper, we report the measured RF performance of these cavities together with the main features of the test facility.

MOPB078 Mode Sensitivity Analysis of 704.4 MHz Superconducting RF Cavities

K. Papke, F. Gerigk, S. Mikulas, S. Papadopoulos (CERN) U. van Rienen (Rostock University, Faculty of Computer Science and Electrical Engineering)

Due to the large variety of beam patterns considered for the superconducting proton linac (SPL) at CERN it is likely that the frequencies of some HOMs are close to machine lines during operation. Hence, in the interest of developing a method to shift HOM frequencies away from machine lines, we study the influence of cavity detuning and re-tuning (e.g. by Lorentz forces, field flatness tuning, frequency tuning during operation) on HOMs. The sensitivity of HOMs with respect to the fundamental mode was studied for a mono-cell and for 5-cell high-beta SPL cavities operating at 704.4 MHz. First, the variation of the HOMs during the flat-field tuning was measured. In this process, several detuning and re-tuning cycles were made to estimate the range of possible HOM frequency shifts. Secondly the effect of the frequency tuner on the HOMs is presented and finally the frequency shifts of all modes due to the cool down.

MOPB079 Analysis of the Test Rate for European XFEL Series Cavities

J. Schaffran, S. Aderhold, D. Reschke, L. Steder, N.J. Walker (DESY) L. Monaco (INFN/LASA)

The main part of the superconducting European XFEL linear accelerator consists of 100 accelerator modules each containing eight RF-cavities. Before the installation to a module, all of these cavities will be tested at cryogenic temperatures in a vertical cryostat in the accelerator module test facility (AMTF) at DESY. This paper discusses the average vertical test rate at the present status. It should be 1 in the ideal case, but actually it's observed to be approximately 1.4. Classification and analysis concerning the reasons for this deviation are given as well as suggestions for a reduction of the test rate for future production cycles.

MOPB080 Update and Status of Test Results of the XFEL Series Accelerator Modules

M. Wienczek, K. Kasprzak, A. Zwozniak (IFJ-PAN) D. Kostin, D. Reschke, N.J. Walker (DESY)

The European X-ray Free Electron Laser is under construction at DESY, Hamburg. During preparation for tunnel installation 100 Cryomodules are tested in a dedicated facility on the DESY campus. Up to now around 50 cryomodules have been measured at 2K. This paper describes the current status of the measurements, especially single cavity limitations. In addition we present a comparison between the vertical test results of the individual cavities and the corresponding performance measurements of the cavities once assembled into the accelerator string inside the cryomodule.

MOPB081 Testing of a Prototype LCLS II Cavity in the Horizontal Test Bed*M.A. Drury, E. Daly, G.K. Davis, C. Grenoble, L.K. King, A.D. Palczewski, T. Powers, J.P. Preble (JLab)*

The Thomas Jefferson National Accelerator Facility is currently engaged, along with several other DOE national laboratories, in the design and prototyping of the Linac Coherent Light Source II project (LCLS II). The SRF Institute at Jefferson Lab will be building 18 cryomodules based on the TESLA / XFEL design. Each cryomodule will contain eight nine-cell, 1.3 GHz cavities with coaxial input power couplers. In preparation for cryomodule production, new cavity processing techniques were investigated that would facilitate the production of cavities with a mean unloaded Q (Q₀) of 2.7×10^{10} at accelerating gradients of at least 16 MV/m. Vertical testing of nitrogen doped cavities has shown that Q₀ at 16 MV/m can exceed 4.0×10^{10} . Horizontal testing was deemed necessary to determine whether this level of cavity performance could be maintained when the cavity was installed in a cryomodule. In April, 2015, a successful horizontal test of a nitrogen doped prototype LCLS II cavity was completed using the Jefferson Lab Horizontal Test Bed (HTB). In the HTB at 16 MV/m and 2.0 K, this cavity had a measured Q₀ of 2.9×10^{10} . This paper will describe the test and discuss the results.

MOPB082 Analysis of Field Emission Reduction Resulting From 2nd-Round Helium Processing of CEBAF Cryomodules*M.A. Drury, F. Humphry, L.K. King (JLab)*

The Continuous Electron Beam Accelerator (CEBA) at the Thomas Jefferson National Accelerator Facility contains 50 cryomodules of three different designs in two linacs. These 50 cryomodules are capable of delivering multi-pass beam energy of up to 12 GeV. In order to ensure that the full potential of these cryomodules is available, Jefferson Lab will subject the cavities in all 50 linac cryomodules to a procedure known as helium processing. Helium processing will, in many cases, reduce the field emission in a given cavity. The benefits of field emission reduction include lower dynamic heat loads, lower waveguide arc rates in the fundamental power couplers and increased life expectancies for various components in or near the cryomodules. Processing will begin in June, 2015 and continue through October, 2015. This will be the second time a large scale helium processing project has been undertaken at Jefferson Lab. This paper will describe the procedure and analyze the results of this round of Helium Processing.

MOPB083 Cooling Front Measurement of a 9-Cell Cavity via the Multi-Cell Temperature-Mapping System at Cornell University*G.M. Ge (Cornell University (CLASSE), Cornell Laboratory for Accelerator-Based Sciences and Education)*

Cooling speed and uniformity affect flux trapping of a nitrogen-doped cavity; hence it determines the surface resistance and the quality factor of the cavity. We measured the temperature distribution of the 9-cell cavity by using the multi-cell T-map system at Cornell University, when it was cooled at different cooling rate. This paper also proposed a method to evaluate the formation of normal conducting islands at different cooling speed. We conclude that the slow cool down generates less normal conducting islands.

MOPB084 Performance of Nitrogen-Doped 9-Cell SRF Cavities in Vertical Tests at Cornell University*G.M. Ge (Cornell University (CLASSE), Cornell Laboratory for Accelerator-Based Sciences and Education)*

Cornell University treated five LCLS-II 9-cell cavities by nitrogen-doped recipes. In this paper, we report the performance of these 9-cell cavities. In the treatment, the nitrogen recipes are slightly different. The cavities have been doped under high nitrogen pressure and low pressure. The comparison of the performance will be shown and concluded.

MOPB085 Efforts of the Improvement of Cavity Q-Value by Plasma Cleaning Technology: Plan and Results from Cornell University*G.M. Ge (Cornell University (CLASSE), Cornell Laboratory for Accelerator-Based Sciences and Education)*

Experience with larger SRF installations shows that occasionally SRF cavities have substandard performance, and an in-situ cleaning mechanism would be highly desirable to recover the performance. Plasma cleaning was successful in reducing field emission in cavities with poor performance. Potentially, it might also be able to improve the quality factor Q₀ not only by reducing field emission, but also by removing bad oxides or other surface contamination. Within this proposal we would study if in-situ plasma cleaning can be effective in recovering or even improving the medium field Q₀ of SRF cavities. Cavity tests in a vertical test Dewar with large scale temperature mapping will be done to study the potential of plasma cleaning in improving the medium field Q₀. Parameters like the gas type and pressure will be varied to explore an optimized method for in-situ cavity cleaning.

MOPB086 Update and Status of Vertical Test Results of the European XFEL Series Cavities*N.J. Walker, D. Reschke, J. Schaffran, L. Steder (DESY) L. Monaco (INFN/LASA) M. Wiencek (IFJ-PAN)*

The series production by two industrial vendors of the 800 1.3-GHz superconducting cavities for the European XFEL has been on-going since the beginning of 2013 and will conclude towards the end of this year. As of publication some 740 cavities (~93%) have been produced at an average rate of 6 cavities per week. As part of the acceptance testing, all cavities have undergone at least one vertical RF test at 2K at the AMTF facility at DESY. The acceptance criterion for module assembly is based on the concept of a "usable gradient", which is defined as the maximum field taking into account Q₀ performance and allowed thresholds for field emission, as well as breakdown limits. Approximate 20% of the cavities have undergone further surface treatment in the DESY infrastructure to improve their usable gradient performance. In this paper we present the performance statistics of the vertical test results, as well as an analysis of the limiting criteria for the usable gradient, and finally the impact of the surface retreatment on both usable gradient and Q₀.

MOPB087 Integrated High-Power Tests of Dressed N-doped 1.3 GHz SRF Cavities for LCLS-II*N. Solyak, T.T. Arkan, M.H. Awida, B.E. Chase, A.C. Crawford, E. Cullerton, A. Grassellino, A. Hocker, J.P. Holzbauer, T.N. Khabiboulline, O.S. Melnychuk, J.P. Ozelis, T.J. Peterson, Y.M. Pischnalnikov, K.S. Premo, A. Romanenko, A.M. Rowe, W. Schappert, D.A. Sergatskov, G. Wu (Fermilab)*

New auxiliary components have been designed and fabricated for the 1.3 GHz SRF cavities comprising the LCLS-II linac. In particular, the LCLS-II cavity's helium vessel, high-power input coupler, higher-order mode (HOM) feedthroughs, magnetic shielding, and cavity tuning system were all designed to meet LCLS-II specifications. Integrated tests of the cavity and these components were done at Fermilab's Horizontal Test Stand (HTS) using several kilowatts of continuous-wave (CW) RF power. The results of the tests are summarized here.

MOPB088 HOM Measurements on the ARIEL eLINAC Cryomodules*P. Kolb, R.E. Laxdal, Y. Ma, Z.Y. Yao, V. Zvyagintsev (TRIUMF, Canada's National Laboratory for Particle and Nuclear Physics)*

The ARIEL eLINAC is a 50 MeV, 10 mA electron LINAC designed for the creation of rare isotopes via photo-fission. Future upgrade plans include the addition of a recirculating beam line to allow for either further energy increase of the beam beyond 50 MeV or to operate a free electron laser in an energy recovery mode. For both recirculating LINAC and ERL the higher order modes (HOM) have to be sufficiently suppressed to prevent beam-break-up. The design of the 1.3 GHz nine-cell cavity incorporated this requirement by including beam line absorbers on both ends of each cavity and an asymmetric beam pipe configuration on the cavity to allow trapped modes to propagate to the beam line absorbers. Measurements of the higher order modes on the completed injector cryomodule and the first cavity in the accelerating cryomodules will be shown and compared to simulations.

MOPB089 1.3 GHz Cavity Test Program for ARIEL

P. Kolb, R.E. Laxdal, Y. Ma, Z.Y. Yao, V. Zvyagintsev (TRIUMF; Canada's National Laboratory for Particle and Nuclear Physics) R.S. Orr (University of Toronto)

The ARIEL eLINAC is a 50 MeV 10 mA electron LINAC. Once finished, five cavities will each provide 10MV of effective accelerating voltage. At the present time two cavities have been installed and successfully accelerated beam with cavity performance above specifications of 10 MV/m at a Q0 of 1010. The next cavities are already in the pipeline and are being processed. In addition, one additional cavity has been produced for our collaboration with VECC, India. This cavity has been through a vertical test program and is being installed in a single cavity cryomodule for beam test at TRIUMF before shipment to India. The progress of the cavity performance after each treatment step has been measured and will be shown. In addition a thermometry system is being developed and first measurements of the temperature dependence of the used resistors have been completed and will be presented.

MOPB090 Analysis of Degraded Cavities in Prototype Modules for the European XFEL

S. Aderhold (Fermilab) S. Aderhold, D. Kostin, A. Matheisen, A. Navitski, D. Reschke (DESY)

In-between the fabrication and the operation in an accelerator the performance of superconducting RF cavities is typically tested several times. Although the assembly is done under very controlled conditions in a clean room, it is observed from time to time that a cavity with good performance in the vertical acceptance test shows deteriorated performance in the accelerator module afterwards. This work presents the analysis of several such cavities that have been disassembled from modules of the prototype phase for the European XFEL for detailed investigation like additional rf tests, optical inspection and replica.

MOPB091 Cavity Processing and Preparation of 650 MHz Elliptical Cell Cavities for PIP-II

A.M. Rowe, A. Grassellino, M. Merio, O.V. Pronitchev (Fermilab) R.C. Murphy, T. Reid (ANL)

The PIP-II project at Fermilab requires fifteen 650 MHz SRF cryomodules as part of the 800 MeV LINAC that will provide beam to NOvA, LBNL and the Mu2e experiments. A total of fifty-seven high-performance SRF cavities will populate the cryomodules and will operate in both pulsed and continuous wave modes. These cavities will be processed and prepared for performance testing utilizing adapted cavity processing infrastructure already in place at Fermilab and Argonne. The processing recipes implemented for these structures will incorporate state-of-the-art processing and cleaning techniques developed for 1.3 GHz SRF cavities for the ILC, XFEL, and LCLS-II projects. This paper describes the details of the processing recipes and associated chemistry, heat treatment, and cleanroom infrastructure adaptations at the Fermilab and Argonne cavity processing facilities.

MOPB092 Economics of Electropolishing Niobium SRF Cavities in Eco-Friendly Aqueous Electrolytes Without Hydrofluoric Acid

E.J. Taylor, T.D. Hall, M.E. Inman, S.T. Snyder (Faraday Technology, Inc.) D. Holmes (AES) A.M. Rowe (Fermilab)

A major challenge for industrialization of SRF cavity fabrication and processing is developing a supply chain to meet the high production demands of the ILC prior to establishment of a long term market need. Conventional SRF cavity electropolishing is based on hydrofluoric-sulfuric acid mixtures. In comparison, FARADAYIC® Bipolar EP applies pulse reverse electrolysis in dilute sulfuric acid-water solutions without hydrofluoric acid and offers substantial savings in operating and capital costs. Based on a preliminary economic analysis of the cavity processing requirements associated with the ILC, we project the cost of FARADAYIC® Bipolar EP to be about 27% that of the Baseline EP. In terms of tangible cost savings, the cost per cavity for the FARADAYIC® Bipolar EP and Baseline EP are \$1,293 and \$4,828, respectively. The "eco-friendly" intangible cost savings are generally accepted although the cost savings in terms of material degradation and maintenance are difficult to quantify at this time. Continued development and validation of FARADAYIC® Bipolar EP on nine cell cavities will contribute greatly to the industrialization of SRF accelerator technology.

MOPB093 Vertical Electropolishing Studies at Cornell

F. Furuta, B. Elmore, G.M. Ge, T. Gruber, G.H. Hoffstaetter, D.K. Krebs, J. Sears (Cornell University (CLASSE), Cornell Laboratory for Accelerator-Based Sciences and Education) T.D. Hall, M.E. Inman, S.T. Snyder, E.J. Taylor (Faraday Technology, Inc.) H. Hayano, T. Saeki (KEK) Y.I. Ida, K.N. Nii (MGH)

Vertical Electro-Polishing (VEP) has been developed and applied on various SRF R&Ds at Cornell as primary surface process of Nb. Recent achievements had been demonstrated with nitrogen doped high-Q cavities for LCLS-II. Five 9-cell cavities processed with VEP and nitrogen doping at Cornell showed the high average Qo value of $3.0 \cdot 10^{10}$ at 16MV/m, 2K, during vertical test. This achievement satisfied the required cavity specification values of LCLS-II ($2.7 \cdot 10^{10}$ at 16MV/m, 2K). We will report the details of these achievements and new VEP collaboration projects between Cornell and companies.

MOPB094 Inspection and Repair Techniques for the EXFEL Superconducting 1.3 GHz Cavities at Ettore Zanon S.p.A: Methods and Results

G. Massaro, G. Corniani, N. Maragno (Ettore Zanon S.p.A.) A. Matheisen, A. Navitski (DESY) P. Michelato, L. Monaco (INFN/LASA)

The quality control of the inner surface of superconducting RF cavities is essential in order to assure high accelerating gradient and quality factor. Ettore Zanon S.p.A. (EZ) has implemented in the serial production an optical system that use an high-resolution camera, in order to detect various types of defects. This system is added to a grinding machine, that was specifically designed and built to repair imperfections of the cavities inner surface. This inspection and repair system is applied to recover performance limited cavities of the 1.3 GHz European XFEL project, where surface irregularities are detected, either by the Obacht inspection system at Desy or the optical system at EZ. The optical system and the grinding procedure are qualified using two series cavities limited in gradient and showing different types of surface defects. The performances of these cavities have been recovered to reach the specifications of the project. Until now, all the series XFEL cavities built by EZ, repaired with this technique, have shown an accelerating gradient well above the EXFEL goal.

MOPB095 SRF Cavity Processing and Chemical Etching Development for the FRIB Linac

I.M. Malloch, E.S. Metzgar, L. Popielarski (FRIB) M.J. LaVere (MSU)

In preparation of a rigorous superconducting RF (SRF) cavity processing and test plan for the production of the Facility for Rare Isotope Beams (FRIB) driver linac, a state-of-the-art chemical etching tool has been installed in the FRIB coldmass production facility. This paper seeks to summarize the etching equipment design, installation, and validation program and subsequent etching results for a variety of SRF cavity types and etching configurations. Bulk etching, light etching, and custom (frequency tuning) etching results for different FRIB cavities are discussed. Special emphasis is placed on the etching removal uniformity and frequency tuning reliability of these processes.

MOPB096 Vertical Electropolishing at TRIUMF

J.J. Keir, P.R. Harmer, D. Lang, R.E. Laxdal, T. Shishido, R. Smith (TRIUMF; Canada's National Laboratory for Particle and Nuclear Physics) T. Shishido (KEK)

A setup for electropolishing of a superconducting niobium single-cell cavity has been installed at TRIUMF. A vertical method was selected to make the setup compact. To increase removal speed at the equator and remove hydrogen bubbles at the iris surface, 4 cathode paddles were rotated in the cavity cell during electropolishing. We will report on our first electropolishing result.

MOPB097 Test Results of the First Plasma Etched SRF Cavity

J. Upadhyay, J.J. Peshl, S. Popović, L. Vušković (ODU) D.S. Im (Old Dominion University) H.L. Phillips, A-M. Valente-Feliciano (JLab)

Plasma processing of SRF cavities will provide the unique opportunity of tailoring the inner surfaces for better SRF properties, in addition to less expensive and more environmentally friendly processing the cavities. The chosen process is using an rf (13.56 MHz) based coaxial capacitively coupled Ar/Cl₂ plasma. An apparatus has been designed and a method has been developed for plasma etching a varied diameter cylindrical structure resembling SRF cavities. The etch rate variation with the process parameters, such as gas pressure, rf power, dc bias on inner electrode, chlorine (Cl₂) content in Ar/Cl₂ mixture and temperature of the niobium (Nb) surface was established. The etch rate mechanism of Nb in an Ar/Cl₂ plasma was determined. The etch rate non-uniformity due to radical depletion along the gas flow direction was overcome by simultaneous movement of electrode and gas flow inlet. The shape of the inner electrode was optimized and a corrugated structured electrode was chosen. The apparatus for cavity plasma etching and rf test result of the first plasma etched cavity will be presented.

MOPB098 Improvement of Temperature Control During Nb 9-Cell SRF Cavity Vertical Electro-Polishing (VEP) and Progress of VEP Quality

K.N. Nii, V. Chouhan, Y.I. Ida, T.Y. Yamaguchi (MGH) H. Hayano, S. Kato, H. Monjushiro, T. Saeki, M. Sawabe (KEK) K. Ishimi (MGI)

Marui Galvanizing Co.,Ltd. has been developing Nb 9-cell SRF cavity vertical electro-polishing (VEP) facility and technique for mass production in collaboration with KEK. Our first 9-cell cavity VEP facility was not enough to control temperature during VEP, so the polishing quality was not so high. In this article, we will report the progress of temperature distribution and polishing quality due to the improvement of temperature control system of electrolyte and cavity during VEP.

MOPB099 Vertical Electropolish of Cu Single Cell Cavities Prior to Nb Film Coating

H.L. Phillips, H. Tian (JLab)

Nb film growth has been studied on various substrates. The resulting film structures confirm that the films characteristics are determined in the early stages of growth by the substrate parameters and the ion incident energy*. In this study, we report the progress for preparing Cu cavities for Nb thin film deposition via vertical electropolish (VEP). The analysis of Cu surface chemistry and morphology via witness samples under different steps of Cu cavity processing will be reported.

MOPB100 Cathode Geometry and Flow Dynamics Impact on Vertical Electropolishing of Superconducting Niobium Cavities

L.M.A. Ferreira (CERN)

CERN has now a fully operating vertical electropolishing installation, which has been used for the processing of 704 MHz high-beta five-cell Superconducting Proton Linac (SPL) niobium cavities. This installation relies only on the electrolyte circulation (HF/H₂SO₄) for power dissipation, evacuation of gases and homogeneous finishing; thus, parameters like cathode geometry, electrolyte flow and temperature become even more crucial when compared with horizontal electropolishing installations. Based on computational simulations performed with Comsol Multiphysics® and on a methodology developed at CERN, it is possible to assess the impact of the different cathode geometries as well as of the flow on the etching rate distribution. The data obtained with two different cathode geometries are presented: electrolyte velocity distribution, etching rate distribution, average current density and minimum working potential. One geometry was defined through a purely electrochemical approach while the second was defined to minimise the difference between the maximum and the minimum electrolyte speed inside the cavity; in both cases, the influence of the electrolyte flow was taken into account.

MOPB101 Electropolishing of Niobium SRF Cavities in Eco-Friendly Aqueous Electrolytes Without Hydrofluoric Acid

M.E. Inman, T.D. Hall, S. Lucatero, S.T. Snyder, E.J. Taylor (Faraday Technology, Inc.) F Furuta, G.H. Hoffstaetter (Cornell University (CLASSE), Cornell Laboratory for Accelerator-Based Sciences and Education) J.D. Mammoser (ORNL) A.M. Rowe (Fermilab)

Electropolishing of niobium cavities is conventionally conducted in high viscosity electrolytes consisting of concentrated sulfuric and hydrofluoric acids. This use of dangerous and ecologically damaging chemicals requires careful attention to safety protocols to avoid harmful worker exposure and environmental damage. We present an approach for electropolishing of niobium materials based on pulse reverse waveforms, enabling the use of low viscosity aqueous dilute sulfuric acid electrolytes without hydrofluoric acid, or aqueous near-neutral pH salt solutions without any acid. Results will be summarized for both cavity and coupon electropolishing for bulk and final polishing steps. With minimal optimization of pulse reverse waveform parameters we have demonstrated the ability to electropolish single-cell niobium SRF cavities and achieve at least equivalent performance compared to conventionally processed cavities. Cavities are electropolished in a vertical orientation filled with electrolyte and without rotation, offering numerous advantages from an industrial processing perspective. Shielding, external cooling and high surface area cathodes are adaptable to the bipolar EP process.

MOPB102 Comments on Electropolishing at Ettore Zanon SpA at the End of EXFEL Production

M. Rizzi, G. Corniani (Ettore Zanon S.p.A.) A. Matheisen (DESY) P. Michelato (INFN/LASA)

In 2013 a new horizontal electropolishing facility was developed and implemented by Ettore Zanon SpA (EZ) for the treatment of cavities for EXFEL series production. More than 300 cavities have been treated. Electropolishing has been used for two applications: bulk removal and recovering of cavities with surface defects. Treatment settings have been analysed and compared with cavities performances to verify possible influence of the various parameters. Main parameters considered are treatment time, voltage and current, that together define average thickness removal. The completion of EXFEL production has shown that the facility can perform five bulk treatments per week (140 micron each) over a long period. A one/two days maintenance every month was necessary to assure stable quality. Facing the new production of cavities for the upgrading of LCLSII, the process will be modified and verified according to specification of Jefferson Lab.

MOPB103 Vertical Electro-Polishing at DESY of a 1.3 GHz Gun Cavity for CW Application

N. Steinhilber-Kühl, R. Bandelmann, D. Kostin, A. Matheisen, M. Schmökel, J.K. Sekutowicz (DESY)

Superconducting gun cavities for cw operation in accelerators are under study. In 2003 a three-and-a-half cell gun cavity was chemically treated with buffered chemical polishing and tested successfully in a collaboration between Helmholtz-Zentrum Dresden-Rossendorf and DESY. For several years a 1.3-GHz 1.6-cell resonator has been under study, which has been built and tested at DESY and elsewhere. For further studies and optimization the gun cavity needed to be electro-polished, which was conducted at DESY for the first time using vertical electro-polishing. The technical set-up for the vertical electro-polishing and high-pressure rising as well as the processing parameters applied and the adaptation of the existing infrastructure to the 1.6-cell geometry at DESY are presented.

MOPB104 Outside BCP Studies of N-doped Cavities

S. Posen, M. Checchin, A. Grassellino, M. Martinello, O.S. Melnychuk, A. Romanenko, D.A. Sergatskov (Fermilab)

Outside BCP was applied to a number of single cell 1.3 GHz cavities with different levels of N-doping. This procedure was performed with the cavities under vacuum to ensure that the etch would not affect the inside surface. The RF performance of the cavities was evaluated before and after this procedure in vertical test. We discuss the interesting effect on the performance of the cavity and describe a possible explanation for the change in performance. A model is developed to explain the changes caused by the alteration only of the outer surface. We conclude with possible applications for this effect.

- MOPB105 Homogeneous Removal of Niobium Superconducting RF Cavity in Vertical Electropolishing**
V. Chouhan, Y.I. Ida, K.N. Nii, T.Y. Yamaguchi (MGH) H. Hayano, S. Kato, H. Monjushiro, T. Saeki, M. Sawabe (KEK) K. Ishimi (MGI)
Vertical electropolishing (VEP) leads several advantages over horizontal EP in respect of easy operation and mechanism of an EP system resulting in lower cost. However, till yet VEP always resulted inhomogeneous removal of a niobium (Nb) cavity along its length and bubble traces especially on the top iris of a vertically set cavity. In this work we performed lab EP and VEP experiments in order to study and solve these two problems. A coupon cavity which contains 6 disk type Nb coupons positioned at beam pipes, irises and equator was vertically electropolished to optimize VEP parameters so as to get almost uniform removal of Nb and a smooth surface of the cavity without bubble traces. Our patented unique i-Ninja cathode having 4 wings was used with an optimized rotation speed to get homogeneous removal of Nb. The homogeneous removal and the surface without bubble traces might be result of a uniform thickness of a viscous layer on the surface of the cavity cell and no accumulation of hydrogen bubbles on the top iris surface. The surfaces of the coupons were studied in detail with surface analytical tools.
- MOPB106 Analysis of High Pressure Rinsing for SRF Cavity Fabrication**
Y. Jung, J. Joo, M.J. Joung, H.J. Kim (IBS)
High pressure rinsing treatment has been widely used in the SRF cavity fabrication. This well-known process helps removes undesirable emission tips effectively from the inner surface of a cavity (Half wave resonator and Quarter wave resonator). Consequently, the HPR treatment improves quality factor by suppressing various field emission from the cavity during the operation. We fabricated a simplified transparent dummy cavity in order to observe with naked eyes how water rinsing was performed inside the cavity. In this paper, we simulated the HPR experiment with the dummy cavity which was intentionally painted inside and we report how rinsing was carried out as a function of the position and the water pressure.
- MOPB107 Investigation of N-Concentration Profiles in N-doped Nb via Witness Samples**
H. Tian, A.D. Palczewski, C.E. Reece (JLab) M.J. Kelley (The College of William and Mary)
In parallel with the single and multi-cell cavity work for LCLS-II and other projects, Nb samples were treated with the same thermal diffusion doping with nitrogen and comparable subsequent electropolish. In order to build a better understanding of the distribution of residual nitrogen within the rf surface and the mechanisms by which this influences the rf surface resistance of doped cavities, we are subjecting these samples to careful material characterization. In this study, we report a detailed depth profile of N doped Nb samples by SIMS using two different systems, surface chemistry under different doping and EP removals by XPS, and depth profiling of a cross section of bi-crystalline Nb. The results matrix together with cavity tests help to build a mechanistic understanding of the material modification that yields the improved rf performance.
- MOPB108 Vertical Electropolishing System for Applying the Pulse Reverse Electropolishing Technique to a Single Cell Nb Cavity**
H. Tian, J. Musson, H.L. Phillips, C.E. Reece, C. Seaton (JLab)
Pulse reverse electropolishing (EP), using a dilute aqueous H₂SO₄ electrolyte without HF has yielded RF performance equivalent to traditional EP. Compared with the presently deployed EP process for Nb SRF cavities, which uses 1: 10 volume ratio of HF (49%) and H₂SO₄ (98%), pulse reverse EP presents an ecologically friendly and relatively benign electrolyte option for cavity processing. In this study, we report on the design and commissioning of a new vertical electropolish (VEP) system with using the pulse reverse electropolishing technique applied to a single cell Nb cavity.
- MOPB109 Analysis of HF-Free Pulse-Reverse Nb Electropolishing Dynamics for SRF Cavities**
H. Tian, H.L. Phillips, C.E. Reece (JLab)
The performance of superconducting radiofrequency (SRF) cavities is greatly affected by the topography of the interior surface, so it is imperative that the surface be clean metal as smooth as possible. A new method that has been developed to smooth the surface is pulse reverse electropolishing (EP). This method uses aqueous H₂SO₄ as the electrolyte and alternating anodic and cathodic pulses to oxidize the niobium (Nb) and then remove the oxide from the surface. Previous studies have shown that pulse reverse EP effectively polishes the surface of Nb SRF cavities. However, mechanism for oxide removal and effect of off time are not well understood. In order to better understand polishing mechanism and optimize the operating parameter for cavity production, systematic electrochemical experiments have been carried out to further explore the oxide removal process, off time between positive and negative pulses, and determine optimum polishing parameters, the results will be reported.
- MOPB110 The Transfer of Improved Cavity Processing Protocols to Industry for LCLS-II - N-Doping and Electropolishing**
C.E. Reece, F. Marhauser, A.D. Palczewski (JLab)
Based on the R&D efforts of colleagues at FNAL, Cornell, and JLab, the LCLS-II project adopted a modification to the rather standard niobium SRF cavity surface processing protocol, which incorporates a high temperature diffusion doping with nitrogen gas. This change was motivated by the resulting higher Q₀ and the prospect of significantly lower cryogenic heat load for LCLS-II. JLab is responsible for managing the cavity procurement for the LCLS-II project. The first phase of the procurement action is to transfer the nitrogen-doping protocol to the industrial vendors. We also seek to exploit improvements in understanding of the niobium electropolishing process as part of the production processing of the LCLS-II cavity set. We will report on the technology transfer activities and progress toward the envisaged performance demonstration of vendor-processed TESLA-style LCLS-II cavities.
- MOPB111 Details on the Nitrogen Doping of SRF Cavities at Fermilab**
M. Merio, M. Checchin, A.C. Crawford, A. Grassellino, M. Martinello, A.M. Rowe, M. Wong (Fermilab) M. Checchin, M. Martinello (Illinois Institute of Technology)
The Fermilab SRF group regularly performs Nitrogen (N₂) doping heat treatments on superconducting cavities in order to improve their RF performances. This paper describes the set up and operations of the Fermilab vacuum furnaces, with a major focus on the implementation and execution of the N₂ doping recipe. Different cavity preparations and N₂ doping recipes will be analyzed and heat treatment data will be reported in the form of plot showing temperature, total pressure and partial pressures over time; cavity test results will also be reported to show how the different doping recipes affect the RF performances. Finally possible upgrades and improvements of the furnace and the N₂ doping process are discussed.
- MOPB112 SRF Quality Assurance Studies and Their Application to Cryomodule Repairs at SNS**
J.D. Mammosser, R. Afanador, D.L. Barnhart, B. DeGraff, B.S. Hannah, J. Saunders (ORNL RAD) M. Doleans, S.-H. Kim (ORNL)
Many of the SRF activities involve interactions to cavities which presents risk for particulate contamination to RF surfaces. In order to understand and reduce contamination in cavities during cleaning, vacuum pumping and purging, and in-situ cryomodule repairs, a Quality Assurance (QA) studies were initiated to evaluate these activities and improve them where possible. This paper covers the results of investigations on the effectiveness of the SNS ultrasonic cleaning systems, particulate control during pumping and purging, procedure development for in-situ cryomodule repairs, the application of these studies to the repair of a linac cryomodule, and discussion of further improvement in these areas.


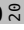
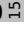
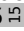
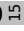
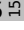
- MOPB113 Study of the Evolution of Artificial Defects on the Surface of Niobium During Electrochemical and Chemical Polishing**
L. Monaco, P. Michelato (INFN/LASA) A. Navitski, J. Schaffran, W. Singer (DESY) C. Pagani (Università degli Studi di Milano & INFN) A.L. Prudnikava (Uni HH)
 The presence of defects on the inner surface of Nb superconducting RF structures might limit its final performance. For this reason, strict requirements are imposed during mechanical production of the cavities, specifically on the quality control of the inner surface of components, to avoid the presence of defects or scratches. Nevertheless, some defects may remain also after control or can arise from the following production steps. Understanding the evolution of the defect might shine new insight on its origin and help in defining possible repair techniques. This paper reports the topographical evolution of defects on a Nb sample polished with the standard recipe used for the 1.3 GHz cavities of the XFEL project. Various artificial defects of different shape, dimensions, and thicknesses/depths, with geometrical characteristics similar to the one that may occur during the machining and handling of cavities, have been “ad hoc” produced on the sample of the same material used for the cell fabrication. Analysis shows the evolution of the shape and profile of the defects at the different polishing steps.
- MOPB114 Multi Analytical Approach for the Study of Residual Contamination During SRF Cavity Production**
F. Saliu, G. Sangiorgi (University of Milano Bicocca) M. Bertucci, P. Michelato, L. Monaco (INFN/LASA) C. Di Benedetto (KAUST) A. Matheisen (DESY) C. Pagani (Università degli Studi di Milano & INFN) D. Rizzetto, M. Rizzi (Ettore Zanon S.p.A.)
 Until now more than 700 superconducting 1.3 GHz cavities for the European XFEL project have been produced, treated and handed over to DESY for 2K RF acceptance test by Ettore Zanon SPA and Research Instrument company. Most of the cavities fulfil immediately the specifications for the European XFEL application. However some issues, related to contaminants accumulating during production, were encountered and could represent an additional cost for the project. Thus, for the early detection of this contamination, recognition of their source and establishment of prevention actions, a multi analytical approach was implemented. In particular, attention was devoted to some organic contaminants origin from piping's in use, that may affect the inner surface of the cavities. Analytical techniques included RGA during high vacuum operation, HPLC and GC-MS for the characterization of the fluids in contact with the cavities, IR and NMR spectroscopy for the study of the solid organic residues, CHNS and SEM/EDX for the inorganic particles. Data were submitted to multivariate statistical analysis in order to highlight significant correlation with the cavities performances.
- MOPB115 Surface Studies of Plasma Processed Nb Samples**
P.V. Tyagi, R. Afanador, M. Doleans, B.S. Hannah, S.-H. Kim, C.J. McMahan (ORNL) B.S. Hannah (ORNL RAD)
 Contaminants present at top surface of superconducting radio frequency (SRF) cavities can act as field emitters and restrict the cavity accelerating gradient. A room temperature in-situ NeO₂ plasma processing technology** for SRF cavities aiming to clean hydrocarbons from inner surface of cavities has been developed at the Spallation Neutron Source (SNS) and RF tests of plasma processed cavities have shown improvement of their accelerating gradient***. Surface studies of plasma processed Nb samples by Secondary ion mass spectrometry (SIMS) and Scanning Kelvin Probe (SKP) show that the plasma processing is very effective to remove carbonaceous contaminants from the top surface and to increase the surface work function. This article will present the results from those surface studies.
- MOPB116 Developments of Horizontal High Pressure Rinsing for SuperKEKB SRF Cavities**
Y. Morita, K. Akai, T. Furuya, A. Kabe, S. Mitsunobu, M. Nishiwaki (KEK)
 The Q factors of the eight superconducting accelerating cavities gradually degraded during the long-term operation of the KEKB accelerator. Since we will re-use those SRF cavities for the SuperKEKB, the performance degradation will be a serious problem. Several cavities degraded their performance significantly at high accelerating fields. The Q degradation is still acceptable for the 1.5 MV operations at SuperKEKB. However, further degradation will make the operation difficult. In order to recover the cavity performance, we developed horizontal high pressure water rinsing (HHPR). This method uses a horizontal high pressure water nozzle and inserts it directly into the cavity module. We applied this method to two degraded cavities and their degraded Q factors recovered above 10⁹ at around 2 MV. In this paper we will present the HHPR method, high power test results after the HHPR and the residual gas analysis.
- MOPB117 Identifying and Evaluation of Contamination Sources During Clean Room Preparation of SRF Cavities**
L. Zhao, G.K. Davis, A.V. Reilly (JLab)
 Particles are one possible cause of field emission issues in SRF cavity operations. During clean room cavity preparation, several processes could contribute to the generation of particles. One of them is friction between materials especially on flanges. It is important to understand the behaviors that generate and propagate particles into cavities. Using a single cell cavity, particle shedding between flange and several materials have been tested. The amount of particles is recorded with airborne particle counter, and the generated particles are examined with microscopies. The migration of particles into a cavity due to different movements is studied. Suggestions are made to reduce particle generation and prevent contamination of cavity interior area.
- MOPB118 Cleanliness and Vacuum Acceptance Tests for the UHV Cavity String of the XFEL Linac**
S. Berry, O. Napolý, B. Visentin (CEA/DSM/IRFU) C. Boulch, C. Cloué, C. Madec, T. Trublet (CEA/IRFU) D. Henning, L. Lilje, A. Matheisen, M. Schmökel (DESY)
 The main linac of the European XFEL will consist of 100 accelerator modules, i.e. 800 superconducting accelerator cavities operated at a design gradient of 23.6MV/m. In this context CEA-Saclay built an assembly facility designed to produce one module per week, ready to be tested at DESY. The facility overcame the foreseen production rate. We would like to highlight and discuss the critical fields: cleanliness and vacuum. A new assembly method to protect final assembly against particulates contamination has been implemented on the production line. Particle transport measurements on components used for the European XFEL accelerator module are presented. The results indicate that the nominal operation of the automated pumping and venting units will not lead to particle transport. Vacuum acceptance tests are of major interest: leak tests and residual gas analysis (RGA) are used to control the absence of air leak and contamination. The RGA specifications have been slightly relaxed to ensure the production rate. The correlation between cavities performances and production parameters will be investigated and discussed.
- MOPB119 Microscopic Investigation of Materials Limitations of Superconducting RF Cavities**
B.G. Oripov, T.M. Tai (CNAM, UMD) S. M. Anlage (UMD)
 Niobium-based SRF particle accelerator cavity performance is sensitive to localized defects that give rise to quenches at high accelerating gradients. A novel near-field magnetic field microwave microscope that enables locating these defects through scanning and mapping of the local electrodynamic response in the multi-GHz frequency range was successfully built using a magnetic writer from a conventional magnetic recording hard-disk drive. This magnetic writer can create an RF magnetic field, localized and strong enough to drive Nb into the vortex state, and may have sub-micron resolution. Using our probe, we study the 3rd harmonic nonlinear response and its dependence on input power and temperature for various materials such as Nb, MgB₂ and the cuprate Bi-Sr-Ca-Cu-O (BSCCO). By raster scanning the samples we are able to locate the regions with enhanced nonlinear response. For example, raster scans of exfoliated BSCCO superconducting samples showed ~10 dB variation in 3rd harmonic response power over a 1 mm line scan. Understanding the mechanism responsible for this non-linear response is important for improving the performance of SRF cavities.

15-Sep-15	08:00 – 10:10	Oral	Sea to Sky Ballroom A
TUAA — Facilities II			
Chair: D. Jeon (IBS)			

- TUAA01 08:00** **Operational Progress in Compact-ERL and Development of ERL-FEL for EUV Light Source at KEK**
H. Kawata (KEK)
 The beam commissioning in KEK-cERL including the first demonstration of energy recovery and the operational experience in gradually increasing beam currents should be presented. Also include the next project in ERL at KEK, the development of ERL-FEL for EUV light source started in collaboration with Japanese companies. Application of SRF technology to the EUV light source in an industrial framework should be discussed.
- TUAA02 08:20** **Commissioning of the SRF Linac for ARIEL**
V. Zvyagintsev, Z.T. Ang, T. Au, S. Calic, K. Fong, P.R. Harmer, B. Jakovljevic, J.J. Keir, D. Kishi, P. Kolb, S.R. Koscielniak, A. Koveshnikov, C. Laforge, D. Lang, R.E. Laxdal, Y. Ma, A.K. Mitra, N. Muller, R.R. Nagimov, W.R. Rawnsley, R.W. Shanks, R. Smith, B.S. Waraich, L. Yang, Z.Y. Yao, Q. Zheng (TRIUMF, Canada's National Laboratory for Particle and Nuclear Physics)
 This talk will report commissioning results for the SRF linac of ARIEL facility at TRIUMF. The talk should focus on the SRF challenges: cavity design and performance, ancillaries design and preparation, cryomodule design and performance, RF system and final beam test results.
- TUAA03 08:40** **BESSY-VSR: A Novel Application of SRF for Synchrotron Light Sources**
A.V. Véléz, J. Knobloch, A. Neumann (HZB)
 CW SRF Cavities have been used very successfully in the past in synchrotron light sources to provide high power acceleration. Here we present a novel application of higher harmonic systems of two frequencies (1.5 GHz and 1.75 GHz) to generate a beating of accelerating voltage. With such a system it is possible to store "standard" (some 10 ps long) and "short" (ps and sub-ps long) pulses simultaneously in the light source. This opens up brand new possibilities for light source users to perform dynamic and high-resolution experiments at the same facility. The demands on the SRF system and RF control are substantial and a new design, based on waveguide damping, is currently being developed. This system will be used for a major upgrade of the BESSY-II facility to the BESSY Variable Pulse Storage Ring (BESSY-VSR) for a next-generation storage-ring light source. We will discuss the concept, challenges and designs for BESSY-VSR.
- TUAA04 09:00** **Rapid Growth of SRF in India**
D. Kanjilal (IUAC)
 The talk shall summarize the recent advances in the SRF program in India. The IUAC, RRCAT and BARC SRF efforts shall each be addressed. In particular include results from the commissioning of the full (three module) heavy ion linac at IUAC, cavity fabrication, processing and results and infrastructure development at BARC and the technology and infrastructure advances at RRCAT.
- TUAA05 09:25** **SRF Development for PIP-II: Status and Challenges**
V.P. Yakovlev (Fermilab)
 The recent progress on R&D in support of the construction of PIP-II is presented. Recent results and progress on low and medium beta cavity development, rf ancillary development, CM prototyping, resonance control, and the front end test facility PXIE are reported.
- TUAA06 09:45** **Recent Progress of ESS Spoke and Elliptical Cryomodules**
G. Olry, S. Bousson (IPN)
 The ESS accelerator high level requirements are to provide a 2.86 ms long proton pulse at 2 GeV at repetition rate of 14 Hz. This represents 5 MW of average beam power with a 4% duty cycle on target. In a framework of a collaboration between IPN Orsay, CEA Saclay and ESS, prototype spoke and medium and high beta elliptical cavities and cryomodules are being constructed for the ESS linac. After a brief description of the accelerator layout, this talk will focus on the recent progress towards realization of the detailed design, the manufacturing of the prototype cryomodules and their associated valves boxes and the first test results of some of the most critical components such as SRF cavities, cold tuning systems and fundamental power couplers.

15-Sep-15	10:40 – 13:00	Oral	Sea to Sky Ballroom A
TUBA — Fundamentals II - Beyond Nb			
Chair: T. Tajima (LANL)			

- TUBA01 10:40** **Status of the HIE Isolde Project Including Cryomodule Commissioning**
W. Venturini Delsolaro (CERN)
 The status and the future steps of the HIE Isolde project shall be presented. The talk should also focus on the challenges, the realisation and the commissioning of the first HIE Isolde cryomodule and recent cavity performance progress.
- TUBA02 11:00** **Thermal Contact Resistance at the Nb-Cu Interface**
V. Palmieri (INFN/LNL)
 For years the main attention of experimentalists has been devoted to the optimization of the cavity internal surface layer. Instead even at superfluid temperatures, at the interface between Helium and the superfluid, it will be always a nanometric thick layer of normal helium and the thickness of this layer depends on the RF power. We have already shown that the status of the external surface of a cavity affects Kapitza Resistance and as a consequence both the Q-factor and the maximum accelerating field. In this talk starting from the well known evidence that Niobium and Copper are not miscible in any region of the phase diagram, we will show that in Niobium Sputtered Copper cavities, the thermal boundary Resistance at the interface can achieve values much bigger than predicted in the past, unless a buffer layer is added between Copper and niobium.

- TUBA03**
11:20  **On the Understanding of Q Slopes of Thin Films**
S. Aull, T. Junginger (CERN) J. Knobloch (HZB) J. Knobloch (University of Siegen) A-M. Valente-Feliciano (JLab)
The Q-Slope of niobium coated copper cavities at medium fields is still the limiting factor for application of the Nb/Cu technology in accelerators. A dedicated study has been carried out comparing the SRF performance of a bulk Nb and a Nb film sample. Both samples have the same grain size, RRR, penetration depth and critical field but show significant differences in terms of RF field dependence, trapped flux and thermal effects. From this study conclusions about the origin of the Q-Slope and the much lower sensitivity to trapped flux can be drawn.
- TUBA04**
11:40  **Nb3Sn Cavities: Material Characterization and Coating Process Optimization**
D.L. Hall, M. Liepe (Cornell University (CLASSE), Cornell Laboratory for Accelerator-Based Sciences and Education)
Recent progress on vapor diffusion coated Nb3Sn SRF cavities makes this material a very promising alternative for CW medium field SRF applications. In this talk we report on several systematic studies to determine the sources currently limiting the performance of Nb3Sn cavities to determine improved coating parameters to overcome these limitations. These include a detailed study of the sensitivity of Nb3Sn to trapped ambient magnetic flux, a first measurement of the field dependence of the energy gap in Nb3Sn and detailed measurements of the stoichiometry of the obtained Nb3Sn coatings with synchrotron x-ray diffraction and STEM. Studies on the impact of the coating process parameters on energy gap, mean free path, and residual resistance, show clear dependencies, and thus directions for process optimization.
- TUBA05**
12:00  **Progress With Multi-Cell Nb3Sn Cavity Development Linked With Sample Materials Characterization**
G.V. Eremeev, M.J. Kelley, C.E. Reece (JLab) M.J. Kelley, U. Pudasaini (The College of William and Mary) J. Tuggle (Virginia Polytechnic Institute and State University)
Exploiting both the new Nb3Sn coating system and the materials characterization tools, we report our progress in low-loss Nb3Sn films development. Nb3Sn films several micrometers thick were grown on Nb coupons as well as single- and multi-cell cavities by Sn-diffusion technique. Films structure and composition were investigated on coated samples and cavity cutouts with characterization tools including SEM/EDS/EBSD, AFM, XPS, SIMS towards correlating film growth and RF loss to material properties and deposition parameters. Cavity coating efforts focused on establishing techniques for coating progressively more complicated RF structures, and understanding limiting mechanisms in coated cavities. Nb3Sn coated 1.5 GHz 1-cell and 1.3 GHz 2-cell cavities have showed quality factors of 10^{10} at 4.3 K, with several cavities reaching above $E_{acc} = 10$ MV/m. The dominant limiting mechanisms were low field quenches and quality factor degradation above 8 MV/m. The surface data indicates a near-stoichiometric Nb3Sn consistent with the transition temperature and gap measurements. The Nb3Sn layer is covered with Nb2O5 and SnO2 native oxides and has little memory of the pre-coating surface.
- TUBA06**
12:15  **Increase in Vortex Penetration Field on Bulk Nb Coated With a MgB2 Thin Film Without an Insulation Layer**
T. Tan, M.A. Wolak, X. Xi (Temple University) L. Civale, T. Tajima (LANL)
Since SRF2013, there has been a remarkable progress in terms of sample measurement. Instead of measuring a flat film that allows magnetic field on both sides of the film, which does not simulate the situation on a SRF cavity correctly, an ellipsoidal bulk Nb (rugby-ball shape with ~8 mm long axis) was coated with a MgB2 film and its vortex penetration field has been measured with a SQUID magnetometer and compared with uncoated samples. After a number of measurements, vortex penetration field has been consistent with maximum critical RF field, superheating field. Here, we show that 100 nm and 200 nm thick MgB2 coating increases the vortex penetration field by up to ~70 mT, e.g., 240 mT (200 nm MgB2 coated Nb) vs. 170 mT (uncoated Nb) at 2.8 K (lowest measurement temperature) with the trend of increasing as temperature goes down. This is consistent with recent theoretical development saying that the increase is possible even without an insulation layer, which makes the coating easier. In this talk, the thickness dependence of the rise and comparison with theory will be shown.
- TUBA07**
12:30  **Theory of Multilayer Coating for Proof-of-Concept Experiments**
T. Kubo (KEK)
Structures of alternating layers of superconducting (SC) and insulating layers formed on a bulk SC are actively discussed these years, because of their great possibility in realizing a high-field and high-Q SCRF cavity. In 2013, theoretical studies of an ideal system with a single SC layer and a single insulator layer formed on a bulk SC were carried out, by which appropriate combinations of materials and optimum thicknesses of SC and insulator layers that can enhance field limit were revealed. A more realistic model with nano-scale surface defects on the SC layer was also studied in 2014. As of this year, a sample-experiment-oriented theoretical study is in progress towards proof-of-concept experiments. Theories are becoming realistic every year. In this talk, I will review progresses after 2013 and provide theoretical equipages to tackle experiments of the multilayer coating(*).
- TUBA08**
12:45  **Growth and Characterization of Multi-Layer NbTiN Films**
A-M. Valente-Feliciano (JLab)
Significant theoretical interest has stimulated efforts to grow and characterize thin multi-layer superconductor/insulator/superconductor structures for their potential capability of supporting otherwise inaccessible surface magnetic fields in SRF cavities. The technological challenges include realization of high quality superconductors with sharp, clean, transition to high quality dielectric materials and back to superconductor, with careful thickness control of each layer. Choosing NbTiN as the first candidate material, we have developed the tools and techniques that produce such SIS film structures and have begun their characterization. Using DC magnetron sputtering and HiPIMS, NbTiN and AlN can be deposited with nominal superconducting and dielectric parameters. Hc1 enhancement is observed for NbTiN layers with a Tc of 16.9 K for a thickness less than 150 nm. The optimization of the thickness of each type of layer to reach optimum SRF performance is underway. This talk describes this work and the rf performance characteristics observed to date.

TUPB — Poster Session

- TUPB001 Progress on Superconducting RF Cavity Development With UK Industry**
A.E. Wheelhouse, R.K. Buckley, L.S. Cowie, P. Goudket, A.R. Goulden, P.A. McIntosh (STFC/DL/ASTeC) J.R. Everard, N. Shakespeare (Shakespeare Engineering)
 As part of a STFC Industrial Programme Support (IPS) Scheme grant, Daresbury Laboratory and Shakespeare Engineering Ltd have been developing the capability to fabricate, process, and test a 9-cell, 1.3 GHz superconducting RF cavity. The objective of the programme of work is to achieve an accelerating gradient of greater than 20 MV/m at an unloaded quality factor of 1.0×10^{10} or better. Processes such as the high pressure rinsing and the buffer chemical polishing are being developed at Daresbury Laboratory and the manufacturing of the cavity half cells and beampipes are being optimised by Shakespeare Engineering to enable this target to be achieved. These are discussed in this paper.
- TUPB002 Elimination of High Frequency Noise From the Beam in the Diamond Light Source Storage Ring**
C. Christou, A. Bogusz, P.J. Marten (DLS)
 High frequency beam motion has been identified as a source of noise in infrared beamlines in a number of synchrotron light sources. Diamond is a third generation synchrotron light source with storage ring current maintained by two superconducting CESR-B cavities powered by IOT-driven RF amplifiers. In our case, undesirable beam motion in the kilohertz range is predominantly driven by spectral content in the voltage across the IOTs arising from the switched mode nature of the high voltage power supply. Spectral noise on the amplifiers and beam has been identified and characterised and efforts to eliminate this noise are described. Care has been taken to maintain the overall stability of the RF at Diamond and tests have been carried out on an infrared beamline to investigate the degree to which beam noise impacts beamline operation in its different operating configurations.
- TUPB003 LCLS-II Cavity Procurement and Qualification Plan for LCLS-II**
F. Marhauser, E. Daly (JLab)
 The LCLS-II project aims to build 35 accelerating cryomodules, which are based on the European XFEL design but modified for operation in CW mode. Each cryomodule houses eight TESLA-style nine-cell superconducting radio-frequency cavities. The activities to assemble the first two prototype cryomodules are ongoing at FNAL and JLab. 264 cavities worth of cavities for the remaining 33 cryomodules will be procured from two industrial vendors in similar quantity considering the option to produce spares. The assembly of cavities into the production cryomodules will be distributed among FNAL (16 cryomodules) and JLab (17 cryomodules). In this paper the cavity procurement and qualification plan for the LCLS-II project is detailed.
- TUPB004 Vertical Test Facility at Fermilab**
O.S. Melnychuk, A. Grassellino, F.L. Lewis, D.F. Orris, J.P. Ozelis, R.V. Pilipenko, Y.M. Pischalnikov, A. Romanenko, D.A. Sergatskov, B. Squires (Fermilab)
 After a recent upgrade, the vertical test facility for SRF cavities at Fermilab features a low level RF system capable of testing 325MHz, 650MHz, 1.3GHz, and 3.9GHz cavities, helium liquefying plant, three test cryostats, and the interlock safety system. The cryostats can accommodate measurements of multiple cavities in a given cryogenic cycle in the range of temperatures from 4.2K to 1.4K. We present a description of the components of the vertical test facility. We also discuss cavity instrumentation that is used for diagnostics of cavity ambient conditions and quench characterization.
- TUPB005 Current Status of the HZB SRF Testing Infrastructure**
B.D.S. Hall (HZB)
 HZB currently has two ongoing SRF accelerator projects, BERLinPro and BESSY-VSR, in addition to SRF basic R&D. All of these programs require that the cavity preparation infrastructure at HZB be upgraded. This has included the construction of an ISO 5 cleanroom, a new high pressure rinsing system, as well as the installation of a vertical testing dewar and plans for the procurement of a larger vertical testing dewar, both of which will be equipped with second sound detection (OSTs). This paper will report on the current status of, and first results from, the high pressure rinsing and measurement of a single cell cavity with OSTs. In addition the first cold mass assembly in the cleanroom will be reviewed.
- TUPB006 The CLS SRF Cryogenic System Upgrade**
C.N. Regier (CLS)
 The Canadian Light Source currently makes use of a 500 MHz CESR-B type SRF cavity in its storage ring. While the performance of this cavity has generally been good, the reliability of the cryostat and cryogenic system has suffered a few setbacks over the 10 years of operation. The position of CLS as a user facility requires reliable beam to be consistently delivered. For this reason CLS is undertaking an upgrade project to improve system reliability and reduce downtime due to planned and unplanned maintenance. The upgrade is to include a redundant helium compressor, and new cryogenic infrastructure. In addition, the spare CESR-B cryomodule will be installed and operating in the storage ring. This talk reviews the problems with the current system to date, and discusses the proposals for the upgrade of the system.
- TUPB007 Progress in the Elliptical Cavities and Cryomodule Demonstrators for ESS**
F. Peauger, C. Arcambal, S. Berry, P. Bosland, E. Cenni, G. Devanz, X. Hanus, P. Hardy, F. Leseigneur, C. Madec, L. Maurice, O. Piquet, J. Plouin, B. Renard, D. Roudier (CEA/DSM/IRFU) C. Darve, N. Elias (ESS) G. Olivier (IPN)
 The European Spallation Source (ESS) is composed of a long pulse superconducting linac delivering a proton beam of 62.5 mA at 2 GeV. In the high energy section of the accelerator, two families of elliptical cavities with a geometrical beta of 0.67 and 0.86 operate at 704.42 MHz in 2 K superfluid helium bath to reach the challenging accelerating gradients of 16.7 and 19.9 MV/m respectively. The SRF cavities are grouped four by four in 6.6 meter long cryomodules, similar for both cavity types. The CEA Saclay in collaboration with the IPN Orsay and ESS is in charge of the design, manufacture and high power tests without beam of two Elliptical Cavities Cryomodule Technological Demonstrators (ECCTD) with medium and high beta cavities. We present the status of the design and fabrication of the cryomodule components housing four cavities, each being equipped with a 1.1 MW power coupler, a Saclay-V type cold tuning system and a cold magnetic shielding. The test results in a vertical cryostat of the two high-beta prototype cavities ordered in two different companies are also discussed.
- TUPB008 A New Cryogenic Control System for the Vertical Test Area at Jefferson Lab**
G.K. Davis, T. Goodman, C. Grenoble, P. Kushnick, T. Powers (JLab)
 The Vertical Test Area at Jefferson Lab, consisting of eight vertical dewars, recently received a major upgrade by replacing the original (1995) cryogenic control system. A new, state-of-the-art, distributed control system (DCS) based on Programmable Logic Controllers (PLCs) was installed and commissioned. The new system increases facility throughput, reliability and cryogenic efficiency, while improving safety. The system employs a touchscreen graphical user interface and a highly redundant architecture on an Ethernet backbone.

- TUPB009 Upgrades of the Jefferson Lab Cryomodule Test Facility for LCLS II**
M.A. Drury, R. Bachimanchi, E. Daly, G.K. Davis, C. Grenoble, C. Hovater, L.K. King, R.M. Nelson, D.J. Seidman (JLab)
 The Thomas Jefferson National Accelerator Facility is currently engaged, along with several other DOE national laboratories, in the Linac Coherent Light Source II project (LCLS II). The SRF Institute at Jefferson Lab will be building 18 cryomodules based on the TESLA / ILC / XFEL design. Each cryomodule will contain eight nine cell cavities with coaxial power couplers operating at 1.3 GHz. All of these cryomodules will be tested in the Cryomodule Test Facility (CMTF) at Jefferson Lab before shipment to the Stanford Linear Accelerator (SLAC). The CMTF is undergoing a major upgrade of its facilities in order to enable testing of these cryomodules. The upgrades will include new high power RF sources along with new low level RF controls, interlock and data acquisition electronics. This paper will give a detailed description of these upgrades.
- TUPB010 Plug Transfer System for GaAs Photocathodes**
P. Murcek, A. Arnold, J. Teichert, R. Xiang (HZDR) A. Burrill (HZB)
 The transport and exchange technology of Cs₂Te photocathode for the ELBE superconducting rf photoinjector (SRF gun) has been successfully developed and tested at HZDR. The next goal is to realize the transport of GaAs photocathode into SRF gun, which will need a new transfer system with XHV 10⁻¹¹ mbar. The key component of the system is the transfer chamber and the load-lock system that will be connected to the SRF-gun. In the carrier four small plugs will be transported, and one of them will be plug on the cathode-body and inserted into the cavity. The new transport chamber allows the transfer and exchange of plugs between HZDR, HZB and other cooperating institutes. In HZDR this transfer system will also provide a direct connection between the SRFGUN and the GaAs preparation chamber in the Elbe-accelerator hall.
- TUPB011 HPRF Waveguide Elements Study and Distributions in TRIUMF Electron Linac System**
Z.T. Ang (TRIUMF; Canada's National Laboratory for Particle and Nuclear Physics)
 TRIUMF e-lianc was commissioning last September for the first stage. High power rf systems were in operation stable. Two 300 kW klystrons and the key waveguide components were tested before feeding rf power to 1.3 GHz 9-cell superconducting cavities. The rf high power divider and 360 degree waveguide phase shifters are working well. The simulations on different waveguide structures for the power dividers, phase shifters have been investigated. The comparisons of the calculation results are given in the paper. The rf signal level tests of the components and waveguide distribution systems will also be present in this paper.
- TUPB012 LCLS-II High Power RF Systems Overview and Progress**
A.D. Yeremian, C. Adolphsen, J. Chan, G. DeContreras, K. Fant, C.D. Nantista (SLAC)
 A second X-ray free electron laser facility, LCLS-II, will be constructed at SLAC. LCLS-II is based on a 1.3 GHz, 4 GeV, continuous-wave (CW) superconducting linear accelerator, to be installed in the first kilometer of the SLAC tunnel. Multiple types of high power RF (HPRF) sources will be used to power different systems on LCLS II. The main 1.3 GHz linac will be powered by 280 1.3 GHz, 3.8 kW solid state amplifier (SSA) sources. The normal conducting buncher in the injector will use four more such SSAs. Two 185.7 MHz, 60 kW sources will power the photocathode dual-feed RF gun. A third harmonic linac section, included for linearizing the bunch energy spread before the first bunch compressor, will require sixteen 3.9 GHz sources at about 1 kW CW. A diagnostic line at 94 MeV, for tuning and characterizing the beam prior to acceleration through the rest of the linac, will contain an S-band transverse deflection cavity (TCAV) to time-resolve the energy spread of the beam. A 2.856 GHz model 5045 pulsed klystron already existing at SLAC will be used to power the TCAV. A description and an update on all the HPRF sources of LCLS-II and their implementation is the subject of this paper
- TUPB013 Fermilab Cryomodule Test Stand Design and Plans**
E.R. Harms, C.M. Baffes, K. Carlson, B.E. Chase, A.L. Klebaner, M.J. Kucera, J.R. Leibfritz, M.W. McGee, P.S. Prieto, J. Reid, R.P. Stanek, D. Sun (Fermilab)
 A facility dedicated to SRF cryomodule testing is under construction at Fermilab. The test stand has been designed to be flexible enough to cool down and power test full length TESLA-style 8-cavity cryomodules as well cryomodules for low-β acceleration. We describe the design considerations, status, and near future plans for utilization of the test stand.
- TUPB014 First Operation of a Superconducting RF Electron Test Accelerator at Fermilab**
E.R. Harms, R. Andrews, C.M. Baffes, D.R. Broemmelsiek, K. Carlson, D.J. Crawford, N. Eddy, D.R. Edstrom, J.R. Leibfritz, A.H. Lumpkin, S. Nagaitsev, P. Piot, P.S. Prieto, J. Reid, V.D. Shiltsev, W.M. Soyars, D. Sun, R.M. Thurman-Keup, A. Valishev, A. Warner (Fermilab)
 A test accelerator utilizing SRF technology recently accelerated its first electrons to 20 MeV at Fermilab. Foreseen enhancements will make acceleration to 300 MeV possible at a maximum beam power of 80 kW. A summary of commissioning steps and first experiments as well as current beam parameters compared to design is presented. Plans for expansion and the future physics program are also summarized.
- TUPB015 A New Cleanroom With Facilities for Cleaning and Assembly of Superconducting Cavities at Helmholtz-Institut Mainz**
F. Schlander, K. Aulenbacher, R.G. Heine (IKP) K. Aulenbacher, W.A. Barth, V. Gettmann, S. Mickat, M. Miski-Oglu (HIM) W.A. Barth, S. Mickat (GSI)
 The Helmholtz-Institut Mainz HIM will operate a clean room facility for the assembly and possible re-treatment of superconducting cavities. This is mandatory for several SRF accelerator projects, like the advanced demonstrator for a dedicated sc heavy ion cw-linac at HIM or other projects pursued by research facilities or universities close by. While the installation of the clean room is in progress, the procurement of the appliances is ongoing. The present equipment planned and the current status of the installation will be presented.
- TUPB016 Progress on Superconducting Linac for the RAON Heavy Ion Accelerator**
H.J. Kim (IBS)
 The RISP (Rare Isotope Science Project) has been proposed as a multi-purpose accelerator facility for providing beams of exotic rare isotopes of various energies. It can deliver ions from proton to uranium. Proton and uranium ions are accelerated upto 600 MeV and 200 MeV/u respectively. The facility consists of three superconducting linacs of which superconducting cavities are independently phased. Requirement of the linac design is especially high for acceleration of multiple charge beams. In this paper, we present the RISP linac design, the prototyping of superconducting cavity and cryomodule.
- TUPB017 1.3 GHz SRF Technology R&D Progress of IHEP**
J.Y. Zhai, J.P. Dai, X.W. Dai, J. Gao, R. Ge, T.M. Huang, X. Huang, S. Jin, S.P. Li, H.Y. Lin, B. Liu, Z.C. Liu, Q. Ma, Z.H. Mi, W.M. Pan, X.H. Peng, L.R. Sun, Y. Sun, Z. Xue, S.W. Zhang, Z. Zhang, H. Zhao, T.X. Zhao, H.J. Zheng (IHEP)
 IHEP started the 1.3GHz SRF technology R&D in 2006 and recently enters the stage of integration and industrialization. After successfully making several single cell and 9-cell cavities of different shape and material, we designed and assembled a short cryomodule containing one large grain low loss shape 9-cell cavity with an input coupler and a tuner etc. This module will perform horizontal test in 2016 with the newly commissioned 1.3GHz 5MW klystron and the 2K cryogenic system. Beam test with a DC photocathode gun is also foreseen in the near future. We report here the problems, key findings and improvements in cavity dressing, clean room assembly, cryomodule assembly and the liquid nitrogen cool down test. A fine grain TESLA 9-cell cavity is also under fabrication in a company as the industrialization study.

TUPB018 **Preparation of the 3.9 GHz System for the European XFEL Injector Commissioning**

P. Pierini, M. Bertucci, A. Bosotti, J.F. Chen, P. Michelato, L. Monaco, M. Moretti, R. Paparella, D. Sertore (INFN/LASA) C. Albrecht, N. Baboi, S. Barbanotti, R. Bospflug, J. Branlard, Th. Buettner, Ł. Butkowski, T. Delfs, H. Hintz, F. Hoffmann, M. Hüning, K. Jensch, R. Jonas, R. Klos, D. Kostin, L. Lilje, C.G. Maiano, W. Maschmann, A. Matheisen, U. Mavrič, W.-D. Möller, C. Müller, P. Pierini, J. Prenting, J. Rothenburg, O. Sawlanski, M. Schlösser, M. Schmökel, A.A. Sulimov, E. Vogel (DESY) E.R. Harms (Fermilab) C.R. Montiel (ANL) C. Pagani (Università degli Studi di Milano & INFN)

The 3.9 GHz cryomodule and RF system for the XFEL Injector is being assembled and delivered to the underground building in summer 2015, for the injector commissioning in Fall 2015. This contribution outlines the status of the activity and reports the preparation stages of the technical commissioning of the system.

TUPB019 **Fermilab PIP-II Cavity and Cryomodule R&D Status**

C.S. Mishra, P. Derwent, S.D. Holmes, V.A. Lebedev, D.V. Mitchell, V.P. Yakovlev (Fermilab)

Proton Improvement Plan-II (PIP-II) is the centerpiece of Fermilab's plan for upgrading the accelerator complex to establish the leading facility in the world for particle physics research based on intense proton beams. PIP-II has been developed to provide 1.2 MW of proton beam power at the start of operations of the Long Baseline Neutrino Experiment (LBNE), while simultaneously providing a platform for eventual extension of LBNE beam power to >2 MW and enabling future initiatives in rare processes research based on high duty factor/higher beam power operations. PIP-II is based on the construction of a new, 800 MeV, superconducting linac, augmented by improvements to the existing Booster, Recycler, and Main Injector complex. PIP-II is currently in the development stage with an R&D program underway targeting the front end and superconducting rf acceleration technologies. This paper will describe the status of the SRF Cavity and Cryomodule and associated technology R&D programs.

TUPB020 **Recent Status New Superconducting CW Heavy Ion LINAC@GSI**

V. Gettmann, W.A. Barth, S. Mickat, S. Yaramyshev (GSI) M. Amberg, F.D. Dziuba, H. Podlech, U. Ratzinger (IAP) M. Amberg, W.A. Barth, S. Mickat (HIM) K. Aulenbacher (IKP)

The demonstrator is a prototype of the first section of the proposed cw-LINAC@GSI, comprising a superconducting CH-cavity embedded by two superconducting solenoids. The sc CH-structure is the key component and offers a variety of research and development. The beam focusing solenoids provide maximum fields of 9.3 T at an overall length of 380 mm and a free beam aperture of 30 mm. The magnetic induction of the fringe is minimized to 50 mT at the inner NbTi-surface of the neighboring cavity. The fabrication of the key components is still in progress and is near to completion. After cold performance testing of the RF cavity, the helium jacket will be welded on. The cryostat is partly assembled and will be finished in the next weeks. The test environment is completely prepared. Advanced emittance measurement is foreseen to prepare for best matching of the heavy ion beam from the injector. Integration of the cryostat into the beam line, the first cool down of the module and commissioning of the RF elements will be performed as next steps towards a complete testing of the demonstrator.

TUPB021 **Measurement of the Cavity Performances of Compact ERL Main Linac Cryomodule During Beam Operation**

H. Sakai, M. Egi, K. Enami, T. Furuya, S. Michizono, T. Miura, F. Qiu, K. Shinoe, K. Umemori (KEK) M. Sawamura (JAEA)

We developed ERL main linac cryomodule for Compact ERL (cERL) in KEK. The module consists of two 9-cell 1.3 GHz superconducting cavities, two 20 kW high power coupler, two mechanical tuner and three HOM dampers. After construction of cERL recirculation loop, beam operation was started in 2013 Dec. First electron beam of 20 MeV successfully passed the main linac cavities. After adjusting beam optics, energy recovery operation was achieved. Main linac cavity was enough stable for ERL beam operation with digital LLRF system and energy recovery was successfully done with CW 80 uA beam. However, field emission was a problem for long term operation. In this paper, we express the measurement of the cavity performances of long term beam operation.

TUPB022 **Low-Beta SRF Cavity Processing and Testing Facility for the Facility for Rare Isotope Beams at Michigan State University**

L. Popielarski (NSCL) B.W. Barker, C. Compton, I.M. Malloch, E.S. Metzgar, J. Popielarski, K. Saito, G.J. Velianoff, D.R. Victory, T. Xu (FRIB)

Major work centers of the new SRF Highbay are fully installed and in use for FRIB pre-production SRF quarter-wave and half-wave resonators, including inspection area, high temperature vacuum furnace for cavity degassing, chemical etching facility and processing and assembly cleanrooms. Pre-production activities focus on optimizing workflow by reducing process time, tracking part status and related data, and identifying bottlenecks. Topics discussed may include; buffered chemical polish (BCP) etching for cavity frequency control, degassing time reduction, automated high pressure rinse, particle control against field emission, pre-production cavity test results and implementation of workflow status programs

TUPB024 **Tuning the Linac With Superconducting Resonator Used as a Phase Detector**

N.R. Lobanov, P. Linardakis, D. Tsifakis (Research School of Physics and Engineering, Australian National University)

The ANU Heavy Ion Facility is comprised of a 15 MV electrostatic accelerator and superconducting linac booster. The beam is double terminal stripped to provide high charge states at the entrance to the linac, which consists of twelve $\beta=0.1$ Split Loop Resonators (SLR). Each SLR needs to be individually tuned in phase and amplitude for optimum acceleration efficiency. The amplitude and phase of the superbuncher and time energy lens also have to be correctly set. The linac set up procedure developed at ANU utilises a beam profile monitor in the middle of a 180 degree achromat and a new technique based on a superconducting resonator operating in a beam bunch detection mode. Both techniques are used to derive a full set of phase distributions for quick and efficient setting up of the entire linac. Verification of the superconducting phase detector is accomplished during routine linac operations and is complemented by longitudinal phase space simulations. The new technique allows better resolution for setting the resonator acceleration phase and better sensitivity to accelerating current.

TUPB025 **Tuning Superconducting Linac at Low Beam Intensities**

N.R. Lobanov, P. Linardakis, D. Tsifakis (Research School of Physics and Engineering, Australian National University)

The ANU Heavy Ion Facility comprises a 15 MV electrostatic accelerator followed by a superconducting linac booster. The beam is foil stripped in the terminal and then stripped again to provide high charge states at the entrance to the linac. Employment of double terminal stripping allows the system to accelerate beams with mass up to 70 amu. The disadvantage of double terminal stripping is low beam intensity of few particle nA delivered to the linac. The linac encompasses twelve $\beta=0.1$ lead tin plated Split Loop Resonators (SLR) housed in four module cryostats. One of the linac set up procedures that developed at ANU utilises U-bend at the end of the linac. One special wide Beam Profile Monitor (BPM) is installed after 90 degrees magnet. The technique allows to set correct phase by observing the displacement of beam profile versus phase shift of the last phase locked resonator. In this paper a simple method has been proposed to improve sensitivity of commercially available BPM for efficient operation with low beam intensities. The system demonstrated very high stability, simplicity of operation and high reliability allowing sustained operation of the LINAC facility.

TUPB026 Cryogenic Performance of the HNOSS Test Facility at the FREIA Laboratory

R. Santiago Kern, K.J. Gajewski, L. Hermansson, R.J.M.Y. Ruber (Uppsala University) P. Bujard, T. Junquera, J.P. Thermeau (Accelerators and Cryogenic Systems)

The FREIA laboratory at Uppsala University is developing part of the RF system and double spoke cavities for ESS. During 2014 it was equipped with HNOSS, a versatile horizontal cryostat system designed for high power RF test of two fully equipped superconducting cavities. In particular, it will be used to characterise the performance of spoke cavities like used in the ESS accelerator. HNOSS is connected to a cryogenic plant providing liquid helium and a sub-atmospheric pumping system enabling operation in the range from 1.8 to 4.5 K. This paper presents a brief description of the major cryogenic components, the cryostat installation, the first cryogenic tests and recent operation with SC cavities. Presently, all the interfaces with the cryogenic infrastructure are operational. HNOSS, with its ancillary components, is integrated into the laboratory control system (EPICS) and all the operation sequences and related supervision procedures are running. First cryogenic operation results, at 4K and 2K, will be presented, as well as the main performances: static losses, cool down and heat up times, pressure and level stability. The test of a complete ESS spoke cavity is under preparation.

TUPB027 Developments on SRF Coatings at CERN

A. Sublet, B. Bártoová, S. Calatroni, T. Richard, G.J. Rosaz, M. Taborelli (CERN)

The thin films techniques applied to Superconducting RF (SRF) has a long history at CERN. A large panel of cavities have been coated from LEP, to LHC. For the current and future projects (HIE-ISOLDE, HL-LHC, FCC) there is a need for further higher RF-performances with focus on minimizing residual resistance R_{res} and maximizing quality factor Q_0 of the cavities. This paper will present CERN's developments on thin films to achieve these goals through the following main axes of research: The first one concerns the application of different coating techniques for Nb (DC-bias diode sputtering, magnetron sputtering and HiPIMS). Another approach is the investigation of alternative materials like Nb₃Sn. These lines of development will be supported by a material science approach to characterize and evaluate the layer properties by means of FIB-SEM, TEM, XPS, XRD, etc. In addition a numerical tool for plasma simulation will be exploited to develop adapted coating systems and optimize the coating process, from plasma generation to thin film growth.

TUPB028 Development of Nb/Al Films Grown by Energetic Condensation

A-M. Valente-Feliciano, C.E. Reece, J.K. Spradlin (JLab)

Avenues for the production of thin films tailored for Superconducting RF (SRF) applications are showing promise with recent developments in vacuum deposition techniques using energetic ions, such as Electron Cyclotron Resonance (ECR) plasma. High quality Nb films are now reliably produced on copper (Cu) substrates. Beyond Cu, another well-suited substrate candidate for Nb film is Aluminum (Al) due to its high thermal conductivity and ease of formability or casting, alluring to the potential of dramatic cost reduction afforded by cavity/cryostat integration and low cost fabrication methods. The controlled incoming ion energy available with ECR plasma enables processes such as enhanced mobility of surface atoms and sub-implantation of impinging ions which lead to improved film structures at lower process temperatures. This paper presents results on surface and material characterization for Nb films produced on Al substrates as a function of the ion energy and thermal energy provided to the substrate.

TUPB029 SRF Performance and Material Quality of Nb Films Grown on Cu via ECR Plasma Energetic Condensation

A-M. Valente-Feliciano, G.V. Eremeev, C.E. Reece, J.K. Spradlin (JLab) S. Aull (CERN) Th. Proslie (ANL)

The RF performance of bulk Nb cavities has continuously improved over the years and is approaching the intrinsic limit of the material. Although some margin seems still available with processes such as N₂ surface doping, long term solutions for SRF surfaces efficiency enhancement need to be pursued. Over the years, Nb/Cu technology, despite its shortcomings, has positioned itself as an alternative route for the future of superconducting structures used in accelerators. Significant progress has been made in recent years in the development of energetic deposition techniques such as Electron Cyclotron Resonance (ECR) plasma deposition. Nb films with very high material quality have then been produced by varying the deposition energy alluding to the promise of performing SRF films. This paper presents RF measurements, correlated with surface and material properties, for Nb films showing how, by varying the film growth conditions, the Nb film quality and surface resistance can be altered and how the Q-slope can be eventually overcome.

TUPB030 Recent Results from the Cornell Sample Host Cavity

J.T. Maniscalco, B. Clasby, T. Gruber, D.L. Hall, M. Liepe (Cornell University (CLASSE), Cornell Laboratory for Accelerator-Based Sciences and Education)

Many novel materials are under investigation for the future of superconducting radio-frequency accelerators (SRF). In particular, thin-film materials such as Nb₃Sn, niobium-coated copper, and niobium multilayers may offer improvements in cost efficiency and RF performance over the standard niobium cavities. To avoid the difficulties of depositing thin films on full cavities, Cornell has developed a TE-mode sample host cavity which allows for RF measurements of large, flat samples at fields up to 100 mT. We present recent measurements and performance results from the cavity, using samples of Nb₃Sn and plain niobium. We also discuss plans for future collaborations.

TUPB031 Deposition of Superconducting Nb Thin Films by Re-crystallization

J. Musson, K. Macha, H.L. Phillips (JLab) H. Elsayed-Ali (Old Dominion University)

Superconducting niobium thin films provide an attractive solution to accelerator cavity production and cryomodule integration, but so far have been deficient in their radio-frequency performance. Physical vapor deposition techniques (ie. sputtering) have been largely favored, but have nearly always resulted in excessive Q-slope. A new deposition method is proposed to produce bulk-structured Nb film, utilizing cold Cu/Al substrates to restrict grain growth. A dense amorphous film is created using modulated pulse-power magnetron sputtering (MPPMS), with thickness well beyond the normal grain competition region. Laser-induced re-crystallization of the film surface results in a large-grain bulk-like crystalline structure, exhibiting random orientation over several penetration depths. Controlled heating for surface re-crystallization is provided by a pulsed, raster-scanned UV HIPPO laser. Also, since surface processing is performed in the vacuum chamber, substrate pre-conditioning is available, as well as opportunities to dope the film during deposition and growth. Results of the new process are presented, including physical film analysis (XRD, SEM, EBSD, AFM) and SC performance (RRR).

TUPB032 Energetic Condensation Growth of Nb on Cu SRF Cavities

K.M. Velas, S. Chapman, I. Irfan, M. Krishnan (AASC)

Alameda Applied Sciences Corporation (AASC) grows Nb thin films via Coaxial Energetic Condensation (CED) from a cathodic arc plasma. The plasma from the cathode consists exclusively of 60-120eV Nb ions (Nb⁺ and Nb²⁺) that penetrate a few monolayers into the substrate and enable sufficient surface mobility to ensure that the lowest energy state (crystalline structure with minimal defects) is accessible to the film. Hetero-epitaxial films of Nb were grown on biased and unbiased copper substrates heated to various temperatures to optimize the coating parameters. AASC is coating 1.3 GHz SRF cavities using a graded anode to ensure uniform film thickness in the beam tube and elliptical regions. Copper cavities are centrifugal barrel polished and electropolished* before coating, to ensure good adhesion and improved film quality. The Nb coated copper cavities will undergo RF tests at JLab and at Fermilab to measure Q_0 vs. E.

TUPB033 Commissioning of the New JLAB Cavity Deposition System for Energetic Condensation of Niobium Films

H.L. Phillips, K. Macha, J. Musson, C.E. Reece (JLab) M.C. Burton (The College of William and Mary)

The influence of energetic condensation of niobium ions on film structure has been studied extensively at Jefferson Lab on small samples, demonstrating the production of very high quality films using this method^{*,**}. A system has been designed and commissioned to deposit niobium films energetically to study RF performance on single cell cavities of copper and aluminum^{***}. The current status of the design and deposition capabilities of this system using the High Peak Power Magnetron Sputtering (HIPPMs) process will be described.

TUPB034 Bulk Nb Polishing and EP Steps for Thinfilm Coated Cu SRF Cavities

M. Krishnan, S. Chapman, I. Irfan, K.M. Velas (AASC) C.E. Reece, J.K. Spradlin, H. Tian (JLab)

Alameda Applied Sciences Corporation (AASC) grows Nb thin films via Coaxial Energetic Condensation (CED) from a cathodic arc plasma. The plasma consists of 60-120eV Nb ions (Nb⁺ and Nb⁺⁺) that penetrate a few monolayers into the substrate and enable sufficient surface mobility to ensure that the lowest energy state (crystalline structure with minimal defects) is accessible to the film. A limitation of CED thinfilms is the presence of Nb macroparticles (~0.1-10 microns) that could be deleterious to high field performance of the SRF cavity. One way to remove such macroparticles^{*} is to grow a thick film (~3-5 microns), followed by mechanical polishing (using the finest media as might be applied in Centrifugal Barrel Polishing) to achieve a 0.4 micron surface figure, and an EP step to remove ~2 microns of Nb that also removes all traces of embedded media in the film. The residual 1-3 micron Nb film should more nearly resemble the surface of a bulk Nb cavity that has been subjected to the same steps. This paper describes experiments conducted on Cu coupons as a prelude to SRF Cu cavity coating.

TUPB035 Development of Superconducting Photocathodes Using the Proximity Effect

M. Warren, J. Zasadzinski (IIT) Th. Proslir (ANL) L.K. Spentzouris, Z.M. Yusof (Illinois Institute of Technology)

A novel approach to superconducting photocathodes for SRF photoinjectors is presented. The concept utilizes a hybrid, (Niobium/M) bilayer structure where M is a relatively high quantum efficiency material such as Cs₂Te or Mg. The idea is that if M is thin enough it may be induced into the superconducting state via the proximity effect creating a superconducting photocathode suitable for SRF injectors. Initial results show that ultra thin layers (15 Å) of Cs₂Te deposited onto high purity Nb disks which exhibit quantum efficiencies of 6%. Such thin layers of semiconducting Cs₂Te may be expected to produce low RF losses. Results of QE vs thickness of thin Mg layers will also be presented. Tests of induced superconductivity in the Mg layer will be done using planar junction tunneling spectroscopy.

TUPB036 Pulsed Energetic Condensation of Nb Thin Films on Cu Cavities

M.C. Burton, R.A. Lukaszew (The College of William and Mary) H.L. Phillips, C.E. Reece (JLab)

Bulk Nb SRF cavities are currently the preferred method for acceleration of charged particles at accelerator facilities around the world. However, bulk Nb cavities can be costly, have poor thermal conductance and impose material and design restrictions on other components of a particle accelerator. A proposed solution to this problem has been to take advantage of the shallow depth of the SRF phenomena by creating cavities of a suitable metal (Cu or Al) and coating the interior with a Nb film. While this approach has been attempted in the past using DC magnetron sputtering (DCMS), cavity performance has never met the bulk Nb level. However, new energetic condensation techniques offer the opportunity to create suitably thick Nb films with improved density and microstructure when compared to traditional DCMS. One such technique recently developed is High Power Impulse Magnetron Sputtering (HiPIMS). Here we present results from initial studies for coating Cu cavities with Nb at Jefferson Lab using HiPIMS and calibration sample results. Also, due to unique capabilities of the Jefferson Lab deposition system, we will show RF results from a Nb/Cu cavity before and after exposure to air.

TUPB037 NbTiN and NbN Thin Films for the Enhancement of SRF Cavities

M.C. Burton, M. Beebe, K. Kaida, R.A. Lukaszew, J.M. Riso (The College of William and Mary) G.V. Ereemeev, A.M. Valente-Feliciano (JLab)

Current superconducting radio frequency (SRF) technology, used in various particle accelerator facilities is reliant upon bulk Nb. Due to technological advancements in the processing of bulk Nb cavities, the facilities have reached accelerating fields very close to material-dependent limits, i.e. ~50 MV/m for bulk Nb. One possible solution to overcome this limit proposed by A. Gurevich consists of the deposition of alternating thin layers of superconducting and insulating materials on the interior surface of the cavities which may prevent early field penetration and thus delay high field breakdown^{*}. Some candidate materials proposed for this scheme are NbN and NbTiN. Here we present experimental results correlating film microstructure and surface morphology with superconducting properties on coupon samples made with NbN and NbTiN. We have achieved thin films with close to bulk-like lattice parameters and transition temperatures, while achieving Hc1 values larger than bulk for films thinner than their London penetration depths. We compare results from samples grown utilizing NbTi targets with different stoichiometries and we will show RF measurements from 2" coupon samples.

TUPB038 CVD/PECVD Superconducting Coatings for SRF Cavities

P. Pizzol (The University of Liverpool) O.B. Malyshev, R. Valizadeh (STFC/DL/ASTeC)

One of the important characteristic in the developing of thin film superconducting cavities is a uniformity of the film thickness. The coating of superconducting cavities currently is synthesised by PVD method which suffers from lack of conformity. By using chemical vapour deposition (CVD), where precursors are introduced into the reaction chamber, it is possible to deposit thin Nb layers uniformly and density very close to bulk material. Using plasma in the reaction (PECVD) it is possible to lower the deposition temperature. This project explores the use of CVD /PECVD techniques to deposit metallic niobium or niobium nitride on copper or bulk niobium with insulation layer. These chemically driven techniques allow a great control over the deposition thickness and growth rate of the desired materials, leading to single or multilayered coatings of known chemical composition and properties. The obtained samples were then characterized via SEM, TEM, XRD, XPS, EDX and other morphological investigation techniques, as well as probing their cryogenic superconductivity capabilities and performances using AC and DC susceptometry and pill box cavity.

TUPB039 Superconducting Niobium Thin Film Synthesised by Ionized Jet Deposition for SRF Cavities

R. Valizadeh, A.N. Hannah, O.B. Malyshev, S. Wilde (STFC/DL/ASTeC) B. Chesca, S. Wilde (Loughborough University) G.B.G. Stenning (STFC/RAL/ISIS)

Niobium thin film deposited on copper cavity has the potential to replace bulk niobium superconducting cavity in particle accelerators. Bulk niobium has a typical heat conductance of about 75 W/m.K at best, while for copper is as high as 300-2000 W/m.K and the cost of copper is a fraction of that of niobium. In this paper we report on synthesising superconducting niobium film deposited on copper substrate with Ionized Jet Deposition (IJD) where a short but very intense discharge is generated by intense electron beam and supported by a gas jet towards the target. The IJD offers a high ion/atom arrival ratio with ion energy ranging from 10 to 100 eV. The films are characterised using scanning and transmission electron microscopy (SEM & TEM), x-ray diffraction and DC SQUID magnetometry. The results showed that the film grain size ranges between 100 to 400 nm with a RRR of 100 and Hc1 of 0.18 T.

- TUPB040 High Power Impulse Magnetron Sputtering of Thin Films for Superconducting RF Cavities**
S. Wilde, B. Chesca (Loughborough University) A.N. Hannah, O.B. Malyshev, S.M. Pattalwar, R. Valizadeh (STFC/DL/ASTeC) G.B.G. Stenning (STFC/RAL/ISIS)
 The production of superconducting coatings for radio frequency cavities is a rapidly developing field that should ultimately lead to acceleration gradients greater than those obtained by bulk Nb RF cavities. Optimizing superconducting properties of Nb and Nb compound thin-films is therefore essential. Nb films were deposited by magnetron sputtering in pulsed DC mode onto Si (100) and MgO (100) substrates and also by high impulse magnetron sputtering (HiPIMS) onto Si (100), MgO (100) and polycrystalline Cu. HiPIMS was then used to deposit NbN and NbTiN thin films onto Si(100) and polycrystalline Cu. The films were characterised using scanning electron microscopy, x-ray diffraction, DC SQUID magnetometry and Q factor for a flat thin film sample.
- TUPB041 Testing Nb₃Sn Coating Using muSR**
R.E. Laxdal, T.J. Buck (TRIUMF, Canada's National Laboratory for Particle and Nuclear Physics) S. Gheidi (UBC) R. Kiefl (UBC & TRIUMF) S. Posen (Fermilab)
 Cornell has reported successful coating of a Niobium 1.3GHz single cell cavity with Nb₃Sn. In this study collaborators at Cornell coat a Nb coin and a Nb ellipsoid sample with Nb₃Sn for characterization using muSR at TRIUMF. Field of first flux entry measurements are performed at M20 on both samples. Interestingly the Nb₃Sn increases the field of first flux entry at 2k over standard Nb samples.
- TUPB042 Low Energy Muon Spin Rotation and Point Contact Tunneling Applied to Niobium Films for SRF Cavities**
T. Junginger (TRIUMF, Canada's National Laboratory for Particle and Nuclear Physics) S. Calatroni (CERN) T. Prokscha, Z. Salmer, A. Suter (PSI) Th. Proslir (ANL) J. Zasadzinski (IIT)
 Muon spin rotation (muSR) and point contact tunneling (PCT) are used since several years for bulk niobium studies. Here we present studies on niobium thin film samples of different deposition techniques (diode, magnetron and HIPIMS) and compare the results with RF measurements and bulk niobium results. It is consistently found from muSR and RF measurements that HIPIMS can be used to produce thin films of high RRR. Hints for magnetism are especially found on the HIPIMS samples. These could possibly contribute to the field dependent losses of superconducting cavities, which are strongly pronounced on niobium on copper cavities.
- TUPB043 Measurement System of Superconducting Characteristics on Thin-Film Samples at KEK**
T. Saeki, H. Hayano, T. Kubo (KEK) Y. Iwashita (Kyoto ICR)
 We are planning to facilitate a measurement system of superconducting characteristics on thin-film samples at KEK. The system can measure critical temperature, critical magnetic field, RRR, SRF resistivity with applying electromagnetic field on thin-film samples. The system includes a small-size cryostat with a compact refrigerator to cool down samples for the measurements of critical temperature and RRR, and a middle-size cryostat to cool down various setups by using liquid helium. The middle-size cryostat can be used in three ways. A thin-film sample is set into a mushroom cavity which is cooled down and the SRF characteristics of the thin-film sample can be measured. In another setup, a sample is set with a small coil and the third harmonic measurement is done on the sample around the critical temperature. Finally, a thin-film sample is set into the bore-center of superconducting magnet and the magnetization of sample is measured with external magnetic field around the critical temperature. This article presents the details of the system and some measurements of samples by the system.
- TUPB044 High Quality Factor Studies in SRF Nb₃Sn Cavities**
D.L. Hall, B. Clasby, H. Conklin, R.G. Eichhorn, T. Gruber, G.H. Hoffstaetter, J.J. Kaufman, M. Liepe (Cornell University (CLASSE), Cornell Laboratory for Accelerator-Based Sciences and Education)
 A significant advantage of Nb₃Sn coated on niobium over conventional bulk niobium is the substantial reduction in the BCS losses at equal temperatures of the former relative to the latter. The quality factor of a Nb₃Sn cavity is thus almost entirely dictated by the residual resistance at temperatures at and below 4.2 K, which, if minimised, offers the ability to operate the cavity in liquid helium at atmospheric pressure with quality factors exceeding $4 \cdot 10^{10}$. In this paper we present results of a systematic study on the sources of residual resistance in state-of-the-art Nb₃Sn cavities, as well as the parameters that affect their impact. In particular, we look at the impact of the coating procedure, cooldown procedure – which is intrinsically linked to the effect of spatial and temporal gradients – and the impact of external ambient magnetic fields.
- TUPB045 Surface Analysis and Material Property Studies of Nb₃Sn on Niobium for Use in SRF Cavities**
D.L. Hall, H. Conklin, T. Gruber, J.J. Kaufman, M. Liepe (Cornell University (CLASSE), Cornell Laboratory for Accelerator-Based Sciences and Education) Th. Proslir (ANL)
 Studies of superconducting Nb₃Sn cavities and samples at Cornell University and Argonne National Lab have shown that current state-of-the-art Nb₃Sn cavities are limited by material properties and imperfections. In particular, the presence of regions within the Nb₃Sn layer that are deficient in tin are suspected to be the cause of the lower than expected peak accelerating gradient. In this study we present results from a comprehensive material study of the Nb₃Sn layer fabricated using the vapour deposition method, with data collected using TEM, EDX, SEM and XRD methods. We conclude with preliminary results of a coating parameter study in which results of the previous material studies have been applied to improve the stoichiometry and uniformity of the Nb₃Sn layer.
- TUPB046 Structure and Composition of Nb₃Sn Diffusion Coated Films on Nb**
J. Tuggle, M.J. Kelley (Virginia Polytechnic Institute and State University) G.V. Ereemeev, M.J. Kelley, C.E. Reece (JLab) M.J. Kelley (The College of William and Mary)
 We have investigated the structure and composition of Nb₃Sn films obtained by diffusion coating of niobium coupons and SRF cavities with x-ray photoelectron spectroscopy (XPS), secondary ion mass spectroscopy (SIMS), and scanning electron microscopy (SEM) with energy-dispersive x-ray spectroscopy (EDS) and electron back-scatter diffraction (EBSD). We examined as-coated surfaces, profiles, and cross-sections, and found that the native surface oxide was made of SnO₂ and Nb₂O₅ and significantly tin-rich. We also found that the grains apparent in the SEM images were individual crystallites having no evident relationship to the substrate or each other.
- TUPB047 Next Generation of SRF-Guns: Low Secondary Electron Yield Based on a Thin Film Approach**
M. Vogel, X. Jiang, C. Schlemper (University Siegen)
 Multipacting is a common issue in the context of cathode units of superconducting radiofrequency photoinjectors (SRF-guns) utilized in linear accelerators under resonant conditions. In this study, Titanium Nitride (TiN) and Carbon thin films have been prepared by DC and RF magnetron sputtering in a Nitrogen and Argon plasma discharge, respectively. Films featuring a thickness of about 600 nm were produced under various deposition conditions on substrates such as Copper, Molybdenum, and Silicon. Materials characterization was carried out utilizing SEM, Raman and FTIR spectroscopy, XRD and AFM. In order to evaluate the SEY a new device is introduced, which is capable of quasi in-situ measurements. The latter is realized by connecting the coating-, the SEY- and a contamination chamber into one setup allowing sample transfer under UHV conditions. Even after an exposure to air carbon shows SEY values down to 0.69. This value, however, turns out to be quite sensitive with respect to the actual surface morphology. Clean TiN surfaces, on the other hand, displayed a SEY value as low as 1.4. In this case the SEY value is strongly affected by potential surface contamination.

TUPB048 **Fermilab Nb₃Sn Cavity R&D Program**

S. Posen, M. Merio, A. Romanenko (Fermilab)

A substantial program has been initiated at FNAL for R&D on Nb₃Sn coated cavities. Since early 2015, design, fabrication, and commissioning has been ongoing on a coating chamber, designed for deposition via vapor diffusion. The volume of the chamber will be large enough to accommodate not just R&D cavities, but full production-style cavities such as TeSLA 9-cells. In this contribution, we overview the development of the chamber and we introduce the R&D program planned for the coming years. We discuss research paths that may yield increased maximum fields and reduced residual resistances as well as new applications that could be explored with larger coated cavities.

TUPB049 **Cutout Study of a Nb₃Sn Cavity**

S. Posen, O.S. Melnychuk, A. Romanenko, D.A. Sergatskov, Y. Trenikhina (Fermilab) D.L. Hall, M. Liepe (Cornell University (CLASSE), Cornell Laboratory for Accelerator-Based Sciences and Education)

The first 1.3 GHz single cell Nb₃Sn cavity coated at Cornell and FNAL to have poor RF performance. Though future cavities showed much higher quality factors, this cavity exhibited Q_0 on the order of 10^9 caused by strong heating concentrated in one of the half cells. This paper presents an investigation into the source of this excess heating. Through the use of temperature mapping both at Cornell and at FNAL, locations with high and low surface resistance were located, cut out from the cavity, and studied with microscopic tools. We present the RF measurements and temperature maps as well as the microscopic analyses, then conclude with implications for avoiding similar high resistance areas in future Nb₃Sn coating procedures.

TUPB050 **Secondary Electron Yield of SRF Materials**

S. Aull, T. Junginger, H. Neupert (CERN) S. Aull, J. Knobloch (University of Siegen) J. Knobloch (HZB)

In the quest of new materials for SRF applications, the secondary electron yield (SEY) needs also to be taken into consideration. A high SEY holds the risk that multipacting becomes again a main performance limitation of an SRF cavity. In the worst case, a too high SEY makes a material completely unsuitable for an RF exposed surface. This contribution will discuss general aspects of the role of the surface condition and present SEY measurements on different SRF relevant materials, i.e. MgB₂, Nb₃Sn and NbTiN.

TUPB051 **Development of Nb₃Sn Coatings by Magnetron Sputtering for SRF Cavities**

G.J. Rosaz, S. Aull, S. Calatroni, F.M. Leaux, F. Motschmann, Z. Mydlarz, M. Taborelli, W. Vollenberg (CERN)

Cost and energy savings are an integral requirement in the design of future particle accelerators. Very low losses SRF accelerating systems, together with high-efficiency cryogenics systems, have the potential of low running costs. The association to the capital cost reduction allowed by thin films coated copper cavities may represent the best overall cost-performance compromise. This strategy has been applied for instance in LEP, the LHC and HIE-ISOLDE with the niobium thin films technology. New materials must be considered to improve the quality factor of the cavities, such as Nb₃Sn, which could also ideally operate at higher temperature thus allowing further energy savings. The study considers the possibility to coat a copper resonator with an Nb₃Sn layer by means of magnetron sputtering using an alloyed target. We present the impact of the process parameters on the as-deposited layer stoichiometry. The latter is in good agreement with previous results reported in the literature and can be tuned by acting on the coating pressure. The effect of post-coating annealing temperature on the morphology, crystallinity and superconducting properties of the film was also investigated.

TUPB052 **HTS Coatings for Impedance Reduction of Beam-Induced RF Image Currents in the FCC**

S. Calatroni (CERN)

The FCC-hh presently under study at CERN will make use of 16 T superconducting dipoles for achieving 100 TeV p-p center-of-mass collision energy in a 100 km ring collider. A copper coated beam screen, like in the LHC, has been envisaged to shield the 1.9 K dipole cold bores from the 28 W/m/beam of synchrotron radiation. Operating temperature should be in the 50 K range, as best compromise among several different requirements, with the final goal of reducing the wall-plug power consumption of the cryogenic system. However, preliminary studies indicate that copper at 50 K might not provide low enough beam coupling impedance in the FCC-hh. It has then been proposed to reduce the beam coupling impedance by adding a thin layer of a High-Temperature Superconductor (HTS), which will thus effectively shield the beam-induced RF image currents. Purpose of this paper is to study the validity of the approach and describe the basic requirements for an HTS film in the RF field induced by beam image currents and exposed to a high magnetic field, and to identify the best candidate materials and coating processes.

TUPB053 **Research on MgB₂ at LANL for the Application to SRF Structures**

T. Tajima (LANL)

Evaluations of MgB₂, a superconductor with a transition temperature of >35 K, have been conducted at LANL. A summary of our research in the last few years will be presented including our effort to optimize coating parameters and design the coating system suited for coating SRF cavities.

TUPB054 **Local Composition and Topography of Nb₃Sn Diffusion Coatings on Niobium**

U. Pudasaini, M.J. Kelley (The College of William and Mary) G.V. Eremeev, M.J. Kelley, C.E. Reece (JLab)

The potential for energy savings and for increased gradient continues to bring attention to Nb₃Sn-coated niobium as a future SRF cavity technology. We prepared these materials by vapor diffusion coating on polycrystalline and single crystal niobium. The effect of changing substrate preparation, coating parameters, and post-treatment was examined by AFM and SEM/EDS. The AFM data were analyzed in terms of power spectral density (PSD). We found little effect of pre-coating topography on the resulting surface roughness. The PSD curves from the coated samples show some surprising kinship to those obtained from BCP-treated surfaces. SEM/EDS revealed no compositional non-uniformities at the micron scale.

TUPB055 **Large Area Superconducting Magnesium Diboride Films on Copper Substrates for SRF Applications Using HPCVD**

W.K. Withanage, N. Lee, T. Tan, M.A. Wolak, X. Xi (Temple University) G.V. Eremeev, A-M. Valente-Feliciano (JLab) R. Kustom, A. Nassiri (ANL) P.B. Welander (SLAC)

Coating superconducting magnesium diboride on the inner walls of copper cavities is a viable alternative to the commonly used bulk Nb SRF cavities. This approach improves the thermal conductivity and can entirely eliminate helium refrigeration and distribution costs as well as reducing operational costs. For this research, we grew MgB₂ films via Hybrid Physical Chemical Vapor Deposition (HPCVD) on Cu substrates. Since Mg and Cu readily form an alloy at higher temperatures, a direct deposition of MgB₂ on Cu is challenging. Buffer layers between the MgB₂ film and the underlying copper substrate can offer a sufficient barrier and reduce the formation of Mg – Cu alloys. In our approach, we employed various buffer layers which were deposited ex-situ before the HPCVD MgB₂ growth. This method led to a successful coating of 2" copper disks with uniform MgB₂ films with transition temperatures of up to 37 K. Characterization experiments carried out on the coated copper disks as well as reference samples at microwave frequencies indicated enhanced superconducting properties. The presented results confirm that MgB₂ coated copper cavities can be a suitable alternative for SRF applications.

TUPB056 Characterization of Nb₃Sn Coated Nb Samples

Y. Trenikhina, S. Posen (Fermilab) D.L. Hall (Cornell University (CLASSE), Cornell Laboratory for Accelerator-Based Sciences and Education) M. Liepe (Cornell University)

Nb₃Sn has a great potential to replace traditional Nb for the fabrication of SRF cavities. The higher critical temperature of Nb₃Sn potentially allows for an increased operational temperature for SRF cavities, which promises cryogenic cost savings. We present preliminary characterization of Nb₃Sn layer grown on flat Nb sample prepared by the same chemical vapor deposition method that is used for the cavity coating. SEM, TEM/EDS, TEM imaging and diffraction characterization was used in order to evaluate any chemical and structural defects that could be responsible for the limited quench field and high residual resistance. Variation of local stoichiometry was found in the Nb₃Sn layer, which is in line with previous studies. Regions of decreased Sn content can have a lower T_c in comparison to the stoichiometric composition, which may be responsible for the limited performance. AES investigations of the Nb₃Sn surface before and after HF-rinse were done in order to explore the mechanism that is responsible for the performance degradation of HF-rinsed Nb₃Sn coated cavities.

TUPB057 Nanometric Multilayers Structural Characterization

C.Z. Antoine (CEA/DSM/IRFU) H. Hayano, S. Kato, T. Kubo, T. Saeki (KEK) M. Hofheinz, J.C. Villegier (CEA/INAC) Y. Iwashita (Kyoto ICR)

Nanometric multilayers deposited onto Nb could improve the efficiency of accelerating cavities as proposed in 2006 by A. Gurevich*. Recently two different approaches have been proposed for the optimization of the thickness of a trilayer SIS systems, taking into account more precisely boundary conditions, showing that thicknesses around 100 nm for the surface superconductor seem to provide the optimum compromise for field enhancement vs field screening^{*,**}. Therefore it would be interesting to evaluate how these predictions evolve with actual thin film samples. Therefore a series of NbN/MgO/Nb layers with NbN thicknesses ranging from 20 nm to 200 nm have been deposited by magnetron sputtering on an MgO (~10 nm)/Nb (250 nm) system, itself deposited onto a sapphire substrate. This paper describes characterization studies conducted on this sample series, mainly structure and composition. These vortex penetration field of these samples will also be measured and compared with the calculated values.

TUPB058 Multilayers Characterization

N. Katyan, C.Z. Antoine (CEA/DSM/IRFU) C.Z. Antoine, C. Marchand (CEA/IRFU) C. B. Baumier, G. Martinet (IPN) F. Fortuna (CSNSM) J.C. Villegier (CEA/INAC)

SIS nanocomposite (Superconductor/Insulator/Superconductor) could improve efficiency of accelerating cavities. The SRF multilayers concept focuses on the enhancement of HC1 using thin layers ($d \sim \lambda$). The use of thin layers makes it easier to avoid avalanche penetration of vortices in case of local defects. Several layers are needed in order to attenuate the external field to values below Nb HC1, decoupled using dielectric layers. We don't know yet how the predicted properties evolve in realistic conditions; hence it seems reasonable to do their optimization. Two parameters need to be measured to study their behavior in cavity operating conditions: HC1 and R_s surface resistance (especially residual). For that purpose two instruments were developed in Saclay and in Orsay. A local magnetometer allows measuring the vortex penetration on samples without the orientation and edge effects encountered in SQUID magnetometers. Its operating conditions range from 2-40 K, with field up to 150 mT, and upgradation to higher field. A pill-box cavity working on TE011 and TE012 modes with removable sample/top measures surface resistance up to 60 mT based on calorimetric method from 1.6-4.5 K.*

TUPB059 Magnetic Field Penetration Experiment on Multilayer S-I-S Structures

O.B. Malyshev, L. Gurran, N. Pattalwar, S.M. Pattalwar, R. Valizadeh (STFC/DL/ASTeC) A.V. Gurevich (Old Dominion University) L. Gurran (Lancaster University) L. Gurran (Cockcroft Institute, Lancaster University) S.M. Pattalwar, R. Valizadeh (Cockcroft Institute)

Superconducting RF cavities made of bulk Nb has reached a breakdown field of about 200 mT which is close to the superheating field for Nb. As it was theoretically shown* a multilayer coating can be used to enhance the breakdown field of SRF cavities. The simple example is a superconductor-insulator-superconductor (S-I-S), for example bulk niobium (S) coated with a thin film of insulator (I) followed by a thin layer of a superconductor (S) which could be a dirty niobium^{**}. To verify such an enhancement in a presence of a DC magnetic field at 4.2 K a simple experimental facility was designed, built and tested in ASTeC. The details of experimental setup and results of the measurements will be shown at the conference.

TUPB060 RF Properties of Multilayer Superconducting Samples Using Calorimetric Measurement Technique

S.I. Sosa Guitron, J.R. Delaysen, A.V. Gurevich (ODU) M.C. Burton, R.A. Lukaszew (The College of William and Mary) E. Chang Beom, C. Sundahl (University of Wisconsin-Madison) J.R. Delaysen, G.V. Ereemeev (JLab)

The Surface Impedance Characterization system at Jefferson Lab has been used extensively for investigating RF properties of superconducting material samples, particularly, measurements of surface resistance using a power compensation technique. SIC consists of a superconducting Nb cylindrical cavity operating in the TE011 mode at 7.38 GHz and a calorimeter for temperature dependent measurements. Recent tests of multilayer superconducting samples using SIC are presented and discussed in this contribution. Specifically, we have tested samples of Nb₃Sn/Nb with Nb₃Sn layer thicknesses of 50 nm and 100 nm, and multilayer structures NbN/MgO/Nb with 50 nm thick NbN layer. These samples were measured in the range 4K - 19K, where screening of Nb by the outer superconducting layer has been observed above the critical temperature of Nb for the Nb₃Sn/Nb sample.

TUPB061 Increase in Vortex Penetration Field on Bulk Nb Coated With a MgB₂ Thin Film Without an Insulation Layer

T. Tan, M.A. Wolak, X. Xi (Temple University) L. Civale, T. Tajima (LANL)

Since SRF2013, there has been a remarkable progress in terms of sample measurement. Instead of measuring a flat film that allows magnetic field on both sides of the film, which does not simulate the situation on a SRF cavity correctly, an ellipsoidal bulk Nb (rugby-ball shape with ~8 mm long axis) was coated with a MgB₂ film and its vortex penetration field has been measured with a SQUID magnetometer and compared with uncoated samples. After a number of measurements, vortex penetration field has been consistent with maximum critical RF field, superheating field. Here, we show that 100 nm and 200 nm thick MgB₂ coating increases the vortex penetration field by up to ~70 mT, e.g., 240 mT (200 nm MgB₂ coated Nb) vs. 170 mT (uncoated Nb) at 2.8 K (lowest measurement temperature) with the trend of increasing as temperature goes down. This is consistent with recent theoretical development saying that the increase is possible even without an insulation layer, which makes the coating easier. In this talk, the thickness dependence of the rise and comparison with theory will be shown.

TUPB062 Evaluation of Sc Property Coated on a Surface

Y. Iwashita, Y. Fuwa (Kyoto ICR) M. Hino (Kyoto University, Research Reactor Institute) T. Kubo, T. Saeki (KEK)

We are trying to deposit thin superconducting material on a substrate for higher accelerating field gradients. In order to evaluate the deposit method, surface properties are under measurement. Some results on measurements at DC and a preparation status toward RF measurement will be reported.

TUPB063 **A Multi-Sample Residual Resistivity Ratio System for High Quality Superconductor Measurements**

J.K. Spradlin, C.E. Reece, A-M. Valente-Feliciano (JLab)

For developing accelerator cavity materials, transition temperature (T_c), transition width (ΔT_c), and residual resistivity ratio (RRR), are useful parameters to correlate with SRF performance and fabrication processes of bulk, thin film, and novel materials. The transition from normal conduction to superconducting is characterized by T_c and ΔT_c . The RRR gauges the purity and structure of the superconductor based on the temperature dependence of electron scattering in the normal conducting state. This system combines a four point probe delta pulse setup with a switch to multiplex the electrical measurement of up to 32 samples per cool down cycle. The samples are measured inside of an isothermal setup in a LHe dewar. The isothermal setup is necessitated by a quasistatic warmup through T_c that is driven by the stratification of the He in the dewar. This contribution will detail the current setup for collecting RRR and T_c data, the current standard of throughput and measurement quality of the setup, and the improvements underway to increase the resolution and ease of use of the system.

TUPB064 **Superconducting Thin Film Test Cavity Commissioning**

P. Goudket, K.D. Dumbell, L. Gurrán, O.B. Malyshev, S.M. Pattalwar, R. Valizadeh, S. Wilde (STFC/DL/ASTeC) G. Burt, P. Goudket, O.B. Malyshev, R. Valizadeh (Cockcroft Institute) G. Burt, L. Gurrán (Cockcroft Institute, Lancaster University) G. Burt, L. Gurrán (Lancaster University) T.J. Jones, E.S. Jordan (STFC/DL) S. Wilde (Loughborough University)

An RF cavity and cryostat dedicated to the measurement of superconducting coatings at GHz frequencies was designed to evaluate surface resistive losses on a flat sample. The cavity consists of two parts: a cylindrical half-cell made of bulk niobium (Nb) and a flat Nb disc. The two parts can be thermally and electrically isolated via a vacuum gap, whereas the electromagnetic fields are constrained through the use of RF chokes. Both parts are conduction cooled hence the system is cryogen free during operation. The flat disc can be replaced with a sample, such as a Cu disc coated with a film of niobium or any other superconducting material. The RF test provides simple cavity Q-factor measurements as well as calorimetric measurements of the losses on the sample. The advantage of this method is the combination of a compact cavity with simple sample geometry. The paper describes the RF mechanical and cryogenic design, commissioning and first results of the system.

TUPB065 **Cryogenic RF Characterization of Superconducting Materials at SLAC with Hemispherical Cavities**

P.B. Welander, M.A. Franzi, S.G. Tantawi (SLAC)

For the characterization of SRF materials, we have commissioned a second-generation, X-band cavity cryostat that can rapidly analyze thin-film coatings or bulk samples. The system operates at 11.4 GHz, at temperatures down to 4 K, and utilizes two interchangeable hemispherical cavities (one Cu, one Nb) that can accommodate 51 mm-diameter samples on the flat side. The cavities are designed to operate with a TE₀₁₃-like mode where the magnetic field is strongest on the sample surface. As a result, the sample accounts for 33% of the overall cavity loss, despite comprising less than 8% of the total surface area. For low-power testing we utilize a programmable network analyzer, while for high-power testing we connect the cavity to a 50 MW XL-4 klystron. With the Nb cavity we can measure surface resistances down to 0.5 microhm, while with the Cu cavity we can measure quenching fields up to 360 mT. X-band operation permits a compact cavity and cryostat design with a reasonable sample size, while the closed-cycle pulse-tube cryorefrigerator allows for rapid sample cycling. We will discuss cryostat design, cavity modeling, measurement limits, and recent sample testing results.

TUPB066 **Commissioning Results of the HZB Quadrupole Resonator**

R. Kleindienst, A. Burrill, S. Keckert, J. Knobloch, O. Kugeler (HZB)

Recent cavity results with niobium have demonstrated the necessity of a good understanding of both the BCS and residual resistance. For a complete picture, and comparison with theory, it is essential that one can measure the RF properties as a function of applied magnetic field, temperature, frequency and ambient magnetic field. Standard cavity measurements are limited in their ability to change all parameters freely and in a controlled manner. On the other hand, most sample measurement setups operate at fairly high frequency, where the surface resistance is always BCS dominated. The quadrupole resonator, originally developed at CERN, is ideally suited for RF characterization of samples at frequencies of 400 and 1300 MHz, between which many of today's SRF cavities operate. We report on a modified version of the QPR with improved RF figures of merit for high-field operation. Experimental challenges in the commissioning run and alternate designs towards a simpler sample change are shown alongside measurement results of a large grain niobium sample.

TUPB067 **Design and First Measurements of an Alternative Calorimetry Chamber for the HZB Quadrupole Resonator**

S. Keckert, R. Kleindienst, J. Knobloch, O. Kugeler (HZB)

The systematic research on superconducting thin films requires dedicated testing equipment. The Quadrupole Resonator (QPR) is a specialized tool to characterize the superconducting properties of circular samples. A calorimetric measurement of the RF surface losses allows the surface resistance to be measured with sub nano-ohm resolution. This measurement can be performed over a wide temperature and magnetic field range, at frequencies of 433, 866 and 1300 MHz. The system at Helmholtz-Zentrum Berlin (HZB) is based on a resonator built at CERN and has been optimized to lower peak electric fields and an improved resolution. An alternative calorimetry chamber has been designed in order to provide flat samples for coating and to ease changing of samples. Furthermore it enables exchangeability of samples between the QPRs at HZB and CERN. With this poster the design and first measurements of the new calorimetry chamber is presented.

TUPB068 **Tunneling Spectroscopy for SRF: A Correlation Study Between the Superconducting Density of States and SRF Performances**

Th. Proslie, N. Groll (ANL) S. Calatroni (CERN) C. Cao, J. Zasadzinski (IIT) G. Ciovati, A-M. Valente-Feliciano (JLab) A. Grassellino, S. Posen, A. Romanenko (Fermilab) D.L. Hall (Cornell University (CLASSE), Cornell Laboratory for Accelerator-Based Sciences and Education) M. Liepe (Cornell University)

The performances of SRF cavities are very sensitive to the surface superconducting properties and their variations over both microscopic and macroscopic scales. Tunneling spectroscopy (TS), in synergy with other surface characterization technique, is a very unique and necessary tool that enables the measurements of the surface superconducting properties and density of states. I'll present an overview of over 4 years of measurement on a large variety of samples relevant for SRF cavity applications in collaboration with Jlab, FNAL, Cornell, CERN from bulk Nb with various surface treatments, Nb films on cooper grown with various deposition techniques to Nb₃Sn films on bulk Nb samples. I'll highlight clear correlations that emerge from the surface data analysis between the superconducting density of states, chemical and structural properties and the SRF performances. The Tunneling spectroscopy is a crucial part of a necessary surface characterization tool portfolio to understand and to some extent predicts the SRF performances of various surface treatments applied to Nb, or new superconducting alloys developed to break the Nb monopoly.

- TUPB069 Point Contact Tunneling Spectroscopy Apparatus for Large Scale Mapping of the Surface Superconducting Properties**
Th. Proslie, N. Groll (ANL) J. Zasadzinski (IIT)
 We describe the design and testing of a point contact tunneling spectroscopy (PCTS) device that can measure a material's surface superconducting properties and density of states (DOS) over large surface areas with size up to mm. The tip's lateral (X,Y) motion, mounted on a (X,Y,Z) piezo stage, was calibrated on a patterned substrate consisting of Nb lines sputtered on a gold film using both normal (Al) and superconducting (PbSn) tips at 1.5K. The tip's vertical (Z) motion control enables the adjustment of the tip-sample junction resistance over 7 orders of magnitudes from a quasi ohmic regime (few hundred Ohms) to the tunnel regime (up to few GOhms). Due to numerous surface treatments applied to cavities, the native oxide thickness 3-10 nm of Nb or impurity phases have impeded the use of vacuum tunneling techniques. In this respect, PCTS combined with other structural and chemical characterization techniques, is a uniquely suited tool to map the surface superconducting properties on sub-micron to mm scales for SRF cavities applications.
- TUPB070 High Power Tests of the Fermilab SSR1 Cavities**
A.I. Sukhanov (Fermilab)
 A cryomodule of 325 MHz Single Spoke Resonator type 1 (SSR1) superconducting RF cavities is being built at Fermilab for the PIP II project. Ten SSR1 cavities were manufactured in industry and delivered to Fermilab. Nine of the produced SSR1 cavities have been successfully tested in the Fermilab Vertical test stand (VTS) before jacketing in Helium vessel. Qualification of the jacketed SSR1 cavities complete with tuner and high power coupler is an important step of the cryomodule assembly. In this paper we report on the ongoing efforts of high power tests of jacketed SSR1 cavities at the Fermilab Spoke test cryostat (STC). We present performance parameters achieved by the cavities during these tests.
- TUPB071 Development and Testing of a 325 MHz $\beta=0.82$ Single-Spoke Cavity**
C.S. Hopper, J.R. Delayen, H. Park (ODU) J.R. Delayen, H. Park (JLab)
 A single-spoke cavity operating at 325 MHz with geometric β of 0.82 has been developed and tested. Initial results* showed high levels of field emission which limited the achievable gradient. Several rounds of helium processing significantly improved the cavity performance. Here we discuss the development process and report on the improved results.
- TUPB072 Report of Vertical Test of the $\beta=0.12$ Half-Wave Resonator at RISP**
G.-T. Park, H.J. Cha, H. Kim, W.K. Kim (IBS) Z.Y. Yao (TRIUMF, Canada's National Laboratory for Particle and Nuclear Physics)
 $\beta=0.12$, $f=162.5$ MHz half-wave resonator for Rare Isotope Science Project (RISP) was recently tested at TRIUMF. We briefly report the vertical test result: At 2K, the cavity achieved $Q_0=2\cdot 10^9$ at $E_{acc}=6.4$ MV/m and the performance was limited at $E_{acc}=7.8$ MV/m by intense field emission. The surface processing was standard: 120 micron buffered chemical polishing followed by high pressure rinsing. After first cold test, 120C baking was done and the corresponding result was also obtained.
- TUPB073 Cold Tests of SSR1 Resonators Manufactured by IUAC for the Fermilab PIP-II Project**
L. Ristori, O.S. Melnychuk (Fermilab) K.K. Mistri, P.N. Potukuchi, A. Rai, J. Sacharias, S.S.K. Sonti (IUAC)
 In the framework of the Indian Institutions and Fermilab Collaboration (IIFC) within the PIP-II project, two Superconducting Single Spoke Resonators were manufactured at the Inter-University Accelerator Centre (IUAC) in New Delhi and tested at Fermilab. The resonators were subject to the routine series of inspections and later processed chemically by means of Buffered Chemical Polishing, heat-treated at 600 C and cold-tested at Fermilab in the Vertical Test Stand. In this paper we present the findings of the inspections and the results of the cold-tests.
- TUPB074 SSR1 Cold Mass: Alignment and Vacuum Measurements**
L. Ristori, M. Parise, D. Passarelli (Fermilab)
 The assembly of SSR1 cryomodules for the PIP-II project at Fermilab poses several challenges. In this paper we present the requirements for the alignment of cold-mass components and the tests performed to validate the assembly and alignment process. A multi-cavity bead pull test was carried out as part of this validation process together with laser tracker measurements. All beamline components in the SSR1 cryomodule have an aperture of just 30 mm and several vacuum tests were performed to evaluate the need of a parallel vacuum manifold to achieve the level of vacuum required for the cryomodule.
- TUPB075 Performance Tests with Low Level RF Power of the Superconducting 217 MHz CH Cavity**
F.D. Dziuba, M. Amberg, M. Basten, M. Busch, H. Podlech (IAP) M. Amberg, K. Aulenbacher, W.A. Barth, S. Mickat (HIM) K. Aulenbacher (IKP) W.A. Barth, S. Mickat (GSI)
 Since in future the existing UNILAC (Universal Linear Accelerator) is used as an injector for the FAIR (Facility for Antiproton and Ion Research) project, a new superconducting (sc) continuous wave (cw) linac at GSI is proposed to keep the Super Heavy Element (SHE) program at a competitive high level. In this context, a sc 217 MHz Crossbar-H-mode (CH) cavity has been designed at the Institute for Applied Physics (IAP) of Frankfurt University and was built at Research Instruments (RI) GmbH, Germany. The cavity serves as a first prototype to demonstrate the reliable operability under a realistic accelerator environment and its successful beam operation will be a milestone on the way to the new linac. In this contribution the results of first measurement on the sc 217 MHz CH cavity at 4K with low level rf power will be presented.
- TUPB076 The Multipacting Study of Niobium Sputtered High-Beta Quarter-Wave Resonators for HIE-ISOLDE**
P. Zhang, W. Venturini Delsolaro (CERN)
 Superconducting quarter-Wave Resonators (QWRs) will be used in the superconducting linac upgrade in the frame of HIE-ISOLDE project at CERN. The cavities are made of bulk copper with thin niobium film coated. They will be operated at 101.28 MHz at 4.5 K providing 6 MV/m accelerating gradient with 10 W power dissipation. Multipacting (MP) has been studied for the high-beta ($\beta=10.9\%$) QWRs and two MP barriers have been found: E_{acc} at around 0.05MV/m and 1.5MV/m. We have used both CST Microwave Studio & Particle Studio and the parallel codes Omega3P & Track3P developed at SLAC. The results from the two codes are consistent and are in good agreement with cavity vertical cold test results. Both MP barriers can be processed by RF during the cavity cold test.
- TUPB077 The Influence of Cooldown Conditions at Transition Temperature on the Quality Factor of Niobium Sputtered Quarter-Wave Resonators for HIE-ISOLDE**
P. Zhang, Y. Kadi, A. Miyazaki, M. Therasse, W. Venturini Delsolaro (CERN)
 Superconducting quarter-wave resonators (QWRs) are to be used in the ongoing linac upgrade of the ISOLDE facility at CERN. The cavities are made of niobium sputtered on copper substrates. They will be operated at 101.28 MHz at 4.5 K providing 6 MV/m accelerating gradient with 10 W power dissipation. In recent measurements, we found the thermal gradient along the cavity during the niobium superconducting transition has an impact on the cavity quality factor. On the other hand, the speed of the cooling down through the superconducting transition turned out to have no influence on the cavity Q-factor.

TUPB078 **Developments on a Cold Bead-Pull Test Stand for SRF Cavities**

A.V. Vélez, A. Burrill, A. Frahm, J. Knobloch, A. Neumann (HZB)

Final tuning and field profile characterization of SRF cavities always takes place at room temperature. However, important questions remain as to what happens when the cavity is cooled to LHe temperature, in particular with multi cell systems. To enable the characterization of cavities in the cold, we have designed and commissioned a "cold bead-pull" test stand at HZB. The present test stand is designed to be integrated in HoBiCaT (Horizontal bi-cavity testing facility) with the ability to provide electric field profile measurements under realistic superconducting conditions ($T=1.8\text{K}$). In this paper mechanical and operational details of the apparatus will be described as well as future plans for the development and usage of this facility.

TUPB079 **Second Sound Quench Detection of Dressed TESLA-Shape SRF Cavities**

Y. Tamashevich (University of Hamburg) E. Elsen, A. Navitski (DESY)

A compact Multi-OST detector for second sound measurements has been developed. The Multi-OST detector allows precise 3D quench localisation within a single unit and can be used even for cavities with mounted Helium tank. The compact device is easily mounted and requires minimum space. It can be used as a part of the standard cold test of cavities, since the requirements for mounting are minimal. The results obtained with the new sensor and a 3D-algorithm have been crosschecked by optical inspection and resistor-based temperature mapping. The resolution is seen to be limited by the sampling rate and the lateral extent of the quench induced heated area on the Nb superconductor.

TUPB080 **Diagnostic Developments at CERN's SRF Testing Facility**

A. Macpherson, S. Aull, A. Benoit, P.F. Fernández López, K.G. Hernández-Chahín, K.M. Schirm, R. Valera Teruel (CERN) K.G. Hernández-Chahín (DCI-UG) T. Junginger (HZB) T. Junginger (TRIUMF, Canada's National Laboratory for Particle and Nuclear Physics)

As part of CERN's re-establishment of an SRF cold testing facility for bulk niobium cavities, diagnostic instrumentation and testing procedures have been upgraded, with particular attention given to quench location, ambient magnetic field control, thermometry and thermal cycling techniques. Detection, characterisation, and localisation of quench spots using Oscillating Superleak Transducer (OST) sensors is presented using both standard a fixed and a new variable velocity algorithm for the relative Helium 1/Helium 2 density wave produced by the quench. Fluxgate observations of ambient magnetic field contributions during the cool down process, and the effect on cavity performance is also presented, for both suppressed and fixed ambient magnetic field configurations, with attention given to monitoring and control of thermal electrical currents during the superconducting transition. Correlation of thermometry measurements to cavity trips, based on resistor thermometry is shown for both elliptical and non-elliptical cavities. Finally, we comment on the LabView/PLC deployment of the diagnostics infrastructure and our new offline analysis and reprocessing in a standard python framework.

TUPB081 **Multi-Cell T-Mapping and Conclusions**

F. Furuta, R.G. Eichhorn, G.M. Ge, D. Gonnella, D.L. Hartill, G.H. Hoffstaetter, J.J. Kaufman, M. Liepe, E.N. Smith (Cornell University (CLASSE), Cornell Laboratory for Accelerator-Based Sciences and Education)

Multi-cell temperature mapping (T-map) system has been developed and applied on SRF Nb cavities vertical tests (VT) at Cornell. It has nearly two thousand thermometers and achieved a 1mK resolution of niobium surface temperature rinsing in superfluid helium. We have upgraded the system to be capable of monitoring the temperature profiles of quench spot on cavity. The recent results of T-map during cavity tests and details will be reported.

TUPB082 **Automatic Surface Defect Detection and Sizing for Superconducting Radio Frequency Cavities Using Haar Cascades**

G.V. Ereemeev (JLab) D.C. Iriks (Santa Rosa Junior College)

Serious albeit tiny surface defects can remain on the surface of superconducting radio frequency (SRF) cavities after polishing and cleaning. These defects reduce the efficiency of cavities and often limit the maximum attainable fields. We applied a Haar cascade artificial vision technique for automated identification, counting, and sizing of defects induced on niobium surface by Nb-H precipitates formed at cryogenic temperatures. The defects were counted and sized by a computer program and also counted and measured manually to estimate detection rate and accuracy of sizing. The overall detection rate was 53%, and the overall false positive rate was 29%. The technique that was used to automatically size the features was found to oversize the features, but oversize them consistently, resulting in a size histogram that represents the defect size distribution on the sample. After scaling the histogram data, the average defect area was found to be 90 square micrometers with the standard deviation of 70 square micrometers.

TUPB083 **Room Temperature Characterization of Superconducting Spoke Cavities at the FREIA Laboratory**

H. Li (IHEP) V.A. Goryashko, R.J.M.Y. Ruber, V.G. Ziemann (Uppsala University)

As part of the development of the ESS spoke linac, the FREIA Laboratory at Uppsala University, Sweden, has been equipped with superconducting cavity test facility. The first horizontal tests of a single and double spoke cavity developed by IPN Orsay have been performed in the new HNOSS horizontal cryostat system. The cavities are equipped with a low power input antenna and a pick-up antenna. Different measurement methods were investigated to measure the weak RF signal coupling from the cavity at room temperature and during cool down. Despite the large signal attenuation we managed to characterize the cavities with low signal-to-noise ratio. Results from the tests confirm the possibility to transport the cavities from France to Sweden without consequences. We present the methods and study results of the cavity performance.

TUPB084 **Vacuum Test of Cavity With Liquid Nitrogen**

H. Kim, H.J. Cha, M.J. Joung, H.J. Kim, J.H. Kim, W.K. Kim, Y. Kim, G.-T. Park, I. Shin (IBS)

Preliminary vacuum test for superconducting cavity with liquid nitrogen is performed. Schematic plan for ROAN vacuum system is introduced and vacuum control system for superconducting cavity test is shown. Pressure of cavity is shown as a function of time and temperature. Outgassing species from cavity is also detected. Detailed experimental procedure is described to test vacuum in cavity with liquid nitrogen.

TUPB085 **Optical Surface Properties of XFEL Cavities and Their Influence on RF Performance**

M. Wenskat, E. Elsen, A. Navitski, L. Steder (DESY)

The optical inspection of the inner surface of superconducting rf cavities is a well-established tool at many laboratories. Its purpose is to recognise and understand field limitations and to allow optical quality assurance during cavity production. Within the ILC-HiGrade programme at DESY, as part of the XFEL cavity production, an automated image processing and analysis algorithm has been developed that recognises structural boundaries. The count of features, the length of boundaries and their orientation can be used for characterisation. Appreciable differences are observed depending on the fabrication process at the vendor and the chemical treatment applied. The potential of this framework for automated quality assurance as an integral part of large-scale cavity production will be outlined. In addition, correlations between geometrical surface properties and the maximal accelerating field of twenty cavities have been found. These observations coincide with quench localisation by second sound of two cavities. The distribution of the limiting cell is vendor dependent, indicating weaknesses in the fabrication procedure.

- TUPB086 Multimode Quench Detection on a 3.9 GHz XFEL Type Large Grain Cavity**
M. Bertucci, A. Bosotti, P. Michelato, L. Monaco, D. Sertore (INFN/LASA) C. Pagani (Università degli Studi di Milano & INFN)
 A 3.9 GHz XFEL type Large Grain cavity shows field quenches in different modes of the fundamental passband. During the cavity test, different OSTs for second sound detection are installed around the cavity. The reconstructed quench positions match with the results obtained by means of RF mode pattern analysis, therefore suggesting that the different quench fields are due to defect in different positions within the 9 cavity cells. The cavity optical inspection confirmed the presence of grain-boundary like structures in the identified points. A preliminary discussion of possible quench mechanism related to the presence of grain boundaries is also presented.
- TUPB087 Development of an X-Ray Fluorescence Probe for Inner Cavity Inspection**
M. Bertucci, P. Michelato, L. Monaco, M. Moretti, C. Pagani (INFN/LASA) A. Navitski (DESY)
 The development of an x-ray fluorescence probe for detection of foreign material inclusions of the inner surface of 1.3 GHz tesla-type Niobium cavities is here presented. The setup dimensions are minimized so to access the inner cavity volume and focus on the surface of equator. Preliminary tests confirmed the system capability to detect and localize with good precision small metal inclusions of few micrograms. The results obtained from the inspection of some 1.3 GHz XFEL series production cavities are also pointed out.
- TUPB088 On the Mystery of Quench Detection Using Second Sound**
S.R. Markham, R.G. Eichhorn (Cornell University (CLASSE), Cornell Laboratory for Accelerator-Based Sciences and Education)
 Quench location detection has provided valuable insight in SRF cavity operation since two decades. While in earlier days temperature maps were used the state of the art technique nowadays is detecting the second sound wave, excited by a quench, using oscillating super-leak detector (OSTs). Typically, many OSTs surround the cavity and the quench location is determined by triangulation of the different OST signals. Convenient as the method is there is a mystery: taking the well-known velocity of the second sound wave, the quench seems to come from a place slightly above the cavity's outer surface. In addition, not all triangulation spheres intersect in one point. We will present a model based on numerical quench propagation simulations that is able to fully explaining this discrepancy.
- TUPB089 High-Precision Measurements of the Quality Factor of Superconducting Cavities at the FREIA Laboratory**
V.A. Goryashko, K.J. Gajewski, L. Hermansson, H. Li, H. Nicander, R.J.M.Y. Ruber, R. Santiago Kern (Uppsala University)
 In this paper we propose a high-precision method of measuring Q0 of SRF cavities. A common way to study the performance of an SRF cavity is to build an oscillator around it that is referred to as a self-exciting loop. In the standard approach, by tuning the loop phase for a maximum field level in the cavity and measuring forward and reflected waves, one finds the cavity coupling. Then, performing a time-decay measurement and finding the total quality factor, one gets Q0. However, this approach suffers from a deficiency originating from a single data-point measurement of the reflection coefficient. In our method by varying the loop phase shift, one obtains amplitudes of the reflection coefficient of the cavity as a function of its phases. The complex reflection coefficient describes a perfect circle in polar coordinates. Fitting the overdetermined set of data to that circle allows more accurate calculation of Q0 via the least-squares procedure. The method has been tested at the FREIA Laboratory on two cavities from IPN Orsay: a single spoke and a prototype ESS double spoke.
- TUPB090 Study of the Mechanical Modes and Microphonics of Spoke Cavities at the FREIA Laboratory**
V.A. Goryashko, K.J. Gajewski, L. Hermansson, H. Li, T. Lofnes, H. Nicander, R.J.M.Y. Ruber, R. Santiago Kern (Uppsala University)
 At the FREIA Laboratory we performed measurements of the Lorentz transfer function and microphonics for spoke cavities designed and built at IPNO. The measurements are done by running the cavity in the self-excited mode and using Digital Cavity Resonance Monitors (DCRM) for tracking the cavity frequency. One DCRM makes use of a commercial oscilloscope that provides directly I and Q data whereas the second one uses an LLRF built in-house. The latter is an FPGA based unit with 6 ADC input channels, 2 at 250 Msps and 4 ADC at 1.25 Gsps and 2 DAC output channels at 1 Gsps. The FPGA is used to downconvert the incoming signal at the ADC to baseband at 1 Msps. After performing loop control filtering at baseband the signal is upconverted to 352 MHz and sent back to the cavity as a feedback signal. This feedback can be used to control both amplitude and phase of the cavity as well as other parameters. The Lorentz transfer function is obtained by modulating the cavity voltage with help of our LLRF and sweeping the modulation frequency across the range of interest.
- TUPB091 Systematic Uncertainties in RF-Based Cavity Quality Factor Measurements**
W. Schappert, Y.M. Pischalnikov, D.A. Sergatskov (Fermilab)
 Measurements of cavity quality factor measurements are subject to at least three potentially large sources of systematic error that have not been previously recognized. Imperfect coupler directivity (cross-talk) can lead to large errors in the cavity coupling factor when the cavity coupling factor is significantly different than unity. Energy re-reflected from the circulator can systematically bias the measured cavity decay time which is used to determine the loaded quality factor. Use of the peak probe power or the minimum of the reflected power to determine the cavity resonance frequency rather than the peak of the probe/forward transfer function may lead to errors in the resonance frequency that can also affect quality factors. Each effect is illustrated with measurements in the Fermilab VTS, simulations and analytic calculations. If the magnitude and phase of the cavity RF signals are measured, these effects can be measured and corrected for. If only signal magnitudes are recorded or these effects are not measured, they must be treated as sources of systematic uncertainty.
- TUPB092 Technology Development of Solid State RF Amplifier for Superconducting Cavities**
J.K. Mishra, V.R. Bala, M.M. Pande, P. Singh (BARC)
 Superconducting RF accelerators utilizes special kind of cavities which are operated in the temperatures of 2-4 K. Due to high quality factor of these cavities, low RF power is needed to generate same accelerating gradient. Solid state RFPAs are best suited for these kinds of applications where RF power requirement is of the order of tens of kW. MOSFET based RFPAs have been designed and developed to deliver 1.0 kW of RF power at 325 MHz. These RFPAs have been tested with feature like power gain of 21.6 dB, efficiency of 70%, harmonic content of < -45 dBc and compact size (power output per unit volume). Wilkinson type power combiner and dividers have been designed and developed for combining of these RFPAs modules. High power RF output has been delivered by combing 8 nos. of RFPAs modules and these Power divider and combiners. 8 kW output RF power have been extracted from this amplifier with 1.0 dB compression power at 7.3 kW. Overall amplifier efficiency has been 68% at 8 kW and 66% at 7.3 kW of output power. Harmonic content of this amplifier is < -50 dBc.
- TUPB093 Initial Commissioning Experience with the Spallation Neutron Source VTA RF System**
M.T. Crofford, J.A. Ball, M. Doleans, S.-H. Kim, S.W. Lee, J.D. Mammosser, J. Saunders (ORNL) T.L. Davidson (ORNL RAD)
 The Spallation Neutron Source (SNS) has developed a vertical test area (VTA) for the testing and qualification of superconducting radio frequency cavities. The associated RF System successfully supported the initial commissioning of the VTA system and has been utilized for cavity testing at both 4 and 2 K. As operational experience was gained, improvements to the RF system were implemented to better utilize the dynamic range of the system along with software updates and additions to meet the operational needs. The system continues to evolve as we gain better understanding of the testing needs.

TUPB094 **JLAB Vertical Test Area RF System Improvements**

T. Powers, M.L. Morrone (JLab)

RF systems for testing critically coupled SRF cavities require the ability to track the cavity frequency excursions while making accurate measurements of the radio frequency (RF) signals associated with the cavity. Two types of systems are being used at Jefferson Lab. The first, the traditional approach, is to use a voltage controlled oscillator configured as a phase locked loop such that it will track the cavity frequency. The more recently developed approach is to use a digital low level RF (LLRF) system in self excited loop (SEL) mode to track the cavity frequency. Using a digital LLRF system in SEL mode has the advantage that it is much easier to lock to the cavity's resonant frequencies and they tend to have a wider capture range. This paper will report on the system designs used to implement the 12 GeV digital LLRF system in the JLAB vertical test area. Additionally, it will report on the system modifications which are being implemented so that the RF infrastructure in the VTA will be ready to support the LCLS II cryomodule production effort, which is scheduled to begin in calendar year 2016.

TUPB095 **Resonance Control for Narrow Bandwidth SRF Cavities**

W. Schappert, J.P. Holzbauer, Y.M. Pischalnikov (Fermilab)

Optimal control techniques have been employed in a variety of applications since they were first developed more than 60 years ago but until now they have been used in few if any accelerator-related applications. The next generation of superconducting accelerators will require both precise control of the gradient and active stabilization of the resonance frequency. Optimal control techniques provide a self-consistent framework within which to construct a combined electro-mechanical controller. Results from recent cold cavity tests at Fermilab are presented.

TUPB096 **Mechanical Damper Study for ISAC-II Quarter Wave Resonators**

L. Yang (TRIUMF, Canada's National Laboratory for Particle and Nuclear Physics)

ISAC-II quarter wave resonators are installed with mechanical dampers to damp out the first mechanical mode of inner conductors. The dampers absorb the oscillating energy of inner conductors which could cause high level of frequency detuning. In the operation, over coupling is required to get a stable bandwidth. Since the beam loading of ISAC-II is negligible, the forward power is almost fully reflected. Current damper design helps reduce the forward power down to 150w for the 106MHz quarter wave resonators. Study is carried out to improve the damping efficiency and further reduce the forward power. This paper will present the methodology.

TUPB097 **The Study on Microphonics of Low Beta HWR Cavity at IMP**

Z. Gao (IMP/CAS)

The superconducting linac of China Accelerator-Driven System Injector II will operate at CW-mode. Mechanical vibrations of the superconducting cavity, also known as microphonics, cause shifts in the resonant frequency of the cavity. In order to understand these effects, microphonics measurements were performed on the half-wave superconducting cavity when it was operated in the test cryostat. And the experimental modal analysis was also performed to understand the cavity structure optimization. The measurement method and results will be shown and analyzed in this paper.

TUPB098 **Error Analysis on RR Measurement Due to Imperfect RR Components**

G. Wu (Fermilab)

An accurate cavity test involves the accurate power measurement and decay time measurement. The directional coupler in a typical cavity test llrf system usually has low directivity due to broadband requirement and fabrication errors. The imperfection of the directional coupler brings unexpected systematic errors for cavity power measurement in both forward and reflect power. An error analysis will be giving and new specification of directional coupler is proposed.

TUPB099 **Magnetic Foils for SRF Cryomodule**

G. Wu, A. Grassellino, D.A. Sergatskov (Fermilab)

High quality factor niobium cavities require minimal residual magnetic field around the high magnetic field region. A typical global magnetic shield takes more material and provides less effective magnetic screening. On the other hand, local magnetic shield has to introduce complex geometries to cover access ports and instrumentation and thermal straps. Local magnetic source and thermal current will increase residual field seen by SRF cavities regardless the complexity of local magnetic shield. Magnetic foils that is cryogenic compatible provides a great benefit to reduce residual magnetic field. This paper will describe the evaluation of such magnetic foils in both vertical and horizontal test.

TUPB100 **CEA Experience and Effort to Limit Magnetic Flux Trapping in Superconducting Cavities**

J. Plouin, F. Leseigneur (CEA/DSM/IRFU) N. Bazin, P. Charon, G. Devanz, H. Dzitko, P. Hardy, J. Neyret (CEA/IRFU)

Protecting superconducting cavities from the surrounding static magnetic field is considered as a key point to reach very good cavity performances. This can be achieved by both limiting the causes of magnetic flux around the cavity in the cryomodule, and enclosing cavities and/or cryomodules into magnetic shields. We will present the effort made at CEA into this direction: shield design, shield material characterization, at room and cryogenic temperature, and search and attenuation of the magnetic background present in the cryomodule during the cavities superconducting transition. This last point will be especially studied for the IFMIF project where the cryomodule houses the focusing magnets. Aspects of the cold magnetic shields for ESS will also be discussed.

TUPB101 **Design of the Thermal and Magnetic Shielding for the LHC High Luminosity Crab-Cavity Upgrade**

N. Templeton, T.J. Jones (STFC/DL) K. Artoos, S. Atieh, R. Calaga, O. Capatina, T. Capelli, F. Carra, G. Favre, P. Freijedo Menendez, S.A.E. Langeslag, C. Zanoni (CERN) S.A. Belomestnykh (Stony Brook University) G. Burt, S.M. Patalwar (Cockcroft Institute) G. Burt (Cockcroft Institute, Lancaster University) G. Burt (Lancaster University) S.U. De Silva, J.R. Delaysen, H. Park (ODU) Z. Li (SLAC) K.B. Marinov, A.J. May, S.M. Patalwar (STFC/DL/ASTeC) T.H. Nicol (Fermilab) R.G. Olave (Old Dominion University) A. Ratti (LBNL) S. Verdú-Andrés, Q. Wu, B. P. Xiao (BNL)

As part of the High Luminosity upgrade of the LHC, two superconducting compact Crab-Cavity designs are to be tested within separate Cryomodules, on the SPS ring at CERN in 2018. A novel side loaded Cryomodule, utilised for both cavities, satisfies tight spatial constraints within SPS and facilitates the strict operating conditions of the cavities while allowing ease of access for assembly, inspection and maintenance. This paper outlines the design and performance of the module's thermal & magnetic shields, which are critical to cavity operational stability. The thermal shield serves as a radiative heat barrier for the cavities and also recycles gaseous helium to intercept and thermalize critical components, such as the fundamental power coupler, ensuring minimal heat leak to the cavities. The design of the magnetic shielding prevents field of more than 1 μ T reaching the cavity surface, it consists of a 'warm' outer shield and two 'cold' inner shields (one per cavity, two cavities per module). The shields adopt the 'side loaded' configuration while the cold shields are suspended within the cavity's 2K liquid helium vessel, leading to various design constraints and considerations.

TUPB102 Validation of Local Magnetic Shielding for FRIB Using a Prototype Cryomodule

S.K. Chandrasekaran, K. Saito (FRIB)

The Facility for Rare Isotope Beams (FRIB) shall employ local magnetic shielding around the niobium SRF cavities in its cryomodules (CM). Each CM shall contain at least one 8 T superconducting (SC) solenoid, whose operation could magnetize components in the CM. The Q of the cavities could degrade if they are cooled through T_c in the presence of magnetic fields from the magnetized components. To prevent such degradation in performance, historically, demagnetization cycles are run using the solenoid prior to warming of the CM. The FRIB solenoid design contains bucking coils, but does not include any iron yoke. The residual magnetic field of the solenoid package, due to hysteresis in the iron, is therefore expected to be small. In addition, the local magnetic shields are expected to attenuate the fields around the cavities further. The magnetic fields before, during, and after operation of a solenoid at 8 T, inside and outside the magnetic shielding, within a prototype CM were measured. The effect of demagnetization cycles and thermal cycling of the CM were also examined. Results from these measurements validated the design and usage of local magnetic shields.

TUPB103 Cryomodule Protection for ARIEL e-Linac

Z.Y. Yao, R.E. Laxdal, W.R. Rawnsley, V. Zvyagintsev (TRIUMF, Canada's National Laboratory for Particle and Nuclear Physics)

The e-Linac cryomodules require high RF power, cryogenics, ultra-high vacuum, and precise mechanical adjustment. They require protection against failures, like quench in the cavity, bad vacuum or multipacting in power couplers, low liquid helium level or high temperatures. The protection unit should stop RF power in the cryomodule in case of the listed failures. An Interlock Box is developed to implement protection function for the cryomodule. The paper will describe the design of Interlock Box for e-Linac cryomodule protection. As quench protection required, quench evolution analysis with RF transient analysis is investigated. The details of quench detection for e-Linac will also be reported.

TUPB104 Series Production of BQU at DESY for the EXFEL Module Assembly at CEA Saclay

B. van der Horst, M. Helmig, A. Matheisen, S. Saegebarth, M. Schalwat (DESY)

Each of the 10^3 XFEL modules foreseen for the EXFEL as well as the 3.9 GHz injector module is equipped with a combination of beam position monitor, superconducting quadrupole and a gate valve connected to the beam position monitor. The subunits are prequalified by the relevant work packages of the EXFEL collaboration and then handed over to the DESY cleanroom. These subunits are assembled in the DESY ISO 4 cleanroom to produce a BQU unit, finally conditioned and quality controlled in respect to cleanliness. When passing all quality control steps the BQU are handed over with the status "ready for assembly in ISO 4 cleanroom" for string assembly in the ISO 4 cleanroom located at CEA France. Series production started with the production of one unit per week which then needed to be ramped up in beginning of 2015 up to five to six units every four weeks (1.25 units per week). Analysis of data taken during production and the optimization of the work flows for higher production rates are presented.

TUPB105 Assembly of a 3.9 GHz String for the EXFEL at DESY

M. Schmökel, R. Bandelmann, A. Daniel, A. Matheisen, P. Schilling (DESY) P. Pierini (INFN/LASA)

For the injector of the EXFEL one so-called 3.9 GHz module is required. This special module houses eight 3.9 GHz s.c. cavities, a beam position monitor and quadrupole package. The cavities were fabricated and vertically tested as an in-kind contribution to the EXFEL by INFN Milano collaborators. The power couplers have been fabricated and conditioned by FNAL. The string assembly took place inside the ISO 4 cleanroom at DESY. A seven meter long alignment and assembly girder for this special string assembly has been designed and fabricated at DESY. The girder facilitates the assembly of the 3.9 GHz resonators with alternating power coupler orientation in ISO 4 cleanrooms. For redundancy and fast action on problems during string assembly, the DESY high pressure rinsing system (HPR) has been modified on the basis of the INFN Milano design for this 3.9 GHz application. The HPR has been qualified by four 3.9 GHz resonators, tested at INFN Milano. The integration of the cavities into Helium vessels, power coupler coupling factor and the power coupler assembly at DESY is qualified by one cavity that has been equipped with Helium tank and a power coupler and tested horizontally.

TUPB106 First Phase HIE-ISOLDE Cryo-Modules Assembly at CERN

M. Therasse, G. Barlow, S. Bizzaglia, J.A. Bousquet, A. Chrul, P. Demarest, J-B. Deschamps, J.A. Ferreira Somoza, J. Gayde, M. Gourragne, A. Harrison, G. Kautzmann, D. Mergelkuhl, V. Parma, M. Struik, W. Venturini Delsolaro, L.R. Williams, P. Zhang (CERN) J. Dequaire (Intitek)

The first phase of the HIE-ISOLDE project aims to increase the energy of the existing REX ISOLDE facilities from 3MeV/m to 5MeV/m. It involves the assembly of two superconducting cryo-modules based on quarter wave resonators made by niobium sputtered on copper. The first cryo-module was installed in the linac in May 2015 followed by the commissioning. The first beam is expected for September 2015. In parallel the second cryo-module assembly started. In this paper, we present the different aspects of these two cryo-modules including the assembly facilities and procedures, the quality assurance and the RF parameters (cavity performances, cavity tuning and coupling).

TUPB107 Development of a Test Bench to Prepare the Assembly of the IFMIF LIPAC Cavity String

N. Bazin, G. Devanz, P. Hardy (CEA/DSM/IRFU) H. Dzitko, J. Neyret (CEA/IRFU) E. Toral (CIEMAT)

The IFMIF LIPAC cryomodule houses eight half-wave resonators and eight solenoids which will be assembled on a support frame in clean room. Due to the short lattice defined by beam dynamics constraints, there is not much room between two elements for the operators' hands to connect them. In order to test, optimize and validate the clean room assembly procedures and the associated tools, a test bench, consisting of a frame, a little bigger than one eighth of the final support has been manufactured. In order to start the tests before the delivery of the actual key components of the cryomodule, a dummy cavity, solenoid and coupler were manufactured and will be used to perform tests outside and inside the clean room to validate the assembly procedure and the tools. The mock-up will then be used to train the operators for the assembly of the whole string.

TUPB108 Connection of EXFEL Cryomodules, Caps, Boxes in EXFEL Main Linac and Injector: Welding of Cryo-Pipes and Assembly of Beam-Line Absorbers Under Requirements of PED Regulation

S. Barbanotti, H. Hintz, K. Jensch, L. Lilje, W. Maschmann (DESY) P. Pierini (INFN/LASA)

The European X-ray Free Electron Laser (EXFEL) cold linac consists of 100 assembled cryomodules, 6 feed-/end-boxes and 6 string connection boxes fixed to the ceiling of the accelerator tunnel; the cold injector consists of a radio frequency gun, one 1.3 GHz and one 3.9 GHz cryomodule, one feed- and one end-cap lying on ground supports. The components are connected together in the tunnel, after cold testing, transport, final positioning and alignment. The cold linac is a pressure equipment and is therefore subjected to the requirements of the Pressure Equipment Directive (PED). This paper describes the welding and subsequent non-destructive testing of the cryo-pipes (with a deeper look at the technical solutions adopted to satisfy the PED requirements), the assembly of the beam line absorbers and the final steps before closing the connection with a DN1000 bellows. A special paragraph will be dedicated to the connection of the injector components, where the lack of space makes this installation a particularly challenging task.

TUPB109 Assembly and Cool-Down Tests of STF2 Cryomodule at KEK

T. Shishido, K. Hara, E. Kako, Y. Kojima, H. Nakai, Y. Yamamoto (KEK)

As the next step of the quantum beam project, the STF2 project is in progress at KEK. Eight 9-cell SC cavities and one superconducting quadrupole magnet were assembled into the cryomodule called CM1. Four 9-cell SC cavities were assembled into the cryomodule called CM2a. These two cryomodules were connected as one unit, and the examination of completion by a prefectural government was carried out. The target value of beam energy in the STF2 accelerator is 400 MeV with a beam current of 6 mA. The first cool down test for low power level RF measurements was performed in autumn of 2014. In this paper, the assembly procedure of the STF2 cryomodules and the results of the low-power measurement are reported.

TUPB110 LCLS-II Cryomodules Design Integration and Assembly at Fermilab

T.T. Arkan, C.M. Ginsburg, Y. He, J.A. Kaluzny, Y.O. Orlov, T.J. Peterson, K. Premo (Fermilab)

LCLS-II is a planned upgrade project for the linear coherent light source (LCLS) at SLAC. The LCLS-II linac will consist of thirty-five 1.3 GHz and two 3.9 GHz superconducting RF continuous wave (CW) cryomodules that Fermilab and Jefferson Lab will assemble in collaboration with SLAC. The LCLS-II 1.3 GHz cryomodule design is based on the European XFEL pulsed-mode cryomodule design with modifications needed for CW operation. Both Fermilab and Jefferson Lab will each assemble and test a prototype 1.3 GHz cryomodule to assess the results of the CW modifications. After prototype cryomodule tests, both laboratories will increase cryomodule production rate to meet the challenging LCLS-II project installation schedule requirements of approximately one cryomodule per month per laboratory. This paper presents the 1.3 GHz CW cryomodule design integration for assembly at Fermilab, and describes Fermilab Cryomodule Assembly Facility (CAF) infrastructure modifications for the LCLS-II cryomodules, and readiness for the required assembly throughput.

TUPB111 Design and Commissioning of a New High Pressure Rinse Tool at Jefferson Lab

A.V. Reilly, S. Castagnola, D. Dail, G.K. Davis, P. Denny, J. Follkie, L. Zhao (JLab)

The Thomas Jefferson National Accelerator Facility is currently engaged in the installation and commissioning of a new high pressure rinse (HPR) tool. The new HPR tool is being installed into the SRF Institute's class 10 clean room facility. The new tool was designed and provided by an equipment manufacturer experienced in the semiconductor industry. The design of the tool is based on an engineering specification developed and provided by the SRF Institute. The HPR tool will upgrade and expand JLab's high pressure rinse capabilities. Features of the new tool include a larger process chamber, PLC control, HEPA filtered air flow, a broad ultrapure water (UPW) flow range and the capability to provide high pressure UPW at both ambient and hot temperatures. The tool is planned to be operational in August 2015. This paper will describe the installation and commissioning of the tool and expand upon the features and HPR capabilities.

TUPB112 Status of the JLab LCLS-II Prototype Cryomodule

A.V. Reilly, E. Daly, G.K. Davis, P. Denny, J.F. Fischer, J. Follkie, D. Forehand, K. Macha, J.P. Preble (JLab)

The Thomas Jefferson National Accelerator Facility is currently engaged, along with several other DOE national laboratories, in the Linac Coherent Light Source II project (LCLS II). The SRF Institute at Jefferson Lab will be building one prototype and 17 production cryomodules based on the TESLA / ILC / XFEL design. Each cryomodule will contain eight nine cell cavities with coaxial power couplers operating at 1.3 GHz. Preparations for the prototype cryomodule are underway. Assembly of the prototype is planned to begin with cavity string assembly in late August 2015 and conclude with cryomodule testing in the winter of 2016. Preparations for the prototype included process procedure development and modifications and additions to assembly infrastructure. The SRF cavities for the prototype have been processed and vertical test qualified at JLab by the SRF Institute's production group. This paper will provide a review of the preparations made, a description of the status of the prototype cryomodule and discuss the plans to complete the prototype cryomodule assembly in preparation for cryogenic performance testing.

TUPB113 JLab Cryomodule Assembly Infrastructure Modifications for LCLS-II

E. Daly, J. Armstrong, M.A. Drury, J.F. Fischer, D. Forehand, J. Henry, K. Macha, J.P. Preble, A.V. Reilly, K.M. Wilson (JLab)

The Thomas Jefferson National Accelerator Facility is currently engaged, along with several other DOE national laboratories, in the Linac Coherent Light Source II project (LCLS II). The SRF Institute at Jefferson Lab will be building 1 prototype and 17 production cryomodules based on the TESLA / ILC / XFEL design. Each cryomodule will contain eight nine cell cavities with coaxial power couplers operating at 1.3 GHz. New and modified infrastructure and assembly tooling is required to construct cryomodules in accordance with LCLS-II requirements. The approach for modifying assembly infrastructure included evaluating the existing assembly infrastructure implemented at laboratories world-wide in support of ILC and XFEL production activities and considered compatibility with existing infrastructure at JLab employed for previous cryomodule production projects. These modifications include capabilities to test cavities, construct cavity strings in a class 10 cleanroom environment, assemble cavity strings into cryostats, and prepare cryomodules for cryogenic performance testing. This paper will give a detailed description of these modifications.

TUPB114 Transient Study of Beam Loading and Feedforward LLRF Control of ARIEL Superconducting RF e-LINAC

E. Thoeng (UBC & TRIUMF) R.E. Laxdal (TRIUMF, Canada's National Laboratory for Particle and Nuclear Physics)

ARIEL e-LINAC is a 1/2 MW-class SRF accelerator operated at 10 mA of average current. In the initial commissioning, e-LINAC will be tested with increasing duty factor from 0.1% up to CW mode. During the pulsed mode operation, beam loading causes cavity gradient fluctuation and therefore transient behavior of SRF Cavity gradient needs to be studied in order to determine how the Low-level RF (LLRF) should be implemented. LLRF control system with and without feed-forward are simulated with Matlab/Simulink to determine the control gain parameters to meet the settling time specification. Furthermore, experimental measurements of cavity gradient and beam energy spread are conducted to quantify the performance of the current feed-forward compensation.

TUPB115 Improvements of the Mechanical, Vacuum and Cryogenic Procedures for European XFEL Cryomodule Testing

J. Świerbleski, M. Bednarski, B. Dzieza, W. Gaj, L. Grudnik, P. Halczyński, A. Kotarba, A. Krawczyk, K. Myalski, T. Ostrowski, B. Prochal, J. Rafalski, M. Sienkiewicz, M. Skiba, M. Wartak, M. Wiencek, J. Zbroja, P. Ziolkowski (IFJ-PAN)

The European X-ray Free Electron Laser is under construction at DESY, Hamburg. The linear accelerator part of the laser consists of 100 SRF cryomodules. Before installation in the tunnel the cryomodules undergo a series of performance tests at the AMTF Hall. Testing procedures have been implemented based on TTF (Tesla Test Facility) experience. However, the rate of testing and number of test benches is greater than in the TTF infrastructure. To maintain the goal testing rate of one module per week, improvement to the existing procedures were implemented at AMTF. Around 50% of the testing time is taken by connection of the cryomodule to the test bench, performing all necessary checks and cool down. Most of the preparation procedures have been optimized to decrease mounting time. This paper describes improvements made to the mechanical connections, vacuum checks and cryogenics operation.

TUPB116 Construction and First Cooling Test of Horizontal Test Cryostat at KEK

K. Umemori, K. Hara, E. Kako, Y. Kobayashi, Y. Kondo, H. Nakai, H. Sakai, S. Yamaguchi (KEK)

A horizontal test cryostat was designed and constructed at AR East building on KEK. Main purposes of test stand are improvement of module assembly technique and effective development of module components. Diameter of vacuum chamber is 1 m and its length is 3 m, which is enough to realize performance test of L-band 9-cell cavity with full assembly, including input couplers, HOM dampers/couplers and frequency tuners. On the sides, several ports are prepared to access to components, such as coupler and tuners. A cold box is placed on the top of the chamber. Liquid He is filled in a 4K-pod and 2K He is supplied through a J-T valve. A He pumping system is prepared. Inside of the chamber was covered with 80K shield, which is cooled by Liquid nitrogen. A cavity is supported on 5K table, which is also used as 5K thermal anchors. First 80 K cooldown test using liquid Nitrogen was successfully carried out and 2K cold test will be planned in this July. In this presentation, details of design and construction of the horizontal test cryostat is described and results of the cooling tests are shown. High power tests will be realized in a future.

TUPB117 Cavities and Cryomodules Managing System at AMTF

M. Wiencek, K. Krzysik, J. Świerbleski (IFJ-PAN) J. Chodak (DESY)

800 SRF cavities and 100 SRF cryomodules are under test in the AMTF Hall at DESY, Hamburg. Testing of such a large volume of components requires a management system which can store the measurement data. In addition the system should simplify tasks which are recurrent. In the case of the system developed at AMTF, communication with external databases has also been developed. An added complication is that not all the test procedures are identical for each component, and therefore the management system keeps track of all work done for each of the individual components. In the case of the vertical acceptance tests for the 800 SRF cavities, the management system provides an interface for specifying a decision of the next step each cavity (e.g. send for module assembly or retreatment). This paper describes the most important parts of this system.

TUPB118 Improvements of the RF Test Procedures for European XFEL Cryomodule Testing

M. Wiencek, K. Kasprzak, D. Konwisorz, S. Myalski, K. Turaj, A. Zwozniak (IFJ-PAN)

The testing of the 100 SRF cryomodules for E-XFEL is currently ongoing at the AMTF Hall, located at DESY, Hamburg. Cold tests for the cryomodules have been developed based on TTF (Tesla Test Facility) experience. However, to be able to test the cryomodules with required test rate of one a week, some improvements to the measurements had to be made. The goal of these improvements was to reduce the time needed for testing without losing any of the important data for the cryomodule. Currently, after testing more than 30% of the cryomodules, gathered experience is now allowing us to skip or combine some of the measurements. This paper describes changes in the cold test procedures which have been made since the testing of the first serial cryomodules delivered by IRFU.

TUPB119 Engineering Design of Bi-Cavity Horizontal Test Stand at RRCAT for Testing Two 650 MHz SCRF Cavities

G. Gilankar, R. Ghosh, P.D. Gupta, A. Jain, P. Khare, P.K. Kush (RRCAT) M. Geynisman, A. Hocker, D.V. Mitchell, T.H. Nicol, J.P. Ozelis, T.J. Peterson, V. Poloubotko, C. Reid (Fermilab)

A Bi-cavity Horizontal Test stand (HTS-2), for testing two 650 MHz “dressed” superconducting RF cavities was designed at Raja Ramanna Centre for Advanced Technology, India (RRCAT) in collaboration with Fermi National Accelerator Laboratory, USA (FNAL). This HTS facility will be used to test two 5-cell 650 MHz SRF cavities in the CW regime for Proton Linear Accelerator of PIP II project at Fermi Lab., USA. HTS of same design will be used for testing two 650 MHz cavities of LINAC for Indian SNS project in future. In order to maximize the utility of this facility, design of facility can also be used to test two dressed 9-cell 1.3 GHz cavities and other similarly-sized devices if required in future. This design work has been carried out under umbrella of Indian Institution and Fermilab Collaboration (IIFC). Design of this test facility was based on the design and operating experience of the existing Horizontal Test Stand-1 (HTS-1) in service at the Meson Detector Building at FNAL (MDB). Design work of HTS has been completed and now procurement process for this test stand is in progress. This paper discusses design considerations, salient features, design calculations and analysis of HTS-2.

TUPB120 The Cryogenic Infrastructure for SRF Testing at TRIUMF

R.R. Nagimov, P.R. Harmer, D. Kishi, A. Koveshnikov, R.E. Laxdal, H. Liu, N. Muller (TRIUMF; Canada's National Laboratory for Particle and Nuclear Physics)


At the moment TRIUMF operates one superconductive radio-frequency (SRF) accelerator and building the second one. Superconducting heavy ion linear accelerator of the Isotope Separation and Acceleration (ISAC) facility utilizes medium beta quarter wave cavities cooled down to 4 K. The Advanced Rare Isotope Laboratory (ARIEL) is a major expansion of the ISAC facility. ARIEL SRF electron linear accelerator (e-linac) operates nine-cell TESLA type cavities at 2 K. Both accelerators have dedicated cryogenic systems including cryoplants and liquid helium (LHe) distribution systems. In addition to accelerator cryogenic support, ISAC cryoplant provides LHe for the SRF testing facility at both 4 K and 2 K temperatures. TRIUMF's SRF development involves both SRF testing facility and accelerators cryogenic support systems. This paper presents the details of the SRF testing cryogenic systems as well as recent commissioning results of the new e-linac cryo-system.

16-Sep-15 08:00 – 09:20 Oral Sea to Sky Ballroom A

WEA1A — Fundamentals III - Frequency dependence

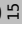
Chair: V. Palmieri (INFN/LNL)

WEA1A01 Microwave Suppression of Nonlinear Surface Resistance and the Extended Q(B) Rise in Alloyed Nb Cavities

08:00  A.V. Gurevich (Old Dominion University)

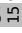
The talk gives a theoretical overview of recent progress in our understanding of the field dependence of the SRF surface resistance $R_s(H)$. A theory of microwave suppression of $R_s(H)$ in the Meissner state of alloyed superconductors under a low-frequency, strong RF field at low temperatures is presented*. Solving equations for $R_s(H)$ derived from a non-equilibrium BCS theory in the dirty limit shows that $R_s(H)$ has a minimum as a function of H, mostly due to field-induced temporal oscillations of the quasiparticle density of states. The calculated field dependence $R_s(H)$ is in good agreement with recent experiments on Ti and N alloyed Nb resonator cavities. The theory suggests that the extended Q(B) rise can be further enhanced by reducing subgap density of states by materials modifications. Applying superimposed dc and ac fields can be used to reduce the rf dissipation by tuning $R_s(H^0)$ with the dc field and also to probe the mechanism of microwave suppression of $R_s(H)$ under equilibrium conditions. Ways of increasing the SRF performance by an optimized dirty layer at the Nb surface, which can withstand magnetic field exceeding the superheating field of Nb is discussed**.

WEA1A02 Surface Resistance Study on Low Frequency (Low Beta) Cavities

08:20  D. Longuevergne (IPN)

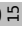
Additional RF tests and temperature treatments (120°C baking, 100K soaking, ...) have been carried out on Spiral2 quarter-wave cavities and ESS double spoke cavities. For each test, residual resistance and BCS resistance have been evaluated by testing the cavities between 4.2K and 1.5K. This talk will summarize the main results and try to highlight the main differences with high frequency cavities.

WEA1A03 Medium Field Q-Slope in Low Beta Resonators

08:35  Z.Y. Yao, P. Kolb, R.E. Laxdal (TRIUMF; Canada's National Laboratory for Particle and Nuclear Physics)

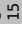
A significant issue in low beta resonators is medium field Q-slope (MFQS) at 4K that in some cases has resulted in projects choosing to operate low frequency cavities at 2K. Recent measurements have been done on QWR (80MHz) and HWR (160MHz) cavities at TRIUMF to study the MFQS of Low Beta Resonators. Quality factor data taken in cooling from 4K to 2K is used to separate the rf surface resistance into BCS and residual components for different surface treatments. These measurements shed light on the mechanisms behind the field dependence in the rf surface resistance.

WEA1A04 The Quadrupole Resonator: An Ideal Tool to Study RF Superconductors

08:50  R. Kleindienst, A. Burrill, S. Keckert, J. Knobloch, O. Kugeler (HZB)

Recent cavity results with niobium have demonstrated the necessity of a good understanding of both the BCS and residual resistance. For a complete picture, and comparison with theory, it is essential that one can measure the RF properties as a function of applied magnetic field, temperature, frequency and ambient magnetic field. Standard cavity measurements are limited in their ability to change all parameters freely and in a controlled manner. On the other hand, most sample measurement setups operate at fairly high frequency, where the surface resistance is always BCS dominated. The quadrupole resonator, originally developed at CERN, is ideally suited for RF characterization of samples at frequencies of 400 and 1300 MHz, between which many of today's SRF cavities operate. We report on a modified version of the QPR with improved RF figures of merit for high-field operation. Experimental challenges in the commissioning run and alternate designs towards a simpler sample change are shown alongside measurement results of a large grain niobium sample.

WEA1A05 Nanostructure of the Penetration Depth in Nb Cavities: Debunking the Myths and New Findings

09:05  Y. Trenikhina, A. Romanenko (Fermilab)


Nanoscale defect structure within the magnetic penetration depth of ~100 nm is key to the performance limitations of niobium superconducting radio frequency (SRF) cavities. Using a unique combination of advanced thermometry during cavity RF measurements, and TEM structural and compositional characterization of the samples extracted from cavity walls at both room and cryogenic temperatures, we directly discover the existence of nanoscale hydrides in SRF cavities limited by the high field Q slope, and show the decreased hydride formation after 120C baking. Crucially, in extended studies we demonstrate that adding 800C hydrogen degassing - both with AND without light BCP afterwards - restores the hydride formation to the pre-120C bake level correlating perfectly with the observed high field Q slope behavior. We also show absence of niobium oxides along the grain boundaries and the modifications of the surface oxide upon 120C bake, which contradicts some of the widely used models of niobium surface. Finally, we report on studies of nanohydride formation in cutouts from nitrogen doped cavities.

16-Sep-15 09:20 – 10:00 Oral Sea to Sky Ballroom A

WEA2A — Cavities I


Chair: V. Palmieri (INFN/LNL)

WEA2A01 High-Velocity Spoke Cavities

09:20  C.S. Hopper, H. Park (ODU)

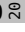
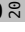
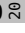
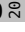
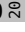
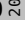
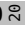
The speaker is asked to present the world-wide activities toward the design, development, and testing of spoke cavities for the acceleration of high-velocity particles.

WEA2A02 High Gradient Tests of the Five-Cell Superconducting RF Module With a PBG Coupler Cell

09:40  S. Arsenyev (MIT/PSFC) C.H. Boulware, T.L. Grimm, A. Rogacki (Niowave, Inc.) W.B. Haynes, D.Y. Shchegolkov, E.I. Simakov, T. Tajima (LANL)

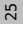
The talk shall present results of high-gradient testing of the first 5-cell superconducting radio frequency (SRF) module with a photonic band gap cell (PBG). The purpose of the PBG cell is to provide higher order mode (HOM) damping and beam acceleration at the same time. Both HOM damping and fundamental power input are done through waveguides attached to the PBG cell. We will first address the design of the structure and issues that arise from incorporating a complex PBG cell into an SRF module. In particular, the module was tuned to have an uneven accelerating gradient profile in order to provide equal surface magnetic field in every cell. We will then cover the fabrication steps and surface treatment of the five-cell niobium structure and shall report results of the high gradient tests at temperatures 4 K and 2 K. We will compare the results to previously obtained data for single PBG cells.

16-Sep-15	10:30 – 12:50	Oral	Sea to Sky Ballroom A
WEBA — Cavities II			
Chair: S.A. Belomestnykh (BNL)			

- WEBA01**
10:30  **Experiences Earned on the Fabrication, Testing, and Operation of the TEM Cavities for ADS**
H.F.S. Feisi (IHEP)
TEM mode cavities (spokes and HWR) are being developed for C-ADS. The talk shall report the progress to date on cavity prototyping including vertical test performance and performance after installation in test cryomodules and during beam tests. The speaker should be aware that an overview talk on C-ADS progress since SRF2013 will also be given.
- WEBA02**
10:50  **RF Measurements for Quality Assurance During SC Cavity Mass Production**
A.A. Sulimov (DESY)
The talk shall describe the comprehensive program and results of RF measurements taken during the mass production of sc cavities for the Eu-XFEL. The speaker should highlight important issues and mitigation strategies to help guide future large projects. A comparison of vertical test data to installed performance should be given where data is available.
- WEBA03**
11:10  **Cavity Fabrication Experience at FRIB**
C. Compton (FRIB)
The speaker is asked to give an overview of the FRIB experience with the fabrication of cavities. This would include partners and vendors interactions, technical and schedule issues and their mitigation strategies. Also include experience with rf frequency control and post-fabrication mitigation strategies.
- WEBA04**
11:30  **Performances of Spiral2 low and high beta cryomodules**
C. Marchand (CEA/IRFU)
All SPIRAL2 cryomodules (twelve with one quarter wave resonator (QWR) at $\beta=0.07$ and seven with two QWRs at $\beta=0.12$) have been produced and qualified, and are now in installation phase on the LINAC at GANIL. We will present a summary of the techniques used for the preparation and integration of the cavities in the cryomodules, and compare the achieved performances with design parameters.
- WEBA05**
11:50  **Achieving High Peak Fields and Small Residual Resistance in Half-Wave Cavities**
Z.A. Conway, A. Barcikowski, G.L. Cherry, R.L. Fischer, S.M. Gerbick, C.S. Hopper, M. Kedzie, M.P. Kelly, S.H. Kim, S.W.T. MacDonald, B. Mustapha, P.N. Ostroumov, T. Reid (ANL)
We have designed, fabricated and tested two new half-wave resonators following the successful development of a series of niobium superconducting quarter-wave cavities. The half-wave resonators are optimized for $\beta = 0.11$ ions, operate at 162.5 MHz and are intended to provide up to 2 MV effective voltages for particle with the optimal velocity. Testing of the first two half-wave resonators is complete with both reaching accelerating voltages greater than 3.5 MV with low-field residual resistances of 2.5 nanoOhms increasing to 6 nanoOhms nominally at 3.5 MV. The performance of these cavities, in terms of both achieved accelerating voltage and residual resistance, is more than double the next best half-wave cavities reported for this velocity regime. The intention of this presentation is to provide insight into how Argonne achieves low-residual resistances and high surface fields in low-beta cavities by describing the cavity design, fabrication, processing and testing.
- WEBA06**
12:10  **Design Studies for QWR Structure and Cryomodule for RIKEN SC-Linac**
N. Sakamoto, O. Kamigaito, H. Okuno, K. Ozeki, K. Suda, Y. Watanabe, K. Yamada (RIKEN Nishina Center) H. Hara, K. Okihira, K. Sennyu, T. Yanagisawa (MHI) E. Kako, H. Nakai, K. Umemori (KEK)
Recently we proposed a new project aimed at intensity upgrade of uranium beams of RIKEN RIBF. In this new project, construction of a superconducting linac is planned replacing the injector cyclotron so called RRC. The RIKEN superconducting linac consists of 14 cryomodules each of which contains four quarter-wave-resonators (QWRs) in each. The QWR operates at an rf frequency of 73 MHz in the continuous wave mode with beta as low as 0.055-1.008. A coaxial probe-type RF fundamental power-coupler which transmits RF power of several kW will be utilized for beam loading of 1.3 kW/resonator at the maximum with Qext of several $\times 10^6$. Tuning of the resonant frequency will be realized with a mechanical tuner pressing the resonator wall in the direction parallel to the beam. This year, we started a development of a test cryomodule with SC-QWRs. In this paper, design studies for a SC-QWR and its cryomodule, e.g., QWR, coupler, and, tuner will be presented together with a construction schedule of the prototype. Prototyping of a superconducting cavity and its test cryomodule was funded by ImpACT Program of Council for Science, Technology and Innovation (Cabinet Office, Government of Japan).
- WEBA07**
12:30  **Beam Commissioning of the 56 MHz QW Cavity in RHIC**
Q. Wu, S.A. Belomestnykh, I. Ben-Zvi, M. Blaskiewicz, L. DeSanto, D. Goldberg, M. Harvey, T. Hayes, G.T. McIntyre, K. Mernick, P. Orfin, S.K. Seberg, F. Severino, K.S. Smith, R. Than, A. Zaltsman (BNL) S.A. Belomestnykh, I. Ben-Zvi (Stony Brook University)
A 56 MHz superconducting RF cavity has been designed, fabricated and installed in the Relativistic Heavy Ion Collider (RHIC). The cavity operates at 4.4 K with a “quiet helium source” to isolate the cavity from environmental acoustic noise. The cavity is a beam driven quarter wave resonator. It is detuned and damped during injection and acceleration cycles and is brought to operation only at store energy. We have observed clear luminosity increase and bunch length reduction in the first operation of the cavity with Au + Au and Au + He3 collisions. The cavity voltage was limited by quenching in the Higher Order Mode coupler. This paper also discusses the cavity beam experiments with no higher order mode coupler in p + p and p + Au RHIC operation.

17-Sep-15 08:00 – 10:10	Oral	Sea to Sky Ballroom A
THAA — Cavities III Chair: A. Facco (FRIB)		

THAA01 Review of SRF Deflecting Cavity Development

08:00  *J.R. Delayen (ODU)*

In the last few years there has been a growing interest in compact superconducting cavities operating in a deflecting mode to be used either in rf separators or crabbing systems. This talk will give an overview of recent progress in global activities towards SRF deflecting mode cavities.

THAA02 SRF Gun Development Overview

08:25  *J.K. Sekutowicz (DESY)*

The most demanding component of a continuous wave (cw) injector is cw operating RF-gun, delivering highly populated low emittance bunches. RF-guns, both working at room temperature and superconducting, when they generate highly populated low emittance bunches have to be operated at high accelerating gradients to suppress space charge effects diluting emittance. Superconducting RF-guns are technically superior to the normal conducting devices because they dissipate orders of magnitude less power when operating at very high gradients in cw mode. In this contribution progress since 2013 in the R&D programs, designing and operation of the SRF-injectors at KEK, HZB, HZDR, PKU and DESY will be discussed.

THAA03 SRF Guns at BNL: First Beam and Other Commissioning Results

08:50  *W. Xu (BNL)*


The talk shall cover two SRF photoemission electron guns under commissioning at BNL: a 704 MHz elliptical ERL gun and a 112 MHz quarter-wave gun for coherent electron cooling experiment. In particular, the speaker shall report on generating first photoemission beam current from the 704 MHz SRF gun, multipacting issues in the SRF guns, photocathode behavior as well as other commissioning experiences and results.

THAA04 Comparison of Cavity Fabrication and Performances Between Fine Grains, Large Grains and Seamless Cavities

09:10  *K. Umemori, H. Inoue, T. Kubo, H. Shimizu, Y. Watanabe, M. Yamanaka (KEK) A. Hocker (Fermilab) T. Tajima (LANL)*

In KEK-CFF, L-band SRF cavity fabrication studies have been actively proceeded. Main target of the R&D is investigation of cavity fabrication methods using different Nb materials. In this talk, we report mainly focus on the experiences obtained from single cell cavity fabrications. First, different Nb materials are compared, between fine grain Nb and large grain(LG) Nb from different vendors including low RRR LG Nb, in which, cavities were fabricated by electron beam welding method. Difficulty on LG cavity fabrication come from deformation due to stressed grain boundaries. In addition to nominal electron beam welded cavities, hydro-formed seamless cavities have been fabricated. Relatively large difference of equator and iris ratio cause difficulty on expansion of Nb pipes. Good qualified Nb pipe is essential and control of hydro-forming steps including annealing of materials is also important. In order to evaluate these cavity performances, vertical tests were carried out. Generally, they showed good performances. In this presentation, fabrication processes, technical difficulties, mitigation strategies and vertical test results are presented.

THAA05 First Results of SRF Cavity Fabrication by Electro-Hydraulic Forming at CERN

09:30  *S. Atieh, FF Bertinelli, R. Calaga, O. Capatina, G. Favre, M. Garlaschè, F. Gerigk, S.A.E. Langeslag, K.M. Schirm, N. Valverde Alonso (CERN) G. Avriilaud, J. Bonafe, E. Mandel, P. Marty, H. Peronnet (Bmax)*

In the framework of many projects relying on RF superconducting technology, shape conformity and processing time are key aspects for the optimization of niobium cavity processing. An alternative technique to traditional shaping methods, such as deep-drawing and spinning, is Electro-Hydraulic Forming (EHF). In EHF, cavities are obtained through ultra-high-speed deformation of blank sheets, using shockwaves induced in water by a pulsed electrical discharge. With respect to traditional methods, such highly dynamic process can yield interesting results in terms of effectiveness, repeatability, final shape precision, higher formability and reduced spring-back. In this paper, the first results of EHF on copper prototypes and ongoing developments for niobium for the Superconducting Proton Linac project at CERN are discussed. The simulations performed in order to master the embedded multi-physics phenomena and to steer process parameters are also presented.




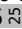
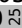
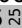
THAA06 Precise Studies on He-Processing and HPR for Recovery From Field Emission by Using X-Ray Mapping System

09:50  *H. Sakai, M. Egi, K. Enami, T. Furuya, K. Shinoe, K. Umemori (KEK) M. Sawamura (JAEA)*

We usually met the degradation of superconducting RF cavity on the cryomodule test and beam operation even if the performance of this cavity is good on the vertical test (V.T). Field emission is the most severe problem for this degradation after reassembly work from vertical test. Not only high pressure rinsing (HPR) but also He-processing, which is more suitable method without the reassembly work for recovery, is recommended and tried to recover this degradation. However, we did not investigate the details of how field emission sources were processed and removed after HPR and He-processing. We deeply investigated the processing procedure during He-processing and how many field emission sources removed after HPR by using rotating X-ray mapping system* in V.T .

17-Sep-15 10:40 – 13:00 Oral Sea to Sky Ballroom A

THBA — Technology**Chair:** M.P. Kelly (ANL)

- THBA01**
10:40  **Plasma Processing to Improve SRF Accelerating Gradient**
M. Doleans, R. Afanador, J.A. Ball, D.L. Barnhart, W. Blokland, M.T. Crofford, B. DeGraff, B.S. Hannah, M.P. Howell, S.-H. Kim, S.W. Lee, J.D. Mammosser, C.J. McMahan, T.S. Neustadt, J. Saunders, S.E. Stewart, W.H. Strong, P.V. Tyagi, D.M. Vandygriff (ORNL)
A new In-situ plasma processing technique is being developed at the SNS (Spallation Neutron Source) to improve the performance of the cavities in operation. The technique utilizes a reactive low-density room-temperature plasma to remove top-surface hydrocarbons. This increases the work function of the cavity surface and reduces the overall amount of electron activity; In particular it increases the field-emission onset, which enables to operate a cavity at higher accelerating gradient. Development of the basic plasma processing parameters and effect on the Niobium surface can be found elsewhere **. Details on the results for in-situ plasma processing of dressed cavities in the SNS HTA (horizontal test apparatus) will be reported here.
- THBA02**
11:00  **Recent Developments in Vertical Electropolishing**
V. Chouhan (MGH)
The talk will provide an overview on the latest advances (since SRF2013) of vertical electro-polishing for SRF applications. The speaker is asked to emphasize issues and present approaches on how to resolve those issues. Examples from other labs (J-Lab, Cornell, CERN, DESY) should be given that help explain the issues, resolutions and progress. Details of the speaker's own work at MGH are expected but should occupy no more than 2/3 of the talk.
- THBA03**
11:20  **Overview of Recent Advances in Coupler Technology, Fabrication and Conditioning**
W. Kaabi (LAL)
The talk will provide an overview on the latest advances (since SRF2013) of Power Coupler development, production and preparation for SRF applications. The speaker is asked to emphasize issues of design, fabrication and conditioning. Examples from other labs (FRIB, SPIRAL-II, ESS, LCLS-II) should be given that help explain the issues and resolutions including the multipacting free coupler at FRIB and the copper free coupler at FNAL. Details of the speaker's own work with the large scale production of power couplers for XFEL are expected but should occupy <=50% of the talk.
- THBA04**
11:45  **Overview of Recent HOM Coupler Development**
B. P. Xiao (BNL)
HOM damping is important for SRF applications, especially for high intensity machines. A good HOM damping design will help to reduce power load to the cryogenic system and to reduce the risk of beam breakup. The design of HOM damping, including antenna/loop HOM couplers, beam pipe HOM absorbers and waveguide HOM couplers, is to solve a multi-physics problem that involves RF, thermal, mechanical, and beam-cavity interaction issues. In this talk, the author provides an overview on the latest advances of the HOM couplers for high intensity SRF applications.
- THBA05**
12:10  **Higher Order Mode Absorbers for High Current SRF Applications**
R.G. Eichhorn, J.V. Conway, T. Gruber, Y. He, G.H. Hoffstaetter, Y. Li, M. Liepe, T.I. O'Connel, P. Quigley, J. Sears, V.D. Shemelin, E.N. Smith, M. Tigner (Cornell University (CLASSE), Cornell Laboratory for Accelerator-Based Sciences and Education)
Efficient damping of the higher-order modes (HOMs) of the superconducting cavities is essential for any high current operation. The talk will provide an overview on the latest advances of HOM absorber development for high intensity SRF applications. As the ideal absorber does not exist, the different conceptual approaches will be presented and the associated issues are outlined. Design examples from various labs will be given that help explain the issues and resolutions. Some focus will be given to the Cornell HOM beamline absorber that was design for high current, short bunch operation with up to 400 W heating. The design will be reviewed and testing results will be reported.
- THBA06**
12:35  **Overview on Magnetic Field Management and Shielding in High Q Modules**
G. Wu (Fermilab)
Maintaining very high cavity Q0 in linac applications creates new challenges for cryomodule design. Magnetic shielding from both external fields and internal fields is required and its importance to thermal gradients during Tc transition is now emerging. This presentation will describe the design challenges and possible mitigation strategies with examples from various applications or laboratories including FRIB, LCLS-II, PIP-II, Cornell University and KEK.

THPB — Poster Session

THPB001 Propagation of the High Frequency Fields in the Chain of the Superconducting Cavities*A. Novokhatski (SLAC)*

Combination with the very high repetition rate requires to use the superconducting cavities to accelerate very short bunches for the FEL operation. In the cavities these bunches excite very high frequency electromagnetic fields. There are severe concerns, that these fields will remain inside the structure for a long time, bring additional heating or even break up the Cooper pairs. We present results of the simulation of the transient dynamics of wake fields of very short bunches. We show how much of the energy is vanishing through the beam pipes immediately and how much energy is staying in the cavity for a long time.

THPB002 Second Harmonic Cavity Design for Synchrotron Radiation Energy Compensator in eRHIC Project*C. Xu, S.A. Belomestnykh, W. Xu (BNL)*

eRHIC project requires a construction of FFAG ring to accelerate electrons and connect to the existing ion ring in Brookhaven national laboratory. This new ring will have the same radius with RHIC ring. Synchrotron radiation lost in the electron ring should be compensated by a CW superconducting Radio frequency cavity, and we propose an 845MHz single cell harmonic cavity. This cavity will also experience the high average current (~0.7A) passing through it. With this consideration, this cavity design requires special design to reduce higher order mode power generation. On the other hand, a large amount of energy is requires compensating back to the beam due to synchrotron radiation, this requires cavity having a high R/Q and operating at relative high gradient of 18Mv/m. Current design would requires fundamental couplers handles 400Kw forward power and HOM couplers extract 2.5Kw HOM power. Comparison with other existing cavity will also show the superb property of this design.

THPB003 Calculations of Cavities with Dissipative Material*F. Marhauser (JLab)*

3D simulations have been performed for a variety of SRF cavities which incorporate Higher Order Mode dampers, either in form of coaxial couplers or waveguide dampers. Instead of utilizing the rather standard approach of matching the output port of the dampers with a broadband coaxial or waveguide port, dissipative materials are modelled for RF field absorption. This for instance not only avoids the otherwise required definition of the number of modes considered for damping, which has an impact on the computational time, but also allows tailoring the load material to conform with experimental data of e.g. non-perfect absorbers. The new calculation scheme is presented. Findings are partially compared with those achieved with the standard waveguide port approach by means of external quality factors. CPU speeds are briefly discussed for both approaches.

THPB004 HOM Calculations for Different Cavities and Beam Induced HOM Power Analysis of ESS*H.J. Zheng, J. Gao (IHEP) J.F. Chen (INFN/LASA) C. Pagani (Università degli Studi di Milano & INFN)*

For different design of ESS superconducting cavities, the higher order modes (HOM's) of monopoles, dipoles, quadrupoles and sextupoles are found. Their R/Q values are also calculated. Main HOM related issues are the beam instabilities and the HOM induced power especially from TM monopoles. The analysis for the beam induced HOM voltage and power in this paper showed that, if the HOM frequency is a few kHz away from the beam spectrum, it is not a problem. In order to understand the effects of the beam structure, analytic expressions are developed. With these expressions, the induced HOM voltage and power were calculated by assuming external Q for each HOM. Our analysis confirm that, with the beam structure of ESS and a good cavity design, no special tight tolerances are required for cavity fabrication and no HOM couplers in the cavity beam pipes are planned.

THPB005 Simulations and Experimental Study of 1.3 GHz and 3.9 GHz CW Couplers for LCLS-II Project*I.V. Gonin, T.T. Arkan, E.R. Harms, A. Hocker, T.N. Khabiboulline, A. Lunin, K.S. Premo, O.V. Prokofiev, N. Solyak, V.P. Yakovlev (Fermilab)*

LCLS-II linac is based on XFEL/ILC superconducting technology. TTF-III fundamental power couplers for the 1.3 GHz and 3.9 GHz 9-cell cavities have been modified to satisfy requirements of LCLS-II, operating in CW regime. In this paper we discuss the results of COMSOL analysis of the possible modification of couplers, working at various operating regimes. We present also the results of experimental study of coupler prototypes.

THPB006 Improvement of Buildcavity Code*J.F. Chen, M. Moretti, C. Pagani, P. Pierini (INFN/LASA) C. Pagani (Università degli Studi di Milano & INFN)*

Recently, we improve the BuildCavity code, which is a graphics interface to SUPERFISH for the study of superconducting cavities of elliptical shape. Now it works with latest SUPERFISH 7 and can be installed also on newer Windows system such as Win 7 and 8. Several improvements have been done in the code. As examples, some designs of ESS median beta cavities with BuildCavity will also be presented.

THPB007 A Study of Resonant Excitation of Longitudinal HOMs in the Cryomodules of LCLS-II*K.L.F. Bane, C. Adolphsen, A. Chao, Z. Li (SLAC)*

The Linac Coherent Light Source (LCLS) at SLAC, the world's first hard X-ray FEL, is being upgraded to the LCLS-II. The major new feature will be the installation of 35 cryomodules (CMs) of TESLA-type, superconducting accelerating structures. It is envisioned that LCLS-II will eventually be able to deliver 300 pC, 1 kA pulses of beam at a rate of 1 MHz. At a cavity temperature of 2K, any heat generated (even on the level of a few watts) is expensive to remove. In the last linac of LCLS-II, L3—where the peak current is highest—the power radiated by the bunch in the CMs is estimated at 14 W (charge 300 pC option, rep rate 1 MHz). But this calculation ignores resonances that can be excited between the bunch frequency and higher order mode (HOM) frequencies in the CMs, which in principle can greatly increase this number. In this report we develop a theory of resonant build up. Then, using 500 numerically obtained modes over the frequency range 3–5 GHz, we estimate the probability of significant resonant build up in L3 of LCLS-II. The effects of small random bunch phase and charge errors will also be addressed.

THPB008 RF Simulations for a 3rd Harmonic Cavity Cryomodule*L. Xiao, C. Adolphsen, Z. Li, T.O. Raubenheimer (SLAC)*

The FNAL designed 3.9GHz third harmonic cavity for XFEL will be used in LCLS-II for linearizing the longitudinal beam profile. The 3.9GHz SRF cavity is scaled down from the 1.3GHz TESLA cavity shape but has a large beampipe radius for the purpose of better HOM damping. Therefore, except for a few ones, the HOM modes are above the beampipe cutoff. The HOM damping up to 9GHz in the 4-cavity cryomodule is simulated using SLAC parallel finite-element electromagnetic code suite ACE3P to investigate possible trapped modes in the cryomodule. The coupler RF kicks produced by the HOM and power couplers in the third harmonic cavity are also evaluated. Different pairs of cavity and cavity arrangement are evaluated, and a possible arrangement is proposed that can better cancel the coupler RF kicks. In this paper we present and discuss the RF simulation results in the third harmonic cavity cryomodule.

- THPB009 Monopole Propagating Mode Studies for PIP-II 650MHz High Beta Cryomodule**
L. Xiao, L. Ge, Z. Li, C.-K. Ng (SLAC)
 Fermilab's Proton Improvement Plan II (PIP-II) will increase proton flux from the booster to the main injector through a new 800MeV, 250m long superconducting linac. The linac consists of five types of SRF cavities operating at 162.5MHz, 325MHz and 650MHz. No Higher-Order-Mode (HOM) couplers are considered for the two current 650MHz cavity designs consisting of five elliptical cells. However, fabrication errors and the operating mode tuning procedure can cause cavities deformed from the ideal one, and thus affect the beam induced HOM frequencies and quality factors. In particular, the monopole modes will generate heat and increase cryogenic loss. In this paper, the parallel finite element code suite ACE3P is employed to calculate the propagating monopole band modes including cavity imperfection within mechanical tolerances in PIP-II 650MHz high beta cryomodule consisting of 6 cavities. Mesh distortion method is used to generate deformed cavities in cryomodule. This will provide useful information for beam dynamics studies and heat load estimation for PIP-II. The simulation results are presented and discussed in the paper.
- THPB010 INFN Milano - LASA Activities for ESS**
P. Michelato, M. Bertucci, A. Bosotti, J.F. Chen, L. Monaco, M. Moretti, R. Paparella, P. Pierini, D. Sertore (INFN/LASA) C. Pagani (Università degli Studi di Milano & INFN) H.J. Zheng (IHEP)
 INFN Milano – LASA is involved in the development and industrialization for the production of 704.4 MHz medium beta ($\beta = 0.67$) cavities for the ESS project. In this framework, we are designing a medium beta prototype cavity exploring both Large Grain and Fine Grain Niobium for its production as well as a high beta ($\beta = 0.86$) Large Grain cavity. In the meanwhile, an activity is ongoing for upgrading the LASA test facility to be able to test these kind of resonators.
- THPB011 Superconducting Travelling Wave Accelerating Structure Development**
R.A. Kostin, P.V. Avrahov, A.D. Didenko, A. Kanareykin (Euclid TechLabs, LLC) T.N. Khabiboulline, Y.M. Pischnalnikov, N. Solyak, V.P. Yakovlev (Fermilab)
 The 3 cell superconducting TW accelerating structure was developed to experimentally demonstrate and to study tuning issues for a new experimental device - the superconducting traveling wave accelerator (STWA), a technology that may prove of crucial importance to the high energy SRF linacs by raising the effective gradient and therefore reducing the overall cost. Recently, a STWA structure with a feedback waveguide has been suggested. The structure was optimized and has phase advance per cell of 105° which provide 24% higher accelerating gradient than in SW cavities. Also STWA structure has no strong sensitivity of the field flatness and its length may be much longer than SW structure. With this presentation, we discuss the current status of a 3-cell L-band SC traveling wave along with the analysis of its tuning issues. Special attention will be paid to feedback loop operation with the two-coupler feed system. We also report on the development and fabrication of a niobium prototype 3-cell SC traveling wave structure to be tested at 2°K in fall 2015.
- THPB012 3 Cell Superconducting Travelling Wave Cavity Tuner**
R.A. Kostin, P.V. Avrahov, A.D. Didenko, A. Kanareykin (Euclid TechLabs, LLC) T.N. Khabiboulline, Y.M. Pischnalnikov, N. Solyak, V.P. Yakovlev (Fermilab)
 The use of a travelling wave (TW) accelerating structure with a small phase advance per cell instead of standing wave may provide a significant increase of accelerating gradient in a superconducting linear accelerator. The TW section achieves an accelerating gradient 1.2-1.4 times larger than TESLA-shaped standing wave cavities for the same surface electric and magnetic fields. However, this cavity needs additional tuner to compensate all the reflections along the structure to obtain TW regime. This paper presents the tuner requirements, design and development.
- THPB013 A Novel Design and Development of 650 MHz, $\beta=0.61$, 5-Cell SRF Cavity for High Intensity Proton Linac**
S.S. Som, P. Bhattacharyya, A. Dutta Gupta, S. Ghosh, A. Mandal, S. Seth (VECC)
 DAE laboratories in India are involved in R&D activities on SRF cavity technology for the proposed high intensity proton linacs for ISNS/IADS and also FERMILAB PIP-II program under IIFC. VECC is responsible for design, analysis and development of a 650 MHz, $\beta=0.61$, 5-cell elliptical cavity. This paper describes the novel design of the cavity, with different aperture and wall angle, having better field flatness and mechanical stability, reliable surface processing facility and less beam loss. The cavity geometry has been optimized to get acceptable values of field enhancement factors, R/Q, Geometric factor, cell-to-cell coupling etc. The effective impedance of transverse and longitudinal HOMs are low enough to get rid of HOM damper for low beam current. 2-D analysis shows no possibility of multipacting. However, 3-D analysis using CST Particle Studio code confirms its presence and it can be suppressed by introducing a small convexity in the equator region. Two niobium half cells and beam pipes for the single cell cavity have been fabricated. Measurement and RF characterisation of half cells, prototype 1-cell and 5-cell and also 1-cell niobium cavities have been carried out.
- THPB014 Mechanical Optimization of High Beta 650 MHz Cavity for Pulse and CW Operation of PIP-II Project**
T.N. Khabiboulline, I.V. Gonin, C.J. Grimm, A. Lunin, T.H. Nicol, V.P. Yakovlev (Fermilab) P. Kumar (RRCAT)
 The proposed design of the 0.8 GeV PIP-II SC Linac employs two families of 650 MHz 5-cell elliptical cavities with 2 different beta. The $\beta=0.61$ will cover the 185-500 MeV range and the $\beta=0.92$ will cover the 500-800 MeV range. In this paper we will present update of RF and mechanical design of dressed high beta cavity ($\beta=0.92$) for pulse regime of operation at 2 mA beam current. In previous CW version of PIP-II project the mechanical design was concentrated on minimization of frequency shift due to helium pressure fluctuation. In current case of pulse regime operation the main goal was Lorentz force detuning minimization. We present the scope of coupled RF-Mechanical issues and their resolution. Also detailed stress analysis of dresses cavity will be presented.
- THPB015 Design of a Medium Beta Half-Wave SC Prototype Cavity at IMP**
A.D. Wu, Y. He, T.C. Jiang, Y.M. Li, W.M. Yue, S.H. Zhang, H.W. Zhao (IMP/CAS)
 Two types of low beta Half-wave superconducting cavities have developed for Chinese Accelerator Driven Sub-critical System (C-ADS) at Institute of Modern Physics. Because of the simple structure, easy to fabrication and surface preparation, it attracts us to research the application on the medium beta section for the high power and high current linear accelerators such as the ADS. A Half-wave superconducting cavity was designed with frequency of 325 MHz and beta of 0.51. The geometry parameters and the two shapes of inner conductors are optimized in details to decrease the peak electro-magnetic fields to obtain higher accelerator gradients. To suppress the operation frequency shift caused by the helium pressure fluctuations and maximize the tuner ranges, the frequency shift and mechanical characters are studied in the electric and magnetic areas separately. At the end, the helium vessel is also designed to keep stability as possible. The fabrication and test will be completed at the beginning of 2016.
- THPB016 Development of a Low Beta High Current Superconducting Half Wave Resonator at Peking University**
F. Zhu, P.L. Fan, K.X. Liu, S.W. Quan, H.T.X. Zhong (PKU)
 More and more projects based on high current ion linear accelerators have been emerged and proposed to better support various fields of science. At Peking University, a $\beta=0.09$ 162.5 MHz HWR cavity has been designed to accelerate several 100 mA proton beam and 50 mA deuteron beam after RFQ. The detailed electromagnetic design, multipacting simulation, mechanical design, beam dynamic simulation and fabrication process of the cavity will be given in this paper.

THPB017 **A Higher Harmonic Cavity at 800 MHz for HL-LHC**

T. Roggen, R. Calaga (CERN)

A superconducting 800 MHz second harmonic system is proposed for HL-LHC. It serves as a cure for beam instabilities with high beam currents by improving Landau damping and will allow for bunch profile manipulation. This can potentially help to reduce intra-beam-scattering, beam induced heating and e-cloud effects, pile-up density in the detectors and beam losses. An overview of the 800 MHz cavity design and RF power requirements is given. In particular the design parameters of the cavity shape and HOM couplers are described. Some other aspects such as RF power requirements and cryomodule layout are also addressed.

THPB018 **A 200 MHz Superconducting RF System for the LHC**

R. Calaga (CERN)

A quarter wave $\beta=1$ superconducting cavity at 200 MHz is proposed for the LHC as an alternative to the present 400 MHz RF system. This system will allow for improved capture efficiency and acceleration of very high intensity bunches. A preliminary design with considerations of the fundamental mode fields, beam loading and RF power are presented. Some challenges related to technology development, input coupling and higher order modes are also addressed.

THPB019 **Bead-Pull Measurements of the Main Deflecting Mode of the Double-Quarter-Wave Cavity for the HL-LHC**

M. Navarro-Tapia, R. Calaga (CERN)

A full-scale model of the double-quarter-wave (DQW) cavity towards the High-Luminosity Large Hadron Collider (HL-LHC) upgrade was built in aluminum to characterize the deflecting mode. Field strength measurements have been carried out for both the transverse and longitudinal electromagnetic fields, by using the bead-pull technique. Perturbation objects of different shapes and material were used to separate the electric and magnetic field components. A reasonably good agreement was found between numerical simulation and measurements, which confirm the reliability and accuracy of the measurements done.

THPB020 **Multipactor Simulation on Superconducting Spoke Cavity**

Y. Iwashita, H. Tongu (Kyoto ICR) E. Cenni (CEA/IRFU) R. Hajima, M. Sawamura (JAEA) T. Kubo, T. Saeki (KEK)

Superconducting spoke cavities for laser Compton scattered (LCS) photon sources is under development. Considering the smaller diameter compared with the elliptical cavity with the same frequency, the operating frequency is targeted at 325-MHz towards 4K operation. Because of the complicated shape of the cavity, it may be suffered from a strong multipactor effect. Results of the multipactor analysis are reported.

THPB021 **Balloon Variant of Single Spoke Resonator**

Z.Y. Yao, R.E. Laxdal (TRIUMF, Canada's National Laboratory for Particle and Nuclear Physics)

Spoke resonators have been widely proposed and optimized for various applications. Good performance has been demonstrated by many cavity tests. Accompanying the great progress, the adverse impact of strong multipacting (MP) is also noted by recent test reports, consistent with modern 3D simulations. This paper will discuss MP behaviors in the single spoke resonator. In particular a phenomenological theory is developed to highlight the details of the geometry that affect MP. The analysis leads to an optimized geometry of a single spoke resonator defined here as the 'balloon geometry'. A 325MHz $\beta=0.3$ single spoke resonator based on 'balloon' concept is under development by the RISP-TRIUMF Collaboration. The RF and mechanical design of this cavity will also be reported.

THPB022 **A Preliminary Study of a New Superconducting Accelerating Structure for Extremely Low Energy Proton Working in Te210 Mode**

Z.Q. Yang, X.Y. Lu, D.Y. Yang, J. Zhao (PKU)

For the application of high intensity continuous wave (CW) proton beam acceleration, a new superconducting accelerating structure for extremely low β proton working in TE210 mode has been proposed at Peking University. The cavity consists of eight electrodes and eight accelerating gaps. The RF frequency is 162.5MHz, and the designed proton input energy is 200keV. A peak field optimization has been performed for the lower surface field. The accelerating gaps are adjusted by phase sweeping based on KONUS beam dynamics. Solenoids are placed outside the cavity to provide transverse focusing. Numerical calculation shows that the transverse defocusing of the KONUS phase is about three times smaller than that of the conventional negative synchronous RF phase. The beam dynamics of a 10mA CW proton beam is simulated by the TraceWin code. The simulation results show that the beam's size is under effective control. Both the simulation and the numerical calculation show that the cavity has a relatively high effective accelerating gradient of 2.6MV/m. Our results show that this new accelerating structure may be a possible candidate for superconducting operation at such a low energy range.

THPB023 **RF Team Experience with E-XFEL Cavity Production at E.ZANON**

A. Gresele, A. Visentin (Ettore Zanon S.p.A., Nuclear Division) G. Corniani (Ettore Zanon S.p.A.) A.A. Sulimov, J.H. Thie (DESY)

In the poster E.Zanon will show some final statistics: shrinkage and welding deformation for different materials (average values, deviations), the stability of cavity length after tuning and possibility of its correction, the comparison of the final frequencies with cold value.

THPB025 **Exchange and Repair of Titanium Service Pipes for the EXFEL Series Cavities**

M. Schawat, S. Barbanotti, A. Daniel, H. Hintz, K. Jensch, A. Matheisen, S. Saegebarth, P. Schilling (DESY) A. Schmidt (XFEL, EU)

Longitudinally-welded 72 mm ID service pipes (HSP) made from titanium grade 2 are used by the two suppliers of the helium tanks for the EXFEL accelerator. From the perspective of the PED DESY is legally designated as the manufacturer and is responsible for conformity to all relevant codes. During module assemblies at CEA Saclay the orbital welds of the interconnection bellows between cavities showed pores with dimensions outside the specifications set by DESY. These welds needed to be redone which caused a project delay of several months. The X-ray examination of the HSP showed that the pipes already exhibited many out-of-DESY spec pores in the longitudinal welds and were most likely the main cause of the problems in the orbital welds. It was decided to replace the extremities of the service pipes with seamless titanium tubes both on "naked" helium tanks as well as on tanks with cavities already welded in. At DESY more than 750 service pipes were exchanged over a period of 2 years. The qualification of the repair line according to PED regulation and the prove with RF test at 2 K that the repairs do not influence the high performance of the s.c. cavities were done.

THPB026 **Update on SRF Cavity Design, Production and Testing for BERLinPro**

A. Neumann, W. Anders, A. Burrill, A. Frahm, H.-W. Glock, J. Knobloch (HZB) K. Brackebusch, U. van Rienen (Rostock University, Faculty of Computer Science and Electrical Engineering) G. Ciovati (JLAB) W.A. Clemens, C. Dreyfuss, D. Forehand, T. Harris, P. Kneisel, R.B. Overton, L. Turlington (JLab) E.N. Zaplatin (FZJ)

The BERLinPro Energy Recovery Linac (ERL) is currently being built at Helmholtz-Zentrum Berlin in order to study the accelerator physics of operating a high current, 100 mA, 50 MeV low emittance ERL utilizing all SRF cavity technology. For this machine three different types of SRF cavities are being developed. For the injector section, consisting of an SRF photoinjector and a three two cell booster cavity module, fabrication is close to completion. The cavities were designed at HZB and manufactured, processed and vertically tested at Jefferson Laboratory. In this paper we will review the design and production process of the two structures and show the latest acceptance tests at HZB prior to installation into the newly designed cryo-module. For the Linac cavity the latest cavity and module design studies are being shown.

THPB027 Welding a Helium Vessel to a 1.3 GHz 9-Cell Nitrogen Doped Cavity at Fermilab for LCLS-II*C.J. Grimm (Fermilab)*

Fermilab has developed a TIG welding procedure that is used to attach a nitrogen doped 1.3 GHz 9-cell niobium (Nb) cavity to a titanium (Ti) helium vessel. These cavities will be used in the two prototype cryomodules for the Linac Coherent Light Source (LCLS-II) upgrade at SLAC National Accelerator Laboratory. Discussion in further detail will include setting up TIG welding parameters and tooling requirements for assembly and alignment of the cavity to the helium vessel. The weld designs and glovebox environment produce the best quality TIG welds that meet ASME Boiler and Pressure Vessel Code. The cavity temperature was monitored to assure the nitrogen doping is preserved, and RF measurements are taken throughout the process to monitor the cavity for excessive cell deformation due to heat loads from welding.

THPB028 ESS Medium Beta Cavity Prototypes Manufacturing*E. Cenni, C. Arcambal (CEA/IRFU) P. Bosland, G. Devanz, X. Hanus, P. Hardy, V.M. Hennion, F. Leseigneur, F. Peauger, J. Plouin, D. Roudier (CEA/DSM/IRFU) G. Costanza (Lund University) C. Darve (ESS)*

The ESS elliptical superconducting linac consists of two types of 704.42 MHz cavities, medium and high beta, to accelerate the beam from 216 MeV (spoke cavity linac) up to the full energy at 2 GeV. The last linac optimization, called Optimus+, has been carried out taking into account the limitations of SRF cavity performance (field emission). The medium and high-beta parts of the linac are composed of 36 and 84 elliptical cavities, with geometrical beta values of 0.67 and 0.86 respectively. We describe here the procedures and numerical analysis leading from half-cells to a complete medium cavity assembly, which take into account not only the frequency of the fundamental accelerating mode but also the higher order modes near the machine line. The half cell selection process to form dumb bells will be described, as well as the reshaping and trimming procedure.

THPB029 MHI's Production Activities of Superconducting Cavity*A. Miyamoto, H. Hara, K. Kanaoka, K. Okihira, K. Sennyu, T. Yanagisawa (MHI)*

Mitsubishi Heavy Industries (MHI) has developed manufacturing process of superconducting cavities for a long time. In this presentation, recent progress will be reported.

THPB030 Fabrication and Evaluation of Low RRR Large Grain 1-Cell Cavity*H. Shimizu, H. Inoue, E. Kako, T. Saeki, K. Umemori, Y. Watanabe, M. Yamanaka (KEK)*

Successive R&D studies of SRF cavities are ongoing at KEK by using existing facilities of Mechanical Engineering Center (MEC) and other equipment of Superconducting Test facility (STF). Recently, there are studies on the low RRR of niobium material with high and uniform concentration of tantalum which could be used for the fabrication of high performance SRF cavity, and hence it could reduce the fabrication cost of cavities*. In order to confirm the advantage of the material, a large-grain single-cell cavity was fabricated at MEC/KEK with sheets sliced from low RRR niobium ingot with high and uniform concentration of tantalum. The resistivity measurement of sample from sliced sheet showed the RRR value of 100, whereas it is about 400 for the nominal qualification of fine-grain sheets at KEK. The large-grain single-cell cavity was already fabricated at MEC/KEK and the quality control of the fabrication processes are well under control. Then the first vertical tests of the cavity were done at STF/KEK. In this presentation, the results of the vertical tests are shown. The potential of the low RRR niobium material for SRF cavity are discussed.

THPB031 Operation Experience with Half Cell Measurement Machine and Cavity Tuning Machine in 3 Years of XFEL Cavity Series Production*J.H. Thie, A. Gössel, J. Iversen, D. Klinke, C. Müller, A.A. Sulimov, D. Tischhauser (DESY)*

For the European XFEL superconducting Cavity series production at both cavity vendors' four manufacturing machines for production key functions, HAZEMEMA and CTM, are supplied by DESY. Among three years of cavity production in two companies a lot of experience is gathered about influence of surroundings and production quality on cycle times, machine drop outs, general stability time of machines and parts subject to wear. Significant factors on cycle time for tuning operation like temperature stability and drift during tuning and measurements, precision of cell trimming before welding and tuning and generally geometrical factors are shown. RF aspects of tuning and production quality control as additional measurements for TM011-mode to estimate quality of its damping is presented. Performed full Cavity RF measurements exceeds XFEL specifications gives a possibility for additional quality control on welding shrinkage stability and it's homogeneously distribution. The use of HAZEMEMA and CTM to assess the impact of asymmetric trimming, including calculation of it's influence on the higher-order modes, is shown.

THPB032 Release Processes and Documentation Methods During Series Treatment of SRF Cavities for the European XFEL by Using an Engineering Data Management System*J. Iversen, J.A. Dammann, A. Matheisen, N. Steinhilber-Kühl (DESY)*

For the European XFEL more than 800 superconducting cavities need to be treated. At least 65 quality documents per cavity have to be emitted and transferred to DESY by the vendor; two acceptance levels must be passed successfully to release a cavity for transportation to DESY. All quality documents, non-conformity reports and acceptance levels are automatically processed by using DESY's Engineering Data Management System (EDMS). We summarize documentation methods, document transfer procedures, review and release processes; we describe the exchange of process information between customer and vendor; and report about experiences.

THPB033 Frequency Measurement and Tuning of a 9-Cell Superconducting Cavity Developed with UK Industry*L.S. Cowie, P. Goudket, A.R. Goulden, P.A. McIntosh, A.E. Wheelhouse (STFC/DL/ASTeC) J.R. Everard, N. Shakespeare (Shakespeare Engineering) B. Lamb, S. Postlethwaite, N. Templeton (STFC/DL)*

As part of an STFC Innovations Partnership Scheme (IPS) grant, in support of enabling UK industry to address the large potential market for superconducting RF structures, Daresbury Laboratory and Shakespeare Engineering Ltd are collaborating to produce a 1.3 GHz 9 cell niobium cavity. This paper describes the procedures to ensure the cavity reaches the required frequency and field flatness. The frequency of each half-cell was measured using a custom measurement apparatus. Combined mechanical and RF simulations were used to compensate for cavity deformation during measurement. Results of Coordinate Measurement Machine measurements of one half-cell are presented. The same procedure will be used to trim the cells at the dumbbell stage, and the full 9-cell cavity will be tuned once welded.

THPB034 Large Scale Superconducting RF Cavity Production for the European XFEL*M. Pekeler (RI Research Instruments GmbH)*

Since September 2010 RI Research Instruments is producing 420 superconducting 1.3 GHz 9-cell cavities for the European XFEL project. The work includes fabrication of the cavities from niobium provided by DESY as well as surface preparation, helium vessel welding and shipping of the cavities under vacuum ready for cold RF test at DESY. In order to carry out the large scale cavity production and surface preparation significant investment in new infrastructure were made at RI. Within the first 2 years of the project a second EB welding machine, a new 120 m² ISO4 clean room with high pressure water rinsing stations, an all metal 800 C annealing furnace, and 120 C baking stations were built. Reference cavities were used to qualify the infrastructure for the series production. The series production started in March 2013 and will be finished in September 2015 with an average delivery rate of about 4 cavities per week.

- THPB035 Fabrication of the 3.9 GHz SRF Structures for the European XFEL**
P. Pierini, M. Bertucci, A. Bosotti, J.F. Chen, P. Michelato, L. Monaco, M. Moretti, R. Paparella, D. Sertore (INFN/LASA) C.G. Maiano, P. Pierini, E. Vogel (DESY) C. Pagani (Università degli Studi di Milano & INFN)
One batch of 10 cavities has been completed and eight structures have been installed in the 3.9 GHz cryomodule for the European XFEL Injector operation. A second batch of 10 RF structures for a spare injector module is under fabrication. The fabrication has been performed according to the European Pressure Vessel regulations, as needed for the EXFEL operation. This paper describes the fabrication, quality control/assurance procedures and frequency preparation steps in order to achieve cavities at the correct frequency and length within the specifications.
- THPB036 Dissimilar Electron Beam Welding of Niobium-to-Titanium for Cavity Fabrication: Process Development and Metallurgical Analysis**
P.R. Carriere, S. Yue (McGill University) V.W. Cheung, R. Edinger (PAVAC)
To form vacuum sealing surfaces, SRF cavity flanges require materials with high hardness and Nb metallurgical compatibility. For historical reasons, a NbTi alloy is used despite the inability to maintain its hardness for extended periods. Commercially pure Ti is an economical alternative, yet joining Nb to Ti directly represents an engineering challenge due to the differences in thermal conductivity and melting temperature. Recent work at PAVAC Industries has shown that proper electron beam welding (EBW) parameters can compensate for these differences, resulting in cost effective, direct, full penetration joints. In this presentation, the welds are analyzed using metallurgical techniques. The fusion and heat affected zones are predicted from a modified Rosenthal heat model. The welds are characterized using SEM with EDS and EBSD, tensile testing and microhardness. These results quantify the weld penetration, strength, segregation, chemistry, hardness and microstructure. Heat induced phase transitions, recovery and recrystallization are also investigated. These results demonstrate that direct Nb-Ti welds are a possible replacement for the conventional Nb-NbTi configuration.
- THPB037 New Technique to Weld Multi-Cell SCRF Cavities by Laser Without Vacuum Environment: Results and Benefits**
P. Khare, R. Ghosh, G. Gilankar, P.D. Gupta, A. Jain, S.C. Joshi, P.K. Kush, S.M. Oak, B.N. Upadhyay (RRCAT)
A new technique to fabricate SCRF cavities with the help of laser welding process was developed at Raja Ramanna Centre for Advanced Technology (RRCAT), Indore, Department of Atomic Energy, India. In this technique, an Nd:YAG laser was used and inert gas environment was maintained during welding. Using this technique a single cell cavity was developed at RRCAT which was successfully processed and tested at Fermi lab, USA., achieving an accelerating gradient of 31.6 MV/m with quality factor of 1×10^{10} at 2K. Now a multi-cell (5-cell) 1.3 GHz SCRF cavity has been fabricated using this laser welding technique. This is the first multi-cell cavity which has been fabricated completely by laser welding technique. The advantages of this fabrication technique are numerous, such as, reduced fabrication cost, small HAZ, no necessity of high vacuum etc. and hence is highly suitable for large scale production of cavities. This paper describes the technique, method of fabrication and experiences in fabrication of multi-cell cavity by this technique.
- THPB038 XFEL Database Structure and Data Loading System**
S. Yasar, P.D. Gall, V. Gubarev (DESY)
XFEL database was designed to store cavity production, preparation, and test data for the whole LINAC on the very detailed level: from half cells up to module tests. To load this amount of data (more than 140 files per cavity) in automatic regime the special Data Loading System was developed.
- THPB039 XFEL Database User Interface**
S. Yasar, P.D. Gall, V. Gubarev, D. Reschke, A.A. Sulimov, J.H. Thie (DESY)
The XFEL database plays an important role for an effective part of the quality control system for the whole cavity production and preparation process for the European XFEL on a very detailed level. Database has the Graphical User Interface based on the web-technologies, and it can be accessed via low level Oracle SQL.
- THPB040 Hydroforming of a Large Grain Niobium Tube**
A. Mapar, F. Pourboghraat (MSU) T.R. Bieler (Michigan State University) C. Compton (FRIB)
Currently most of Niobium (Nb) cavities are manufactured from fine grain Nb sheets. As-cast ingots go through a series of steps including forging, milling, and rolling with intermediate annealing, before they are deep-drawn into a half-cell shape and subsequently electron beam welded to make a full cavity. Tube hydroforming, a manufacturing technique where a tube is deformed into a die using a pressurized fluid, is an alternative to the current costly manufacturing process. A whole cavity can be made from a tube using tube hydroforming. This study focuses on deformation of large-grain Nb tubes during hydroforming. The crystal orientation of the grains was recorded, and the tube was marked with a circle-grid which is used to measure the local strains after deformation. The deformation of the tube is modeled with crystal plasticity finite element model and compared with the experiment to assess the accuracy of the model.
- THPB041 Hydroforming SRF Cavities from Seamless Niobium Tubes**
M. Yamanaka (KEK)
The authors are developing the manufacturing method for superconducting radio frequency (SRF) cavities by using a hydroforming instead of an electron beam welding, which is the major manufacturing method. We expect a cost reduction by hiring the hydroforming. To realize this development, getting a high-purity seamless niobium tube with good forming ability and an advancement of hydroforming technique are necessary. We got the seamless niobium tube made by ATI Wah Chang with the cooperation of Fermilab, and succeeded to manufacture the 1-cell cavity by hydroforming. The accelerating gradient attained to 36 MV/m, and we confirmed it was available to use as the SRF cavity.
- THPB042 Advance Additive Manufacturing Method for SRF Cavities of Various Geometries**
P. Frigola, R.B. Agustsson, L. Faillace, A.Y. Murokh (RadiaBeam) W.A. Clemens, P. Dhakal, F. Marhauser, R.A. Rimmer, J.K. Spradlin, R.S. Williams (JLab) D. Espalin, J. Mireles, P.A. Morton, R.B. Wicker (University of Texas El Paso, W.M. Keck Center for 3D Innovation) S.M. Gaytan (Advanced Technology Center at El Paso Community College) O. Harrysson, T. Horn, H.A. West (NCSU)
An alternative fabrication method for superconducting radio frequency (SRF) cavities is presented. The novel fabrication method, based on 3D printing (or additive manufacturing, AM) technology capable of producing net-shape functional metallic parts of virtually any geometry, promises to greatly expand possibilities for advance cavity and end-group component designs. A description of the AM method and conceptual cavity designs are presented along with material analysis and RF measurement results of additively manufactured niobium samples.

- THPB043 Alternative Fabrication Methods for the ARIEL e-Linac SRF Separator Cavity**
D.W. Storey (Victoria University) R.E. Laxdal, N. Muller (TRIUMF, Canada's National Laboratory for Particle and Nuclear Physics)
 The ARIEL e-Linac SRF separator cavity is a 650 MHz deflecting mode cavity that will allow simultaneous beam delivery to both the Rare Isotope Beam program and an Energy Recovery Linac. The cavity will be operated at 4K and with deflecting voltages of up to 0.6MV, resulting in a dissipated RF power of less than 1W and peak surface fields of 19MV/m and 24mT. Due to the low performance requirements, alternative methods are being employed for the fabrication of this cavity. These include fabricating the entire cavity from reactor grade Niobium and welding the cavity on site at TRIUMF using tungsten inert gas (TIG) welding in a high purity Argon environment. A post purification heat treatment will be performed in an RF induction oven to increase the cavity performance. The results of weld acceptance tests and fabrication progress will be presented.
- THPB044 A Superconducting RF Deflecting Cavity for the ARIEL e-Linac Separator**
D.W. Storey (Victoria University) R.E. Laxdal, L. Merminga, B.S. Waraich, Z.Y. Yao, V. Zvyagintsev (TRIUMF, Canada's National Laboratory for Particle and Nuclear Physics)
 A 650 MHz SRF deflecting mode cavity has been designed for the ARIEL e-Linac to separate interleaved beams heading towards either Rare Ion Beam production or a recirculation loop for energy recovery, allowing the e-Linac to provide beam delivery to multiple users simultaneously. The cavity geometry has been optimized for the ARIEL specifications, resulting in a very compact cavity with high shunt impedance and low dissipated power. Analyses have been performed on the susceptibility to multipacting, input coupling considering beam loading and microphonics, and extensive studies into the damping of transverse and longitudinal higher order modes. The pressure sensitivity, frequency tuning, and thermal behaviour have also been studied using ANSYS. The cavity design and higher order mode damping scheme required to meet the specifications will be discussed.
- THPB045 Progress in IFMIF Half Wave Resonators Manufacturing and Test Preparation**
G. Devanz, N. Bazin, G. Disset, F. Éozénou, P. Hardy, O. Piquet, J. Plouin (CEA/DSM/IRFU) H. Dzitzko, H. Jenhani, J. Neyret (CEA/IRFU)
 The IFMIF accelerator aims to provide an accelerator-based D-Li neutron source to produce high intensity high energy neutron flux to test samples as possible candidate materials to a full lifetime of fusion energy reactors. The first phase of the project aims at validating the technical options for the construction of an accelerator prototype, called LIPAc (Linear IFMIF Prototype Accelerator). A cryomodule hosting 8 Half Wave Resonators (HWR) at 175 MHz will provide the acceleration from 5 to 9 MeV. We report on the progress of the HWR manufacturing. A pre-series cavity will be used to assess and optimize the tuning procedure of the HWR, as well as the processing steps and related tooling. A new horizontal test cryostat (SATHORI) is also being set up at Saclay in the existing SRF test area. The SATHORI is dedicated to the IFMIF HWR performance check, fully equipped with its power coupler and cold tuning system. A 30kW-RF power will be available for these tests.
- THPB046 Design and Development of Superconducting Spoke Cavity for Compact Photon Source**
M. Sawamura (Japan Atomic Energy Agency (JAEA), Gamma-ray Non-Destructive Assay Research Group) E. Cenni (CEA/IRFU) R. Hajima (JAEA) H. Hokonohara, Y. Iwashita, H. Tongu (Kyoto ICR) T. Kubo, T. Saeki (KEK)
 The spoke cavity is expected to have advantages for compact ERL accelerator for X-ray source based on laser Compton scattering. We have been developing the spoke cavity under a research program of MEXT, Japan to establish the fabrication process. Since our designed shape of the spoke cavity is complicated due to increase the RF properties, we have been designing the mold including the process of press work and the support parts for vacuum tolerance with the mechanical simulation. In this paper we present status of the spoke cavity fabrication.
- THPB047 Tests Analysis of a 750 MHz SRF Dipole for Crabbing Applications**
A. Castilla, J.R. Delayen (ODU) J.R. Delayen (JLab)
 There is a growing interest in using rf transverse deflecting structures for a plethora of applications in the current and future high performance colliders. In this paper, we present the results of a proof of principle superconducting rf dipole, designed as a prototype for a 750 MHz crabbing corrector for the Medium Energy Electron-Ion Collider (MEIC), that has been successfully tested at 4.2 K and 2 K at the Jefferson Lab's Vertical Testing Area (VTA). The analysis of its rf performance during cryogenic testing, along with Helium pressure sensitivity, Lorentz detuning, surface resistance, and multipacting processing analysis are presented in this work. Detailed calculations of losses at the port flanges are included for completeness of the cavity's cryogenic performance studies.
- THPB048 Design of a Compact Superconducting Crab-Cavity for LHC Using Nb-on-Cu-Coating Technique**
A. Grudiev, S. Atieh, R. Calaga, S. Calatroni, O. Capatina, F. Carra, G. Favre, L.M.A. Ferreira, J.-F. Poncet, T. Richard, A. Sublet, C. Zanoni (CERN)
 The design of a compact superconducting crab-cavity for LHC using Nb-on-Cu-coating technique is presented. The cavity shape is based on the ridged waveguide resonator with wide open apertures to provide access to the inner surface of the cavity for coating. It also provides natural damping for HOMs and rather low longitudinal and transverse impedances. The results of the cavity shape optimization taking into account RF performance, coating, and thermo-mechanical considerations as well as the design and fabrication plans of the first prototype for coating and cold tests are presented.
- THPB049 Engineering Design of RF Dipole Crabbing Cavity for LHC High Luminosity Upgrade**
H. Park, S.U. De Silva, J.R. Delayen (ODU) Z. Li (SLAC) T.H. Nicol (Fermilab) H. Park (JLab)
 The Center for Accelerator Science at ODU and SLAC have been working on electromagnetic and mechanical design of an RF Dipole crabbing cavity for the LHC high luminosity upgrade. Based on the analyses and considering the aspects of fabrication, ODU and CERN concluded an engineering design of the cavity. The engineering design includes the interface with the fundamental power coupler, helium vessel, tuner, and higher order mode damper. In this paper, we present the engineering design of the cavity and the prototype fabrication status.
- THPB050 Performance Evaluation of HI-LHC Crab Cavity Prototypes in a CERN Vertical Test Cryostat**
K.G. Hernández-Chahín (DCI-UG) G. Burt (Cockcroft Institute) C. Christophe, A. Macpherson, M. Navarro-Tapia, R. Torres-Sanchez (CERN) S.U. De Silva (JLab) S. Verdú-Andrés (BNL)
 As part of the high luminosity upgrade of the LHC, transverse deflecting cavities are foreseen for luminosity enhancement and leveling. Three proof-of-principle compact cavity designs have been fabricated in bulk niobium and cold tested at their home labs, as a first validation step towards the High Luminosity LHC project. As an additional step, all three designs have been tested in one of the vertical cryostats in CERN's cold test facility, as means of a cross calibration of the crab cavity designs, as well as a cross-check of the CERN cold test facilities with respect to the other test sites. Performance assessment on the CERN test stand in terms of achievable transverse deflecting voltage at both liquid helium and super fluid helium temperatures is presented. In addition, secondary performance indicators are discussed in terms of the monitoring data taken during the tests. This indicators temperature-mapping profiles, quench detection and location with oscillating superleak transducers, ambient magnetic field and trapped magnetic flux effects, and some estimates on the influence of the cool down speed procedure on cavity performance.

THPB051 Lorentz Detuning for a Double-Quarter Wave Cavity

S. Verdú-Andrés, S.A. Belomestnykh, Q. Wu, B. P. Xiao (BNL) S.A. Belomestnykh (Stony Brook University)

The Lorentz detuning is the resonant frequency change in an RF cavity due to the radiation pressure on the cavity walls. We present benchmarking studies of Lorentz detuning calculations for a Double-Quarter Wave Crab Cavity (DQWCC) using the codes ACE3P. The results are compared with the Lorentz detuning measurements performed during the cold tests of the Proof-of-Principle DQWCC at BNL.

THPB052 Thermal Losses in Couplers of a SPS Double-Quarter Wave Crab Cavity

S. Verdú-Andrés, S.A. Belomestnykh, Q. Wu, B. P. Xiao (BNL) S.A. Belomestnykh (Stony Brook University) G. Burt (Cockcroft Institute, Lancaster University) G. Burt (Lancaster University) R. Calaga, O. Capatina, F. Carra, C. Zanoni (CERN) F. Carra (Politecnico di Torino)

The Double-Quarter Wave Crab Cavity for beam tests at SPS will be equipped with a Fundamental Power Coupler (FPC), three HOM filters and one pickup. FPC and HOM couplers are located in high magnetic field region and have a hook shape. The FPC will be made in copper while HOM and pickup are in niobium. This paper explains the material choice for the FPC, HOM and pickup couplers given the calculated power dissipation for fundamental and selected high order modes. It also describes the envisaged cooling system and corresponding thermal distribution for each coupler.

THPB053 Electromagnetic Design of 400 MHz RF-Dipole Crabbing Cavity for LHC High Luminosity Upgrade

S.U. De Silva, J.R. Delayen, H. Park (ODU) Z. Li (SLAC)

The beam crabbing proposed for the LHC High Luminosity Upgrade requires two crabbing systems operating in both horizontal and vertical planes. In addition, the crabbing cavity design needs to meet strict dimensional constraints and functional specifications of the cavities. This paper presents the detailed electromagnetic design including em properties, multipole analysis, multipacting levels of the 400 MHz rf-dipole crabbing cavity.

THPB054 Design of the HOM Couplers for RF-Dipole Crabbing Cavity for LHC High Luminosity Upgrade

S.U. De Silva, J.R. Delayen, H. Park (ODU) Z. Li (SLAC)

Current impedance calculations carried out for the LHC High Luminosity Upgrade require to re-address the higher order mode damping for the proposed crabbing cavities. The HOM couplers for the rf-dipole cavities have been improved to damp the higher order modes more effectively. This paper presents the detailed electromagnetic design of the updated horizontal and vertical HOM couplers, including thermal and mechanical analysis.

THPB055 RF Performance Results of the 2nd ELBE SRF Gun

A. Arnold, H. Büttig, M. Freitag, P.N. Lu, P. Murcek, J. Teichert, H. Vennekate, R. Xiang (HZDR) G.V. Eremeev, P. Kneisel, M. Stirbet, L. Turlington (JLab)

As in 2007 the first 3.5 cell superconducting radio frequency (SRF) gun was taken into operation at Helmholtz-Zentrum Dresden-Rossendorf, it turned out that the specified performance to realize an electron energy of 9.4 MeV has not been achieved. Instead, the resonator of the gun was limited by field emission to about one third of this value and the measured beam parameters remained significantly below its expectations. However, to demonstrate the full potential of this electron source for the ELBE linear accelerator, a second and slightly modified SRF gun was developed and built in collaboration with Thomas Jefferson National Accelerator Facility. We will report on commissioning of this new SRF gun and present a full set of RF performance results. Additionally, investigations are shown that try to explain a particle contamination that happened recently during our first cathode transfer.

THPB056 SRF Gun Cavity R&D at DESY

D. Kostin, C. Albrecht, A. Brinkmann, Th. Buettner, J. Eschke, T. Feldmann, A. Gössel, D. Klinke, A. Matheisen, W.-D. Möller, D. Reschke, M. Schmökel, J.K. Sekutowicz, W. Singer, X. Singer, N. Steinhau-Kühl, J. Ziegler, B. van der Horst (DESY) M. Barlak, W.C. Grabowski, J.A. Lorkiewicz, R. Nietubyć (NCBJ)

SRF Gun Cavity is an ongoing accelerator R&D project at DESY, being developed since several years. Currently several SRF Gun cavity prototypes were simulated, built and tested in our Lab and elsewhere. Lately the 1.6 cells Pb thin film cathode niobium cavity was tested in a vertical cryostat with a different cathode plug configurations. Cathode plug design was improved, as well as SRF Gun Cavity cleaning procedures. Results of the last cavity performance tests are presented and discussed.

THPB057 ELBE SRF Gun II - Emittance Compensation Schemes

H. Vennekate, A. Arnold, D. Janssen, P.N. Lu, P. Murcek, J. Teichert, R. Xiang (HZDR) P. Kneisel (JLab)

In May 2014 the first SRF photo injector at HZDR has been replaced by a new gun, featuring a new resonator and cryostat. The intention for this upgrade has been to reach for higher beam energies, bunch charges and therefore an increased average beam current, which is supposed to be injected into the superconducting, CW ELBE accelerator, where it can be used for multiple purposes, such as THz generation or Compton backscattering. Because of the increased bunch charge of this injector compared to its predecessor, it demands upgrades of the existing and/or novel approaches to alleviate the transverse emittance growth. One of these methods is the integration of a superconducting solenoid into the cryostat. Another method, the so called RF focusing, is realized by displacing the photo cathode's tip and retracting it from the last cell of the resonator. In this case, part of the accelerating field is sacrificed for a better focus of the electron right at the start of its generation. Besides particle tracking simulations, a recent study, investigating on the exact position of the cathode tip with respect to the cell's back plane after tuning and cool down, has been performed.

THPB058 Commissioning of the 112 MHz SRF Gun

S.A. Belomestnykh, I. Ben-Zvi, J.C. Brutus, V. Litvinenko, G. Narayan, P. Orfin, I. Pinayev, T. Rao, J. Skaritka, K.S. Smith, R. Than, J.E. Tuozzolo, E. Wang, Q. Wu, B. P. Xiao, A. Zaltsman (BNL) S.A. Belomestnykh, I. Ben-Zvi, V. Litvinenko, T. Xin (Stony Brook University)

A 112 MHz superconducting RF photoemission gun was designed, fabricated and installed in RHIC for the Coherent electron Cooling Proof-of-Principle (CeC PoP) experiment at BNL. The gun was commissioned first without beam. This was followed by generating the first photoemission beam from a multi-alkali cathode. The paper presents the commissioning results.

THPB059 Design, Fabrication and Performance of SRF-Gun Cavity

T. Konomi, E. Kako, Y. Kobayashi, K. Umemori, S. Yamaguchi (KEK) R. Matsuda (Mitsubishi Heavy Industries Ltd. (MHI)) T. Yanagisawa (MHI)

The development of superconducting RF gun has been started at KEK. The performance targets are that average current is 100 mA, normalized emittance is less than 1 $\mu\text{m}\cdot\text{rad}$, beam energy is 2 MeV and energy spread is less than 0.1 %. The SRF gun consists of 1.3 GHz and 1.5 cell elliptical cavity and backward illuminated photocathode. The cavity shape was designed by using SUPERFISH and GPT. The cavity has been fabricated by Japanese industry. Accelerating field tuning and vertical test without cathode plug was done. The surface peak electric field reached 66 MV/m, and this meet the target value 42 MV/m sufficiently. For next vertical test, cathode rod without photocathode is in preparation. In the workshop, the SRF-Gun concepts and vertical test results will be reported.

THPB060 Development of SRF Cavity Tuners for CERN

K. Artoos, R. Calaga, O. Capatina, T. Capelli, F. Carra, L. Dassa, N. Kuder, R. Leuxe, P. Minginette, W. Venturini Delsolaro, C. Zanoni, P. Zhang (CERN) G. Burt (Cockcroft Institute, Lancaster University) J.R. Delayen, H. Park (ODU) T.J. Jones, N. Templeton (STFC/DL) S. Verdú-Andrés, B. P. Xiao (BNL)

Superconducting RF cavity developments are currently on-going for new accelerator projects at CERN such as HIE ISOLDE and HL-LHC. Mechanical RF tuning systems are required to compensate cavity frequency shifts of the cavities due to temperature, mechanical, pressure and RF effects on the cavity geometry. A rich history and experience is available for such mechanical tuners developed for existing RF cavities. Design constraints in the context of HIE ISOLDE and HL-LHC such as required resolution, space limitation, reliability and maintainability have led to new concepts in the tuning mechanisms. This paper will discuss such new approaches, their performances and planned developments.

THPB061 Static and Dynamic Performance of the Double-Lever Tuner Mechanism for SSR1 Resonators

L. Ristori, D. Passarelli (Fermilab)

The first double-lever tuner for the SSR1 cavity was fabricated and tested in various conditions. Warm tests were performed to qualify the components in terms of stiffness and overall performance. The mechanism was later installed on the first production SSR1 and tested in the STC cryostat as part of a fully integrated cold test. In this paper we present the performance of the device in terms of range, hysteresis, dynamic response.

THPB062 Accelerated Life Testing of LCLS-II Cavity Tuner Motor

N.A. Huque, M.E. Abdelwhab, E. Daly (JLab) Y.M. Pischalnikov (Fermilab)

An Accelerated Life Test (ALT) of the Phytron stepper motor used in the LCLS-II cavity tuner is being carried out at JLab. Since the motor will reside inside the cryomodule, any failure would lead to a very costly and arduous repair. As such, the motor will be tested for the equivalent of five lifetimes before being approved for use in the production cryomodules. The 9-cell LCLS-II cavity will be simulated by disc springs with an equivalent spring constant. Hysteresis plots of the motor's stroke vs. current, and force (measured via an installed LVDT) vs. current will be used to determine any drift from the required performance. The titanium spindle will also be inspected for loss of lubrication. This paper outlines the ALT plan and latest results.

THPB063 BNL 56 MHz HOM Damper Prototype Production at JLab

N.A. Huque, W.A. Clemens, E. Daly (JLab) S. Bellavia, G.T. McIntyre, S.K. Seberg, Q. Wu (BNL)

The Higher-Order Mode (HOM) Dampers for the Relativistic Heavy-Ion Collider's (RHIC) 56 MHz cavity at Brookhaven National Laboratory (BNL) were fabricated at JLab. The coaxial damper is primarily constructed with high RRR niobium, with sapphire rings as the filter assembly. Several design changes have been made with respect to the performance of a prototype damper – also fabricated at JLab – which was found to quench at low power. The production dampers were tuned and tested in the JLab VTA prior to delivery and installation at BNL. Two completed HOM dampers have been delivered to BNL; they are to be used in the RHIC in November, 2015. This paper outlines the challenges faced in the fabrication process, and the improved performance due to the design changes.

THPB064 Radiation Hardness Tests of the LCLS II Piezo-Tuner with Gamma Rays

Y.M. Pischalnikov, B. Hartman, J.C. Yun (Fermilab)

LCLS II fast tuner designed with low voltage piezo-electrical actuators. Actuators will be operate at high radiation environment during many years. Stability of the piezo-actuators parameters versus overall gamma ray dose irradiation will be analyzed and discussed.

THPB065 Reliability of the LCLS II SRF Cavity Tuner

Y.M. Pischalnikov, J.P. Holzbauer, W. Schappert, J.C. Yun (Fermilab)

SRF cavity tuner for LCLS II installed inside cryomodule and must to work reliably for more than 20 years. Tuner's active components- electromechanical actuator and piezo-actuators must work reliable inside insulating vacuum environment for life of the machine. Summary of the accelerated lifetime tests of the piezo actuators inside cold/ insulated vacuum environment will be presented.

THPB066 RF Analysis of Equator Welding Stability for the European XFEL Cavities

A.A. Sulimov (DESY)

The problems with HOM damping during the European XFEL cavities manufacturing were required the detailed analysis of mechanical quality production. The mechanical measurements are enough precise to control the shape of cavity parts, but cannot be used for welded cavity. To estimate the shape deformation during equator welding, the eigenfrequencies of cavity cells can be compared with frequencies of cavity parts. This simple RF analysis can indicate irregularity of 9 equator welds.

THPB067 HOM Coupler Notch Filter Tuning for the European XFEL Cavities

A.A. Sulimov (DESY)

The notch filter (NF) tuning prevent the extraction of fundamental mode (1.3 GHz) RF power through HOM couplers. The procedure of NF tuning was optimized at the beginning of serial European XFEL cavities production. It allows keeping the filter more stable to temperature and pressure changes during cavity cool down. Some statistics of NF detuning before Module cold tests is presented.

THPB068 Practical Aspects of HOM Suppression Improvement for TM011

A.A. Sulimov, A. Ermakov, J.H. Thie (DESY) A. Gresele (Ettore Zanon S.p.A., Nuclear Division)

Some HOM pass bands were controlled during cryo-tests at DESY for the Eu-XFEL Cavities. The second monopole mode (TM011) showed the most instabilities and damping degradations. The authors will explain this phenomenon and present the practical method of TM011 damping improvement.

THPB069 Engineering Design and Prototype Fabrication of HOM couplers for HL-LHC Crab Cavities

C. Zanoni, K. Artoos, S. Atieh, I. Aviles Santillana, R. Calaga, O. Capatina, T. Capelli, F. Carra, L. Dassa, G. Favre, P. Freijedo Menendez, M. Garlaschè, J.-M. Geisser, N. Kuder, S.A.E. Langeslag, R. Leuxe, L. Marques Antunes Ferreira, F. Motschmann, D. Pognat, E. Rigutto (CERN) S.A. Belomestnykh, S. Verdú-Andrés, Q. Wu, B. P. Xiao (BNL) G. Burt (Lancaster University) S.U. De Silva, J.R. Delayen, R.G. Olave, H. Park (ODU) T.J. Jones, N. Templeton (STFC/DL) Z. Li (SLAC) A.J. May, S.M. Pattalwar (STFC/DL/ASTeC) T.H. Nicol (Fermilab) A. Ratti (LBNL)

The High-Luminosity upgrade for the LHC relies on a set of RF Crab Cavities for reaching its goals. Two parallel concepts, the Double Quarter Wave (DQW) and the RF Dipole (RFD), are going through a comprehensive design process along with preparation of fabrication in view of extensive tests with beam in SPS. High Order Modes (HOM) couplers are critical in providing damping in RF cavities for operation in accelerators. HOM prototyping and fabrication have recently started at CERN. In this paper, an overview of the final shape is provided along with an insight in the mechanical and thermal analyses performed to validate the design of these critical components. Emphasis is also given to test campaigns, material selection, prototyping and initial fabrication that are aimed at fulfilling the highly demanding tolerances of the couplers.

THPB070 Design of Dressed Crab Cavities for the High Luminosity LHC Upgrade

C. Zaroni, K. Artoos, S. Atieh, I. Aviles Santillana, J.P. Brachet, R. Calaga, O. Capatina, T. Capelli, F. Carra, L. Dassa, G. Faure, P. Freijedo Menendez, M. Garlaschè, M. Guinchard, N. Kuder, S.A.E. Langeslag, R. Leuxe, L. Prever-Loiri (CERN) S.A. Belomestnykh, S. Verdú-Andrés, Q. Wu, B. P. Xiao (BNL) G. Burt (Lancaster University) S.U. De Silva, R.G. Olave, H. Park (ODU) J.R. Delayen (JLab) T.J. Jones, N. Templeton (STFC/DL) Z. Li (SLAC) K.B. Marinov, A.J. May, S.M. Patalwar (STFC/DL/ASTeC) T.H. Nicol (Fermilab) A. Ratti (LBNL)

RF Crab Cavities are one of the key systems for increasing the LHC luminosity by a factor 10 beyond the design value. In view of extensive tests with beam in SPS, two concepts for the design of such systems are being developed: the Double Quarter Wave (DQW) and the RF Dipole (RFD). Cavities built out of thin niobium plates require external stiffeners in order to sustain the loads applied through their lifetime. Adequate cooling and efficient magnetic shielding are necessary to reach the required kick gradients and maintain the performance. To minimize the deformation of the cavity during assembly and operation, a design of the He-vessel with bolts, for structural strength, and superficial welds, to guarantee vacuum integrity, is proposed. This approach, which is not standard practice for He-tanks, will be reviewed in this paper. At the same time, an overview of the design and fabrication status of the cavity and its components will be provided.

THPB071 Developments of SiC Dampers for SuperKEKB Superconducting Cavity

M. Nishiwaki, K. Akai, T. Furuya, A. Kabe, S. Mitsunobu, Y. Morita (KEK)

Upgrade works for SuperKEKB is in the final stage and the commissioning operation will start in this JFY. Eight superconducting accelerating cavities were operated for more than ten years at the KEKB electron ring and will be used at SuperKEKB. The cavity operation at those high current accelerators requires sufficient absorption of the beam-induced HOM power. In KEKB, the absorbed HOM power of 16 kW in two ferrite dampers attached to each cavity was achieved at the beam current of 1.4 A. On the other hand, the expected HOM power at SuperKEKB is calculated to be 37 kW in the beam current of 2.6 A. To cope with the HOM power issue, we developed additional HOM dampers made of SiC to be installed to the downstream of the cavity module. From precise calculations, it was found that the additional dampers reduce the HOM power loads of the ferrite dampers more effectively than the large beam pipe model of cavity module, which is another option to reduce the HOM loads. New SiC dampers were fabricated and high power-tested. Those SiC dampers successfully absorbed the expected HOM power. In this report, we will describe the results of calculations and high-power RF tests of new SiC dampers.

THPB072 Higher Order Mode Damping in a Higher Harmonic Cavity for the Advanced Photon Source Upgrade

S.H. Kim (ANL)

A superconducting higher-harmonic cavity (HHC) is under development for the Advanced Photon Source Upgrade based on a Multi-Bend Achromat lattice. This cavity will be used to improve the Touschek lifetime and the single bunch current limit by lengthening the electron beam. A single-cell 1.4 GHz (the 4th harmonic of the main RF) cavity is designed based on the TESLA shape. Two adjustable fundamental mode power couplers are included. The harmonic cavity voltage of 0.9 MV will be driven by the 200 mA (4.2 mA/bunch) beam. The RMS bunch length with the harmonic cavity is >50 ps. Higher-order modes (HOM) must be extracted and damped to minimize heating of RF structures such as the superconducting cavity and/or couplers and suppress possible beam instabilities. The HHC system is designed such that 1) most monopole and dipole HOMs are extracted along the beam pipes and damped in the 'beamline' silicon carbide absorbers and 2) a few HOMs resulting from introduction of the couplers are extracted through the coupler and dissipated in a room temperature water-cooled load. We will present time and frequency domain simulation results and discuss damping of HOMs.

THPB073 Beamline Silicon Carbide Higher Order Mode Damper for the Advanced Photon Source Upgrade Harmonic Cavity

S.H. Kim (ANL)

A superconducting higher harmonic cavity (HHC) is under development for Advanced Photon Source Upgrade based on a Multi-Bend Achromat lattice. The HHC improves the Touschek lifetime and the single bunch current limit by lengthening the bunch. A TESLA-shaped single-cell 1.4 GHz (4th harmonic of the main RF) cavity will be used. Monopole and dipole higher order modes (HOMs) will be extracted primarily along the beam pipes and damped in a pair of 'beamline' silicon carbide (SiC) HOM dampers. These water-cooled SiC dampers will be placed just outside of the cryomodule. Maximum power dissipation in both SiC HOM dampers is estimated to be 1.7 kW at the beam current of 200 mA total and 4.2 mA max/bunch with the bunch length of RMS >50 ps. The SiC cylinder is cooled by a precision fit copper sleeve with water cooling channels. The thermal contact conductance at the interface between SiC and copper has been experimentally measured. In this paper, we will present design details of the SiC HOM dampers and experimental results of the thermal contact conductance at the interface.

THPB074 HOM Damping Scheme for 422 MHz Cavity

W. Xu, S.A. Belomestnykh, I. Ben-Zvi, H. Hahn (BNL)

A 422 MHz cavity was designed for high current FFA lattice ERLs for high luminosity eRHIC. The cavity was optimized to be able to propagate all the HOMs out of the cavity for high BBU threshold current and low HOM power (loss factor). Coupling the full spectrum (up to 30 GHz) HOMs out of the cavity and delivering the HOM power (up to 8 kW) out of the cryomodule is a challenge. A damping scheme with 6 coaxial line HOM couplers for low frequency HOMs and 3 waveguide HOM dampers for high frequency (so that the waveguide is small) is proposed to damp the full spectrum and high power HOMs. This paper will present the cavity design and HOM damping scheme.

THPB075 Coupler Quality Control at the Production Sites and the Evolution of the Acceptance Criteria

A. Gallas, H. Guler, W. Kaabi, D.J.M. Le Pinvidic, C. Magueur, M. Oublaid, A. Thiebault, A. Verguet (LAL) W.-D. Möller (DESY)

The coupler quality requested in the specifications evolved during the 3 production phases: prototyping, ramp up and mass production. Improvement and adaptation of the controls were necessary for some critical processes (copper coating). The tolerance range, especially the mechanical tolerance, the size and the criticality of some defects had been adapted to the industrial capability and the users requirement with the return of experience. The paper will explain how the mass production can affect and impact the procedure from R&D and initial industrialization procedures and how the communication and the additional control set in place to support an intensive weekly production.

THPB076 Quality Control of Welding, Brazing Joints and Cu Deposition on XFEL Coupler Parts

A. Ermakov, D. Kostin, W.-D. Möller (DESY)

In frames of XFEL Project the quality control of fundamental 1.3GHz power couplers is very important task. The power coupler consists of the number of parts including itself the different types of welding and brazing joints between ceramic, copper and stainless steel components. The quality of these joints is subject to be investigated and controlled according to XFEL Coupler specification taking into account the different Coupler manufacturers involved. The quality of Cu deposition on some XFEL coupler parts is also the issue to be qualified according to Specs. The number of microscope images of different types of joints and Cu deposition on some XFEL 1.3GHz coupler parts are presented.

THPB077 Modified TTF3 Couplers for LCLS-II

C. Adolphsen, K. Fant, Z. Li, C.D. Nantista, J. Tice, L. Xiao (SLAC) I.V. Gonin, K. Premo, N. Solyak (Fermilab)

The LCLS-II 4 GeV SC electron linac will use 280 TESLA cavities and TTF3 couplers, modified for CW operation with input power up to about 7 kW. The coupler modifications include shortening the antenna to achieve higher Qext and thickening the copper plating on the warm section inner conductor to lower the peak temperature. Another change is the use a waveguide transition box that is machined out of a solid piece of aluminum, significantly reducing its cost and improving its fit to the warm coupler window section. This paper describes the changes, simulations of the coupler operation (heat loads and temperatures), rf processing results and CW tests with LCLS-II dressed cavities.

THPB078 Status of the Power Couplers for the ESS Elliptical Cavity Prototypes

C. Arcambal (CEA/IRFU) P. Bosland, M. Desmons, G. Devanz, G. Ferrand, A. Hamdi, P. Hardy, H. Jenhani, F. Leseigneur, C. Marchand, F. Peauger, O. Piquet, D. Roudier, C. Servouin (CEA/DSM/IRFU) C. Darve (ESS)

In the frame of the European Spallation Source (ESS) project, a linear accelerator composed of a superconducting section is being developed. This accelerator owns two kinds of cavities called "medium beta cavity" ($\beta=0.67$) and "high beta cavity" ($\beta=0.86$). These cavities are equipped with RF power couplers whose main characteristics are: fundamental frequency: 704.42MHz, peak RF power: 1.1MW, repetition rate: 14Hz, RF pulse width>3.1ms. These couplers are common to the two cavities. The CEA Saclay is responsible for the design, the manufacture, the preparation and the conditioning of the couplers used for the Elliptical Cavities Cryomodule Technological Demonstrators (ECCTD). This work is performed in collaboration with ESS and the IPNO. This paper describes the coupler architecture, its different components, the main characteristics and the specific features of its elements (RF performance, dissipated power, cooling, coupler box test for the conditioning). The status of the manufacture of each coupler part is also presented.

THPB079 Improved Capacitive Coupling RF Power Couplers for a Cryomodule with Two 9-Cell Cavities

D.H. Zhuang, P.L. Fan, L.W. Feng, L. Lin, K.X. Liu, S.W. Quan, F. Wang, Z.L. Wang (PKU)

A capacitive coupling RF power coupler was used for the DC-SRF photoinjector at Peking University. Recently, improved capacitive coupling power couplers, which will be used for a new cryomodule with two 9-cell cavities have been designed and fabricated. The main modifications include enlarging the supporting rods of inner conductors in order to increase heat conduction, moving the bellows from the quarter-wave transformer to the 50 Ω coaxial line to avoid the mismatch during Qext adjusting, and changing the design of inner conductor to reduce the electric field of cold window. In this paper, detailed design based on multi-physics analysis and the conditioning of this improved capacitive coupling RF Power coupler will be presented.

THPB080 Next Generation Cavity and Coupler Interlock for the European XFEL

D. Tischhauser, A. Gössel, M. Mommertz (DESY)

The safe operation of cavities and couplers in the European XFEL accelerator environment is secured by a new technical interlock (TIL) design, which is based on the XFEL crate standard (MTCA(TM).4). The new interlock is located inside the accelerator tunnel. Several remote test capabilities ensure the correct operation of sensors for light, temperature and free electrons. Due to the space costs and the very high number of channels, the electronic concept was moved from a conservative, mostly analog electronic approach, with real comparators and thresholds, to a concept, where the digitizing of the signals is done at a very early stage. Filters, thresholds and comparators are moved into the digital part. The usage of an FPGA and an additional watchdog increase the flexibility dramatically, with respect to be as reliable as possible. An overview of the system is shown.

THPB081 FPC and HOM Test Boxes for HL-LHC Crab Cavities

A.R.J. Tutte, G. Burt (Cockcroft Institute, Lancaster University) R. Calaga, A. Macpherson, E. Montesinos (CERN) S.U. De Silva (ODU) Z. Li (SLAC) B. P. Xiao (BNL)

The LHC luminosity upgrade will involve the installation of thirty-two 400 MHz SRF crab cavities. The cavities have two variants known as the RF dipole and double quarter-wave crab cavities. Each cavity has a fundamental power coupler (FPC) at 400 MHz and two or three HOM couplers. Before integration onto the cavities it is necessary to condition the FPC, and to measure the transmission on the HOM couplers at low power to ensure the operate as designed, each requiring a special test box. The FPC test box should provide a high transmission between two couplers without creating high surface fields. The low power HOM test boxes should be terminated to a load such that the natural stop and pass-bands of the couplers are preserved allowing the reflection to be measured and compared to simulations. In addition, due to the possibility of high HOM power in the LHC crab cavities, the concept of creating a broadband high power HOM coupler test box in order to condition and test the couplers at high power has been investigated. The Rf design of all test boxes is presented and discussed.

THPB082 Design of QWR Power Coupler for the Rare Isotope Science Project in Korea

I. Shin, M.O. Hyun (IBS) E. Kako (KEK) C.K. Sung (Korea University Sejong Campus)

A power coupler has been designed and is being prototyped for the Rare Isotope Science Project (RISP) in South Korea. The power couplers will provides 4 kW RF power to 81.25 MHz superconducting quarter wave resonators with $\beta=0.047$. Design studies of the coupler are presented.

THPB083 Energetic Copper Coating on Stainless Steel Power Couplers for SRF Application

I. Irfan, S. Chapman, M. Krishnan, K.M. Velas (AASC)

Delivering RF power from the outside (at room temperature) to the inside of SRF cavities (at $\sim 4^\circ\text{K}$ temperature), requires a power coupler to be thermally isolating, while still electrically conducting on the inside. Stainless steel parts that are coated on the insides with a few skin depths of copper can meet these conflicting requirements. The challenge has been the adhesion strength of copper coating on stainless steel coupler parts when using electroplating methods. These methods also require a nickel flash layer that is magnetic and can therefore pose problems. Alameda Applied Sciences Corporation (AASC) uses Coaxial Energetic Condensation (CED) from a cathodic arc plasma to grow copper films directly on stainless steel coupler parts with no Ni layer and no electrochemistry. The vacuum arc plasma consists of $\sim 100\text{eV}$ Cu ions that penetrate a few monolayers into the stainless steel substrate to promote growth of highly adhesive films with crystalline structure. Adhesion strength and coating quality of copper coatings* on complex stainless steel structures (mock coupler parts), are discussed.

THPB084 Design of Input Coupler for RIKEN Superconducting Quarter-Wavelength Resonator

K. Ozeki, O. Kamigaito, N. Sakamoto, K. Suda, Y. Watanabe, K. Yamada (RIKEN Nishina Center) E. Kako, H. Nakai, K. Umemori (KEK) K. Okihira, K. Sennyu, T. Yanagisawa (MHI)

In RIKEN Nishina Center, for the purpose of development of elemental technology for the superconducting linear accelerator, the designing and construction of accelerator system based on superconducting quarter-wavelength resonator are carried out. The basic designs of the input coupler are as follows: The resonance frequency of the cavity is 75.5 MHz and assumed beam loading is about 1 kW. Double vacuum windows, which are disk-type, are adopted. A thermal anchor of 40 K is installed near the cold-window. The optimum positions of the cold-window and the thermal anchor depending on the effective RRR of copper-plate are being studied. In this contribution, the details of these designs will be reported. This work was funded by ImPACT Program of Council for Science, Technology and Innovation (Cabinet Office, Government of Japan).

- THPB085 Design of LCLS-II Fundamental Power Coupler for CW Operation**
K.S. Premo, I.V. Gonin, O.V. Prokofiev, N. Solyak (Fermilab) C. Adolphsen (SLAC)
 LCLSII is a planned upgrade project for the linear coherent light source (LCLS) at SLAC. The LCLSII linac will consist of thirtyfive 1.3 GHz and two 3.9 GHz superconducting RF continuous wave (CW) cryomodules that will be assembled in collaboration with SLAC. The LCLSII 1.3 GHz cryomodule design is based on the European XFEL pulsedmode cryomoduledesign with modifications needed for CW operation. Due to increased heating during CW operation modifications were required to the TTF3 type fundamental power coupler. This paper presents the design modifications required for CW operation in the LCLS-II cryomodules.
- THPB086 LCLS-II Fundemantal Power Coupler Mechanical Integreation**
K.S. Premo, T.T. Arkan, Y.O. Orlov, N. Solyak (Fermilab)
 LCLSII is a planned upgrade project for the linear coherent light source (LCLS) at SLAC. The LCLSII linac will consist of thirtyfive 1.3 GHz and two 3.9 GHz superconducting RF continuous wave (CW) cryomodules that Fermilab and Jefferson Lab will assemble in collaboration with SLAC. The LCLSII 1.3 GHz cryomodule design is based on the European XFEL pulsed mode cryomodule design with modifications needed for CW operation. The 1.3 GHz cryomodules for LCLSII will utilize a modified TTF3 syle fundamental power coupler design. Due to CW operation heat removal from the power coupler is critical. This paper presents the details of the mechanical integration of the power coupler into the cryomodule. Details of thermal braids, connections, and other interfaces are discussed.
- THPB087 Design and Simulation of High Power Input Coupler for C-ADS Linac 5-Cell Elliptical Cavities**
K.X. Gu, H.Y. Lin (Institute of High Energy Physics (IHEP), Chinese Academy of Sciences) T.M. Huang, Q. Ma, W.M. Pan (IHEP)
 Two 650 MHz elliptical cavity sections (elliptical 063, elliptical 082) are chosen to cover energy from about 150 MeV to 1.5 GeV for C-ADS Linac. RF power up to 150 kW in CW mode is required for the 5-cell elliptical cavity each by a fundamental power coupler (FPC). A planar RF window coaxial coupler has been designed to meet the power and RF coupling requirements. The coupler features a single cold window to enable assembling to cavity in class 10 clean room. This paper presents the coupler RF and thermal design, multipacting simulations of the C-ADS 5-cell elliptical coupler.
- THPB088 20 kW Power Couplers for the APS-U Harmonic Cavity**
M.P. Kelly, A. Barcikowski, Z.A. Conway, D. Horan, S.H. Kim, P.N. Ostroumov (ANL) S.V. Kutsaev (RadiaBeam)
 A pair of fundamental RF power couplers optimized for operation at 1.4 GHz will be used to extract up to 32 kW of continuous (CW) RF power from a bunch lengthening superconducting cavity installed into the APS Upgrade electron storage ring. The couplers provide the flexibility to maintain the required 0.9 MV harmonic cavity voltage over a range of beam currents and to avoid the Robinson instability. Each coupler will extract half of the power from the harmonic cavity, and will use a pair of simple rugged disc-shaped 80 mm diameter ceramic windows with a 50 Ω matching section. Results of electromagnetic and thermal simulations, as well as, prototyping and initial RF testing are presented.
- THPB089 HOM Coupler Performance in CW Regime in Horizontal and Vertical Tests**
N. Solyak, A. Grassellino, C.J. Grimm, A. Hocker, J.P. Holzbauer, T.N. Khabiboulline, O.S. Melnychuk, A.M. Rowe, D.A. Sergatskov, N. Solyak (Fermilab) J.K. Sekutowicz (DESY)
 Power dissipation in HOM coupler antenna can limit cavity gradient in cw operation. XFEL design of HOM coupler, feedthrough and thermal connection to 2K pipe was accepted for LCLS-II cavity based on simulation results. Recently a series of vertical and horizontal test was done to prove design for cw operation. In vertical test was found no effect of HOM coupler heating on high-Q cavity performance. In HTS HOM coupler was tested up-to 23MV/m cw mode. Result proves that XFEL HOM coupler meets LCLS-II specifications.
- THPB090 Study of LCLS-II Fundamental Coupler Thermal Connection**
N. Solyak, Y.O. Orlov, K.S. Premo, O.V. Prokofiev (Fermilab)
 LCLS-II fundamental coupler will operate at 7kW RF power in cw regime. To remove dissipated power at cryogenic environment a good design of straps is required to keep temperature of coupler under control. A test setup was built to study different configurations of straps and investigate effect of thermal contacts. For low temperature boundary condition a liquid nitrogen is used. Results of measuremets and cross-check with simulation are presented.
- THPB091 Mechanical Design of a High Power Coupler for the PIP-II 325 MHz SSR1 RF Cavity**
O.V. Pronitchev, S. Kazakov (Fermilab)
 The Project X Injector Experiment (PXIE) at Fermilab will include one cryomodule with eight 325 MHz single spoke superconductive cavities (SSR1). Each cavity requires approximately 2 kW CW RF power for 1 mA beam current operation. A future upgrade will require up to 8 kW RF power per cavity. Mechanical design of the Coupler, along with production status, are presented.
- THPB092 Mechanical Design of a High Power Coupler for the PIP-II 162.5 MHz RF Quadrupole**
O.V. Pronitchev, S. Kazakov, T.N. Khabiboulline, J. Steimel (Fermilab)
 Project X Injector Experiment (PXIE) at Fermilab will utilize a 162.5 MHz CW RFQ accelerating cavity. Mechanical design of a main coupler for PXIE RFQ is reported. Two identical couplers will deliver approximately 100 kW total CW RF power to RFQ. Fermilab has designed, procured and tested two couplers for the CW RFQ accelerating cavity. Mechanical design of the Coupler, along with production status, are presented.
- THPB093 A 1.3 GHz Waveguide to Coax Coupler for Superconducting Cavities With a Minimum Kick**
J.A. Robbins, C. Egerer, R.G. Eichhorn, V. Veshcherevich (Cornell University (CLASSE), Cornell Laboratory for Accelerator-Based Sciences and Education)
 Transversal forces as a result of asymmetric field generated by the fundamental power couplers have become a concern for low emittance beam in future accelerators. In pushing for smallest emittances, Cornell has finished a physics design for a symmetric coupler for superconducting accelerating cavities. This coupler consists of a rectangular waveguide that transforms into a coaxial line inside the beam pipe, eventually feeding the cavity. We will report on the RF design yielding to the extremely low transversal kick. In addition, heating, heat transfer and thermal stability of this coupler has been evaluated.
- THPB094 Status of the Fundamental Power Coupler Production for the European XFEL Accelerator**
S. Sierra, G. Garcin, C. Lievin, G. Vignette (TED) A. Gallas, W. Kaabi (LAL) M. Knaak, M. Pekeler, L. Zweibaeumer (RI Research Instruments GmbH)
 For the XFEL accelerator, Thales, RI Research Instrument and LAL are working on the manufacturing, assembly and conditioning of fundamental power couplers. 670 couplers have to be manufactured according to strict specifications. The paper describes the full production activity from the program starting to the currentphase with main measurements for the coupler characteristic: copper and TiN coating characteristics. The status of the production is given with an output rate of 8 couplers per week. The status for more than 500 couplers manufactured and conditionned is presented.

- THPB095 Automatic RF Conditioning Test Bench of Fundamental Power Couplers for the European XFEL Accelerator**
S. Sierra, C. Lievin, P. Rouillon (TED) H. Guler, W. Kaabi, A. Verguet (LAL)
 In order to perform the RF conditioning of the fundamental coupler for the XFEL accelerator, Thales and LAL developed together a test bench being able to make the automatic RF conditioning. The capability of this test bench is of 4 pairs of coupler at the same time with automatic sequences of increasing the RF power. The test bench is composed of the overall RF station providing up to 5 MW peak power at 1.3 GHz. The waveguide distribution allows 4 individual RF lines for conditioning, and the automatic sequence applied to the couplers in respect with all signals monitored and controlled during the RF process. The paper will also provide some examples of such process.
- THPB096 Lesson Learned on the Manufacturing of Fundamental Power Couplers for the European XFEL Accelerator**
S. Sierra, G. Garcin, C. Lievin, G. Vignette (TED) M. Knaak, M. Pekeler (RI Research Instruments GmbH)
 In this paper we described lesson learned during the production of Fundamental Power Coupler for the European XFEL accelerator and different steps necessary for obtaining a rate of 8 couplers a week. From the manufacturing of individual components up to the RF conditioning. This paper also propose some possible ways to be optimized for a future mass production of such components. With comparison of processes and adaptation which could benefit to an increase rate or a more secure program. Some of them which could be studied from the coupler definition to the manufacturing process in order to obtain a stable and possible increased rate or lower cost of production by decreasing the risks on programs. This analysis is based on a current production of more than 500 couplers
- THPB097 New Possible Configuration of 3.9 GHz Main Coupler**
S. Kazakov (Fermilab)
 LCLS-II superconducting accelerator supposes to use 3.9 GHz (3-d harmonic) superconductive cavities. New possible of configuration of 3.9 GHz main coupler is presented. This configuration contains two coaxial ceramic windows, cold and warm. Inner conductors of windows connected through capacitive gape and have no mechanical contact. It allows to avoid bellows and problem with bellow heating and cooling. Windows have protecting shields again electrons which prevents charging of ceramics. Results of computer simulation of coupler are posted.
- THPB098 Testing of 325 MHz Couplers at Test Stand in Resonance Mode**
S. Kazakov, B.M. Hanna, O.V. Pronitchev (Fermilab)
 Linear accelerator of PIP-II program utilizes two types of 325 MHz Single Spoke resonator cavities, SSR-I and SSR-II. Operating power of SSR-II is about 20 kW. It requires input couplers which can reliably work at power level > 20 kW with full reflection with any reflected phase. Currently only 10 kW RF power supply is available for coupler testing. To increase testing power the special resonance configuration were used. This configuration allows to increase RF power about 3 times. The testing scheme and results are discussed in the paper.
- THPB100 Nb Coatings on Bellows Used in SRF Accelerators**
S. Chapman, I. Irfan, M. Krishnan, K.M. Velas (AASC) S.A. Belomestnykh, J.C. Brutus, B. P. Xiao (BNL) S.A. Belomestnykh (Stony Brook University) N.Z. Khalil (SBU)
 Alameda Applied Sciences Corporation (AASC) is developing bellows with the strength and flexibility of stainless steel and the low surface impedance of a superconductor. Such unique bellows would enable alignment of cavity sections with greatly reduced RF losses. To that end, we grow Nb thin films via Coaxial Energetic Deposition (CED) from a cathodic arc plasma. The plasma from the cathode consists exclusively of 60-120eV Nb ions (Nb⁺ and Nb²⁺) that penetrate a few monolayers into the substrate and enable sufficient surface mobility to ensure that the lowest energy state (crystalline structure with minimal defects) is accessible to the film. Hetero-epitaxial films of Nb were grown on biased and unbiased stainless steel bellows, with and without an intermediate layer of Cu deposited via the same technique, to produce a working bellows with a well-adhered superconducting inner layer. The Nb-coated bellows have undergone tests conducted by our collaborators at Brookhaven National Laboratory to evaluate their RF performance.
- THPB101 Forward Power Couplers for CADS**
T.M. Huang, X. Chen, H.Y. Lin, Q. Ma, W.M. Pan (IHEP) K.X. Gu (Institute of High Energy Physics (IHEP), Chinese Academy of Sciences)
 Forward Power couplers are key components of the superconducting system for China Accelerator Driven sub-critical System (CADS) project. CADS includes four types of superconducting cavities (SCCs) of two frequencies, 162.5 MHz and 325 MHz up to the energy of 25 MeV. Two kinds of power couplers for injector-I 325 MHz Spoke012 SCC and injector-II 162.5 MHz HWR010 SCC have been designed, fabricated, high power tested, assembled with cavities and operated with beam. The design of the main linac power couplers has also been completed recently. This paper will describe the development status of the forward power couplers for CADS in details.
- THPB102 RF Conditioning of the XFEL Power Couplers at the Industrial Scale**
W. Kaabi, A. Gallas, H. Guler, D.J.M. Le Pinvidic, C. Magueur, M. Oublaïd, A. Thiebault, A. Verguet (LAL)
 LAL has in charge the production monitoring and the RF conditioning of 800 power couplers to equip 100 XFEL cryomodules. The conditioning process and all the preceding preparation steps are performed in a 70m² clean room. This infrastructure, its equipment and the RF station are designed to allow the treatment of 8 couplers in the same time, after a ramp-up phase. Clean room process and conditioning results are presented and discussed.
- THPB103 High Power Coupler Test for Ariel SC Cavities**
Y. Ma, P.R. Harmer, D. Lang, R.E. Laxdal, B.S. Waraich, V. Zvyagintsev (TRIUMF, Canada's National Laboratory for Particle and Nuclear Physics)
 TRIUMF ARIEL (The Advanced Rare Isotope Laboratory) project employs five 1.3 GHz 9-cell superconducting elliptical cavities for acceleration of 10 mA electron beam up to energy of 50 MeV. 100 kW CW RF power will be delivered into each cavity by means of pair of Power Couplers: 50 kW per each coupler. Before installing the power couplers with the cavities, they are to be assembled and conditioned with a 30 kW IOT. Six couplers have been conditioned under room temperature and four of them have been installed and tested during beam commissioning. In this paper, test results of the power couplers will be described.
- THPB104 Coupler Design for 800 MHz Superconducting Cavity**
Ya. V. Shashkov, N.P. Sobenin (MEPhI)
 During the superconducting resonator development it is necessary to consider the input power geometry that will be able to provide wide range of external quality factor. Unfortunately power coupler may break axial symmetry of the field in the structure leading to appearance of transverse voltage on the axis resulting in beam emittance increase. Geometry of the coupler placed in the drift tube was optimized in order to reduce these negative effects. An option with power input placed to quarter-wave resonator attached to the drift tube and two power couplers were analyzed. Comparison of these options is also given.

- THPB105 Demonstration of Coaxial Coupling Scheme at 26 MV/M for 1.3 GHz TeslaType SRF Cavities**
Y. Xie, A. Kanareykin (Euclid TechLabs, LLC) T.N. Khabiboulline, A. Lunin, V. Poloubotko, A.M. Rowe, N. Solyak, V.P. Yakovlev (Fermilab) J. Rathke (AES)
Superconducting ILC-type cavities have an rf input coupler that is welded on. A detachable input coupler will reduce conditioning time (can be conditioned separately), reduce cost and improve reliability. The problem with placing an extra flange in the superconducting cavity is about creating a possible quench spot at the seal place. Euclid Techlabs LLC has developed a coaxial coupler which has an on the surface with zero magnetic field (hence zero surface current). By placing a flange in that area we are able to avoid disturbing surface currents that typically lead to a quench. The coupler is optimized to preserve the axial symmetry of the cavity and rf field. The surface treatments and rf test of the proto- type coupler with a 1.3 GHz ILC-type single-cell cavity at Fermilab will be reported and discussed.
- THPB106 Results of the RF Conditioning of the SPIRAL2 Couplers**
Y. Gómez Martínez, M.A. Baylac, P. Boge, T. Cabanel, P. De Lamberterie, M. Marton, R. Micoud (LPSC)
All the high power couplers for SPIRAL2 have been prepared and successfully tested inside the cryomodules. The results of the RF conditioning for the 28 couplers and main technical difficulties encountered are presented.
- THPB107 Optimization of FRIB HWR Cavities' Power Coupler**
Z. Zheng (FRIB)
The baseline power coupler for FRIB HWR cavities requires multipacting conditioning at operating RF power. Conditioning takes a lot of time and RF power, and its elimination is highly desirable. To significantly shorten the RF conditioning, we developed a multipacting-free coupler design. This paper reports the latest progress in the optimization of multipacting-free coupler. The choke structure is removed and coupler geometry is further modified to keep the coupler RF window screened from the electron bombardment.
- THPB109 ESS Spoke Cryomodule and Test Valve Box**
D. Reynet, S. Bousson, S. Brault, P. Duchesne, P. Duthil, N. Gandolfo, G. Olry, M. Pierens, E. Rampnoux (IPN)
ESS project aims being the world's most powerful neutron source feeding multidisciplinary researches. The superconducting part of the ESS linear accelerator includes 28 b=0.5 352.2 MHz SRF niobium double Spoke cavities. Paired in 13 cryomodules and held at 2K in a saturated helium bath those cavities will generate of an accelerating field of 9MV/m. The prototype Spoke cryomodule holds two cavities and their RF power couplers and integrates all the interfaces necessary to be operational within the linac machine. It is now being fabricated and its assembly will be performed with dedicated tooling and procedures in and out of the clean room. This prototype will be tested by the end of 2015 at IPNO site and then at full power at FREIA (Uppsala university) test stand. A valve box has thus been designed to take into account the specific features of this prototype cryomodule and of the cryogenic environments of both test sites. This valve box is also considered as a prototype of the cryogenic distribution of the linac Spoke section. This element will then be used for the tests of the series cryomodules. We propose to present this prototype Spoke cryomodule for ESS and the test valve box.
- THPB110 Procurements for LCLS-II Cryomodules at JLab**
E. Daly, G. Cheng, G.K. Davis, M.A. Drury, T. Hiatt, N.A. Huque, F. Marhauser, H. Park, K.M. Wilson (JLab) J.P. Preble (JLAB)
The Thomas Jefferson National Accelerator Facility is currently engaged, along with several other DOE national laboratories, in the Linac Coherent Light Source II project (LCLS II). The SRF Institute at Jefferson Lab will be building 1 prototype and 17 production cryomodules based on the TESLA / ILC / XFEL design. Each cryomodule will contain eight nine cell cavities with coaxial power couplers operating at 1.3 GHz. Procurement of components for cryomodule construction has been divided amongst partner laboratories in a collaborative manner. JLab has primary responsibility for six procurements include the dressed cavities, cold gate valves, higher-order-mode (HOM) and field probe feedthroughs, beamline bellows cartridges, cavity tuner assemblies and HOM absorbers. For procurements led by partner laboratories, JLab collaborates and provides technical input on specifications, requirements and assembly considerations. This paper will give a detailed description of plans and status for JLab procurements.
- THPB111 Cooling Optimization for High Q Dressed Cavities in Cryomodule**
G. Wu, A. Grassellino, J.A. Kaluzny, T.J. Peterson (Fermilab)
Maintaining very high cavity Q0 in linac applications creates new challenges for cryomodule design. Increasing thermal gradients during Tc transition in a horizontal dressed cavity became an important operational requirement to expel the magnetic flux as much as possible. To obtain the high thermal gradient, many cryogenic operational parameters can be optimized such as mass flow through the helium vessel, pressure variation through the helium circuit, two phase component ratio and etc. This paper will describe experimental data, compare that to simulation and correlate the thermal gradient to magnetic flux expulsion and cavity performance. New design and operational procedures will be proposed.
- THPB113 Electromagnetic Induced Heating in RF Cables of LCLS-II 1.3 GHz Cryo-Module**
M.H. Awida, T.N. Khabiboulline, N. Solyak (Fermilab)
Electromagnetic heating is a critical issue in the RF cables of LCLS-II cryo-modules given the relatively large amount of RF power expected to flow out of the higher order mode (HOM) cavity ports, which can be up to 10W. The large amount of RF power flowing out of the HOM ports can significantly raise the temperature on the cable well beyond acceptable limits. A careful design for the thermal strapping to cool the cable is needed. Moreover, low loss cables (<0.3dB/m) are needed to avoid the excessive heating that can produce a quench on the HOM feed-through. Also static heat load to cryogenic system should be as low as possible. In this paper, we analyze the RF heating in the RF cables assuming various scenarios for cable loss and cable strapping.
- THPB114 Thermo-Mechanical Study of the Support Frame for the IFMIF Cavity String**
N. Bazin (CEA/DSM/IRFU)
The IFMIF LIPAc cryomodule houses eight half-wave resonators and eight solenoids cooled at liquid helium temperature. All these components are supported by a 5-meter long frame and precisely aligned before closing the vacuum tank and cooling down the system. As the support frame is one of the key elements of the alignment system of the cavity string, great care must be taken to limit its mechanical deformation. The scope of the study is to analyze the mechanical behavior of the frame during cooling. The paper will present the actions taken to improve the cooling time while limiting the thermal gradient in the support frame.
- THPB115 ARIEL e-Linac Cryomodule - Design and Performance**
N. Muller, P.R. Harmer, J.J. Keir, A. Koveshnikov, D. Lang, R.E. Laxdal, Y. Ma, W.R. Rawnsley, B.S. Waraich, Z.Y. Yao, V. Zvyagintsev (TRIUMF, Canada's National Laboratory for Particle and Nuclear Physics)
TRIUMF's ARIEL project includes a 50 MeV-10mA electron linear accelerator (e-Linac) using 1.3 GHz superconducting technology. The accelerator consists of three cryomodules; an injector cryomodule with one cavity and two accelerating cryomodules with two cavities each. One injector and one accelerator have been assembled and commissioned at TRIUMF with a second injector cryomodule being assembled for VECC in Kolkata. Both Injector and Accelerator cryomodules utilize a top-loaded cold mass design contained in a box-type cryomodule; design and early test results of both cryomodules are presented.

- THPB116 Modified ELBE Type Cryomodules for the Mainz Energy Recovering Superconducting Accelerator MESA**
T. Stengler, K. Aulenbacher, R.G. Heine, F. Schlender, D. Simon (IKP) M. Pekeler, D. Trompetter (RI Research Instruments GmbH)
 At the Institut für Kernphysik of Johannes Gutenberg-Universität Mainz, the new multiturn energy recovery linac MESA is under construction. Two modified ELBE-type cryomodules with two 9-cell TESLA/XFEL cavities each will provide an energy gain of 50 MeV per turn. Those are currently in the production process at RI Research Instruments GmbH, Bergisch Gladbach, Germany. Modifications for the tuner and the HOM damper are under development. In addition, a 4K/2K Joule Thomson expansion stage will also be integrated into the cryomodule. The current status of the development of the cryomodules and their modifications will be discussed.
- THPB117 Thermal Load and Assembly for QWR, HWR, SSR1 and SSR2**
W.K. Kim, H. Kim, H.J. Kim, Y. Kim (IBS)
 The heavy ion accelerator that will be built in Daejeon, Korea utilizes superconducting cavities operating in 2 K, 4.5K. The cavities are QWR (quarter wave resonator), HWR (half wave resonator), SSR1 (sing spoke resonator 1) and SSR2 (sing spoke resonator 2). The main role of the cryomodule is supplying thermal insulation for cryogenic operation of the cavities and maintaining cavities' alignment. Thermal and structural consideration such as thermal load by heat leak and heat generation, cryogenic fluid management, thermal contraction, and so on. This paper describes detailed design considerations and current results have being done including thermal load estimation.
- THPB118 First Cool-Down Test of HWR Cryomodule for RAON**
Y. Kim, Y.W. Jo, H. Kim, H.J. Kim, W.K. Kim, M. Lee (IBS)
 The prototyping of the cryomodules that will be utilized for the heavy ion accelerator in Korea had been done in 2014. One of the cryomodules that contains two HWR (Half Wave Resonator) cavities was tested. It was cooled down to liquid helium temperatures and the static thermal load is measured at both 4.2 K and 2.5 K. Also, it was successfully cooled down below lambda point of the helium with warm vacuum pumping system. No cold leak and superleak was observed during the cool-down. The detailed specifications of the cryomodule and the experimental results are reported in this paper.
- THPB119 LCLS-II 1.3 GHz Cryomodule Design – Modified TESLA-Style Cryomodule for CW Operation**
T.J. Peterson, T.T. Arkan, C.M. Ginsburg, Y. He, J.A. Kaluzny, M.W. McGee, Y.O. Orlov (Fermilab)
 We will present the design of the 1.3 GHz cryomodule for the Linear Coherent Light Source upgrade (LCLS-II) at SLAC. Fermilab is responsible for the design of this cryomodule, a modified TESLA-style cryomodule to accommodate continuous wave (CW) mode operation and LCLS-II beam parameters, consisting of eight 1.3 GHz superconducting RF cavities, a corrector magnet package, and instrumentation. Thirty-five of these cryomodules, approximately half built at Fermilab and half at Jefferson Lab, will become the main accelerating elements of the 4 GeV linac. The modifications and special features of the cryomodule include: thermal and cryogenic design to handle high heat loads in CW operation, magnetic shielding and cool-down configurations to enable high quality factor (Q0) performance of the cavities, liquid helium management to address the different liquid levels in the 2-phase pipe with 0.5% SLAC tunnel longitudinal slope, support structure design to meet California seismic design requirements, and with the overall design consistent with space constrains in the existing SLAC tunnel. The prototype cryomodule assembly will begin in August 2015 and is to be completed in early 2016.
- THPB120 Status of LCLS-II QA Systems Collaboration Cryomodule Construction at TJNAF & FNAL**
E.A. McEwen, V. Bookwalter, J. Leung (JLab) J.N. Blowers, J.B. Szal (Fermilab)
 At the Thomas Jefferson National Accelerator Facility (JLab), we are supporting the LCLS-II Project at SLAC. The plan is to build thirty-five 1.3 GHz continuous wave cryomodules, production to be split between JLab and FNAL (Fermilab). This has required a close collaboration between the partner labs, including enhancing our existing quality systems to include this collaboration. This over view describes the current status of the Quality System development as of August 2015, when the partner labs start the assembly of the prototype cryomodules.

18-Sep-15 08:00 – 10:00	Oral	Sea to Sky Ballroom A
FRAA — Cryomodules		
Chair: E. Kako (KEK)		

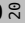
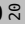

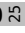
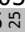
- FRAA01 08:00** **Overview of Recent Tuner Development on Elliptical and Low-Beta Cavities**
R. Paparella (INFN/LASA)
 The talk will provide an overview on the latest advances of tuner development for SRF applications. Issues and present approaches on how to resolve them will be emphasized for both TM and TEM cavities and examples from various labs and projects (XFEL, LCLS-II, ESS, SPL, ARIEL, SPIRAL2, FRIB, ANL, IFMIF) will be given in order to better explain issues and solutions. Details on author's contributions to European-XFEL tuner activity for 1.3 GHz and 3.9 GHz cavities will be also shown.
- FRAA02 08:20** **Module Performance in XFEL Cryomodule Mass-Production**
O. Napoly (CEA/DSM/IRFU)
 The European XFEL cryomodule assembly is executed in CEA-Saclay premises and infrastructure by an industrial company, Alsym, under the supervision of CEA. The nominal assembly throughput and delivery rate of one cryomodule per week has been reached with XM15 in October 2015. With a throughput of 4 days in place in January 2015 with XM26, the delivery of XM100 is currently foreseen before mid-2016. This contribution will present the status of this large scale production project, insisting on the challenges, both technical and organizational, for achieving the quantitative production goal, and on the enhanced quality control put in place in parallel to achieve the qualitative goals in term of module conformance and RF performance. Mitigation of non-conformities generated by the accelerator components, by the assembly tools and finally by the assembly process is essential to eliminate their impact on the production schedule and, especially for the last category, on the module acceptance. The most significant module test results will be discussed with emphasis on their correlation (or lack of thereof) to detailed assembly conditions and their evolution.
- FRAA03 08:40** **High Gradient Performance in Fermilab ILC Cryomodule**
E.R. Harms, C.M. Baffes, K. Carlson, B.E. Chase, D.J. Crawford, E. Cullerton, D.R. Edstrom, A. Hocker, M.J. Kucera, J.R. Leibfritz, J.N. Makara, D. McDowell, O.A. Nezhevenko, D.J. Nicklaus, Y.M. Pischalnikov, P.S. Prieto, J. Reid, W. Schappert, W.M. Soyars, P. Varghese (Fermilab)
 Fermilab has assembled an ILC like cryomodule using U.S. processed high gradient cavities and achieved an average gradient of 31.5 MV/m for the entire cryomodule. Test results and challenges along the way will be discussed.
- FRAA04 09:00** **Performance of the Cornell ERL Main Linac Prototype Cryomodule**
F. Furuta, B. Clasby, R.G. Eichhorn, B. Elmore, G.M. Ge, D. Gonnella, D.L. Hall, G.H. Hoffstaetter, R.P.K. Kaplan, J.J. Kaufman, M. Liepe, J.T. Maniscalco, T.I. O'Connel, S. Posen, P. Quigley, D.M. Sabol, J. Sears, E.N. Smith, V. Veshcherevich (Cornell University (CLASSE), Cornell Laboratory for Accelerator-Based Sciences and Education)
 Cornell has designed, fabricated, and tested (by the time of the conference) a high current (100 mA) CW SRF prototype cryomodule for the Cornell ERL. This talk will report on the design and performance of this very high Q0 CW cryomodule including design issues and mitigation strategies.
- FRAA05 09:20** **Conditioning and Beam Test of a 1.3 GHz Cryomodule with 2X9-Cell Cavity**
F. Zhu, K.X. Liu (PKU)
 For a future FEL project based on an SRF accelerator in China, a 1.3GHz cryomodule containing two 9-cell cavities has been designed and assembled at Peking University. The conditioning and beam test of this cryomodule using a DC-SRF gun as an injector shall be presented. Cryomodule design features and issues, mitigation strategies and results of engineering tests and beam tests should be presented.
- FRAA06 09:40** **Construction and Performance of FRIB Quarter Wave Prototype Cryomodule**
S.J. Miller, B. Bird, G.D. Bryant, B. Bullock, N.K. Bultman, F. Casagrande, C. Compton, A. Facco, P.E. Gibson, J.D. Hulbert, D. Morris, J. Popielarski, L. Popielarski, M.A. Reaume, R.J. Rose, K. Saito, M. Shuptar, J.T. Simon, B.P. Tousignant, J. Wei, K. Witgen, T. Xu (FRIB) A. Facco (INFN/LNL)
 The driver linac for the Facility for Rare Isotope Beams (FRIB) will require the production of 48 cryomodules. FRIB has completed the fabrication and testing of a $\beta=0.085$ quarter-wave cryomodule as a pre-production prototype. This cryomodule qualified the performance of the resonators, fundamental power couplers, tuners, and cryogenic systems of the $\beta=0.085$ quarter-wave design. In addition to the successful systems qualification; the ReA6 cryomodule build also verified the FRIB bottom up assembly and alignment method. The lessons learned from the ReA6 cryomodule build, as well as valuable fabrication, sourcing, and assembly experience are applied to the design and fabrication of FRIB production cryomodules. This paper will report the results of the $\beta=0.085$ quarter-wave cryomodule testing, fabrication, and assembly; production implications to future cryomodules will also be presented. Authors:

18-Sep-15 10:30 – 12:20

Oral

Sea to Sky Ballroom A

FRBA — Closing Session**Chair:** R.E. Laxdal (TRIUMF, Canada's National Laboratory for Particle and Nuclear Physics)

- FRBA01**
10:30  **Technical and Logistical Challenges for IFMIF-LIPAC Cryomodule Construction**
H. Dzitko, N. Bazin, S. Chel, G. Devanz (CEA/IRFU) D. Gex, G. Phillips (F4E) J. Knaster (IFMIF/EVEDA) D. Regidor, F. Toral (CIEMAT)
This paper provides an overview of the final design and fabrication status of the IFMIF cryomodule, including the design issues, and deal with the strategies implemented in order to mitigate the magnetic risk, take into account seismic constraints, optimize operations and take into account the licensing requirements. The transportation issue, assembly process, and integration on the beam line are also addressed. The IFMIF cryomodule presented here will be part of the LIPAc project (Linear IFMIF Prototype Accelerator). It is a full scale prototype of one of the IFMIF accelerators, from the injector to the first cryomodule, aiming at validating the technical options for the future accelerator-based D-Li neutron source to produce high intensity high energy neutron flux. The cryomodule contains all the equipment to transport and accelerate a 125 mA deuteron beam from an input energy of 5 MeV up to 9 MeV. It consists of a horizontal cryostat of around 6 m long, 3 m high and 2 m wide, which includes 8 superconducting HWRs for beam acceleration working at 175 MHz and at 4.5 K, 8 power couplers to provide RF power to cavities, and 8 Solenoid Packages as focusing elements.
- FRBA02**
10:50  **Crab Cavity and Cryomodule Development for HL-LHC**
F. Carra, K. Artoos, S. Atieh, I. Aviles Santillana, A.B. Boucherie, K. Brodzinski, R. Calaga, O. Capatina, T. Capelli, L. Dassa, T. Dijoud, H.M. Durand, G. Favre, P. Freijedo Menendez, M. Garlaschè, M. Guinchard, N. Kuder, S.A.E. Langeslag, R. Leuxe, A. Macpherson, P. Minginette, E. Montesinos, C. Parente, V. Rude, M. Sosin, G. Vandoni, G. Villiger, C. Zanoni (CERN) S.A. Belomestnykh, S. Verdú-Andrés, Q. Wu, B. P. Xiao (BNL) G. Burt (Lancaster University) S.U. De Silva, J.R. Delayen, R.G. Olave, H. Park (ODU) T.J. Jones, N. Templeton (STFC/DL) Z. Li (SLAC) K.B. Marinov, S.M. Patilwar (STFC/DL/ASTeC) T.H. Nicol (Fermilab) A. Ratti (LBNL)
The HL-LHC project aims at increasing the LHC luminosity by a factor 10 beyond the design value. The installation of a set of RF Crab Cavities to increase bunch crossing angle is one of the key upgrades of the program. Two concepts, Double Quarter Wave (DQW) and RF Dipole (RFD) have been proposed and are being produced in parallel for test in the SPS beam before the next long shutdown of CERN accelerator's complex. In the retained concept, two cavities are hosted in one single cryomodule, providing thermal insulation and interfacing with RF coupling, tuning, cryogenics and beam vacuum. This paper overviews the main design choices for the cryomodule and its different components, which have the goal of optimizing the structural, thermal and electro-magnetic behavior of the system, while respecting the existing constraints in terms of integration in the accelerator environment. Prototyping and testing of the most critical components, manufacturing, preparation and installation strategies are also described.
- FRBA03**
11:10  **SRF and Compact Accelerators for Industry and Society**
R.D. Kephart (Fermilab)
Accelerators developed for Science now are used broadly for industrial, medical, and security applications. Over 30,000 accelerators touch over \$500B/yr in products producing a major impact on our economy, health, and well being. Industrial accelerators must be cost effective, simple, versatile, efficient, and robust. Many industrial applications require high average beam power. Exploiting recent advances in Superconducting Radio Frequency (SRF) cavities and RF power sources as well as innovative solutions for the SRF gun and cathode system, a collaboration of Fermilab-CSU-NIU has developed a design for a compact SRF high-average power electron linac. Capable of 3-50 kW average power and continuous wave operation this accelerator will produce electron beam energies up to 10 MeV and small and light enough to mount on mobile platforms, such accelerators will enable new in-situ environmental remediation methods and new applications involving in-situ crosslinking of materials. More importantly, we believe this accelerator will be the first of a new class of simple, turn-key SRF accelerators that will find broad application in industry, medicine, security, and science.
- FRBA04**
11:30  **SRF for Future Circular Colliders**
R. Calaga, O. Brunner, A.C. Butterworth, E. Jensen (CERN)
The future circular colliders (FCC) will require superconducting RF systems for the proton-proton, electron-positron and lepton-hadron modes of the collider operation. The SCRF systems will accelerate the protons beams to 50 TeV and the lepton beams from 45.5 to 175 GeV in a staged approach with a possible 60 GeV energy recovery linac for the lepton-hadron to option as an intermediate step. The expected stored beam currents in some modes exceed 1 A with very short bunch lengths. A first conceptual design of the FCC RF system is proposed along with highlights of specific R&D topics to reach the design performance. Challenges related to RF structure design, intensity limitations due to beam loading, RF powering and higher order modes are addressed. Synergies between the different collider modes and the present LHC are identified.
- FRBA05**
11:55  **Keynote Talk: Scientific Opportunities at LCLS-II - the High Repetition Rate Revolution**
W.F. Schlotter (SLAC)
Keynote Talk: Scientific Opportunities at LCLS-II

Author Index

Boldface papercodes indicate primary authors

— A —

Abdelwhab, M.E. THPB062
 Abidi, S.H. MOPB050
 Aderhold, S. MOPB079, **MOPB090**
 Adolphsen, C. TUPB012, THPB007, THPB008, **THPB077**, THPB085
 Afanador, R. MOPB115, THBA01, MOPB112
 Agustsson, R.B. THPB042
 Akai, K. MOPB116, THPB071
 Albrecht, C. MOPB076, TUPB018, THPB056
 Amberg, M. MOPB065, MOPB066, MOPB067, TUPB020, TUPB075
 Anders, W. THPB026
 Andrews, R. TUPB014
 Ang, Z.T. TUA002, **TUPB011**
 Anlage, S. M. MOPB119
 Antoine, C.Z. **TUPB057**, TUPB058
 Arcambal, C. TUPB007, THPB028, **THPB078**
 Arkan, T.T. MOPB087, **TUPB110**, THPB005, THPB086, THPB119
 Armstrong, J. TUPB113
 Arnold, A. TUPB010, **THPB055**, THPB057
 Arsenyev, S. **WEA2A02**
 Artoos, K. TUPB101, **THPB060**, THPB069, THPB070, FRBA02
 Atieh, S. TUPB101, **THAA05**, THPB048, THPB069, THPB070, FRBA02
 Au, T. TUA002
 Aulenbacher, K. MOPB066, MOPB067, TUPB015, TUPB075, TUPB020, THPB116
 Aull, S. **TUBA03**, TUPB029, **TUPB050**, TUPB051, TUPB080
 Aviles Santillana, I. THPB069, THPB070, FRBA02
 Avrakhov, P.V. THPB011, THPB012
 Avrillaud, G. THAA05
 Awida, M.H. MOPB087, **THPB113**

— B —

Baars, D.C. MOPB045
 Baboi, N. TUPB018
 Bachimanchi, R. TUPB009
 Baffes, C.M. TUPB013, TUPB014, FRAA03
 Bala, V.R. TUPB092
 Ball, J.A. TUPB093, THBA01
 Bandelmann, R. MOPB103, TUPB105
 Bane, K.L.F. **THPB007**
 Barbanotti, S. TUPB018, **TUPB108**, THPB025
 Barcikowski, A. WEBA05, THPB088
 Barker, B.W. TUPB022
 Barlak, M. THPB056
 Barlow, G. TUPB106
 Barnhart, D.L. THBA01, MOPB112
 Barth, W.A. MOPB066, MOPB067, TUPB020, TUPB075, TUPB015

Bártová, B. TUPB027
 Basovic, M. **MOPB047**
 Basten, M. MOPB065, **MOPB066**, MOPB067, TUPB075
 Baumier, C. B. TUPB058
 Baylac, M.A. THPB106
 Bazin, N. **TUPB107**, THPB045, **THPB114**, MOPB063, TUPB100, FRBA01
 Bednarski, M. TUPB115
 Beebe, M. TUPB037
 Bellavia, S. THPB063
 Belomestnykh, S.A. **MOAA04**, WEBA07, THPB002, THPB051, THPB052, **THPB058**, THPB069, THPB070, THPB074, THPB100, FRBA02, TUPB101
 Ben-Zvi, I. WEBA07, THPB058, THPB074
 Benoit, A. TUPB080
 Benson, S.V. MOPB061
 Berry, S. **MOPB118**, TUPB007
 Bertinelli, F.F. THAA05
 Bertucci, M. MOPB077, MOPB114, TUPB018, **TUPB086**, **TUPB087**, THPB010, THPB035
 Bhattacharyya, P. THPB013
 Bieler, T.R. MOPB007, MOPB018, MOPB045, MOPB048, MOPB054, MOPB056, MOPB057, THPB040
 Bird, B. FRAA06
 Bishop, P. MOPB033
 Bizzaglia, S. TUPB106
 Blaskiewicz, M. WEBA07
 Blokland, W. THBA01
 Boge, P. THPB106
 Bogusz, A. TUPB002
 Bonafe, J. THAA05
 Bosland, P. TUPB007, THPB028, THPB078
 Bosotti, A. MOPB076, MOPB077, TUPB018, TUPB086, THPB010, THPB035
 Bospflug, R. MOPB076, TUPB018
 Boucherie, A.B. FRBA02
 Boudjaoui, L. MOPB063
 Boulch, C. MOPB118
 Boulware, C.H. WEA2A02
 Bousquet, J.A. TUPB106
 Bousson, S. TUA006, THPB109
 Brachet, J.P. THPB070
 Branlard, J. MOPB076, TUPB018
 Brault, S. THPB109
 Brinkmann, A. THPB056
 Brodzinski, K. FRBA02
 Broemmelsiek, D.R. TUPB014
 Brunner, O. FRBA04
 Brutus, J.C. THPB058, THPB100
 Bryant, G.D. FRAA06
 Buck, T.J. MOPB050, MOPB051, TUPB041
 Buckley, R.K. TUPB001
 Büttig, H. THPB055
 Buettner, Th. TUPB018, THPB056
 Bujard, P. TUPB026
 Bullock, B. FRAA06

Bultman, N.K.	FRAA06	Christou, C.	TUPB002
Burrill, A.	TUPB010, TUPB066, TUPB078, WEA1A04, THPB026	Chrul, A.	TUPB106
Burt, G.	TUPB064, TUPB101, THPB050, THPB052, THPB060, THPB081, THPB069, THPB070, FRBA02	Ciovati, G.	MOBA07, MOPB001 , MOPB030, TUPB068, THPB026
Burton, M.C.	TUPB033, TUPB036 , TUPB037 , TUPB060	Civale, L.	TUBA06, TUPB061
Busch, M.	MOPB065 , MOPB066, TUPB075	Clasby, B.	MOBA08, MOPB041, TUPB030, TUPB044, FRAA04
Butkowski, Ł.	MOPB076, TUPB018	Clemens, W.A.	THPB026, THPB042, THPB063
Butterworth, A.C.	FRBA04	Cloué, C.	MOPB118
— C —		Compton, C.	MOPB007, MOPB018, MOPB045, MOPB054, MOPB056, MOPB057, TUPB022, WEBA03 , THPB040, FRAA06, MOPB048
Cabanel, T.	THPB106	Conklin, H.	MOPB033, TUPB044, TUPB045
Calaga, R.	TUPB101, THAA05, THPB017, THPB018 , THPB019, THPB048, THPB052, THPB060, THPB069, THPB070, THPB081, FRBA02, FRBA04	Conway, J.V.	THBA05
Calatroni, S.	TUPB027, TUPB042, TUPB051, TUPB052 , TUPB068, THPB048	Conway, Z.A.	MOPB068, WEBA05 , THPB088
Calic, S.	TUAA02	Corniani, G.	MOPB094, MOPB102, THPB023
Cao, C.	MOPB053, TUPB068	Costanza, G.	THPB028
Capatina, O.	TUPB101, THAA05, THPB048, THPB052, THPB060, THPB069, THPB070, FRBA02	Cowie, L.S.	TUPB001, THPB033
Capelli, T.	TUPB101, THPB060, THPB069, THPB070, FRBA02	Crawford, A.C.	MOPB028, MOPB029, MOPB033, MOPB087, MOPB111
Carlson, K.	TUPB013, TUPB014, FRAA03	Crawford, D.J.	TUPB014, FRAA03
Carra, F.	TUPB101, THPB048, THPB052, THPB060, THPB069, THPB070, FRBA02	Crofford, M.T.	TUPB093 , THBA01
Carriere, P.R.	THPB036	Cubizolles, R.	MOPB063
Casagrande, F.	FRAA06	Čučkov, F.	MOPB047
Castagnola, S.	TUPB111	Cullerton, E.	MOPB087, FRAA03
Castilla, A.	THPB047	— D —	
Cenni, E.	TUPB007, THPB020, THPB028 , THPB046	Dai, J.P.	TUPB017
Cha, H.J.	TUPB072, TUPB084	Dai, X.W.	TUPB017
Chan, J.	TUPB012	Dail, D.	TUPB111
Chandrasekaran, S.K.	TUPB102	Daly, E.	MOPB081, TUPB003, TUPB009, TUPB112, TUPB113 , THPB062, THPB063, THPB110
Chang Beom, E.	TUPB060	Dammann, J.A.	THPB032
Chao, A.	THPB007	Daniel, A.	TUPB105, THPB025
Chapman, S.	TUPB032, TUPB034, THPB083, THPB100	Darve, C.	TUPB007, THPB028, THPB078
Charon, P.	TUPB100	Dassa, L.	THPB060, THPB069, THPB070, FRBA02
Chase, B.E.	MOPB087, TUPB013, FRAA03	Davidson, T.L.	TUPB093
Checchin, M.	MOBA05 , MOPB014, MOPB015, MOPB016, MOPB020 , MOPB021 , MOPB022 , MOPB025, MOPB026, MOPB028, MOPB029, MOPB033, MOPB053, MOPB104, MOPB111	Davis, G.K.	MOPB040, MOPB081, TUPB008 , TUPB009, TUPB111, TUPB112, THPB110
Chel, S.	FRBA01	De Lamberterie, P.	THPB106
Chen, J.F.	MOPB077, TUPB018, THPB004, THPB006 , THPB010, THPB035	De Silva, S.U.	THPB050, MOPB003, TUPB101, THPB049, THPB053 , THPB054 , THPB069, THPB070, THPB081, FRBA02
Chen, X.	THPB101	DeContreras, G.	TUPB012
Cheng, G.	THPB110	DeGraff, B.	THBA01, MOPB112
Cherry, G.L.	WEBA05	Dehn, M.	MOPB051
Chesca, B.	TUPB039, TUPB040	Delayen, J.R.	TUPB060, TUPB071, THPB047, THPB070, MOPB003, TUPB101, THAA01 , THPB049, THPB053, THPB054, THPB060, THPB069, FRBA02
Chetri, S.	MOPB048, MOPB052	Delfs, T.	MOPB076, TUPB018
Cheung, V.W.	THPB036	Demarest, P.	TUPB106
Chodak, J.	TUPB117	Denny, P.	TUPB111, TUPB112
Chouhan, V.	MOPB098, MOPB105 , THBA02	Dequaire, J.	TUPB106
Christophe, C.	THPB050	Derwent, P.	TUPB019
		DeSanto, L.	WEBA07
		Deschamps, J-B.	TUPB106

Author Index

Desmons, M.	THPB078	Favre, G.	TUPB101, THAA05, THPB048, THPB069, THPB070, FRBA02
Devanz, G.	TUPB007, TUPB107, THPB028, THPB045 , THPB078, TUPB100, FRBA01	Feisi, H.E.S.	WEBA01
Dhakal, P.	MOBA07, MOPB001, MOPB030 , MOPB039, MOPB052, THPB042	Feldmann, T.	THPB056
Di Benedetto, C.	MOPB114	Feng, L.W.	THPB079
Didenko, A.D.	THPB011, THPB012	Fernández López, P.F.	TUPB080
Dijoud, T.	FRBA02	Ferrand, G.	THPB078, MOPB063
Disset, G.	THPB045	Ferreira Somoza, J.A.	TUPB106
Doleans, M.	MOPB069, MOPB112, MOPB115, TUPB093, THBA01	Ferreira, L.M.A.	MOPB100 , THPB048
Douglas, D.	MOPB061	Fischer, J.F.	MOPB035, TUPB112, TUPB113
Dreyfuss, C.	THPB026	Fischer, R.L.	WEBA05
Drury, M.A.	MOPB081 , MOPB082 , TUPB009 , TUPB113, THPB110	Follkie, J.	TUPB111, TUPB112
Dubois, F.	MOPB023	Fong, K.	TUAA02
Duchesne, P.	THPB109	Ford, D.C.	MOPB046
Dumbell, K.D.	TUPB064	Forehand, D.	TUPB112, TUPB113, THPB026
Durand, H.M.	FRBA02	Fortuna, F. F.	TUPB058
Duthil, P.	THPB109	Foster, B.	MOPB073
Dutta Gupta, A.	THPB013	Fouaidy, M.	MOPB023
Dzieza, B.	TUPB115	Frahm, A.	TUPB078, THPB026
Dzitko, H.	TUPB100, TUPB107, THPB045, FRBA01	Franzi, M.A.	TUPB065
Dziuba, E.D.	MOPB065, MOPB066, MOPB067, TUPB020, TUPB075	Freijedo Menendez, P.	TUPB101, THPB069, THPB070, FRBA02
— E —		Freitag, M.	THPB055
Eddy, N.	TUPB014	Frigola, P.	THPB042
Edinger, R.	MOPB071 , THPB036	Furuta, F.	MOBA08, MOPB033, MOPB040, MOPB041, MOPB093 , MOPB101, TUPB081 , FRAA04
Edstrom, D.R.	TUPB014, FRAA03	Furuya, T.	MOPB116, TUPB021, THAA06, THPB071
Egerer, C.	THPB093	Fuwa, Y.	TUPB062
Egi, M.	TUPB021, THAA06	— G —	
Eichhorn, R.G.	MOBA08, MOPB010, MOPB011, MOPB012, MOPB013 , MOPB033, MOPB041, TUPB044, TUPB081, TUPB088, THBA05 , THPB093, FRAA04	Gaj, W.	TUPB115
Elias, N.	TUPB007	Gajewski, K.J.	TUPB026, TUPB089, TUPB090
Elmore, B.	MOBA08, MOPB041, MOPB093, FRAA04	Galambos, J.	MOPB069
Elsayed-Ali, H.	TUPB031	Gall, P.D.	THPB038, THPB039
Elsen, E.	MOPB072, MOPB073, TUPB079, TUPB085	Gallas, A.	THPB075 , THPB094, THPB102
Enami, K.	TUPB021, THAA06	Gandolfo, N.	THPB109
Éozénou, F.	THPB045	Gao, J.	MOPB070, TUPB017, THPB004
Erdelyi, B.	MOPB068	Gao, Z.	TUPB097
Eremeev, G.V.	MOPB002 , TUBA05 , TUPB029, TUPB037, TUPB046, TUPB054, TUPB055, TUPB060, TUPB082 , THPB055	Garcin, G.	THPB094, THPB096
Ermakov, A.	THPB068, THPB076	Garlaschè, M.	THAA05, THPB069, THPB070, FRBA02
Eschke, J.	MOPB076, THPB056	Gastineau, B.	MOPB063
Espalin, D.	THPB042	Gayde, J.	TUPB106
Everard, J.R.	TUPB001	Gaytan, S.M.	THPB042
— F —		Ge, G.M.	MOBA08, MOPB033, MOPB040, MOPB041, MOPB083 , MOPB084 , MOPB085 , MOPB093, TUPB081, FRAA04
Facco, A.	FRAA06	Ge, L.	THPB009
Faillace, L.	THPB042	Ge, R.	TUPB017
Fan, P.L.	THPB016, THPB079	Geisser, J.-M.	THPB069
Fant, K.	TUPB012, THPB077	Geng, R.L.	MOBA07, MOPB035
		Gerbick, S.M.	WEBA05
		Gerigk, F.	MOPB078, THAA05
		Gettmann, V.	MOPB066, TUPB020 , MOPB067, TUPB015
		Gex, D.	FRBA01
		Geynisman, M.	TUPB119
		Gheidi, S.	MOPB051 , TUPB041
		Ghosh, R.	TUPB119, THPB037
		Ghosh, S.	THPB013

Gibson, P.E.	FRAA06	Hannon, F.E.	MOPB002
Gilankar, G.	TUPB119 , THPB037	Hanus, X.	TUPB007, THPB028
Ginsburg, C.M.	TUPB110, THPB119	Hara, H.	MOPB032, WEBA06, THPB029
Gössel, A.	MOPB076, THPB031, THPB056, THPB080	Hara, K.	TUPB109, TUPB116
Goldberg, D.	WEBA07	Hardy, P.	TUPB007, TUPB107, THPB028, THPB045, THPB078, MOPB063, TUPB100
Gómez Martínez, Y.	THPB106	Harmer, P.R.	MOPB096, TUA002, TUPB120, THPB103, THPB115
Gonin, I.V.	MOPB024, THPB005 , THPB014, THPB077, THPB085	Harms, E.R.	MOPB076, TUPB013 , TUPB014 , TUPB018, THPB005, FRAA03
Gonnella, D.	MOBA03 , MOBA08, MOPB004, MOPB006, MOPB028, MOPB033, MOPB040, MOPB041 , MOPB042 , TUPB081, FRAA04	Harris, T.	THPB026
Goodman, T.	TUPB008	Harrison, A.	TUPB106
Goryashko, V.A.	TUPB083, TUPB089 , TUPB090	Harrysson, O.	THPB042
Goudket, P.	TUPB064 , TUPB001, THPB033	Hartill, D.L.	TUPB081
Goulden, A.R.	TUPB001, THPB033	Hartman, B.	THPB064
Gourragne, M.	TUPB106	Harvey, M.	WEBA07
Grabowski, W.C.	THPB056	Hayano, H.	MOPB093, MOPB098, MOPB105, TUPB043, TUPB057
Grassellino, A.	MOBA06 , MOPB014, MOPB015, MOPB016, MOPB019, MOPB020, MOPB021, MOPB022, MOPB026, MOPB027, MOPB028 , MOPB029 , MOPB033, MOPB037, MOPB038, MOPB041, MOPB043, MOPB044, MOPB053, MOPB055, MOPB087, MOPB091, MOPB104, MOPB111, TUPB004, TUPB068, TUPB099, THPB089, THPB111	Hayes, T.	WEBA07
Grenoble, C.	MOPB081, TUPB008, TUPB009	Haynes, W.B.	WEA2A02
Gresele, A.	THPB023 , THPB068	He, Y.	MOPB041, THBA05, TUPB110, THPB119
Grimm, C.J.	MOPB028, MOPB033, MOPB041, THPB014, THPB027 , THPB089	He, Y.	MOAA03 , THPB015
Grimm, T.L.	WEA2A02	Heilmann, M.	MOPB067
Groll, N.	MOPB053, TUPB068, TUPB069	Heine, R.G.	TUPB015, THPB116
Gruber, T.	MOBA08, MOPB005, MOPB033, MOPB042, MOPB093, TUPB030, TUPB044, TUPB045, THBA05	Helmig, M.	TUPB104
Grudiev, A.	THPB048	Henning, D.	MOPB118
Grudnik, L.	TUPB115	Hennion, V.M.	THPB028
Gu, K.X.	THPB087 , THPB101	Henry, J.	TUPB113
Gubarev, V.	THPB038, THPB039	Hermansson, L.	TUPB026, TUPB089, TUPB090
Guinchard, M.	THPB070, FRBA02	Hernández-Chahín, K.G.	MOPB074, TUPB080, THPB050
Guler, H.	THPB075, THPB095, THPB102	Hiatt, T.	THPB110
Gupta, P.D.	TUPB119, THPB037	Hino, M.	TUPB062
Gurevich, A.V.	TUPB060, TUPB059, WEA1A01	Hintz, H.	TUPB018, TUPB108, THPB025
Gurran, L.	TUPB059, TUPB064	Hocker, A.	MOPB028, MOPB033, MOPB087, TUPB119, THAA04, THPB005, THPB089, FRAA03
— H —			
Hahn, H.	THPB074	Hoffmann, F.	MOPB076, TUPB018
Hajima, R.	THPB020, THPB046	Hoffstaetter, G.H.	MOBA08, MOPB033, MOPB041, MOPB093, MOPB101, TUPB044, TUPB081, THBA05, FRAA04
Halczyński, P.	TUPB115	Hofheinz, M.	TUPB057
Hall, B.D.S.	TUPB005	Hokonohara, H.	THPB046
Hall, D.L.	MOBA08, MOPB006, MOPB033, MOPB041, TUBA04 , TUPB030, TUPB044 , TUPB045 , TUPB049, TUPB056, TUPB068, FRAA04	Holmes, D.	MOPB092
Hall, T.D.	MOPB092, MOPB093, MOPB101	Holmes, S.D.	TUPB019
Hamdi, A.	THPB078	Holzbauer, J.P.	MOPB087, TUPB095, THPB065, THPB089
Hanna, B.M.	THPB098	Hopper, C.S.	WEBA05, TUPB071 , WEA2A01
Hannah, A.N.	TUPB039, TUPB040	Horan, D.	THPB088
Hannah, B.S.	MOPB115, THBA01, MOPB112	Horn, P.	MOPB049
		Horn, T.	THPB042
		Hovater, C.	TUPB009
		Howell, M.P.	MOPB069, THBA01
		Huang, T.M.	MOPB070, TUPB017, THPB087, THPB101
		Huang, X.	TUPB017
		Hüning, M.	MOPB076, TUPB018
		Hulbert, J.D.	FRAA06
		Humphry, F.	MOPB082
		Huque, N.A.	THPB062 , THPB063 , THPB110
		Hyun, M.O.	THPB082

Author Index

— I —

Ida, Y.I. MOPB093, MOPB098, MOPB105
 Im, D.S. MOPB097
 Inman, M.E. MOPB092, MOPB093, **MOPB101**
 Inoue, H. MOPB032, THAA04, THPB030
 Irfan, I. TUPB032, TUPB034, **THPB083**, THPB100
 Iriks, D.C. TUPB082
 Ishimi, K. MOPB098, MOPB105
 Iversen, J. THPB031, **THPB032**
 Iwashita, Y. TUPB043, TUPB057, **TUPB062**, **THPB020**, THPB046

— J —

Jain, A. TUPB119, THPB037
 Jakovljevic, B. TUA002
 Janssen, D. THPB057
 Jenhani, H. THPB078, THPB045
 Jensch, K. MOPB076, TUPB018, TUPB108, THPB025
 Jensen, E. FRBA04
 Jeon, D. **MOAA05**
 Jiang, T.C. THPB015
 Jiang, X. TUPB047
 Jin, S. TUPB017
 Jo, Y.W. THPB118
 Jonas, R. MOPB076, TUPB018
 Jones, T.J. TUPB064, TUPB101, THPB060, THPB069, THPB070, FRBA02
 Joo, J. MOPB106
 Jordan, E.S. TUPB064
 Joshi, S.C. THPB037
 Joung, M.J. MOPB106, TUPB084
 Jung, Y. **MOPB106**
 Junginger, T. TUBA03, TUPB050, TUPB080, **MOPB049**, MOPB050, MOPB051, **TUPB042**
 Junquera, T. TUPB026

— K —

Kaabi, W. **THBA03**, THPB075, THPB094, THPB095, **THPB102**
 Kabe, A. MOPB116, THPB071
 Kadi, Y. TUPB077
 Kaida, K. TUPB037
 Kako, E. MOPB032, TUPB109, TUPB116, WEBA06, THPB030, THPB059, THPB082, THPB084
 Kaluzny, J.A. TUPB110, THPB111, THPB119
 Kamigaito, O. WEBA06, THPB084
 Kanaoka, K. THPB029
 Kanareykin, A. MOPB024, THPB011, THPB012, THPB105
 Kang, D. MOPB018, **MOPB045**, MOPB054, MOPB057
 Kanjilal, D. **TUA004**
 Kaplan, R.P.K. FRAA04
 Kasprzak, K. MOPB080, TUPB118
 Kato, S. MOPB098, MOPB105, TUPB057
 Katyan, N. **TUPB058**
 Kaufman, J.J. MOBA08, MOPB033, MOPB041, TUPB044, TUPB045, TUPB081, FRAA04

Kautzmann, G. TUPB106
 Kawata, H. **TUA001**
 Kazakov, S. THPB091, THPB092, **THPB097**, **THPB098**
 Keckert, S. TUPB066, **TUPB067**, WEA1A04
 Kedzie, M. WEBA05
 Keir, J.J. **MOPB096**, TUA002, THPB115
 Kelley, M.J. TUBA05, TUPB046, TUPB054, MOPB107
 Kelly, M.P. WEBA05, **THPB088**
 Kephart, R.D. **FRBA03**
 Khabiboulline, T.N. MOPB025, MOPB087, THPB005, THPB011, THPB012, **THPB014**, THPB089, THPB092, THPB105, THPB113
 THPB100
 Khalil, N.Z. TUPB119, **THPB037**
 Khare, P. MOPB050, MOPB051, TUPB041
 Kiefl, R. TUPB072, **TUPB084**, THPB117, THPB118
 Kim, H. MOPB106, **TUPB016**, TUPB084, THPB117, THPB118
 Kim, H.J. TUPB084
 Kim, J.H. **MOPB069**, MOPB112, MOPB115, TUPB093, THBA01
 Kim, S.-H. WEBA05, **THPB072**, **THPB073**, THPB088
 Kim, S.H. TUPB072, TUPB084, **THPB117**, THPB118
 Kim, W.K. TUPB084, THPB117, **THPB118**
 Kim, Y. MOPB081, MOPB082, TUPB009
 King, L.K. TUA002, TUPB120
 Kishi, D. TUPB013
 Klebaner, A.L. **TUPB066**, TUPB067, **WEA1A04**
 Kleindienst, R. THPB031, THPB056
 Klinke, D. MOPB076, TUPB018
 Klos, R. THPB094, THPB096
 Knaak, M. FRBA01
 Knaster, J. MOPB001, THPB026, THPB055, THPB057
 Kneisel, P. MOPB017, MOPB019, TUA003, TUBA03, TUPB050, TUPB066, TUPB067, TUPB078, WEA1A04, THPB026
 Knobloch, J. TUPB116, THPB059
 Kobayashi, Y. MOPB049
 Koettig, T. TUPB109
 Kojima, Y. MOPB050, **MOPB088**, **MOPB089**, TUA002, WEA1A03
 Kolb, P. TUPB116
 Kondo, Y. MOPB032, **THPB059**
 Konomi, T. TUPB118
 Konwisorz, D. MOPB046
 Korczakowski, A. TUA002
 Koscielniak, S.R. MOPB076, MOPB080, MOPB090, MOPB103, TUPB018, **THPB056**, THPB076
 Kostin, D. **MOPB024**, **THPB011**, **THPB012**
 Kostin, R.A. TUPB115
 Kotarba, A. MOBA08, **MOPB004**, MOPB041, MOPB042
 Koufalis, P.N. TUA002, TUPB120, THPB115
 Koveshnikov, A. TUPB115
 Krawczyk, A. MOPB093
 Krebs, D.K. TUPB032, **TUPB034**, THPB083, THPB100
 Krishnan, M. MOPB075
 Krupka, N. TUPB117
 Krzysik, K. TUPB117

Kubo, T. **MOPB008**, **MOPB009**, MOPB032, **TUBA07**, TUPB043, TUPB057, TUPB062, THAA04, THPB020, THPB046
 Kucera, M.J. TUPB013, FRAA03
 Kuder, N. THPB060, THPB069, THPB070, FRBA02
 Kugeler, O. MOPB017, **MOPB019**, TUPB066, TUPB067, WEA1A04
 Kulina, G. MOPB033
 Kumar, P. THPB014
 Kush, P.K. TUPB119, THPB037
 Kushnick, P. TUPB008
 Kustom, R. TUPB055
 Kutsaev, S.V. THPB088

— L —

Laforge, C. TUA02
 Lagotzky, S. **MOPB058**, **MOPB059**
 Lang, D. MOPB096, TUA02, THPB103, THPB115
 Langeslag, S.A.E. TUPB101, THAA05, THPB069, THPB070, FRBA02
 Larbalestier, D.C. MOPB052, MOPB048
 LaVere, M.J. MOPB095
 Laxdal, R.E. **MOPB050**, MOPB051, MOPB071, MOPB088, MOPB089, MOPB096, TUA02, **TUPB041**, TUPB103, TUPB114, TUPB120, WEA1A03, THPB021, THPB043, THPB044, THPB103, THPB115
 Le Pinvidic, D.J.M. THPB075, THPB102
 Leaux, F.M. TUPB051
 Lebedev, V.A. TUPB019
 Lee, M. THPB118
 Lee, N. TUPB055
 Lee, P.J. MOPB018, MOPB048, MOPB052
 Lee, S.W. TUPB093, THBA01
 Leibfritz, J.R. TUPB013, TUPB014, FRAA03
 Leseigneur, F. TUPB007, TUPB100, THPB028, THPB078
 Leuxe, R. THPB060, THPB069, THPB070, FRBA02
 Lewis, F.L. TUPB004
 Li, H. **TUPB083**, TUPB089, TUPB090
 Li, S.P. TUPB017
 Li, Y. THBA05
 Li, Y.M. THPB015
 Li, Z. TUPB101, THPB007, THPB008, THPB009, THPB049, THPB053, THPB054, THPB069, THPB070, THPB077, THPB081, FRBA02
 Liao, K.C. MOPB049
 Liepe, M. MOPB028, TUPB056, TUPB068, **MOBA08**, MOPB004, MOPB005, MOPB006, **MOPB033**, MOPB040, MOPB041, MOPB042, TUBA04, TUPB030, TUPB044, TUPB045, TUPB049, TUPB081, THBA05, FRAA04
 Lievin, C. THPB094, THPB095, THPB096
 Lilje, L. MOPB118, TUPB018, TUPB108
 Lin, H.Y. TUPB017, THPB101, THPB087
 Lin, L. THPB079
 Linardakis, P. TUPB024, TUPB025
 Litvinenko, V. THPB058

Liu, B. TUPB017
 Liu, H. TUPB120
 Liu, K.X. THPB016, THPB079, FRAA05
 Liu, Z.C. MOPB070, TUPB017
 Lobanov, N.R. **TUPB024**, **TUPB025**
 Lofnes, T. TUPB090
 Longuevergne, D. MOPB023, **WEA1A02**
 Lorkiewicz, J.A. THPB056
 Lu, P.N. THPB055, THPB057
 Lu, X.Y. MOPB036, THPB022
 Lucatero, S. MOPB101
 Lukaszew, R.A. TUPB036, TUPB037, TUPB060
 Lumpkin, A.H. TUPB014
 Lunin, A. THPB005, THPB014, THPB105

— M —

Ma, Q. TUPB017, THPB087, THPB101
 Ma, Y. MOPB088, MOPB089, TUA02, **THPB103**, THPB115
 Ma, Y.Y. MOPB050
 MacDonald, S.W.T. WEA05
 Macha, K. TUPB031, TUPB033, TUPB112, TUPB113
 Macpherson, A. MOPB049, **MOPB074**, **TUPB080**, THPB050, THPB081, FRBA02
 Madec, C. **MOPB063**, TUPB007, MOPB118
 Mäder, D. MOPB066
 Maesen, P. MOPB074
 Magueur, C. THPB075, THPB102
 Maiano, C.G. **MOPB076**, TUPB018, THPB035, MOPB077
 Makara, J.N. FRAA03
 Malloch, I.M. **MOPB095**, TUPB022
 Malyshev, O.B. TUPB064, TUPB038, TUPB039, TUPB040, **TUPB059**
 Mammosser, J.D. TUPB093, THBA01, MOPB069, **MOPB112**
 Mandal, A. THPB013
 Mandel, E. THAA05
 Maniscalco, J.T. MOBA08, MOPB004, **MOPB005**, **MOPB006**, MOPB033, MOPB041, MOPB042, **TUPB030**, FRAA04
 Mapar, A. MOPB045, **MOPB056**, **MOPB057**, **THPB040**
 Maragno, N. MOPB094
 Marchand, C. THPB078, TUPB058, **WEBA04**
 Marhauser, F. **MOPB061**, MOPB110, **TUPB003**, **THPB003**, THPB042, THPB110
 Marinov, K.B. TUPB101, THPB070, FRBA02
 Markham, S.R. **TUPB088**
 Marques Antunes Ferreira, J. THPB069
 Marten, P.J. TUPB002
 Martinello, M. **MOPB014**, **MOPB015**, **MOPB016**, MOPB020, MOPB021, MOPB022, MOPB025, MOPB026, MOPB028, MOPB029, MOPB033, MOPB053, MOPB104, MOPB111
 Martinet, G. TUPB058
 Marton, M. THPB106
 Marty, P. THAA05
 Maschmann, W. MOPB076, TUPB018, TUPB108
 Massaro, G. **MOPB094**

Oripov, B.G. **MOPB119**
 Orlov, Y.O. TUPB110, THPB086, THPB090, THPB119
 Orr, R.S. MOPB089
 Orris, D.F. TUPB004
 Ostroumov, P.N. **MOPB068**, WEBA05, THPB088
 Ostrowicz, T. TUPB115
 Oublaid, M. THPB075, THPB102
 Overton, R.B. THPB026
 Ozeki, K. WEBA06, **THPB084**
 Ozelis, J.P. MOPB028, MOPB033, MOPB087, TUPB004, TUPB119

— P —

Pagani, C. TUPB087, THPB006, MOPB077, MOPB113, MOPB114, TUPB018, TUPB086, THPB004, THPB010, THPB035
 Palczewski, A.D. **MOBA07**, MOPB033, **MOPB039**, **MOPB040**, MOPB081, MOPB107, MOPB110, MOPB117
TUBA02
 Palmieri, V. MOAA03, TUPB017, THPB087, THPB101
 Pan, W.M. TUPB092
 Pande, M.M. MOPB078
 Papadopoulos, S. MOPB076, MOPB077, TUPB018, THPB010, THPB035, **FRAA01**
 Paparella, R. **MOPB078**
 Papke, K. FRBA02
 Parente, C. TUPB074
 Parise, M. **TUPB072**, TUPB084, **MOPB064**
 Park, G.-T. **MOPB003**, TUPB071, **THPB049**, THPB110, TUPB101, WEA2A01, THPB053, THPB054, THPB060, THPB069, THPB070, FRBA02
 Parma, V. TUPB106
 Passarelli, D. TUPB074, THPB061
 Pattalwar, N. TUPB059
 Pattalwar, S.M. TUPB059, TUPB101, TUPB040, TUPB064, THPB069, THPB070, FRBA02
 Peauger, F. **TUPB007**, THPB028, THPB078
 Pekeler, M. **THPB034**, THPB094, THPB096, THPB116
 Peng, X.H. TUPB017
 Peronnet, H. THAA05
 Pes, C. MOPB063
 Peshl, J.J. MOPB097
 Peters, B.J. MOPB049
 Peterson, T.J. MOPB087, TUPB110, TUPB119, THPB111, **THPB119**
 Phillips, G. FRBA01
 Phillips, H.L. MOPB097, **MOPB099**, MOPB108, MOPB109, TUPB031, **TUPB033**, TUPB036
 Pichoff, N. MOPB063
 Pierens, M. THPB109
 Pierini, P. MOPB076, **TUPB018**, **THPB035**, MOPB077, TUPB105, TUPB108, THPB006, THPB010
 Pilipenko, R.V. TUPB004
 Pillon, F. MOPB074
 Pinayev, I. THPB058
 Piot, P. TUPB014

Piquet, O. TUPB007, THPB045, THPB078
 Pischalnikov, Y.M. MOPB087, TUPB004, TUPB091, TUPB095, THPB011, THPB012, THPB062, **THPB064**, **THPB065**, FRAA03
 MOPB076
TUPB038
 Pivovarov, S. TUPB007, **TUPB100**, THPB028, THPB045
 Pizzol, P. MOPB023
 Plouin, J. MOPB065, MOPB066, MOPB067, TUPB020, TUPB075
 Pochon, O. TUPB119, THPB105
 Podlech, H. MOPB018, MOPB048
 THPB048
 Poloubotko, V. TUPB022, FRAA06
 Polyanskii, A. MOPB095, FRAA06, **TUPB022**
 Poncet, J.-E. MOPB047, MOPB097
 Popielarski, J. FRAA04, MOPB015, MOPB022, MOPB029, **MOPB104**, TUPB041, **TUPB048**, **TUPB049**, TUPB056, TUPB068
 Popielarski, L. TUPB073
 Popović, S. MOPB045, MOPB056, MOPB057, THPB040
 Posen, S. MOPB081, TUPB008, **TUPB094**
 MOPB081, TUPB112, TUPB113, THPB110
 TUPB110, THPB077
 MOPB087, THPB005, **THPB085**, **THPB086**, THPB090
 Potukuchi, P.N. TUPB018
 Pourboghrat, F. THPB070
 Powers, T. TUPB013, TUPB014, FRAA03
 Preble, J.P. TUPB115
 Premo, K. THPB005, THPB085, THPB090
 Premo, K.S. TUPB042
 MOPB091, **THPB091**, **THPB092**, THPB098
 MOPB046, **MOPB053**, TUPB029, TUPB035, TUPB042, TUPB045, **TUPB068**, **TUPB069**
 MOPB059, MOPB073, MOPB113
 TUBA05, **TUPB054**
 THPB069
 Prenting, J. TUPB021
 Prever-Loiri, L. THPB016, THPB079
 Prieto, P.S. MOBA08, MOPB033, MOPB041, THBA05, FRAA04
 Prochal, B. TUPB018
 Prokofiev, O.V. THPB005, THPB085, THPB090
 Prokscha, T. TUPB042
 Pronitchev, O.V. MOPB091, **THPB091**, **THPB092**, THPB098
 Proslier, Th. MOPB046, **MOPB053**, TUPB029, TUPB035, TUPB042, TUPB045, **TUPB068**, **TUPB069**
 MOPB059, MOPB073, MOPB113
 TUBA05, **TUPB054**
 THPB069
 Prudnikava, A.L. TUPB021
 Pudasaini, U. THPB016, THPB079
 Pugnât, D. MOBA08, MOPB033, MOPB041, THBA05, FRAA04

— Q —

Qiu, F. TUPB021
 Quan, S.W. THPB016, THPB079
 Quigley, P. MOBA08, MOPB033, MOPB041, THBA05, FRAA04

— R —

Rafalski, J. TUPB115
 Rai, A. TUPB073
 Rampnoux, E. THPB109
 Rao, T. THPB058
 Rathke, J. THPB105
 Ratti, A. TUPB101, THPB069, THPB070, FRBA02
 Ratzinger, U. MOPB065, MOPB067, TUPB020
 Raubenheimer, T.O. THPB008
 Rawnsley, W.R. TUBA02, TUPB103, THPB115
 Reaume, M.A. FRAA06

Author Index

Reece, C.E.	MOBA07, MOPB033, MOPB039, MOPB107, MOPB108, MOPB109, MOPB110 , TUBA05, TUPB028, TUPB029, TUPB033, TUPB034, TUPB036, TUPB046, TUPB054, TUPB063 FRBA01	Sangiorgi, G.	MOPB114
Regidor, D.	TUPB006	Santiago Kern, R.	TUPB026 , TUPB089, TUPB090
Regier, C.N.	TUPB119	Sato, M.	MOPB032
Reid, C.	TUPB013, TUPB014, FRAA03	Saunders, J.	TUPB093, THBA01, MOPB112
Reid, J.	MOPB091, WEBA05	Sawabe, M.	MOPB098, MOPB105
Reid, T.	MOPB117, TUPB111 , TUPB112 , TUPB113	Sawamura, M.	TUPB021, THAA06, THPB020, THPB046
Reilly, A.V.	TUPB007	Sawlanski, O.	MOPB076, TUPB018
Renard, B.	MOAA02 , MOPB079, MOPB080, MOPB086, MOPB090, THPB039, THPB056	Schaffran, J.	MOPB072, MOPB079 , MOPB086, MOPB113
Reschke, D.	THPB109	Schalwat, M.	TUPB104, THPB025
Reynet, D.	TUPB027, THPB048	Schappert, W.	MOPB087, TUPB091 , TUPB095 , THPB065, FRAA03
Richard, T.	THPB069	Schilling, P.	MOPB075, TUPB105, THPB025
Rigutto, E.	THPB042	Schirm, K.M.	MOPB074, TUPB080, THAA05
Rimmer, R.A.	TUPB037	Schlender, F.	TUPB015 , THPB116
Riso, J.M.	TUPB073 , TUPB074 , THPB061	Schlemper, C.	TUPB047
Ristori, L.	MOPB114	Schlösser, M.	TUPB018
Rizzetto, D.	MOPB102 , MOPB114	Schmidt, A.	THPB025
Rizzi, M.	MOPB011 , THPB093	Schmökel, M.	MOPB076, MOPB077, MOPB103, MOPB118, TUPB018, TUPB105 , THPB056
Robbins, J.A.	WEA2A02	Schwarz, M.	MOPB066
Rogacki, A.	THPB017	Sears, J.	MOBA08, MOPB005, MOPB033, MOPB093, THBA05, FRAA04
Roggen, T.	MOBA02 , MOPB014, MOPB015, MOPB016, MOPB019, MOPB020, MOPB021, MOPB022, MOPB025 , MOPB026 , MOPB027, MOPB029, MOPB033, MOPB041, MOPB043, MOPB044, MOPB053, MOPB055, MOPB087, MOPB104, TUPB004, TUPB048, TUPB049, TUPB068, WEA1A05	Seaton, C.	MOPB108
Romanenko, A.	TUPB027, TUPB051	Seberg, S.K.	WEBA07, THPB063
Rosaz, G.J.	FRAA06	Seidman, D.J.	TUPB009
Rose, R.J.	MOBA01	Sekutowicz, J.K.	MOPB103, THAA02 , THPB056, THPB089
Ross, M.C.	MOPB076, TUPB018	Sellami, N.	MOPB063
Rothenburg, J.	TUPB007, THPB028, THPB078	Sennyu, K.	MOPB032, WEBA06, THPB029, THPB084
Roudier, D.	THPB095	Sergatskov, D.A.	MOPB014, MOPB015, MOPB016, MOPB019, MOPB021, MOPB022, MOPB028, MOPB029, MOPB033, MOPB041, MOPB087, MOPB104, TUPB004, TUPB049, TUPB091, TUPB099, THPB089
Rouillon, P.	MOPB028, MOPB029, MOPB033, MOPB087, MOPB091 , MOPB092, MOPB101, MOPB111, THPB089, THPB105	Sertore, D.	MOPB076, MOPB077 , TUPB018, TUPB086, THPB010, THPB035
Rowe, A.M.	TUPB026, TUPB083, TUPB089, TUPB090 FRBA02	Servouin, C.	THPB078
Ruber, R.J.M.Y.		Seth, S.	THPB013
Rude, V.		Severino, F.	WEBA07
		Sha, P.	MOPB070, MOPB034
		Shakespeare, N.	TUPB001
		Shanks, R.W.	TUAA02
		Shashkov, Ya.V.	THPB104
		Shchegolkov, D.Y.	WEA2A02
		Shemelin, V.D.	THBA05
		Shiltsev, V.D.	TUPB014
		Shimizu, H.	MOPB032, THAA04, THPB030
		Shin, I.	TUPB084, THPB082
		Shinoe, K.	MOPB032, TUPB021, THAA06
		Shishido, T.	MOPB096, TUPB109
		Shishido, T.	MOPB096
		Shuptar, M.	FRAA06
		Sienkiewicz, M.	TUPB115
		Sierra, S.	THPB094 , THPB095 , THPB096
		Simakov, E.I.	WEA2A02
		Simon, D.	THPB116
		Simon, J.T.	FRAA06
		Singer, W.	MOPB113, THPB056
		Singer, X.	THPB056

— S —

Sabol, D.M.	MOBA08, MOPB033, MOPB041, FRAA04
Sacharias, J.	TUPB073
Sacristan De Frutos, O.	MOPB078
Saegebarth, S.	MOPB075, TUPB104, THPB025
Saeki, T.	MOPB093, MOPB098, MOPB105, TUPB043 , TUPB057, TUPB062, THPB020, THPB030, THPB046
Saito, K.	MOAA01 , TUPB022, TUPB102, FRAA06
Sakai, H.	MOPB032, TUPB021 , TUPB116, THAA06
Sakamoto, N.	WEBA06 , THPB084
Saliu, F.	MOPB114
Salman, Z.	TUPB042
Samolov, A.	MOPB047

Author Index

Vennekate, H. THPB055, **THPB057**
 Venturini Delsolaro, W. **TUBA01**, TUPB076, TUPB077, TUPB106, THPB060
 Verdú-Andrés, S. TUPB101, THPB050, **THPB051**, **THPB052**, THPB060, THPB069, THPB070, FRBA02
 Verguet, A. THPB075, THPB095, THPB102
 Veshcherevich, V. MOBA08, MOPB033, MOPB041, THPB093, FRAA04
 Victory, D.R. TUPB022
 Vignette, G. THPB094, THPB096
 Villegier, J.C. TUPB057, TUPB058
 Villiger, G. FRBA02
 Visentin, A. THPB023
 Visentin, B. MOPB118
 Vogel, E. MOPB076, TUPB018, THPB035
 Vogel, M. **TUPB047**
 Vogt, J.M. **MOBA04**, **MOPB017**, MOPB019, MOPB028
 Vollenberg, W. TUPB051
 Vostrikov, A. **MOPB027**
 Vušković, L. MOPB047, MOPB097

— W —

Walker, N.J. MOPB079, MOPB080, **MOPB086**
 Wang, E. THPB058
 Wang, F. THPB079
 Wang, M. **MOPB018**, MOPB048
 Wang, Z.L. THPB079
 Waraich, B.S. TUA002, THPB044, THPB103, THPB115
 Warner, A. TUPB014
 Warren, M. MOPB046, **TUPB035**
 Wartak, M. TUPB115
 Watanabe, Y. THAA04, THPB030
 Watanabe, Y. WEBA06, THPB084
 Wei, J. MOAA01, FRAA06
 Weingarten, W. **MOPB010**
 Welander, P.B. TUPB055, **TUPB065**
 Wenskat, M. **TUPB085**
 West, H.A. THPB042
 Wheelhouse, A.E. **TUPB001**, THPB033
 Wicker, R.B. THPB042
 Wiencek, M. **MOPB080**, MOPB086, TUPB115, **TUPB117**, **TUPB118**
 Wilde, S. TUPB039, **TUPB040**, TUPB064
 Williams, L.R. TUPB106
 Williams, R.S. THPB042
 Wilson, K.M. TUPB113, THPB110
 Witgen, K. FRAA06
 Withanage, W.K. **TUPB055**
 Wolak, M.A. TUBA06, TUPB055, TUPB061
 Wong, M. MOPB111
 Wright, N.T. MOPB007
 Wu, A.D. **THPB015**
 Wu, G. MOPB028, MOPB033, MOPB087, **TUPB098**, **TUPB099**, **THBA06**, **THPB111**
 Wu, Q. TUPB101, **WEBA07**, THPB051, THPB052, THPB058, THPB063, THPB069, THPB070, FRBA02

— X —

Xi, X. TUBA06, TUPB055, TUPB061
 Xiang, R. TUPB010, THPB055, THPB057
 Xiao, B. P. TUPB101, **THBA04**, THPB051, THPB052, THPB058, THPB060, THPB069, THPB070, THPB081, THPB100, FRBA02
 Xiao, L. **THPB008**, **THPB009**, THPB077
 Xie, Y. **THPB105**, **MOPB043**, **MOPB044**
 Xin, T. **MOPB060**, THPB058
 Xu, C. **THPB002**
 Xu, P. **MOPB007**
 Xu, T. FRAA06
 Xu, T. TUPB022
 Xu, W. **THAA03**, THPB002, **THPB074**
 Xue, Z. TUPB017

— Y —

Yakovlev, V.P. **TUAA05**, TUPB019, THPB005, THPB011, THPB012, THPB014, THPB105
 Yamada, K. WEBA06, THPB084
 Yamaguchi, S. TUPB116, THPB059
 Yamaguchi, T.Y. MOPB098, MOPB105
 Yamamoto, Y. TUPB109
 Yamanaka, M. MOPB032, THAA04, THPB030, **THPB041**
 Yanagisawa, T. MOPB032, WEBA06, THPB029, THPB059, THPB084
 Yang, D.Y. MOPB036, THPB022
 Yang, L. MOPB050, TUA002, **TUPB096**
 Yang, Z.Q. **MOPB036**, **THPB022**
 Yaniche, J.-F. MOPB023
 Yao, Z.Y. MOPB050, MOPB088, MOPB089, TUA002, TUPB072, **TUPB103**, **WEA1A03**, **THPB021**, THPB044, THPB115
 Yaramyshev, S. MOPB067, TUPB020
 Yasar, S. **THPB038**, **THPB039**
 Yeremian, A.D. **TUPB012**
 Yue, S. THPB036
 Yue, W.M. THPB015
 Yun, J.C. THPB064, THPB065
 Yusof, Z.M. TUPB035

— Z —

Zaltsman, A. WEBA07, THPB058
 Zanoni, C. TUPB101, THPB048, THPB052, THPB060, **THPB069**, **THPB070**, FRBA02
 Zaplatin, E.N. MOPB024
 Zasadzinski, J. **MOPB046**, MOPB053, TUPB035, TUPB042, TUPB068, TUPB069
 Zbroja, J. TUPB115
 Zhai, J.Y. **MOPB070**, **TUPB017**
 Zhang, P. **TUPB076**, **TUPB077**, TUPB106, THPB060
 Zhang, S.H. THPB015
 Zhang, S.W. TUPB017
 Zhang, Z. TUPB017
 Zhao, H. TUPB017
 Zhao, H.W. THPB015
 Zhao, J. MOPB036, THPB022

Zhao, L.	MOPB117 , TUPB111	Zhuang, D.H.	THPB079
Zhao, T.X.	TUPB017	Ziegler, J.	THPB056
Zhao, Z.	MOPB054	Ziemann, V.G.	TUPB083
Zheng, H.J.	MOPB070, TUPB017, THPB004 , THPB010	Ziolkowski, P.	TUPB115
Zheng, Q.	TUAA02	Zvyagintsev, V.	MOPB088, MOPB089, TUAA02 , TUPB103, THPB044, THPB103, THPB115
Zheng, Z.	THPB107	Zweibaeumer, L.	THPB094
Zhong, H.T.X.	THPB016	Zwozniak, A.	MOPB080, TUPB118
Zhu, F.	THPB016 , FRAA05		